Exploring the Multi-scale character of infectious disease dynamics

by

MUFOYA BLESSINGS

A Thesis Presented to the

UNIVERSITY OF VENDA

In Fulfilment of the Requirements for the Degree

of

Doctor of Philosophy (Mathematics)

in the

Department of Mathematical & Computational Sciences

Faculty of Science, Engineering & Agriculture

Supervisor: Prof W. Garira

Co-Supervisor: Prof D. Mathebula

Submitted: January 2023

Declaration of Authorship

I, MUFOYA BLESSINGS, testify that this thesis titled, 'Exploring the Multi-scale character of infectious disease dynamics' has been prepared fully by myself. I also testify that this work has not been previously submitted, partly or wholly, for a degree qualification at any institution. Unless mentioned otherwise by acknowledgment or reference, this work is completely mine.

Signed: 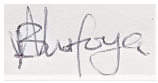

Date: 21/02/2022

Abstract

This research study characterised multiscale models of infectious disease dynamics. This was achieved by establishing when it is appropriate to implement particular mathematical methods for different multiscale models. The study of infectious disease systems has been elucidated ever since the discovery of mathematical modelling. Due to the vast complexities in the dynamics of infectious disease systems, modellers are increasingly gravitating towards multiscale modelling approach as a favourable alternative. Among the diseases that have persistently plagued most developing countries are vector-borne diseases like Malaria and directly transmitted diseases like Foot-and-Mouth disease (FMD). Globally, FMD has caused major losses in the economic sector (particularly agriculture) as well as tourism. On the other hand, Malaria remains amongst the most severe public health problems worldwide with millions of people estimated to live in permanent risk of contracting the disease. We developed multiscale models that can describe both local transmission and global transmission of infectious disease systems at any hierarchical level of organization using FMD and Malaria disease as paradigms. The first stage in formulating the multiscale models in this study was to integrate two submodels namely: (i) the between-host submodel and (ii) within-host submodel of an infectious disease system using the nested approach. The outcome was a system of nonlinear ordinary differential equations which described the local transmission mechanism of the infectious disease system. The next step was to incorporate graph theoretic methods to the system of differential equations. This approach enabled modelling the migration of humans/animals between communities (also called patches or geographical distant locations) thereby describing the global transmission mechanism of infectious disease systems. At whole organism-level we considered the organs in a host as patches and the transmission within-organ scale as direct transmission represented by ordinary differential equations. However, at between-organ scale there was movement of pathogen between the organs through the blood. This transmission mechanism called global transmission was represented by graph-theoretic methods. At macrocommunity-level we considered communities as patches and established that at within-community scale there was direct transmission of pathogen represented by ordinary differental equations and at between-community scale there was movement of infected individuals. Furthermore, the systems of differential equations were extended to stochastic differential equations in order to incorporate randomness in the infectious disease dynamics. By adopting a cocktail of computational and analytical tools we sufficiently analyzed the impact of the transmission mechanisms in the different multiscale models. We established that once we used a graph-theoretic method at host level it would be difficult to extend this to community level. However, when we used different methods then it was easy to extend to community level. This was the main aspect of the characterization of multiscale models that we investigated in this thesis which has not been done before. We also established distinctions between local transmission and global transmission mechanisms which enable us to implement intervention strategies targeted torwards both local transmission such as vaccination and global transmission such as travel restrictions. In spite of the fact that the results collected in this study are restricted to FMD and Malaria, the multiscale modelling frameworks established are suitable for other directly transmitted diseases and vector-borne diseases.

Acknowledgements

Firstly, I would like to thank our Lord and God, Jesus Christ for giving me this opportunity to do my PhD research. I am grateful for His provision and preservation that has enabled this work to be completed successfully. I would like to express my sincere gratitude to my supervisor, Prof. Winston Garira, for his encouragement, endurance and recommendations for the duration of my PhD research work. Furthermore, I would like to thank my co-supervisor, Prof. Dephney Mathebula, for her efforts and support throughout the research study. I would like to also thank and express my deepest appreciation to Dr. Rendani Netshikweta for his suggestions and counselling. My sincere gratitude goes to all the members from the Department of Mathematical and Computational Sciences for their contributions throughout my PhD study.

I would like to extend my sincere gratitude to my wife Violet and our children Tinotenda Daniel, Tinevimbo Beautitude, Makanakaishe Bethel, Taropafadzwa Rachel Kudakwashe and Nenyasha Rebecca, for their unconditional love, encouragement and support throughout my PhD study.

To my late parents, I am truly indebted and thankful for the values you instilled in me. The support and contributions you made in my life will forever be remembered.

Finally, I would like to extend my appreciation to my siblings Admire, Progress, Prosper, Prudence and their families for their support.

Contents

List of Figures

List of Tables

Chapter 1

Introduction

1.1 Background

This thesis characterises multiscale models of infectious disease systems. Previously, infectious disease dynamics have been modelled in an effort to prevent, control and eradicate these diseases. However, there is need to look at some characteristic features of multiscale models that are common and try to understand them. Therefore, this thesis looks at these aspects and characterises the multiscale models of infectious disease systems. Some of the issues that need to be characterised are that modellers have understood how to use ordinary differential equation methods and also how to use graph-theoretic methods. However, they have not been able to establish when is it appropriate to use graph-theoretic methods. This is a new idea that has not been characterised and we address that issue in this thesis. Another issue which needs to be characterised is that at community level there is local transmission or exchange of pathogen that occurs within the community. This happens due to direct contact between an infected individual and a susceptible individual (called direct transmission) or contact between the pathogen and a susceptible individual (called environmental transmission). This local transmission or exchange of pathogen is modelled using ordinary differential equations methods. However, at between-community level it is difficult to represent the contact of communities directly. Therefore, individuals have to move between communities and this is how contact is achieved. This movement of individuals is global transmission or global exchange of pathogen and can be represented using the graph-theoretic approach. This aspect is a new idea that has not been characterised and we address it in this thesis. Over the years, some progress has been made in developing multiscale models. However, there is need to look at general features of these multiscale models. Some of the characterisations that have been established include the categorization of multiscale models [2]. However, mathematically we need to establish which methods are appropriate for the different multiscale models. There are mathematical models that have been used but the challenge with all this

information is that there has not been any systematic characterisation.

Previously, the study of the dynamics of diseases primarily focused on two fundamental ideas, the causation theory of infectious disease and transmission theory of infectious disease [3]. The causation theory of infectious disease is associated with a group of ideas that have been sequentially upgraded to clarify the causes of infectious diseases and considers the infectious disease as systems [3]. On the other hand, the transmission mechanism theory of infectious disease affirms that the dynamics of infectious diseases has the prominent process being transmission. The exchange of pathogens involved in the transmission of an infectious disease system consists of local transmission or global transmission for different scales (microscale and macroscale) and levels of organisation of infectious disease systems [4]. The transmission mechanisms developed from the traditional SIR-type models (including their variations) to the recent multiscale models have been formulated separately, that is, local transmission [5–7] or global transmission [8–13]. It is of paramount importance to formulate a modelling framework that incorporates both the local and global transmission mechanisms to characterise multiscale models of infectious disease systems. Furthermore, it is important to be able to decide when it is appropriate to implement the graph-theoretic methods to describe global transmission. Some of the key factors that contribute to the transmission of infectious disease systems include movement of people, goods and animals. Mathematical models have been developed to address various aspects concerning the transmission dynamics of infectious disease systems. Some aspects of infectious diseases have already been established in terms of how they are transmitted and include Vector-borne transmission mechanism models, Direct transmission mechanism models and Environmental transmission mechanism models.

(a) **Environmental transmission disease systems**
The following are various kinds of environmental transmission disease systems:

(i) *Type I environmental transmission disease systems* : At within-host scale there is no replication of pathogen (for example, Schistosomiasis) [1].

(ii) *Type II environmental transmission disease systems*: Replication of the pathogen takes place strictly at the within-host scale (for example, FMD as well as Influenza) [1].

(iii) *Type III environmental transmission disease systems*: Replication of pathogen takes place at the within-host scale as well as at the between-host scale (for example, Cholera as well as Anthrax) [1].

(b) **Vector-borne transmission disease systems**
The following are various kinds of vector-borne transmission disease systems:

(i) *Type I vector-borne transmission disease systems*: The pathogen has a component of its life cycle outside the hosts. Examples of diseases of this kind include Amebiasis, Cryptosporidiosis and Giardiasis [14].

(ii) *Type II vector-borne transmission disease systems*: The pathogen life cycle is intrinsic to the two hosts. Examples of diseases of this type include Malaria, Chikungunya and Zika [14].

This aspect of the transmission mechanisms of infectious disease systems has been characterised but it is not enough to systematically characterise multiscale models of infectious disease systems. This thesis seeks to establish the appropriate methods for different multiscale models to give different results.

Infectious disease systems result from interactions of three subsystems namely: host, pathogen and environment [1] which have been recently termed the *epidemiological triad* [15]. Nevertheless, the traditional compartmental SIR-type models that have previously been developed focus on the transmission mechanism of pathogen for host populations without modelling the pathogen dynamics explicitly. [15]. The compartmental models of SIR type are inadequate to distinguish transmission processes at between-host scale (where the pathogen is transmitted from a vector, another host or a contaminated environment) and within-host infection process (where pathogens invade host, replicate and cause clinical symptoms). In order to address this flaw mathematical modellers have turned to a novel modelling approach called the multiscale modelling approach [1, 2, 4–6, 9, 14, 16–18]. Multiscale modelling approach involves numerous models that coupled collectively at different scales are used simultaneously to describe a complex system. In relation to multiscale modelling, a theory was recently developed that encorporates both transmission and replication called the theory of replication-transmission relativity[1].

Some of the characterisation that have been done involve the categorization of multiscale models of infectious disease systems. There are five such categories of multiscale models of infectious disease system that have been identified namely: (i) Individual-based multiscale models (IMSMs), (ii) Coupled multiscale models (CMSMs), (iii) Nested multiscale models (NMSMs), (iv) Embedded multiscale models (EMSMs), and (v) Hybrid multiscale models (HMSMs) [2]. We now highlight these categories of multiscale models that have been used to characterise these multiscale models of infectious disease systems below.

(i) *Individual-based multiscale models (IMSMs):* This category of multiscale models incorporates heterogeneity (that is to say, (i) heterogeneity in host susceptibility to infection, (ii) heterogeneity in the ability of hosts to transmit pathogens to other hosts, (iii) heterogeneity in host immune response, (iv) heterogeneity in host behaviour) into the multiscale model. However, this heterogeneity increases the burden of computation to solve the multiscale model. The main flaw of IMSMs is that even though they can describe the microscale explicitly, they are unable to describe the macroscale for each level of organisation of an infectious disease used as a level of observation. The microscale submodel results are normally converted by summing up, averaging, or carrying out some statistical analysis of them into macroscale variables for interpretation at that scale. Another advantage of implementing the IMSMs over the other categories of multiscale models (NMSMs, HMSMs, CMSMs and EMSMs) is that they require minimal mathematical expertise [4].

(ii) *Coupled multiscale models (CMSMs):* This category of multiscale models incorporates multiple levels of organisation of infectious disease system, multiple host species such as vector borne diseases, multiple pathogen species/strains, multiple communities, multiple organs. Models in this category are developed using the other four categories of multiscales (NMSMs, HMSMs, IMSMs and EMSMs) as submodels. Typical examples of coulped multiscale models include malaria in [19], Guinea worm in [20] and human onchocerciasis in [4]. The coupled multiscale models we developed by implementing either (i) a cocktail of a nested multiscale model for the host where the pathogen has a replication cycle at within-host scale and an embedded multiscale model for the host where pathogen does not have a replication cycle at within-host scale as in malaria [19] or a cocktail of embedded multiscale models where pathogen does not have replication at within-host in both hosts (human host and vector host) as in human onchocerciasis in [4].

(iii) *Nested multiscale models (NMSMs):* This category of multiscale models are developed based on the presumption that there is only unidirectional flow of information. Nested multiscale models facilitate simple reduction of the dimensions of the multiscale model, for example through slow and fast time-scale analysis, making it easier to analyze the multiscale model. An example of nested multiscale models includes HIV/AIDS in humans at host level [21]. Nested multiscale models are usually used for infectious disease systems in which the pathogen has replication cycle at the within-host scale.

(iv) *Embedded multiscale models (EMSMs):* This category of multiscale models are developed for infectious disease systems where the pathogen does not have a replication cycle at microscale. An example of these infectious disease systems is soil transmitted helminths infections such as hookworm [1]. For these infectious disease systems, the pathogen load at the within-host scale increases through super-infection (that is, repeated infection before the host recovers from an infectious phase).

(v) *Hybrid multiscale models (HMSMs):* This category of multiscale models incorporates freedom to describe the microscale and the macroscale using different mathematical representations for each level of organisation of an infectious disease system. Hence, HMSMs take the form of either NMSMs or EMSMs except that in this case the microscale and the macroscale have different mathematical formulations. Some examples of such paired formalisms include (i) deterministic/stochastic, (ii) discrete time/continuous time, (iii) ODE/PDE [4].

The characterisation of the categories of multiscale models has made major contributions in elucidating various aspects. This categorisation integrated the within-host scale and between-host scale of infectious disease systems resulting in immuno-epidemiological models. However, this is not enough to establish appropriate mathematical methods for different multiscale models of infectious disease systems.

Another aspect of infectious diseases that has been characterised in terms of the levels of organisation of infectious disease systems includes the cell level, tissue level, organ level, microecosystem level, host level, community level and macrocommunity level as indicated in Figure 1.1.

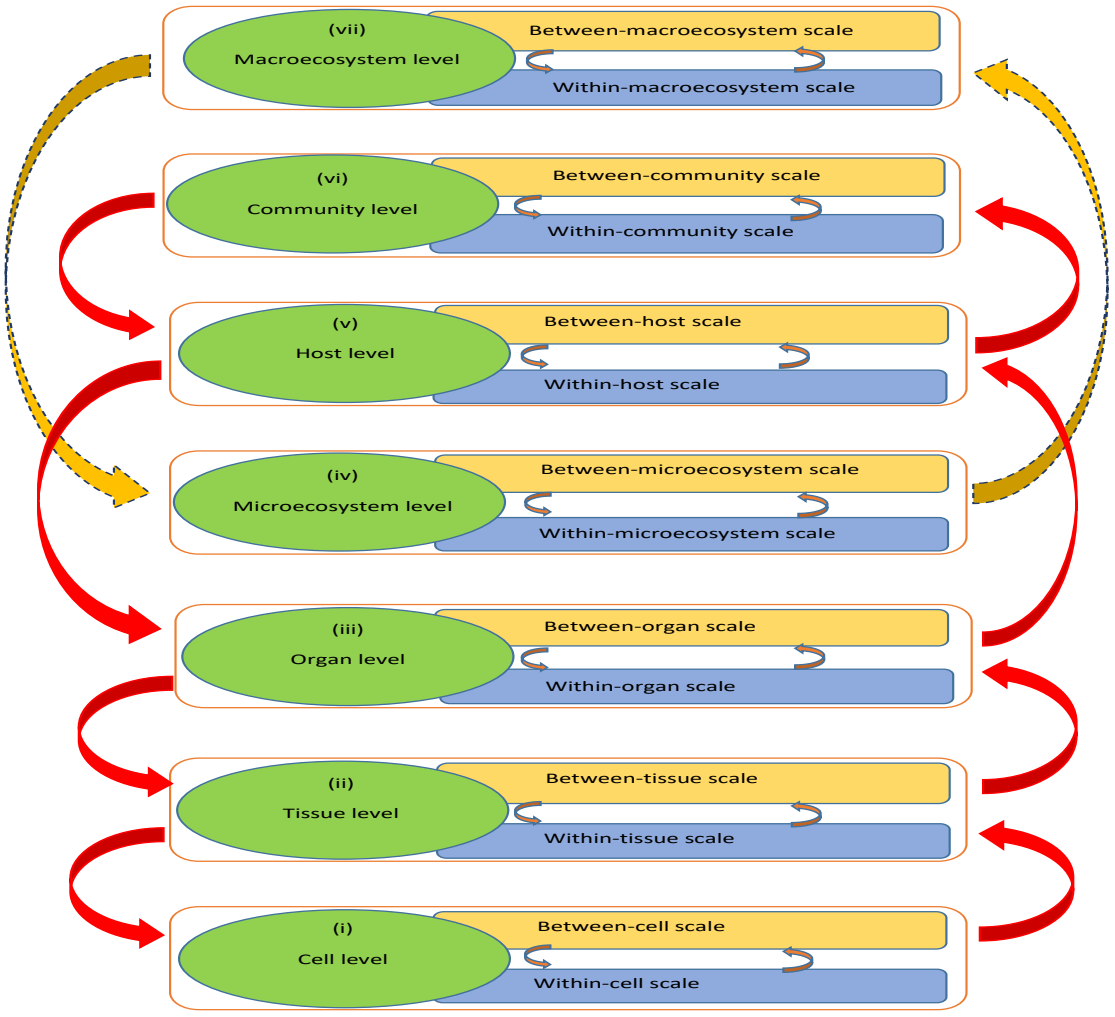

Figure 1.1: Conceptual diagram of the seven hierarchical levels of organization of an infectious disease system and the associated macroscale and microscale for each hierarchical level adopted from [1].

(a) *Cell level* consists of two scales namely: within cell as well as between cell. For levels of observation numerous cells are involved including epithelial cells in the case of FMD or red blood cells in the case of Malaria.

(b) *Tissue level* consists of two scales namely: the within tissue as well as between tissue. For levels of observation numerous forms of tissues can be examined that comprise granuloma [22] for Tuberculosis or Microabscess [23] caused by some bacterial infections.

(c) *Organ level* consists of two scales namely: within organ as well as between organ. For levels of observation numerous forms of organs can be examined that include the brain, kidney, lung, blood, stomach and heart [1].

(d) *Microecosystem level* consists of two scales namely: the within-micro ecosystem scale (microscale) and the between-microecosystem scale (macroscale). At this level we develop models of the evolution as well as the ecology disease systems [4].

(e) *Host level* contains two scales namely: within host as well as between host scale. When formulating multiscale models of infectious disease dynamics numerous hosts can be examined that include vertebrate host in the case of humans and vector host in the case of mosquitoes. In order to formulate the multiscale models of infectious disease systems at this level of organization we use the host level as the level of multiscale observation [1].

(f) *Community level* consists of two scales namely: within community as well as between-community. For levels of observation different forms of communities are used that include districts, provinces and countries.

(g) *Macroecosystem level* consists of three fundamental sub-levels including local community, national and regional level. Each of the sub-levels can be regarded as an ecosystem [4].

This aspect of multiscale models has been characterised to give new insights on infectious disease systems. However, there is need to establish the methods that are appropriate to extend the various multiscale models to higher levels for example, from host level to community level. Furthermore, there is need to group these levels of organisation to three levels in order to characterise the multiscale models.

These levels of organisation of multiscale models can be further grouped into three levels namely: primary level, secondary level and tertiary level. The traditional ODEs have been used to model direct transmission of pathogen at cell level, tissue level or host level of infectious disease systems. Multiscale models of infectious disease systems can be characterised to establish some aspects that enable well informed decision making and implementation of various interventions.

1.2 Characterisation of multiscale models

This thesis chacterises multiscale models. There are certain aspects that arise when we consider various levels of organisation of infectious disease systems. These levels of organisation can be grouped into three main levels namely: primary level, secondary level and tertiary level of multiscale cycle.

(i) *Primary level of multiscale cycle:* This level constitutes the cell level, tissue level and host level. There is strictly local exchange of pathogen or local transmission. The transmission can be direct transmission which occurs when there is direct contact between an infected cell/tissue/host and a susceptible cell/tissue/host or the transmission can be environmental transmission which occurs when there is contact between the pathogen and a susceptible cell/tissue/host. At the primary levels of multiscale observation the pathogens transmitted are either single pathogen species or single pathogen strain at single community.

(ii) *Secondary level of multiscale cycle:* This level constitutes the microcommunity level and macrocommunity level. At organ level, the within-organ level constitutes local transmission similar to the primary level, that is, direct transmission or environmental transmission which can be modelled using Ordinary differential equations (ODEs). However, at between-organ it is difficult to represent direct contact between organs. Therefore the pathogen is moved through blood to other organs. This transport of blood is global transmission which can be modelled using graph-theoretic approach. At community level, the within-community level constitutes local transmission as in the primary level which is through direct contact. Therefore, the ODEs are used to model this local transmission or local exchange of pathogen. However, at between-community level it is difficult to represent the contact of communities directly. Therefore, individuals have to move between communities and this is how contact is achieved at community level. This movement of individuals is global transmission or global exchange of pathogen. This global transmission can be represented using graph-theoretic approach. My thesis wants to characterise this aspect which has not been investigated before to establish when it is appropriate to use graph-theoretic methods. At the secondary level of multiscale observation the pathogens transmitted are single pathogen species or single pathogen strains at multiple communities. Therefore, when we consider only one community then we have strictly local transmission at primary level.

(iii) *Tertiary level of multiscale cycle:* This level constitutes the microecosystem level and macroecosystem level. The transmission occurs in a single community as at the primary level of multiscale observation or in multiple communities as at the secondary level of multiscale observation. In other words, in a single community there is direct contact between infectedes and susceptibles resulting in local transmission or local exchange of pathogen as at primary level. This local transmission or local exchange of pathogen is represented by ODE methods. However, in the case of multiple communities there is movement of individuals between the communities which describes global transmission or global exchange of pathogen. This movement is represented by implementing graph-theoretic approach. This is a new idea that has not been investigated before and my thesis wants to characterise this aspect to establish when it is appropriate to use graph-theoretic methods. The only difference between the tertiary level of multiscale observation and other levels is that at the tertiary level of multiscale observation there are multiple pathogen species or multiple host species whereas the primary level of multiscale observation and the secondary level of multiscale observation have single pathogen species or single host species.

A study was conducted to characterise patterns of sexual contacts in Britain and Zimbabwe [24]. In Britain, the dynamics of an STI like HIV was restricted to people with risk behaviours (prostitutes). The population of prostitutes tends to be much smaller than the general population in any location. This means that there was a sexual contact network with a few nodes (prostitutes) having many connections (high degree distribution) whereas the majority of nodes had few connections. However, a key aspect that was not addressed is that these nodes could be cells, tissues or whole organisms at primary level that are directly transmitting pathogen (local transmission). Therefore, there is need to investigate if this can

be extended to community level to describe global transmission. This is a new idea that has not been addressed before and is investigated in chapter 2 and chapter 5.

In [25], a study was conducted to characterise the dynamics of FMD in pigs. Furthermore, in [7], a model was formulated to investigate the dynamics of the FMDV in cattle. The transmission mechanism of both these models were single scale, that is, local transmission. However, a key aspect that was not addressed is that at the primary level we have cells level, tissues level or whole organisms level that are directly transmitting pathogen (local transmission). Therefore, there is need to investigate if this can be extended to community level to describe global transmission. This is a new idea that has not been addressed before and is investigated in chapter 3.

In[26], a model was developed to characterise the impact of the movement of people on the burden of Malaria disease. In order to illustrate the transmission dynamics of Malaria between various patches an SIR model was formulated. It is important to note that the transmission mechanism in that model was global transmission or global exchange of pathogen. However, an aspect that was not addressed is that there are two transmission modes at the community level namely: local transmission and global transmission. Within the community there is exchange of pathogen when infected cells/tissues/hosts are in direct contact with susceptible cells/tissues/hosts or when the pathogen is in direct contact with susceptible cells/tissues/hosts. This local transmission is modelled using ODEs methods. At between-community level there is movement of infected individuals between the communities resulting in global transmission or global exchange of pathogen. This movement of infected individuals is modelled using graph-theoretic methods. This is a new aspect that has not been addressed and it is investigated in chapter 4 and chapter 6. Furthermore, this community level can be extended to macroecosystem level when there are multiple pathogen species or multiple pathogen strains. This is a new idea that has not been investigated before.

1.3 Classification of individual-based network modelling multiscale models

We have already stated the five categories of multiscale models for disease dynamics which include Coupled, Nested, Individual-based, Embedded and Hybrid multiscale models [2]. Individual-based multiscale models are further classified into four classes namely: Hybrid, Simulation, Network and Empirical data modelling individual-based multiscale models [2, 18]. Network models can formulated through various network modelling techniques that include lattice, random, small-world, spatial, and scale-free [27]. Below are the five network-based techniques:

(i) Lattice networks are characterised by high clustering (due to the localized nature of connections) and long path lengths [28], and can be one-dimensional to form rings or two-dimensional to form grids [29]. Disease spread is considered to be slowest on regular lattices than on the other networks [29]. The main advantage of using a lattice network is that it naturally takes into account spatial separation of sites [30].

(ii) Random networks can be identified by short path length as well as low clustering [28]. Epidemics on random networks spread faster than the other networks except scale-free networks where pathogen spread is extremely rapid [29].

(iii) Small-world networks can be identified by short path lengths as well as high clustering [28]. They are generated from regular lattices by rewiring the edges described in [31], where each edge has a probability of being reconnected to a different vertex [29]. Due to high clustering the majority of infections occur locally [27].

(iv) Scale-free networks- Epidemic spread is considered to be fastest on scale-free networks [29] compared to other networks. These networks can be identified by a power-law decay formed due to preferential attachment [24, 32], that is, linking to the most highly connected existing nodes. A variety of social, biological and communication systems [33–35] have been adequately described by some complex networks where nodes represent individuals (computers) and links show interactions among them, for example, internet and world-wide-web [36, 37].

(v) Spatial networks are considered to be one of the most flexible forms of networks on which it is possible to formulate a variety of other networks [27]. The strength of infection depends on the geographical distance between two individuals or nodes.

This aspect of multiscale models has been characterised by outlining various features of network-based models [27, 36, 37]. However, there is need to establish when it is appropriate to use the graph-theoretic approach. This issue is addressed in this thesis.

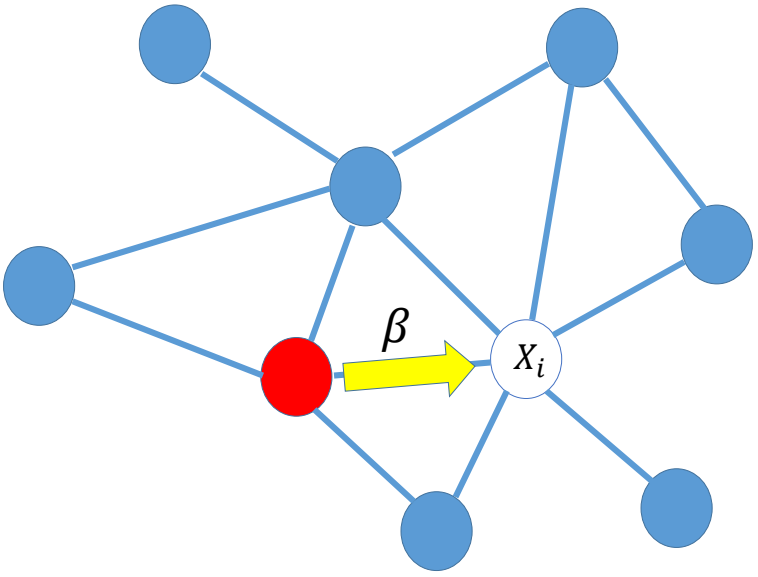

Figure 1.2: The diagram represents the dynamics of infectious disease systems like Foot-and-Mouth disease or Malaria at macrocommunity-level. At macrocommunity-level the communities are considered as patches and there is exchange of pathogen between the communities through global transmission (transport) of infection.

Figure 1.2 represents the dynamics of infectious disease systems like Foot-and-Mouth disease or Malaria at macrocommunity-level. At macrocommunity-level the communities are considered as patches and there is exchange of pathogen between the communities through global transmission (transport) of infection.

1.4 Stability Theory of Differential Equations

Stability theory of differential equations has been implemented to characterise numerous aspects of infectious disease systems. Stability theory addresses the stability of solutions of differential equations and of trajectories of dynamical systems under small perturbations of initial conditions [38]. The heat equation, for example, is a stable partial differential equation because small perturbations of initial data lead to small variations in temperature at a later time as a result of the maximum principle. Stability theory of differential equations was explored by LaSalle who implemented nonautonomous systems for Lyapunov functions to establish their stability [39]. However, there were challenges encountered in the analysis of stability using Lyapunov's direct approach [40]. One of the main problems with using the Lyapunov theory is developing a suitable Lyapunov function. These difficulties were resolved with the application of the fixed point theory. The ideas of stability can be classified into various groups which include Lyapunov stability, Poincare stability and Laplace stability. In the case of Laplace stability, a system is considered to be stable if all the solutions of the differential equations are bounded as time t goes to infinity. In the case of Lyapunov stability, solutions which are initially close together should always remain close together in the future as functions of time [41, 42]. In the case of Poincare stability, a trajectory Ω is stable (orbital stability) if neighbouring half paths which are once near Ω will remain near Ω. The Center manifold theory simplifies dynamical systems to reduce the dimensions of the system, at least near equilibria [43]. The use of center manifold theorem ensures the local stability of the endemic equilibrium of disease systems [44–48]. Furthermore, the theorem establishes the existence of backward bifurcation in the dynamical system. Birfucation theory addresses the changes of behaviour of dynamical systems due to perturbation of some parameters of these dynamical systems [49, 50].

1.5 Stochastic Differential Equations

Stochastic differential equations have been used previous to characterise different aspects of infectious disease dynamics. A stochastic differential equation (SDE) is a differential equation in which one or more of the terms is a stochastic process, that results in a solution which is also a stochastic process. Stochastic differential equations are used to model various phenomena such as stock prices or physical systems subject to thermal fluctuations [51]. Usually, SDEs have a variable which describes random white noise calculated as the derivative of Brownian motion or the Wiener process. However, other types of random behaviour are possible, such as jump processes [51, 52]. SDEs have been used in the study of numerous infectious disease systems to incorporate the randomness effect of infection dynamics due to the random white noise [53–56].

1.6 Numerical Simulation Method

Numerical simulation methods have been used to characterise some features of infectious disease dynamics. Numerical simulation methods can be implemented when analytical methods cannot be used to establish the solutions of a dynamical system. Examples of numerical simulation methods for ordinary differential equations include Euler's method, Backward Euler method, Trapezoidal method, Taylor method and Runge-Kutta method [57, 58]. Numerical simulation methods for stochastic differential equations include Monte Carlo simulation method, Euler-Maruyama method and Milstein method [59–63]. The simplest numerical method for solving the initial value problem is the Euler's method. Euler's method is not an efficient numerical method, however, numerous ideas centred on numerical solutions of differential equations are introduced using this approach. The Backward Euler method is similar to Euler's method in that it is of first order accuracy, however, the main difference between the two methods is that Euler's method uses forward difference approximation where as the Backward Euler's method uses backward difference approximation. The main setback of both the Euler method and the backward Euler method is the low convergence order. The Trapezoidal method has a higher convergence order and is useful in solving initial value problems. The Taylor method is conceptually simpler to work with, however, it is tedious and time-consuming to have to calculate the higher-order derivatives. In order to avoid the need for the higher-order derivatives, the Runge-Kutta methods evaluate the function at more points, at the same time attempting to maintain the accuracy of the Taylor approximation. Monte Carlo simulation methods are numerical methods in which random numbers are implemented to perform computational experiments. The numerical solutions of stochastic differential equations can be observed as a kind of Monte Carlo calculation in which the entire system is simulated many times. The Euler-Maruyama method is one of the simplest numerical approximations for the stochastic differential equation. This is achieved when we truncate Ito's formula of the stochastic Taylor series after the first order terms. Another numerical approximation method for stochastic differential equations is the Milstein method. We obtain the Milstein method if we truncate the stochastic Taylor series after second order terms. In this study we implemented the Milstein method for the numerical simulation of SDEs and the fourth order Runge-Kutta method for the numerical simulation of Ordinary differential equations.

1.7 Mathematical models of infectious disease systems

Numerous models have been developed over the years to characterise different aspects of infectious disease systems. Spatial explicit models were characterised to provide a good description of cholera epidemics [10]. In [10], transmission was mediated by water, hence direct contacts between individuals were less important for disease transmission, where as a crucial role was played by spatial connectivity. The analysis proposed in this paper was based on spatially explicit models that explicitly account for the environmental matrix along which the disease can spread (e.g. river networks and water reservoirs). Nodes represented water reservoirs and human communities (cities, towns and villages) in which the disease

can grow. The edges represented links between the communities, typically hydrological links. An extension of the study was done by [64] were they took into account long-distance dissemination of the pathogen Vibrio cholerae due to host mobility. Other models have been characterised incorporating the optimal control of numerous infectious disease systems like Malaria and Ebola virus [65–68]. Complex networks were characterised to model communication systems [53]. Epidemics on the internet [69] have become more diverse [70] and include computer viruses and computer worms [71]. The internet can be considered as a high traffic network in which data sources and sinks are interconnected by a network routers. The scale-free network was characterised on telephone network traffic to model the behaviour of telephone users [72]. Each user had a fixed set of acquaitances with whom the user may communicate, and the number of acquaintances followed a power-law distribution. The vanishing epidemic threshold for viruses spreading on scale-free networks showed that traditional methods applied to reduce a virus spreading rate cannot succeed in eradicating an epidemic [73]. Bias was placed on curing or vaccinating the highly connected nodes (hubs) which can restore a finite epidemic threshold and eradicate or control a virus [74]. Many diseases required 80% - 100% immunization. Similarly for internet, in order to stop computer viruses required almost 100% immunization [74]. Spatial models were characterised to represent spreading patterns of infectious diseases involving human mobility [75] in the airline transportation [9]. Multi-scale networks obtained here were integrated into the global epidemic and mobility (GLEaM) model, a computational platform that uses a metapopulation stochastic model on a global scale to simulate the large-scale spreading of influenza-like illnesses [11, 76]. It can be noted that the global epidemic behavior was governed by the long-range airline traffic that determines the arrival of infectious individuals on a worldwide scale [12]. However, at the local level, the short-range epidemic coupling induced by commuting flows created a synchrony between neighboring regions and a local diffusive pattern with the epidemic flowing from subpopulations with major hubs into the neighboring subpopulations [77]. These results clearly showed that the level of detail on the mobility networks can be chosen according to the scale of interest. There are numerous models that have been characterised in order to control and eliminate the spread of Foot-and-Mouth disease over the years [78]. In [25], a study was carried out to investigate the early viral dynamics of foot-and-mouth disease within infected pigs. A within-host model was developed to investigate whether individual variation can be explained by the effect of the initial dose of foot-and-mouth disease virus. In [7], a within-host model was developed to investigate the within-host dynamics of the foot-and-mouth disease virus in cattle using previously published data. The transmission mechanism for both these models were single scale, that is, local transmission. In [79], a stochastic farm-based model was characterised in France and depended upon the spatial distance between the numerous farms in that country, on species of animals and the animal farm's status at any particular day. Simulations of the model under study showed local disease transmission when movement of animals was limited. The other control strategies put in place were culling and vaccination. In [80], a mathematical modelling framework was characterised based on geographically aligned data sources and with appropriate flexibility that partitions the modelling of disease spread into two distinct but coupled levels. First was a top-level stochastic simulation with patches (or nodes) interacting via a contact network defined on a lattice consisting of all short- and long-distance interactions [81] relevant for disease transmission. Within each node was a "hidden"

second level, internal to a patch, where disease spread followed the standard mean-field SIR-like ordinary differential equations. They made use of U.S. county-level aggregated data on animal populations and parameters from literature to simulate epidemic spread of two different animal diseases agents: foot-and-mouth disease and highly pathogenic avian influenza. The mitigation strategies evaluated were quarantine, culling and movement controls. However, the overall efficacy of mitigation and movement controls was largely uncertain. Geography and the spatial clustering of animals [82] even at a regional level are key to consider for developing mitigation strategies and applying available resources. In [83], an event-driven multiscale network-based hybrid model was characterised that used a deterministic equation-based model (EBM) to model within-herd spread of foot-and-mouth disease and a stochastic, spatially-explicit agent-based model (ABM) to model between-herd spread and control. The meta-population under investigation was heterogeneous, thereby indicating the multiple species of domestic cloven-hoofed animals that are susceptible to foot-and-mouth disease. The network through which the meta-population sites could be linked was multi-layered, thereby indicating how foot-and-mouth disease spreads via direct contact, indirect contact and aerosols [84]. In [85], a model was characterised based on the Ross-Macdonald model taking into account the rate of immigration and emigration of humans among Q patches. This model explored the way that prevalence and reproduction number (the two important measures of mosquito-borne pathogen transmission) display a complex non-monotonic relationship as a result of spatial heterogeneity in mosquito density and human mobility. The heterogeneity in mosquito density and mosquito bionomic patterns affecting vectorial capacity drive spatially heterogeneous bitting patterns, while human mobility connected isolated areas that can have very different mosquito populations. Results suggested that the relationship between reproduction number and prevalence was intertwined with the interaction between host movement and the degree of spatial heterogeneity in a region. Furthermore, transmission heterogeneity generally promotes persistence in host-parasite systems. In [86], a model was characterised to investigate the efficacy of border screening and local level disease control in the presence of human migrations during an epidemic. Results showed that when border screening fails, then other control measures can be implemented that include treating or isolating infectious people and controlling the mosquito population. Furthermore, the conditions of the efficacy of border screening and local treatment in each settlement were established. In [19], a coupled multiscale model was characterised with the aim of informing policy and guide malaria control and elimination. The formulation of this model was based on the integration of four submodels into a single coupled multiscale model. The model described the mechanics of malaria transmission in terms of the major components of the complete malaria parasite life-cycle. In [26], a model was characterised to assess the impact of human mobility on the burden of malaria disease in South Sudan. an SIR-type model was formulated that describes the transmission dynamics of malaria disease between multiple patches. The model developed was a system of stochastic differential equations consisting of ordinary differential equations perturbed by a stochastic Wiener process. Results showed that the disease tends to persist in the low transmission patches when there is human inflow in these patches.

To the best of my knowledge there is no model that was characterised to establish when is it appropriate to implement the graph-theoretic methods. Furthermore, There is no model that has been characterised that

established the mathematical methods that enable multiscale models to be extended to higher levels.

Modellers have understood how to implement graph-theoretic methods as well as ODE methods. However, they have not been able to establish when it is appropriate to use graph-theoretic methods. This is the major aspect of characterization that we are investigating in this thesis which has not been done before. An advantage of this characterisation is that when we make these distinctions between local transmission and global transmission then we are able to implement interventions targeted torwards global transmission such as travel restrictions to prevent global transmission. On the other hand, the interventions targeted torwards local transmission include wearing of masks and sanitizing (in case of Coronavirus). Therefore, this study is seeking to address these aspects and we implement Foot-and-Mouth disease and Malaria disease as examples.

1.8 Research Limitation

The models used in this study offer insights into the multiscale character of infectious disease dynamics, however, there are some notable limitations of these models. The use of Individual-based multiscale models in this study incorporates heterogeneity (for example, heterogeneity in host susceptibility to infection, heterogeneity in the ability of hosts to transmit pathogens to other hosts and heterogeneity in host immune response) into the multiscale models. However, the incorporation of heterogeneity into the multiscale model comes at the cost of increased computational burden in solving the multiscale model. The major weakness of Individual-based multiscale models is that although they can represent the microscale explicitly, they do not explicitly represent the macroscale for each level of organization of an infectious disease used as the level of multiscale observation in the development of the multiscale models. Furthermore, the bifurcation analysis in multi-patch models for the entire population is difficult to perform because for each patch i there is a corresponding reproduction number $\mathcal{R}_{0i}$. However, the overall $\mathcal{R}_0$ for the entire population cannot be used explicitly to perform the bifurcation analysis.

1.9 Problem Statement

Multiscale models have been characterised to address various aspects of infectious disease systems. These infectious diseases are a serious challenge on humans and animals across the world with the greatest impact being in developing countries. In most developing countries where livestock and crop production are important for subsistence agriculture, outbreaks of infectious diseases have severe impact on economic growth and food security. Amongst these diseases is Foot and Mouth disease [87]. A body of literature indicates that globally, FMD has caused major losses in the economic sector (agriculture in particular) as well as tourism [88]. On the other hand, Malaria is amongst the most severe public health problems globally [89]. The majority of all malaria cases come from sub-Saharan Africa and over $12 billion is used annually on malaria in Africa. Researchers have established the basis of ordinary differential equation

methods and also graph-theoretic methods. However, they have not established when it is appropriate to use these mathematical methods for the multiscale models.

The implementation of mathematical models has been essential to acquire understanding of numerous features of infectious diseases, particularly foot-and-mouth disease and malaria. This understanding gained can help us to implement intervention measures. Present modelling frameworks established from compartmentalizing hosts into SIRS type models (and their variations) and graph-theoretic methods have been used to give insights of local transmission mechanisms and global transmission mechanisms of FMD and Malaria separately. However, to the best of my knowledge there is no model that has been characterised which establishes when it is appropriate to use graph theoretic methods for various multiscale models. The latest work that has been done which is more appropriate in modelling the progression of infectious disease systems based on replication-transmission relativity theory is the multiscale modelling appproach. The multiscale modelling of global transmission mechanisms of infectious diseases is better achieved through the use of graph theoretic methods while the standard SIR models address the local transmission mechanisms. Furthermore, this study establishes the mathematical methods that make it possible for multiscale models to be extended to higher levels of organisation. The mathematical framework we propose characterises the local transmission and global transmission mechanisms of infectious disease dynamics. Our main ideas are centred on developing a multiscale modelling approach in tandem with graph theoretic methods at different levels of organisation. Nodes represent communities (geographical distant locations) while possible transmission of pathogen (transport of infected individuals) is represented by edges. Finally, in this study, we seek to establish when it is appropriate to use particular mathematical methods for different multiscale models.

1.10 Aim and Objectives of study

The main aim of the study is to characterise multiscale models in order to establish appropriate mathematical methods for these multiscale models at different levels of organisation.

The main objectives of this study are to:

- characterise a host-level individual-based multi-scale network model of directly transmitted viral diseases with special consideration to Foot-and-Mouth disease.
- characterise a host-level differential equation average-based model of directly transmitted viral diseases with application to FMD. The within-cattle submodel is unidirectionally coupled to the between-cattle transmission dynamics submodel.
- characterise a macrocommunity-level multiscale multi-patch model for FMD extended from the host-level average-based model.

- characterise a whole organism-level multiscale model of a vector-borne diseases with application to Malaria infection.
- characterise a macrocommunity-level multiscale multi-patch model of a vector-borne disease with special consideration to Malaria.

1.11 Stucture of the Study

The thesis is structured as follows.

(i) In **Chapter** 2, we characterise the spread of the Foot-and-Mouth disease virus taking into account both the dynamics of Foot-and-Mouth disease viral growth at within-host scale (microscale) and the interactions (direct contact) between individuals at between-host scale (macroscale). We implement an individual-based network modelling multiscale model of Foot-and-Mouth disease at host-level and establish if this model can be extended to higher levels using graph-theoretic methods.

(ii) In **Chapter** 3, we characterise the spread of the Foot-and-Mouth disease virus taking into account both the dynamics of Foot-and-Mouth disease viral growth at within-host scale (microscale) and the interactions (direct contact) between individuals at between-host scale (macroscale). We implement a nested modelling multiscale model approach of Foot-and-Mouth disease at host-level and establish if this model can be extended to higher levels using graph-theoretic methods.

(iii) In **Chapter** 4, we characterise the spread of the Foot-and-Mouth disease taking into account both the dynamics of Foot-and-Mouth disease at within-community scale (microscale) and the interactions (direct contact) between communities at between-community scale (macroscale). We implement a nested modelling multiscale model of Foot-and-Mouth disease from **Chapter** 3 together with graph theoretic method at community-level and establish if this model can be further extended to higher levels of organisation using graph-theoretic methods.

(iv) In **Chapter** 5, we characterise the spread of Malaria disease taking into account both the dynamics of plasmodium parasite at within- whole organism scale (microscale) and the interactions (direct contact) between whole organism at between-whole organism scale (macroscale). We implement an individual-based network modelling multiscale model of Malaria disease at whole organism-level and establish if this model can be extended to higher levels of organisation using graph-theoretic methods.

(v) In **Chapter** 6, we characterise the spread of Malaria disease taking into account both the dynamics of Malaria disease at within-community scale (microscale) and the interactions (direct contact) between communities at between-community scale (macroscale). We implement a coupled modelling multiscale model of Malaria disease together with graph theoretic method at community-level and establish if this model can be extended to higher levels of organisation using graph-theoretic methods.

(vi) In **Chapter**, 7 we give conclusions and directions for future research.

Chapter 2

Host-level Multiscale Network-based model for Foot-and-Mouth disease in the cattle population

2.1 Introduction

The study of infectious disease dynamics at each hierarchical level of organisation has made enormous contributions in grasping, hypothesizing and interpreting the dynamics of numerous infectious diseases. The implementation of multiscale models enables us to express infectious disease systems at different scales giving new insights into the dynamics of these infectious disease systems [1, 2, 4, 14, 17, 18]. This chapter seeks to establish whether the model we present can be extended to a higher level (community level) since this is a critical level for the control and eradication of infectious diseases. We characterise this multiscale model by investigating some aspects that distinguish multiscale models of infectious disease systems. We formulate an individual-based network modelling multiscale model for directly-transmitted disease systems at host-level using network modelling techniques. The model we develop characterises the spread of Foot-and-Mouth disease virus taking into account both the dynamics of Foot-and-Mouth disease viral growth at within-host scale (microscale) and the interactions between individuals at between-host scale (macroscale). Therefore, we investigate the impact of the variation in transmission of Foot-and-Mouth disease virus both at within-cattle scale and between-cattle scale.

Foot-and-Mouth disease is a viral disease caused by a virus called Foot-and-Mouth disease virus. It affects animals with cloven-hoofs like cattle as well as certain wildlife animals. The fundamental varieties

of the virus include SAT1, SAT2, SAT3, O, C, A and Asia1. The various transmission routes include air-borne spread, animal-to-animal contact and contamination of the environment [90]. In cattle FMDV usually gains entry through the epithelial cells of the respiratory tract. FMDV is able to replicate rapidly in the tissues of the upper respiratory system making it a site of persistence [91]. Early upon infection there is detectible antibody response (IgA, IgM and IgG) in the secretion of the upper respiratory tract [92]. Spread of Foot-and-Mouth disease virus between cattle and between pigs is usually rapid so that frequently 90% of the animals may be showing signs [93]. The latent period varies between 2 and 14 days. The formation of painful blisters in epithelial sites of the mouth as well as on the feet can result in debilitation of the animal. Typical control measures of foot-and-mouth disease include movement restriction; quarantine; vaccination; educational awareness and culling of detected infected animals [94]. Vaccination is increasingly being accepted as a far-reaching tool in controlling FMD [95, 96]. Different approaches to manage FMD have been developed depending on the stage of the disease [97]. Laboratory diagnosis of any suspected case of FMD includes virus isolation, genome identification techniques such as polymerase chain reaction (PCR) assays and serological tests such as the virus neutralization test. There is no specific treatment for FMD, however available treatment includes mouth washing with sodium bicarbonate, foot washing with copper sulphate as well as antibiotics for lesions. Vaccination of ruminants may stop disease but may not stop infection hence vaccines have being used as a second line of defence [93]. There are presently only three interventions practiced in sub-Saharan Africa against FMD [98]. Within Africa FMD is considered to be the sole most paramount animal disease having a negative impact on trade [98]. Morbidity is high and mortality is very low, although high mortality of young stock can occur [99]. This disease is an environmentally-transmitted disease that is important to both domestic and wildlife livestock and has been reported both locally and globally.

2.2 The mathematical model

The formulation of this model involves differential equations illustrating the initial transmission of FMDV taking into account immune response and then placing the cattle population in a spatial network. Earlier work was done by Howey [7], who investigated the dynamics of this disease in cattle. For each individual i there is interplay between antibody, A_i, virions in blood, V_i, interferon, I_i, uninfected epithelial cells, U_i, infected epithelial cells, F_i, non-infectious material denoted by J_i, virus-antibody complexes, C_i and protected cells, P_i. Given below is the set of differential equations:

$$
\begin{aligned}
\frac{dV_i}{dt} &= \zeta F_i - \phi_A \omega V_i + \sum_{i=1, i\neq j}^{n} \beta_{ij} V_j, \ .....(1) \\
\frac{dF_i}{dt} &= \epsilon U_i V_i - \zeta F_i, \ .....(2) \\
\frac{dU_i}{dt} &= -\kappa U_i \left(I_i - \frac{\mu}{\xi} \right), \ .....(3) \\
\frac{dP_i}{dt} &= \kappa U_i \left(I_i - \frac{\mu}{\xi} \right), \ .....(4) \\
\frac{dI_i}{dt} &= \mu - \xi I_i + \phi_U(U) \eta C_i, \ .....(5) \\
\frac{dA_i}{dt} &= \phi_V(V, J) \phi_A, \ .....(6) \\
\frac{dC_i}{dt} &= \phi_A \omega (V_i + J_i) - \sigma C_i, \ .....(7) \\
\frac{dJ_i}{dt} &= \gamma \zeta F_i - \phi_A \omega J_i \ .....(8)
\end{aligned}
\tag{2.2.1}
$$

where

$$\beta_{ij} = \beta \left(1 - \delta_{ij}\right) e^{-\alpha |i-j|},$$

δ_{ij} is Kronecker's delta, β and α are non-negative. Small values of α implies a widespread influence of infection while bigger values of α implies local spread. The elements β_{ji} of the transmission matrix **B**, representing the strength of transmission from j to i depend on spatial factors. β represents the overfall strength of transmission [100]. All the parameters in the multiscale model system (2.2.1) are constant. We consider non-negative initial conditions $\{V_i(0) \geq 0, F_i(0) \geq 0, U_i(0) \geq 0, P_i(0) \geq 0, I_i(0) \geq 0, A_i(0) \geq 0, C_i(0) \geq 0, J_i(0) \geq 0\}\ \forall t \geq 0, i = 1, ..., n$. Furthermore, $\phi_U(U) = 1$ whenever $U \geq 0.01$ and $\phi_U(U) = 0$ otherwise; $V_i(t) = 0$ for t in $[0, \tau)$ and $V_i(\tau) = 1$ (τ being the time at which virus replication is observable); $\phi_V(V, J) = 1$ whenever $V + J \leq 0.1$ and $\phi_V(V, J) = 0$ otherwise. The antibody is modelled by ϕ_A due to initial abundance of virus so that produced antibody is immediately used and the levels do not increase until the virus is sufficiently cleared.

Equation 1 of model (2.2.1) represents the concentration of infectious virion in blood. The first term on the right hand side represents the infected epithelial cells that burst to release more infectious virion in the blood. The second term is the infectious virion cleared as it complexes with antibody. The third term describes the rate of growth of the viral population due to external sources of the virus. The Equation 2 of model (2.2.1) represents the infected epithelial cells created at a rate of ϵ. The last part of Equation 2 is the infected epithelial cells which burst to become infectious virion. Equation 3 of model (2.2.1) represents proportion of the uninfected epithelial cells that become protected by interferon from infection when interferon is above background level, μ/ξ. Equation 4 of model (2.2.1) represents the proportion of protected epithelial cells. These cells are recruited from uninfected cells when interferon is above background level, μ/ξ. Equation 5 of model (2.2.1) represents interferon which is produced at rate, η, corresponding to the virus-antibody complexes, C. Equation 6 of model (2.2.1) represents antibody production in relation to the virus that must be neutralized. Equation 7 of model (2.2.1) represents infectious virion and non-infectious material that has been neutralized by antibody. The last part of Equation 7 is the clearance of

viral-antibody complex. In Equation 8 of model (2.2.1) the first part is the recruitment of non-infectious material from infected cells. The second part is the non-infectious material that is neutralized by antibody.

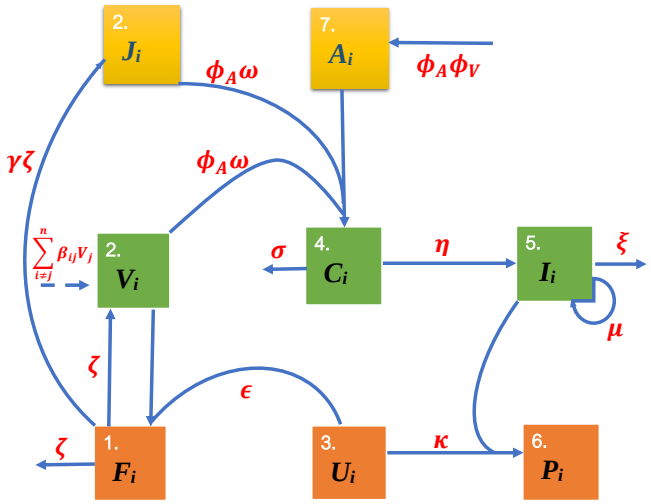

Figure 2.1: Schematic diagram of foot-and-mouth disease dynamics in a network. For each individual i there is interplay between antibody, A_i, virions in blood, V_i, interferon, I_i, uninfected epithelial cells, U_i, infected epithelial cells, F_i, non-infectious material denoted by J_i, virus-antibody complexes, C_i and protected cells, P_i.

Table 2.1: Description of individual-based model variables for the ith individual.

Variable	Description	Units	Initial value
F_i	Infected cells	TCID_{50} ml^{-1}	0
C_i	Virus-antibody complexes	TCID_{50} ml^{-1} equiv.	0
P_i	Protected cells	Cell	0
U_i	Uninfected cells	Cell	1
A_i	Antibody	LPBE-titre	0
V_i	Conc. of virions in blood	TCID_{50} ml^{-1}	0
J_i	Non-infectious material	TCID_{50} ml^{-1} equiv.	0
I_i	Interferon	IU ml^{-1}	$\frac{\mu}{\xi}$

2.2.1 Feasible region of the model

The model that we formulate has to be biologically meaningful. Therefore, we establish the non-negativity and boundedness of all the state variables as well as their solutions, respectively, in the region Φ, where

$$\Phi = \left\{(U_i, V_i, F_i, P_i, I_i, A_i, C_i, J_i) \in \mathbb{R}_+^8\right\}, i = 1, .., n \tag{2.2.1}$$

2.2.1.1 Positivity of solutions

Theorem 2.1. *A non-negative solution* $(V_i(t), F_i(t), U_i(t), P_i(t), I_i(t), A_i(t), C_i(t), J_i(t))$ *exists for all* $t \geq 0$

Proof. The positivity of solutions of the multiscale model system (2.2.1) is proved using the integrating factor technique. We consider (1) in the multiscale model system (2.2.1)

$$\frac{dV_i}{dt} = \vartheta F_i - \phi_A \omega V_i + \sum_{i=1, i\neq j}^{n} \beta_{ij} V_j \tag{2.2.2}$$

We re-write (2.2.2) as follows

$$\frac{dV_i}{dt} + \phi_A \omega V_i = \vartheta F_i + \sum_{i=1, i\neq j}^{n} \beta_{ij} V_j \tag{2.2.3}$$

The integrating factor for (2.2.3) is

$$\text{Integrating factor (IF)} = e^{\int_0^t \phi_A \omega ds} = e^{\phi_A \omega t} \tag{2.2.4}$$

When we multiply (2.2.3) by the integrating factor $e^{\phi_A \omega t}$ to get

$$e^{\phi_A \omega t}\frac{dV_i}{dt} + e^{\phi_A \omega t}\phi_A \omega V_i = e^{\phi_A \omega t}\left(\vartheta F_i + \sum_{i=1, i\neq j}^{n} \beta_{ij} V_j\right) \tag{2.2.5}$$

From the product rule we obtain

$$\frac{d}{dt}(e^{\phi_A \omega t}.V_i) = e^{\phi_A \omega t}\left(\vartheta F_i + \sum_{i=1, i\neq j}^{n} \beta_{ij} V_j\right) \tag{2.2.6}$$

We integrate both sides of (2.2.6) with respect to t and obtain

$$e^{\phi_A \omega t}.V_i(t) = e^{\phi_A \omega (0)}.V_i(0) + \int_0^t e^{\phi_A \omega s}\left(\vartheta F_i(s) + \sum_{i=1, i\neq j}^{n} \beta_{ij} V_j(s)\right) ds \tag{2.2.7}$$

Dividing both sides of (2.2.7) by the integrating factor $e^{\phi_A \omega t}$ we get

$$V_i(t) = e^{-\phi_A \omega t}.\left[V_i(0) + \int_0^t e^{\phi_A \omega s}\left(\vartheta F_i(s) + \sum_{i=1, i\neq j}^{n} \beta_{ij} V_j(s)\right) ds\right] \geq 0 \tag{2.2.8}$$

Similarly, the results for (2), (5), (7) and (8) of the multiscale model system (2.2.1) can also be obtained by the integrating factor technique.

We now consider (3) of the multiscale model system (2.2.1)

$$\frac{dU_i}{dt} = -\kappa U_i \left(I_i - \frac{\mu}{\xi} \right) \tag{2.2.9}$$

Positivity of the solution of (3) of the multiscale model system (2.2.1) is proved using the separation of variables as follows

$$\frac{1}{U_i} dU_i = -\kappa \left(I_i - \frac{\mu}{\xi} \right) dt \tag{2.2.10}$$

We integrate both sides of (2.2.10) with respect to t to get

$$\int_0^t \frac{1}{U_i} dU_i = -\kappa \int_0^t \left(I_i(s) - \frac{\mu}{\xi} \right) ds \tag{2.2.11}$$

Integrating the left side gives

$$\ln \frac{U_i(t)}{U_i(0)} = -\kappa \int_0^t \left(I_i(s) - \frac{\mu}{\xi} \right) ds \tag{2.2.12}$$

Removing $\ln$ we have the following result

$$U_i(t) = U_i(0) exp \left\{ -\kappa \int_0^t \left(I_i(s) - \frac{\mu}{\xi} \right) ds \right\} \geq 0 \tag{2.2.13}$$

Positivity of (4) of the multiscale model system (2.2.1) is proved by integrating both sides of (2.2.14).

$$\frac{dP_i}{dt} = \kappa U_i \left(I_i - \frac{\mu}{\xi} \right) \tag{2.2.14}$$

This gives

$$\int_0^t dP_i = \int_0^t \kappa U_i(s) \left(I_i(s) - \frac{\mu}{\xi} \right) ds \tag{2.2.15}$$

We get the following result

$$P_i(t) = P_i(0) + \int_0^t \kappa U_i(s) \left(I_i(s) - \frac{\mu}{\xi} \right) ds \geq 0 \tag{2.2.16}$$

since the protected cells P_i are recruited from uninfected cells when interferon I_i is above background level, $\frac{\mu}{\xi}$, that is, $I_i(t) > \frac{\mu}{\xi}$. Similarly, the result of (6) of the multiscale model system 2.2.1 is a positive solution since both $\phi_V(V, J)$ and ϕ_A are positive constants.

Consequently, $V_i(t) \geq 0$, $F_i(t) \geq 0$, $U_i(t) \geq 0$, $P_i(t) \geq 0$, $I_i(t) \geq 0$, $A_i(t) \geq 0$, $J_i(t) \geq 0$ and $C_i(t) \geq 0$ for all time $t > 0$. □

2.2.1.2 Boundedness of solutions

We show that all eight equations are ultimately bounded for $t \geq 0$. From the third equation, the viral infection reduces the population of the uninfected cells so that at the onset of the infection, the population of uninfected cells must be greater or equal to the total cell population at $t > 0$. The population of uninfected cells is also reduced as a proportion of the cells become protected. The fifth equation reduces to $\frac{\mu}{\xi}$ while the remaining equations reduce to zero at disease-free equilibrium.

This leaves (3) of the multiscale model system (2.2.1) given by

$$\frac{dU_i}{dt} = -\kappa U_i \left(I_i - \frac{\mu}{\xi} \right) \tag{2.2.17}$$

$$U_i(t) = U_i(0) exp \left\{ -\kappa \int_0^t \left(I_i(s) - \frac{\mu}{\xi} \right) ds \right\} \tag{2.2.18}$$

Initially, the interferons equal to $\frac{\mu}{\xi}$. However, when the interferons are above background level, that is, $\frac{\mu}{\xi}$ is implies that $\left(I_i(s) - \frac{\mu}{\xi} \right) > 0$. Therefore, from (2.2.18) we have

$$\lim_{t \to \infty} \sup U_i(t) \leq \lim_{t \to \infty} \sup U_i(0) = U_i(0) = N_i \tag{2.2.19}$$

Thus, the multiscale model system (2.2.1) is bounded above by N_i and bounded below by 0. Since the multiscale model system (2.2.1) is positive and bounded, it is well-posed (epidemiologically and mathematically) in the region Φ. □

2.3 Determination of disease free equilibrium and its stability

2.3.1 The disease-free equilibrium point

In order to establish the disease-free equilibrium point of the multiscale model system in the disease compartment we set the right-hand side of the equations of multiscale model system (2.2.1) to zero. When the equilibrium is disease-free then infectious virions in the blood of an individual will not exist resulting no transmission of infection. Therefore, the disease-free equilibrium of the multiscale model system (2.2.1) is given by

$$E^0 = \left(U_i^0, V_i^0, F_i^0, P_i^0, I_i^0, A_i^0, C_i^0, J_i^0\right) = \left(N_i, 0, 0, 0, \frac{\mu}{\xi}, 0, 0, 0\right), \quad i = 1, ..., n \tag{2.3.1}$$

where N_i, a constant, is the initial number of uninfected epithelial cells. $A_i^0 = 0$ since this is the time during which virus replication is not yet observable.

2.3.2 The model reproductive number

The reproductive number, $\mathcal{R}_0$ is described as the average number of secondary infections generated by an infectious individual host brought into an entirely susceptible population [101, 102]. It is an important parameter which helps to examine outbreak of disease. For the vast majority of disease outbreaks, if $\mathcal{R}_0 < 1$, this implies that the outbreak dies out, while when $\mathcal{R}_0 > 1$, this implies that the outbreak persists. For FMDV infection in cattle, $\mathcal{R}_0$ describes the anticipated number of cattle FMDV infections generated by an individual animal throughout the whole cycle of virulence of the animal placed in a totally susceptible cattle population. Hence, $\mathcal{R}_0$ quantifies transmission of FMDV from animal to animal. In order to evaluate the basic reproductive number we implement the next generation operator approach [101]. The multiscale model system (2.2.1) can be expressed as follows:

$$\begin{cases} \dfrac{dX}{dt} = f(X, Y, Z), \\ \dfrac{dY}{dt} = g(X, Y, Z), \\ \dfrac{dZ}{dt} = h(X, Y, Z), \end{cases} \tag{2.3.1}$$

where

$$X = (U_i, P_i)$$

$$Y = (J_i, C_i)$$

$$Z = (F_i, V_i).$$

The elements of X stand for the number of susceptibles as well as other groups of non-infectious individuals. The elements of Y stand for the number of infected individuals who are unable to transmit the

disease. The elements of Z stand for the number of infected individuals able to transmit the disease. We define $\tilde{g}(X^*, Z)$ from [101] by

$\tilde{g}(X^*, Z) = \dfrac{\epsilon U_i^0 V_i}{\zeta}$

Suppose $A = D_Z h(X^*, \tilde{g}(X^*, 0), 0)$ so that A is expressed as $A = M - D$.

Then from (1) and (2) of multiscale model system (2.2.1) A becomes

$$A = \begin{bmatrix} \sum_{i \neq j}^{n} \beta_{ij} - \phi_A(t)\omega & \zeta \\ \epsilon U_i^0 & -\zeta \end{bmatrix} \tag{2.3.2}$$

with

$$M = \begin{bmatrix} \sum_{i \neq j}^{n} \beta_{ij} & 0 \\ \epsilon U_i^0 & 0 \end{bmatrix} \tag{2.3.3}$$

and

$$D = \begin{bmatrix} \phi_A(t)\omega & \zeta \\ 0 & -\zeta \end{bmatrix} \tag{2.3.4}$$

Therefore, the inverse of matrix D is

$$D^{-1} = \begin{bmatrix} \dfrac{1}{\phi_A(t)\omega} & \dfrac{1}{\phi_A(t)\omega} \\ 0 & \dfrac{1}{\zeta} \end{bmatrix} \tag{2.3.5}$$

When we multiple M and D^{-1} we get

$$MD^{-1} = \begin{bmatrix} \sum_{i \neq j}^{n} \beta_{ij} & 0 \\ \epsilon U_i^0 & 0 \end{bmatrix} \begin{bmatrix} \dfrac{1}{\phi_A(t)\omega} & \dfrac{1}{\phi_A(t)\omega} \\ 0 & \dfrac{1}{\zeta} \end{bmatrix} \tag{2.3.6}$$

This simplifies to

$$MD^{-1} = \begin{bmatrix} \dfrac{\sum_{i \neq j}^{n} \beta_{ij} + \epsilon U_i^0}{\phi_A(t)\omega} & 0 \\ \dfrac{\epsilon U_i^0}{\zeta} & 0 \end{bmatrix} \tag{2.3.7}$$

$\mathcal{R}_0$ is the spectral radius (dominant eigenvalue) of MD^{-1} and so we have the following expression

$$\mathcal{R}_0 = \rho\left(MD^{-1}\right)$$

$$\mathcal{R}_{0i} = \frac{\sum_{i\neq j}^{n} \beta_{ij} + \epsilon U_i^0}{\phi_A(t)\omega} \tag{2.3.8}$$

$$\mathcal{R}_0 = max\left\{\mathcal{R}_{0i}\right\} \tag{2.3.9}$$

Therefore, the reproductive number $\mathcal{R}_0$, is composed of microscale and macroscale disease parameters ϵ, ω and β_{ij} respectively. When we refer to the formulation for $\mathcal{R}_0$ from Equation (2.3.8) we can gather the following.

(i) The macroscale transmission parameter, β_{ij} from Equation (2.3.8) representing the strength of transmission between individuals j and i due to their separation distance contribute to the spread of FMD infection. The constant α controls the strength of transmission such that when α is small then the probability of transmission β_{ij} from j to i is high and for bigger values of α the transmission between individuals is low.

(ii) The microscale transmission parameters ϵ, the infection rate of epithelial cells as well as ω, which controls rate of clearance of virus from Equation (2.3.8) have an effect on the spread of virus. The immune response, including ω, helps to reduce FMDV transmission.

Therefore, it can be concluded that both macroscale and microscale factors have an impact on the spread of FMDV.

2.3.3 Local Stability of the disease free equilibrium (DFE)

In this section we establish the local stability of disease-free equilibrium of the multiscale model system (2.2.1).

$$E^0 = \left(U_i^0, V_i^0, F_i^0, P_i^0, I_i^0, A_i^0, C_i^0, J_i^0\right) = \left(N_i, 0, 0, 0, \frac{\mu}{\xi}, 0, 0, 0\right), \quad i = 1, ..., n \tag{2.3.1}$$

where N_i, a constant, is the initial number of uninfected epithelial cells.

The Jacobian matrix of the multiscale model system (2.2.1) can be calculated at the disease-free equilibrium state to give:

$$J(E^0) = \begin{bmatrix} d_2 & d_6 & 0 & 0 & 0 & 0 & 0 & 0 \\ d_7 & -d_6 & 0 & 0 & 0 & 0 & 0 & 0 \\ 0 & 0 & 0 & 0 & -d_4 & 0 & 0 & 0 \\ 0 & 0 & 0 & 0 & d_4 & 0 & 0 & 0 \\ 0 & 0 & 0 & 0 & -d_8 & 0 & d_3 & 0 \\ 0 & 0 & 0 & 0 & 0 & 0 & 0 & 0 \\ d_1 & 0 & 0 & 0 & 0 & 0 & -d_9 & d_1 \\ 0 & d_5 & 0 & 0 & 0 & 0 & 0 & -d_1 \end{bmatrix} \tag{2.3.2}$$

where

$$\begin{cases} d_1 = \phi_A \omega, \\ d_2 = -\phi_A \omega + \sum_{i \neq j}^{n} \beta_{ij}, \\ d_3 = \phi_U(U)\eta, \\ d_4 = \kappa N_i, \\ d_5 = \gamma\zeta, \\ d_6 = \zeta, \\ d_7 = \epsilon N_i, \\ d_8 = \xi, \\ d_9 = \sigma \end{cases} \tag{2.3.3}$$

In order to establish the stability of the disease-free-equilibrium we evaluate the eigenvalues of the Jacobian matrix (2.3.2). Given below is the characteristic equation for the eigenvalues.

$$\lambda^3 (-d_8 - \lambda)(-d_9 - \lambda)(-d_1 - \lambda)[(d_2 - \lambda)(-d_6 - \lambda) - d_6 d_7] = 0 \tag{2.3.4}$$

We have three zero eigenvalues and $\lambda_1 = -d_8, \lambda_2 = -d_9, \lambda_3 = -d_1$. We now consider the remaining expression

$$[(d_2 - \lambda)(-d_6 - \lambda) - d_6 d_7] = 0 \tag{2.3.5}$$

The equation above gives the eigenvalues

$$\lambda_0 = \frac{-(d_6 - d_2) \pm \sqrt{(d_6 - d_2)^2 + 4d_6 d_1 (\mathcal{R}_0 - 1)}}{2} \tag{2.3.6}$$

Therefore, the two eigenvalues are

$$\lambda_{01} = \frac{-\left[(d_6 - d_2) - \sqrt{(d_6 - d_2)^2 + 4d_6 d_1 (\mathcal{R}_0 - 1)}\right]}{2} \tag{2.3.7}$$

and

$$\lambda_{02} = \frac{-\left[(d_6 - d_2) + \sqrt{(d_6 - d_2)^2 + 4d_6 d_1 (\mathcal{R}_0 - 1)}\right]}{2}, \tag{2.3.8}$$

Therefore, the eigenvalues of the characteristic equation are

$$\begin{aligned}
\lambda_1 &= 0, \\
\lambda_2 &= 0, \\
\lambda_3 &= 0, \\
\lambda_4 &= -d_8, \\
\lambda_5 &= -d_9, \\
\lambda_6 &= -d_1, \\
\lambda_7 &= \frac{-\left[(d_6 - d_2) - \sqrt{(d_6 - d_2)^2 + 4d_6 d_1 (\mathcal{R}_0 - 1)}\right]}{2}, \\
\lambda_8 &= \frac{-\left[(d_6 - d_2) + \sqrt{(d_6 - d_2)^2 + 4d_6 d_1 (\mathcal{R}_0 - 1)}\right]}{2}
\end{aligned}$$

If $\mathcal{R}_0 < 1$, then this implies $\lambda_7 < 0$. Therefore, all eigenvalues of the multiscale model system (2.2.1) will be zero or negative. Due to the existence of zero eigenvalues, further analysis on the stability of E^0 is performed by implementing the center manifold theorem in section (2.4.3). From the proof of Theorem 2.6 the analysis establishes that the disease-free equilibrium point E^0, of the model system (2.2.1) is locally asymptotically stable whenever $\mathcal{R}_0 < 1$ and unstable otherwise. This result is summarized as follows.

Theorem 2.2. *The disease-free equilibrium point E^0, of the multiscale model system (2.2.1) is locally asmptotically stable whenever $\mathcal{R}_0 < 1$ and unstable otherwise.*

2.3.4 Global stability of the disease-free equilibrium

To determine the global stability of DFE of the multiscale model system (2.2.1), we use (Theorem 2) in [103] to establish that the DFE is globally asymptotically stable whenever $\mathcal{R}_0 < 1$ and unstable when $\mathcal{R}_0 > 1$. In this section, we write down two conditions that when satisfied, also warrant the global asymptotic stability of the disease free state. Therefore, writing the multiscale model system (2.2.1) in the following way we get:

$$\begin{cases} \dfrac{dX}{dt} = F(X,Z), \\ \\ \dfrac{dZ}{dt} = G(X,Z), \quad G(X,0) = 0 \end{cases} \tag{2.3.1}$$

where $X = (U_i, P_i)$ stands for all uninfected components and $Z = (V_i, F_i, I_i, A_i, C_i, J_i)$ stands for all infected and infectious components;

$$U_0 = (X^*; 0_8) \text{ where } X^* = \left(N_i, \frac{\mu}{\xi}\right), \quad i = 1, ..., n \tag{2.3.2}$$

stands for the disease-free equilibrium of the multiscale model system (2.2.1). In order to ensure that the equilibrium is globally asymptotic stable, the conditions $(H1)$ and $(H2)$ below should be satisfied [101]:

(H1) For $\dfrac{dX}{dt} = F(X, 0_8)$, X^* is globally asymptotically stable (g.a.s);

(H2) $G(X,Z) = AZ - \hat{G}(X,Z), \hat{G}(X,Z) \geq 0$ for $(X,Z) \in \mathbb{R}^8_+$, $A \in M(6 \times 6)$
where the Jacobian $A = \dfrac{\partial G}{\partial Z} = D_Z G(X^*, 0_8)$ is an M-matrix (the off diagonal elements of A are non-negative) and $\mathbb{R}^8_+$ is the region where the model makes biological sense.

Here we have

$$F(X, 0_8) = \begin{bmatrix} -\kappa U_i \left(I_i - \dfrac{\mu}{\xi}\right) \\ \kappa U_i \left(I_i - \dfrac{\mu}{\xi}\right) \end{bmatrix} \tag{2.3.3}$$

Interferon production, I_i is stopped when most of the uninfected cells are protected.

Therefore, we can deduce from (2.3.3) that $X^* = \left(N_i; \dfrac{\mu}{\xi}\right)$ is globally asymptotically stable.

$$G(X,Z) = \begin{bmatrix} \zeta F_i - \phi_A(t)\omega V_i + \sum_{i\neq j}^{n} \beta_{ij} V_j \\ \epsilon U_i V_i - \zeta F_i \\ \mu - \xi I_i + \phi_U(U)\eta C_i \\ \phi_V(V,J)\phi_A \\ \phi_A\omega(V_i + J_i) - \sigma C_i \\ \omega\zeta F_i - \phi_A\omega J_i \end{bmatrix} \tag{2.3.4}$$

$$A = \begin{bmatrix} \sum_{i\neq j}^{n} \beta_{ij} - \phi_A(t)\omega & \zeta & 0 & 0 & 0 & 0 \\ \epsilon N_i & -\zeta & 0 & 0 & 0 & 0 \\ 0 & 0 & -\xi & 0 & \phi_U(U)\eta & 0 \\ 0 & 0 & 0 & 0 & 0 & 0 \\ \phi_A\omega & 0 & 0 & 0 & -\sigma & \phi_A\omega \\ 0 & \gamma\zeta & 0 & 0 & 0 & -\phi_A\omega \end{bmatrix} \tag{2.3.5}$$

Therefore we have

$$G(X,Z) = \begin{bmatrix} \zeta F_i - \phi_A(t)\omega V_i + \sum_{i\neq j}^{n} \beta_{ij} V_j \\ \epsilon U_i V_i - \zeta F_i \\ \mu - \xi I_i + \phi_U(U)\eta C_i \\ \phi_V(V,J)\phi_A \\ \phi_A\omega(V_i + J_i) - \sigma C_i \\ \omega\zeta F_i - \phi_A\omega J_i \end{bmatrix} = \begin{bmatrix} \sum_{i\neq j}^{n} \beta_{ij} - \phi_A(t)\omega & \zeta & 0 & 0 & 0 & 0 \\ \epsilon N_i & -\zeta & 0 & 0 & 0 & 0 \\ 0 & 0 & -\xi & 0 & \phi_U(U)\eta & 0 \\ 0 & 0 & 0 & 0 & 0 & 0 \\ \phi_A\omega & 0 & 0 & 0 & -\sigma & \phi_A\omega \\ 0 & \gamma\zeta & 0 & 0 & 0 & -\phi_A\omega \end{bmatrix} Z - \hat{G}(X,Z) \tag{2.3.6}$$

$$\hat{G}(X,Z) = \begin{bmatrix} \hat{G}_1(X,Z) \\ \hat{G}_2(X,Z) \\ \hat{G}_3(X,Z) \\ \hat{G}_4(X,Z) \\ \hat{G}_5(X,Z) \\ \hat{G}_6(X,Z) \end{bmatrix} = \begin{bmatrix} 0 \\ \epsilon N_i V_i - \epsilon U_i V_i \\ 0 \\ 0 \\ 0 \\ 0 \end{bmatrix} \tag{2.3.7}$$

$$= \begin{bmatrix} 0 \\ \epsilon V_i(N_i - U_i) \\ 0 \\ 0 \\ 0 \\ 0 \end{bmatrix} \tag{2.3.8}$$

The result clearly shows that A is an M-matrix, as it has non-negative off diagonal elements. Since $0 \leq U_i \leq N_i$, then it implies that $\hat{G}(X, Z) \geq 0$. It is also clear that the disease-free equilibrium point $X^* = \left(N_i; \frac{\mu}{\xi}\right)$ is globally asymptotically stable (GAS) equilibrium of $\frac{dX}{dt} = F(X, 0)$. Hence, the disease-free equilibrium $E_0 = (X^*, 0_8)$ is globally asymptotically stable. □

Theorem 2.3. *The disease-free equilibrium of the multiscale model system (2.2.1) is globally asymptotically stable if $\mathcal{R}_0 \leq 1$ and the assumptions (H1) and (H2) are satisfied.*

Remark 2.4. This result rules-out the existence of backward bifurcation in this model setting since the disease-free equilibrium is globally-asymptotically stable when $\mathcal{R}_0 \leq 1$.

2.4 The endemic equilibrium and its stability

At the endemic equilibrium the cattle population is invaded by the FMD virus. The endemic equilibrium is given as follows:

$$E^* = (U_i^*, V_i^*, F_i^*, P_i^*, I_i^*, A_i^*, C_i^*, J_i^*), \quad i = 1, ..., n \tag{2.4.1}$$

satisfies

$$\begin{cases} 0 = \zeta F_i^* - \phi_A \omega V_i^* + \sum_{i=1, i\neq j}^{n} \beta_{ij} V_j^*, \\ 0 = \epsilon U_i^* V_i^* - \zeta F_i^*, \\ 0 = -\kappa U_i^* \left(I_i^* - \dfrac{\mu}{\xi} \right), \\ 0 = \kappa U_i^* \left(I_i^* - \dfrac{\mu}{\xi} \right), \\ 0 = \mu - \xi I_i^* + \phi_U(U) \eta C_i^*, \\ 0 = \phi_V(V_i, J_i) \phi_A(t), \\ 0 = \phi_A \omega (V_i^* + J_i^*) - \sigma C_i^*, \\ 0 = \gamma \zeta F_i^* - \phi_A \omega J_i^* \end{cases} \tag{2.4.2}$$

for all $U_i^*, V_i^*, F_i^*, P_i^*, I_i^*, A_i^*, C_i^*, J_i^* > 0, \quad i = 1, ..., n.$

2.4.1 The endemic equilibrium

The endemic value of the proportion of uninfected cells is given by

$$U_i^* = \frac{\phi_A \omega V_i^* - \sum_{i=1, i\neq j}^{n} \beta_{ij} V_j^*}{\epsilon V_i^*} \tag{2.4.1}$$

We deduce from Equation (2.4.1) that the equilibrium state associated with the proportion of uninfected cells is proportional to the rate at which virus is cleared, the amount of antibody produced, the strength of transmission between individuals within a spatial network as well as the rate of infection of cells in the blood. The endemic value of infected cells is expressed as follows:

$$F_i^* = \frac{\phi_A \omega V_i^* - \sum_{i=1, i\neq j}^{n} \beta_{ij} V_j^*}{\vartheta} \tag{2.4.2}$$

We deduce from Equation (2.4.2) that the equilibrium state related to the infected cells corresponds to the rate of infected cells bursting, the amount of antibody produced, the strength of transmission between

individuals within a spatial network, the rate of infection of cells in the blood and to the clearance rate of virus. The endemic value of the non-infectious material is given by

$$J_i^* = \frac{\gamma\zeta F_i^*}{\phi_A\omega} \tag{2.4.3}$$

We deduce from Equation (2.4.3) that the equilibrium state associated with the non-infectious material from the burst infected cells is proportional to the rate at which the virus is cleared, the amount of antibody produced and the rate of infected cells bursting. The endemic value of the virus-antibody complex is given by

$$C_i^* = \frac{\phi_A\omega(V_i^* + J_i^*)}{\sigma} \tag{2.4.4}$$

We deduce from Equation (2.4.4) that the equilibrium state related to virus-antibody complex corresponds to the amount of antibody produced, the rate of clearance of virus-antibody complexes and the clearance rate of the virus. The endemic value of virions in blood is given by

$$V_i^* = \frac{\zeta F_i^*}{\epsilon U_i^*} \tag{2.4.5}$$

We deduce from Equation (2.4.5) that the equilibrium state associated with virions in blood corresponds to the rate of bursting of infected cells as well as the rate of infection of cells from the blood. The endemic value of the interferon is given by

$$I_i^* = \frac{\mu}{\xi} + \frac{\phi_U(U)\eta C_i^*}{\xi} \tag{2.4.6}$$

We deduce from Equation (2.4.6) that the equilibrium state associated with the background production of interferon, background clearance of interferon as well as production rate of interferon. Therefore, the endemic equilibrium of the multiscale model system (2.2.1) given by Equations (2.4.1)-(2.4.6) depend on both microscale and macroscale parameters.

2.4.2 The Existence of the Endemic Equilibrium State

This section gives some solutions regarding the existence of an endemic equilibrium for the multiscale model system (2.2.1) implementing the threshold parameter, $\mathcal{R}_0$.

Theorem 2.5. *The multiscale model system (2.2.1) formulated in terms of proportions has at least one endemic equilibrium solution given by*

$$E^* = (U_i^*, V_i^*, F_i^*, P_i^*, I_i^*, A_i^*, C_i^*, J_i^*), \quad i = 1, ..., n \tag{2.4.1}$$

with $U_i^*, V_i^*, F_i^*, P_i^*, I_i^*, A_i^*, C_i^*, J_i^*$ *all non-negative for all* $i = 1, ..., n$*, whose existence and properties are determined by the threshold parameter* $\mathcal{R}_0$ *where*

$$\mathcal{R}_{0i} = \frac{\sum_{i\neq j}^{n} \beta_{ij} + \epsilon U_i^0}{\phi_A \omega} \tag{2.4.2}$$

Proof. Let $E^* = (U_i^*, V_i^*, F_i^*, P_i^*, I_i^*, A_i^*, C_i^*, J_i^*)\,, \quad i = 1, ..., n$ be a constant solution of the multiscale model system (2.2.1). We can simply present $U_i^*, F_i^*, P_i^*, I_i^*, A_i^*, C_i^*, J_i^*, \quad i = 1, ..., n$ in terms of V_i^* in the form

$$\begin{cases} U_i^* = \dfrac{\phi_A\omega(1-\mathcal{R}_{0i}) + \epsilon U_i^0}{\epsilon}, \\ F_i^* = \dfrac{V_i^*[\phi_A\omega(1-\mathcal{R}_{0i}) + \epsilon U_i^0]}{\zeta}, \\ I_i^* = \dfrac{\mu\sigma + \phi_U(U)\eta(V_i^*\phi_A\omega + \gamma V_i^*[\phi_A\omega(1-\mathcal{R}_{0i}) + \epsilon U_i^0])}{\xi\sigma}, \\ C_i^* = \dfrac{V_i^*\phi_A\omega + \gamma V_i^*[\phi_A\omega(1-\mathcal{R}_{0i}) + \epsilon U_i^0]}{\sigma} \end{cases} \tag{2.4.3}$$

We substitute the equations in (2.4.3) into the expression for V_i to give the following:

$$\frac{dV_i}{dt} = \zeta F_i - \phi_A\omega V_i + \sum_{i\neq j}^{n} \beta_{ij} V_j \tag{2.4.4}$$

$$= V_i^*[\phi_A\omega(1-\mathcal{R}_{0i}) + \epsilon U_i^0] - \phi_A\omega V_i^* + \sum_{i\neq j}^{n} \beta_{ij} V_j^*$$

$$= V_i^*[\phi_A\omega(1-\mathcal{R}_{0i}) + \epsilon U_i^0 - \phi_A\omega + \sum_{i\neq j}^{n} \beta_{ij}] \tag{2.4.5}$$

where $V_i^* \neq 0$

Consequently, there exists one unique endemic equilibrium for the multiscale model system (2.2.1) whenever $\mathcal{R}_0 > 1$. □

2.4.3 Local stability of the Endemic Equilibrium

In this section we find the local asymptotic stability of the endemic steady state of the multiscale model system (2.2.1) through the implementation of the center manifold theory detailed in [101]. Therefore, by applying the theory we change variables of the multiscale model system (2.2.1). We now set $V_i = x_1$, $F_i = x_2$, $U_i = x_3$, $P_i = x_4$, $I_i = x_5$, $A_i = x_6$, $C_i = x_7$ and $J_i = x_8$. We also apply the vector notation $\mathbf{x} = (x_1, x_2, x_3, x_4, x_5, x_6, x_7, x_8)^T$ so that the multiscale model system (2.2.1) can be expressed as follows:

$$\frac{d\mathbf{x}}{dt} = \mathbf{f}(\mathbf{x}, \epsilon^*) \tag{2.4.1}$$

where

$$\mathbf{f} = (f_1, f_2, f_3, f_4, f_5, f_6, f_7, f_8) \tag{2.4.2}$$

Therefore, the multiscale model system (2.2.1) can be rewritten as

$$\begin{aligned}
\frac{dx_1}{dt} &= f_1 = \zeta x_2 - \phi_A \omega x_1 + \sum_{i \neq j} \beta_{ij} x_1, \\
\frac{dx_2}{dt} &= f_2 = \epsilon x_3 x_1 - \zeta x_2, \\
\frac{dx_3}{dt} &= f_3 = -\kappa x_3 \left(x_5 - \frac{\mu}{\xi} \right), \\
\frac{dx_4}{dt} &= f_4 = \kappa x_3 \left(x_5 - \frac{\mu}{\xi} \right), \\
\frac{dx_5}{dt} &= f_5 = \mu - \xi x_5 + \phi_U(U) \eta x_7, \\
\frac{dx_6}{dt} &= f_6 = \phi_V(V, J) \phi_A, \\
\frac{dx_7}{dt} &= f_7 = \phi_A \omega (x_1 + x_8) - \sigma x_7, \\
\frac{dx_8}{dt} &= f_8 = \gamma \zeta x_2 - \phi_A \omega x_8
\end{aligned} \tag{2.4.3}$$

The approach encompasses calculating the Jacobian matrix of the multiscale system (2.4.3) at the disease-free equilibrium E_0 signified by $J(E_0)$. The matrix corresponding to the multiscale system (2.4.3) evaluated at the disease-free equilibrium is given by

$$J(E^0) = \begin{bmatrix} d_2 & d_6 & 0 & 0 & 0 & 0 & 0 & 0 \\ d_7 & -d_6 & 0 & 0 & 0 & 0 & 0 & 0 \\ 0 & 0 & 0 & 0 & -d_4 & 0 & 0 & 0 \\ 0 & 0 & 0 & 0 & d_4 & 0 & 0 & 0 \\ 0 & 0 & 0 & 0 & -d_8 & 0 & d_3 & 0 \\ 0 & 0 & 0 & 0 & 0 & 0 & 0 & 0 \\ d_1 & 0 & 0 & 0 & 0 & 0 & -d_9 & d_1 \\ 0 & d_5 & 0 & 0 & 0 & 0 & 0 & -d_1 \end{bmatrix} \tag{2.4.4}$$

where

$$\begin{cases} d_1 = \phi_A \omega, \\ d_2 = -\phi_A \omega + \sum_{i=1, i \neq j}^{n} \beta_{ij}, \\ d_3 = \phi_U(U)\eta, \\ d_4 = \kappa N_i, \\ d_5 = \gamma\zeta, \\ d_6 = \zeta, \\ d_7 = \epsilon^* N_i, \\ d_8 = \xi, \\ d_9 = \sigma \end{cases} \tag{2.4.5}$$

By making the use of of an approach similar to the one in section (2.3.3), we can obtain the basic reproductive number of the multiscale system (2.4.3) given by

$$\mathcal{R}_{0i} = \frac{\sum_{i=1, i \neq j}^{n} \beta_{ij} + \epsilon^* U_i^0}{\phi_A \omega} \tag{2.4.6}$$

Setting $\epsilon = \epsilon^*$ as the bifurcation parameter and also, letting $\mathcal{R}_0 = 1$ and determining ϵ^* in (2.4.6), this gives

$$\epsilon^* = \frac{\phi_A \omega - \sum_{i=1, i\neq j}^{n} \beta_{ij}}{U_i^0} \tag{2.4.7}$$

We can highlight that the linearized system of the transformed equations (2.4.3) with bifurcation point ϵ^* has a simple zero eigenvalue. Consequently, the center manifold theory [101] can be utilized to examine the dynamics of the multiscale system (2.4.3) close to ϵ^*.

Theorem 2.6. *Consider the following general system of ordinary differential equations with parameter ϕ:*

$$\frac{dx}{dt} = f(x, \phi) \tag{2.4.8}$$

$$f : \boldsymbol{R}^n \times \boldsymbol{R} \to \boldsymbol{R}. \quad f : \boldsymbol{C}^2 \left(\boldsymbol{R}^2 \times \boldsymbol{R}\right).$$

where 0 is an equilibrium of the system, that is, $f(0, \phi) = 0$ for all ϕ, and assume that

(A1) $A = D_x f(0,0) = ((\partial f_i / \partial x_j)(0,0))$ is a linearization matrix of the multiscale system (2.4.3) around the equilibrium 0 with ϕ evaluated at 0. Zero is a simple eigenvalue of A, and other eigenvalues have negative real parts.

(A2) matrix A has a right eigenvector u and a left eigenvector v corresponding to the zero eigenvalues.

Let f_k be the kth component of f and

$$\begin{cases} a = \displaystyle\sum_{k,i,j=1}^{n} u_k v_i v_j \frac{\partial^2 f_k}{\partial x_i \partial x_j}(0,0), \\ \\ b = \displaystyle\sum_{k,i,j=1}^{n} u_k v_i \frac{\partial^2 f_k}{\partial x_i \partial \phi}(0,0), \end{cases} \tag{2.4.9}$$

The local dynamics of (2.4.8) around 0 are totally governed by a and b and are summarized as follows.

(i) $a > 0$ and $b > 0$. When $\phi < 0$ with $|\phi| \ll 1$, 0 is locally asymptotically stable, and there exists a positive unstable equilibrium: when $0 < \phi \ll 1$, 0 is unstable and there exists a negative and

locally asymptotically stable equilibrium.

(ii) $a < 0$ *and* $b < 0$. *When* $\phi < 0$ *with* $|\phi| \ll 1$, *0 is unstable, when* $0 < \phi \ll 1$, *0 is asymptotically stable, and there exists a positive unstable equilibrium.*

(iii) $a > 0$ *and* $b < 0$. *When* $\phi < 0$ *with* $|\phi| \ll 1$, *0 is unstable, and there exists a locally asymptotically stable negative equilibrium; when* $0 < \phi \ll 1$, *0 is stable and a positive unstable equilibrium appears.*

(iv) $a < 0$ *and* $b > 0$. *When* ϕ *changes from negative to positive, 0 changes its stability from stable to unstable. Correspondingly a negative unstable equilibrium becomes positive and locally asymptotically stable.*

To implement Theorem 2.6, the following calculations are neccessary (note that ϵ^* is the bifurcation parameter instead of ϕ in Theorem 2.6).

When $\mathcal{R}_0 = 1$, we can demonstrate that the Jacobian matrix of the multiscale system (2.4.3) at ϵ^* (denoted by J_{ϵ^*}) has a right eigenvector corresponding to the zero eigenvalue expressed below:

$$\mathbf{u} = (u_1, u_2, u_3, u_4, u_5, u_6, u_7, u_8)^T, \tag{2.4.10}$$

such that

$$\begin{bmatrix} d_2 & d_6 & 0 & 0 & 0 & 0 & 0 & 0 \\ d_7 & -d_6 & 0 & 0 & 0 & 0 & 0 & 0 \\ 0 & 0 & 0 & 0 & -d_4 & 0 & 0 & 0 \\ 0 & 0 & 0 & 0 & d_4 & 0 & 0 & 0 \\ 0 & 0 & 0 & 0 & -d_8 & 0 & d_3 & 0 \\ 0 & 0 & 0 & 0 & 0 & 0 & 0 & 0 \\ d_1 & 0 & 0 & 0 & 0 & 0 & -d_9 & d_1 \\ 0 & d_5 & 0 & 0 & 0 & 0 & 0 & -d_1 \end{bmatrix} \begin{bmatrix} u_1 \\ u_2 \\ u_3 \\ u_4 \\ u_5 \\ v_6 \\ v_7 \\ v_8 \end{bmatrix} = \begin{bmatrix} 0 \\ 0 \\ 0 \\ 0 \\ 0 \\ 0 \\ 0 \\ 0 \end{bmatrix} \tag{2.4.11}$$

where

$$\begin{cases} u_1 = 1, \\ u_2 = 1, \\ u_3 = 0, \\ u_4 = u_4 > 0, \\ u_5 = 0, \\ u_6 = u_6 > 0 \\ u_7 = 0, \\ u_8 = \dfrac{\gamma\zeta}{\phi_A\omega} \end{cases} \tag{2.4.12}$$

Furthermore, the left eigenvector of the jacobian matrix in (2.4.4) corresponding to the zero eigenvalue at ϵ^* such that

$$\begin{bmatrix} v_1 & v_2 & v_3 & v_4 & v_5 & v_6 & v_7 & v_8 \end{bmatrix} \begin{bmatrix} d_2 & d_6 & 0 & 0 & 0 & 0 & 0 & 0 \\ d_7 & -d_6 & 0 & 0 & 0 & 0 & 0 & 0 \\ 0 & 0 & 0 & 0 & -d_4 & 0 & 0 & 0 \\ 0 & 0 & 0 & 0 & d_4 & 0 & 0 & 0 \\ 0 & 0 & 0 & 0 & -d_8 & 0 & d_3 & 0 \\ 0 & 0 & 0 & 0 & 0 & 0 & 0 & 0 \\ d_1 & 0 & 0 & 0 & 0 & 0 & -d_9 & d_1 \\ 0 & d_5 & 0 & 0 & 0 & 0 & 0 & -d_1 \end{bmatrix} = \begin{bmatrix} 0 & 0 & 0 & 0 & 0 & 0 & 0 & 0 \end{bmatrix} \tag{2.4.13}$$

and satisfying the condition $\mathbf{v}.\mathbf{u} = \mathbf{1}$.

From (2.4.13) we obtain:

$$\mathbf{v} = (v_1, v_2, v_3, v_4, v_5, v_6, v_7, v_8)^T, \tag{2.4.14}$$

where

$$\begin{cases} v_1 = \dfrac{[-(d_1d_6 + d_5d_7)\,\zeta\phi_A\omega + d_6\,(d_2 + d_7)\,\gamma\zeta\epsilon^* N_i]}{[-(d_1d_6 + d_5d_7)\,\zeta\phi_A\omega + (d_2d_5 - d_1d_6)\,\epsilon^* N_i\phi_A\omega + d_6\,(d_2 + d_7)\,\gamma\zeta\epsilon^* N_i]}, \\ v_2 = \dfrac{[(d_2d_5 - d_1d_6)\,\epsilon^* N_i\phi_A\omega]}{[-(d_1d_6 + d_5d_7)\,\zeta\phi_A\omega + (d_2d_5 - d_1d_6)\,\epsilon^* N_i\phi_A\omega + d_6\,(d_2 + d_7)\,\gamma\zeta\epsilon^* N_i]}, \\ v_3 = v_3 > 0, \\ v_4 = 0, \\ v_5 = 0 \\ v_6 = 0, \\ v_7 = 0, \\ v_8 = 0 \end{cases} \tag{2.4.15}$$

When we determine the dot product **v.u** $= 1$ we obtain

$$\begin{cases} \mathbf{v.u} = v_1.u_1 + v_2.u_2 \\ = \left(\dfrac{[-(d_1d_6 + d_5d_7)\,\zeta\phi_A\omega + d_6\,(d_2 + d_7)\,\gamma\zeta\epsilon^* N_i]}{[-(d_1d_6 + d_5d_7)\,\zeta\phi_A\omega + (d_2d_5 - d_1d_6)\,\epsilon^* N_i\phi_A\omega + d_6\,(d_2 + d_7)\,\gamma\zeta\epsilon^* N_i]}\right) \\ + \left(\dfrac{[(d_2d_5 - d_1d_6)\,\epsilon^* N_i\phi_A\omega]}{[-(d_1d_6 + d_5d_7)\,\zeta\phi_A\omega + (d_2d_5 - d_1d_6)\,\epsilon^* N_i\phi_A\omega + d_6\,(d_2 + d_7)\,\gamma\zeta\epsilon^* N_i]}\right) \\ = \left(\dfrac{[-(d_1d_6 + d_5d_7)\,\zeta\phi_A\omega + (d_2d_5 - d_1d_6)\,\epsilon^* N_i\phi_A\omega + d_6\,(d_2 + d_7)\,\gamma\zeta\epsilon^* N_i]}{[-(d_1d_6 + d_5d_7)\,\zeta\phi_A\omega + (d_2d_5 - d_1d_6)\,\epsilon^* N_i\phi_A\omega + d_6\,(d_2 + d_7)\,\gamma\zeta\epsilon^* N_i]}\right) \\ = 1 \end{cases} \tag{2.4.16}$$

We now calculate the parameters of bifurcation a and b, by determining the value of the nonzero second-order mixed derivatives of **F** in regard to the variables and ϵ^* to get the signs of a and b. The sign of a corresponds to, the following nonvanishing partial derivatives of **F**:

$$\begin{cases} \dfrac{\partial^2 f_2}{\partial x_3 \partial x_1} = \dfrac{\partial^2 f_2}{\partial x_1 \partial x_3} = \epsilon^* \\ \\ \dfrac{\partial^2 f_4}{\partial x_3 \partial x_5} = \dfrac{\partial^2 f_4}{\partial x_5 \partial x_3} = \kappa \end{cases} \tag{2.4.17}$$

Similarly, the sign of b corresponds to the following non-vanishing partial derivatives of $\mathbf{F}$:

$$\frac{\partial^2 f_2}{\partial x_1 \partial \epsilon^*} = x_3 = N_i \tag{2.4.18}$$

Substituting expression (2.4.12), (2.4.15) and (2.4.17) into (2.4.9), we get

$$\begin{cases} a &= 2u_2 v_3 v_1 \dfrac{\partial^2 f_2}{\partial x_3 \partial x_1} \\ \\ &= 2\dfrac{\left[-\left(d_1 d_6 + d_5 d_7\right)\zeta \phi_A \omega + d_6\left(d_2 + d_7\right)\gamma\zeta\epsilon^* N_i\right]}{\left[-\left(d_1 d_6 + d_5 d_7\right)\zeta \phi_A \omega + \left(d_2 d_5 - d_1 d_6\right)\epsilon^* N_i \phi_A \omega + d_6\left(d_2 + d_7\right)\gamma\zeta\epsilon^* N_i\right]}\epsilon^* v_3 \end{cases} \tag{2.4.19}$$

On the other hand, when we substitute expressions (2.4.12), (2.4.15) and (2.4.18) into (2.4.9), we get

$$\begin{cases} b &= u_2 v_1 \dfrac{\partial^2 f_2}{\partial x_1 \partial \epsilon^*} \\ \\ &= \dfrac{\left[-\left(d_1 d_6 + d_5 d_7\right)\zeta \phi_A \omega + d_6\left(d_2 + d_7\right)\gamma\zeta\epsilon^* N_i\right]}{\left[-\left(d_1 d_6 + d_5 d_7\right)\zeta \phi_A \omega + \left(d_2 d_5 - d_1 d_6\right)\epsilon^* N_i \phi_A \omega + d_6\left(d_2 + d_7\right)\gamma\zeta\epsilon^* N_i\right]}N_i \end{cases} \tag{2.4.20}$$

When $d_2 d_5 > d_1 d_6$ then $a > 0$ and $b > 0$. It follows that the foot-and-mouth disease model (2.4.3) exhibits a backward bifurcation whenever the threshold parameter $\mathcal{R}_0$ crosses unity. This shows the co-existence of disease-free and endemic equilibrium at $\mathcal{R}_0$ slightly less than unity. Implementing Theorem 2.6, item (i), enables us to establish the following result which is only valid for $\mathcal{R}_0 > 1$ but near 1. When forward bifurcation occurs, the condition $\mathcal{R}_0 < 1$ is usually a necessary and sufficient condition for disease eradication, however, it is no longer sufficient when a backward bifurcation occurs. In the case of backward bifurcation there exists a subcritical transcritical bifurcation at $\mathcal{R}_0 = 1$ and a saddle-node bifurcation at $\mathcal{R}_0 = \mathcal{R}_0^{sn} < 1$. On the other hand, when $d_2 d_5 < d_1 d_6$ then $a < 0$ and $b < 0$. Implementing Theorem 2.6, item (ii), enables us to establish the following result which is only valid for $\mathcal{R}_0 > 1$ but near 1.

Theorem 2.7. *The FMD endemic steady state of model system (2.2.1) guaranteed by theorem 2.6 is locally asymptotically stable for $\mathcal{R}_0 > 1$ near 1.*

2.5 Numerical analysis

This section presents computer simulations for the multiscale model system (2.2.1)'s behaviour performed using Python program version 3.6 on the Windows 10 operation system. The numerical simulations of the multiscale model system (2.2.1) were carried out to explain some of the systematic results that we got. We used the estimated parameter values presented in Table 2.2 for sensitivity and numerical analysis. A certain amount of the parameter values implemented in the simulations are results from publications and the others are estimates. The following are initial conditions implemented for these simulations: $V_i(0) = 0, F_i(0) = 0, U_i(0) = 500, P_i(0) = 0, I_i(0) = \frac{\mu}{\xi}, A_i(0) = 0, C_i(0) = 0, J_i(0) = 0$ for each individual i. We considered a population of $n = 100$ individuals in a spatial network.

Symbol	Description	Value	Unit	Source
ϵ	Rate of infection of cells from the blood	0.03	$\text{TCID}_{50}\text{mlday}^{-1}$	[7]
ζ	Bursting rate of infected cells	0.23	day^{-1}	[7]
γ	Non-infectious material per $\text{TCID}_{50}\text{ml}^{-1}$	0.01	None	[7]
σ	Rate of clearance of virus-antibody complexes	0.009	day^{-1}	[7]
η	Rate at which interferon is produced per complexes	0.03	$\text{TCID}_{50}^{-1}\text{mlday}^{-1}$	[7]
κ	Protection rate of uninfected cells	0.001	$\text{cell}^{-1}\text{day}^{-1}$	[7]
μ	Interferon rate of production	0.06	$\text{IU ml}^{-1}\text{ day}^{-1}$	[7]
ξ	Interferon rate of clearance	0.056	day^{-1}	[7]
ϕ_A	Production rate of antibody	10	$\text{LPBE-titre day}^{-1}$	[7]
β_{ij}	Transmission rate of FMDV virus between hosts	0.5		Estimate
ω	Clearance rate of virus	0.06	LPBE-titre^{-1}	[7]

Table 2.2: Model parameter values corresponding to the transmission dynamics of FMD.

2.5.1 Sensitivity Analysis

This section presents the analysis of sensitivity for the FMDV transmission indicators obtained from the multiscale model to the model parameters. The transmission indicator we consider is the basic reproductive number, $\mathcal{R}_0$ that generally describes the dynamics for a disease at the beginning of an infection. For any particular epidemic model that illustrates the disease dynamics within a particular population, a sensitivity analysis study is important to perform since it enables us to establish model parameters which can be marked for control, elimination as well as eradication of disease. Therefore, the analysis of sensitivity of the FMDV metric $\mathcal{R}_0$, in relation to the variation of FMD multiscale model parameters is carried out by implementing Latin Hypercube Sampling and Partial Rank Correlation Coefficients (PRCCs). In order to explore the influence of each model parameter on the basic reproduction number, $\mathcal{R}_0$ we perfomed 1000 simulations per run. The results of sensitivity of $\mathcal{R}_0$ to the model parameters are presented by the Tornado plot, Fig. 2.2

According to the sensitivity analysis results of $\mathcal{R}_0$ to the multiscale model system (2.2.1)'s parameters obtained in Fig. 2.2, we deduce these outcomes:

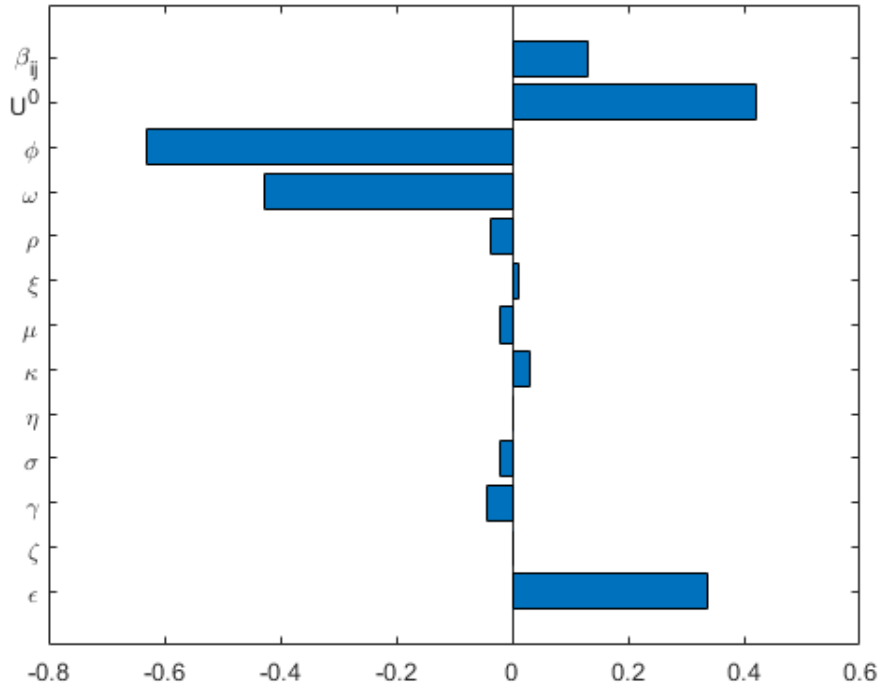

Figure 2.2: *Tornado plot of partial rank correlation coefficients (PRCCs) of the multiscale model parameters that impact the FMDV transmission indicator* $\mathcal{R}_0$

(a) The multiscale model system (2.2.1)'s parameters have both positive PRCCs and negative PRCCs. This implies that parameters with positive PRCCs will increase the value of $\mathcal{R}_0$ as they are increased, where as parameters with negative PRCCs will decrease the value for $\mathcal{R}_0$ as they are increased. For example, an increase in a parameter like rate of infection of cells from the blood, ϵ at the within-host level will consequently increase the value of $\mathcal{R}_0$, and also increasing a parameter like rate at which virus is cleared, ω leads to decrease in $\mathcal{R}_0$.

(b) The FMDV transmission metric $\mathcal{R}_0$ is extremely sensitive to five of the disease parameters of the multiscale model system (2.2.1), ($\beta_{ij}, U^0, \phi, \omega, \epsilon$). We note that $\mathcal{R}_0$ indicates spread of FMDV during the beginning of the outbreak. The following conclusions regarding sensitivity of $\mathcal{R}_0$ to the FMDV multiscale model system (2.2.1)'s parameters can be established.

(i) Since $\mathcal{R}_0$ is significantly sensitive to $(\beta_{ij}, U^0, \phi, \omega, \epsilon)$, this implies that caution must be applied on the accuracy of these five FMDV multiscale model system (2.2.1)'s parameters during the collection of data if the effectiveness and usefulness of the FMDV multiscale model system (2.2.1) is to be intensified.

(ii) In view of the fact that $\mathcal{R}_0$ is responsive to the transmission rate between the cattle, β_{ij} (the between-host level parameter) it implies that FMD interventions such as quarantines would be more effective to control the spread of FMD infection at the beginning of the outbreak.

(iii) Since $\mathcal{R}_0$ is significantly sensitive to the initial susceptible epithelial cells, U^0 (the within-host level parameter) and the rate of infection of cells from the blood, ϵ this implies that FMD interventions such as vaccination (which reduces susceptible epithelial cells within the cattle) would be more effective to control the spread of FMD infection at the beginning of outbreak.

(iv) Since $\mathcal{R}_0$ is significantly sensitive to the rate of production of antibodies, ϕ_A and rate at which FMDV virus is cleared, ω this implies that FMD interventions such as vaccination (which increases the rate of antibody production and clearance of FMDV virus) would be more effective to control the spread of FMD infection at the beginning of outbreak.

2.5.1.1 Influence of within-host scale parameters of the FMD multiscale model dynamics

In this section, we demonstrate by implementing numerical simulations the impact of within-host scale parameters

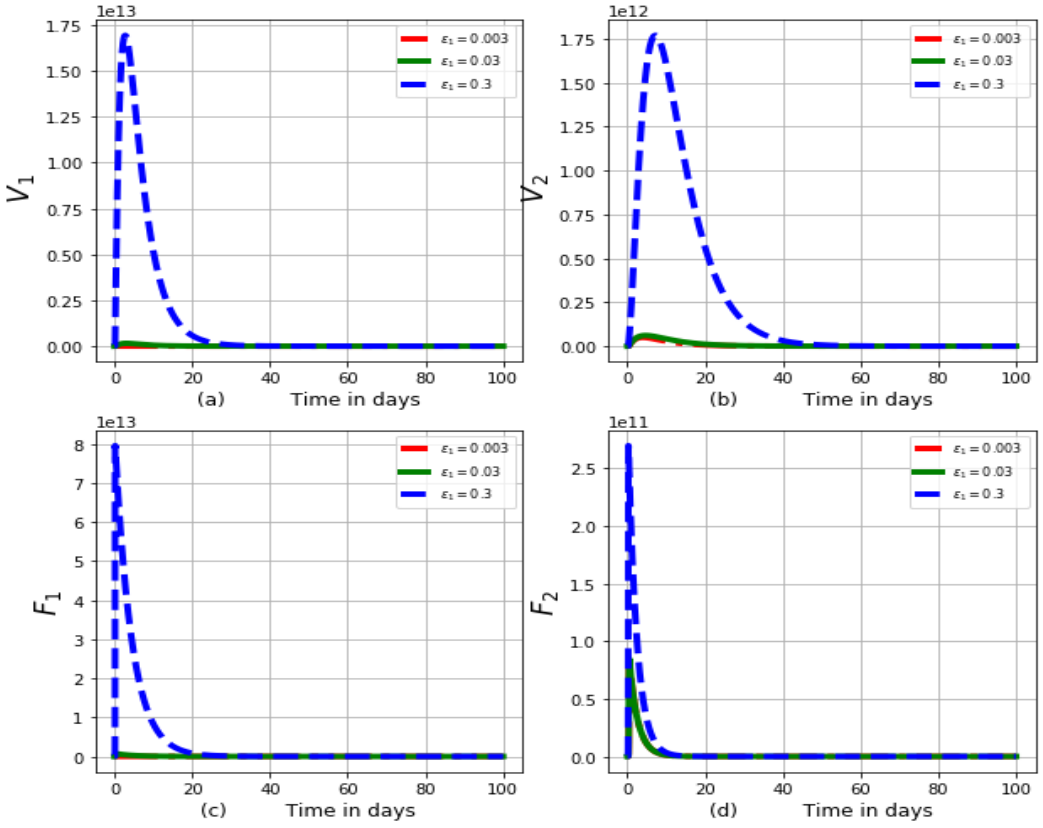

Figure 2.3: Graphs of numerical results of the model system (2.2.1) demonstrating the advancement with time of (a) concentration of virions in the blood for individual 1, V_1, (b) concentration of virions in the blood for individual 2, V_2, (c) infected cells for individual 1, F_1, (d) infected cells for individual 2, F_2 for variant values of infection rate of cells from the blood for individual 1, ϵ_1 : $\epsilon_1 = 0.003$, $\epsilon_1 = 0.03$ and $\epsilon_1 = 0.3$

Figure 2.3 represents the graphs of numerical results of model system (2.2.1) demonstrating the progression in time of (a) concentration of virions in the blood for individual 1, V_1, (b) concentration of virions in the blood for individual 2, V_2, (c) infected cells for individual 1, F_1, (d) infected cells for individual 2, F_2 for variant values of infection rate of cells from the blood for individual 1, $\epsilon_1 : \epsilon_1 = 0.003, \epsilon_1 = 0.03$ and $\epsilon_1 = 0.3$. From these results we can see that as the rate of infection of cells from the blood for individual 1, ϵ_1 increases, there is significant increase in the concentration of virions in the blood for individual 1, concentration of virions in the blood for individual 2, infected cells for individual 1, infected cells for individual 2. These results reflect that interventions such as vaccination of cattle will reduce the rate of infection of cells from the blood leading to a reduced risk of transmission of FMD for the individual in the community.

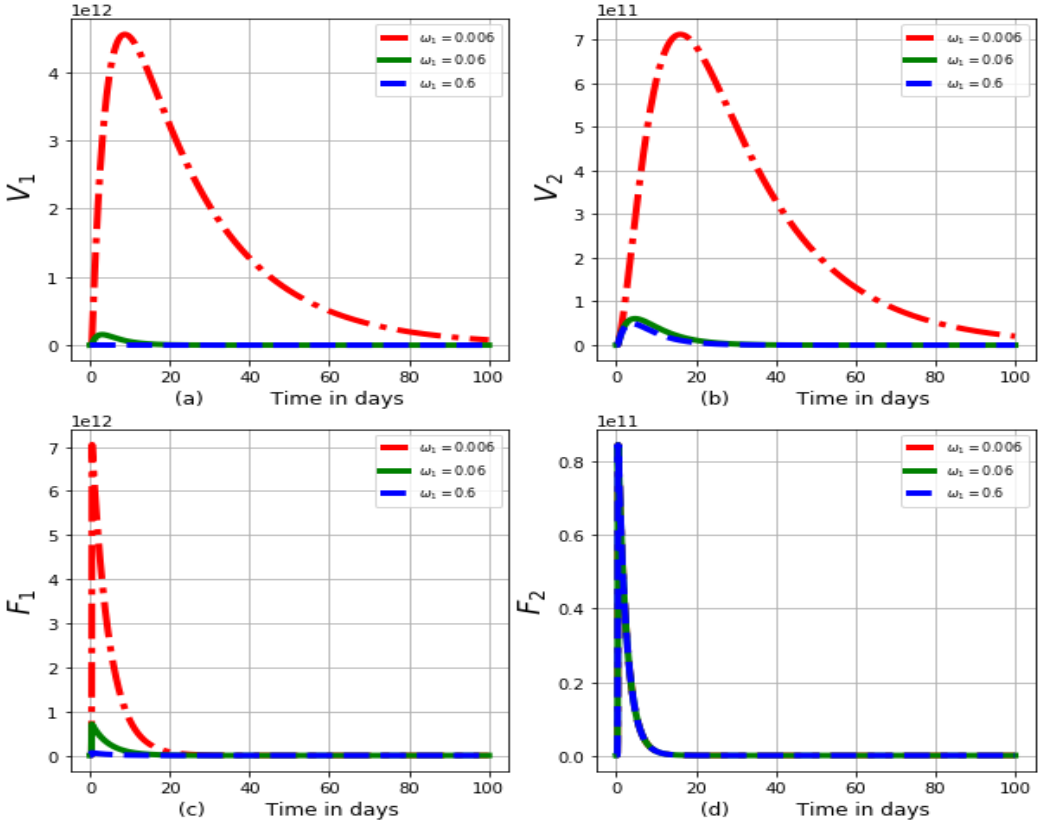

Figure 2.4: Graphs of numerical results of the model system (2.2.1) demonstrating the advancement with time of (a) concentration of virions in the blood for individual 1, V_1, (b) concentration of virions in the blood for individual 2, V_2, (c) infected cells for individual 1, F_1, (d) infected cells for individual 2, F_2 for variant values of rate at which virus is cleared for individual 1, $\omega_1 : \omega_1 = 0.006, \omega_1 = 0.06$ and $\omega_1 = 0.6$

Figure 2.4 demonstrates the impact of variation of rate at which virus is cleared, $\omega_1 : \omega_1 = 0.006, \omega_1 = 0.06$ and $\omega_1 = 0.6$ on the within-host scale variables $V_i, F_i, U_i, P_i, I_i, A_i, C_i, J_i$. The outcomes demonstrate that a decrease in ω is related to an increment in the within-cattle scale variables $(V_i, F_i, I_i, C_i, J_i)$. An increment in the within-cattle scale variables like V_i and F_i implies that there is an increase in FMDV shedding into the environment and an increase in the strength of transmission of FMDV , β, throughout the cattle population. The within-host scale variables I_i, C_i, A_i represent the early immune response which

intensifies as rate at which virus is cleared decreases.

2.5.1.2 Influence of between-host scale parameters of the FMD multiscale model dynamics

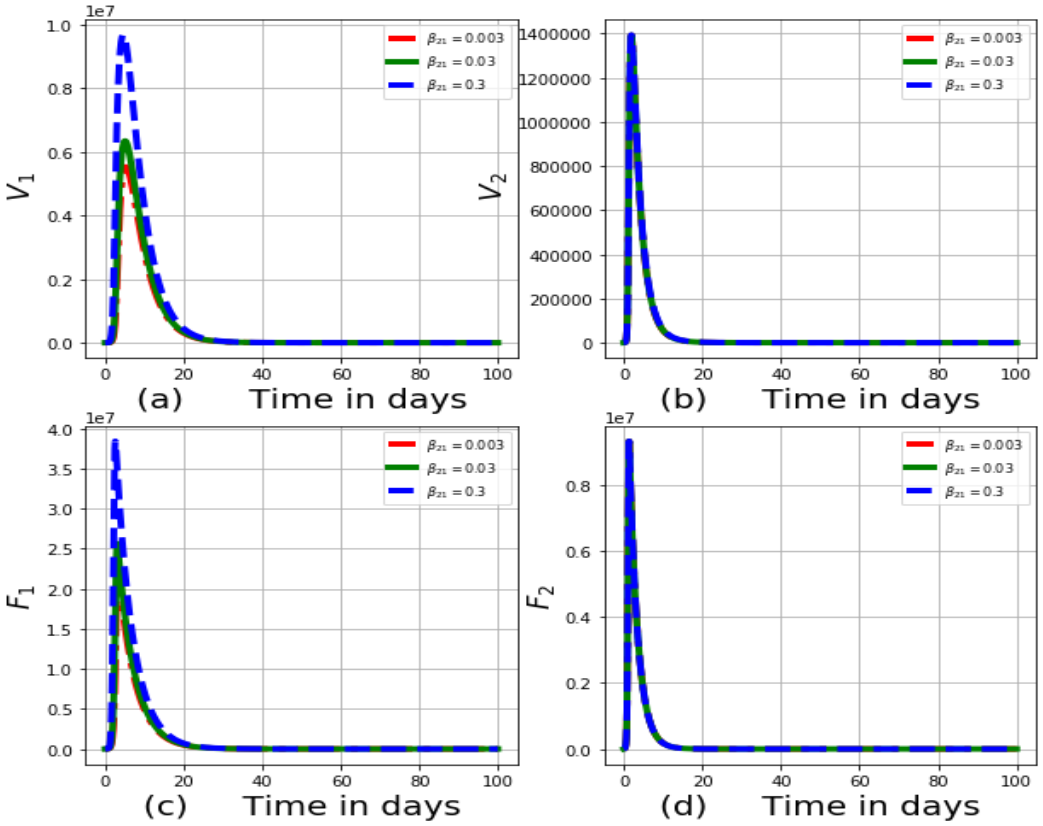

Figure 2.5: Graphs of numerical results of the model system (2.2.1) demonstrating the advancement with time of all model variables for variant values of rate of transmission of virus from individual 2 to individual 1, β_{21} : $\beta_{21} = 0.003$, $\beta_{21} = 0.03$ and $\beta_{21} = 0.3$

Figure 2.5 represents the graphs of numerical results of the model system (2.2.1) demonstrating the advancement with time of all model variables for variant values of rate of transmission of virus from individual 2 to individual 1, β_{21} : $\beta_{21} = 0.003$, $\beta_{21} = 0.03$ and $\beta_{21} = 0.3$. Results indicate that as the rate of transmission of virus from individual 2 to individual 1 increases, there is an increase in the within-cattle scale variables like V_1 and F_1.

2.5.1.3 Network of cattle population

Figure 2.6: The diagram represents the network degree distribution in the cattle population

In Figure 2.6 the diagram represents a network of a population of 50 cattle that has been generated using age-dependent data. The size of each node represents the number of contacts of cattle in the network. The nodes that have the same colour represent cattle of the same age group.

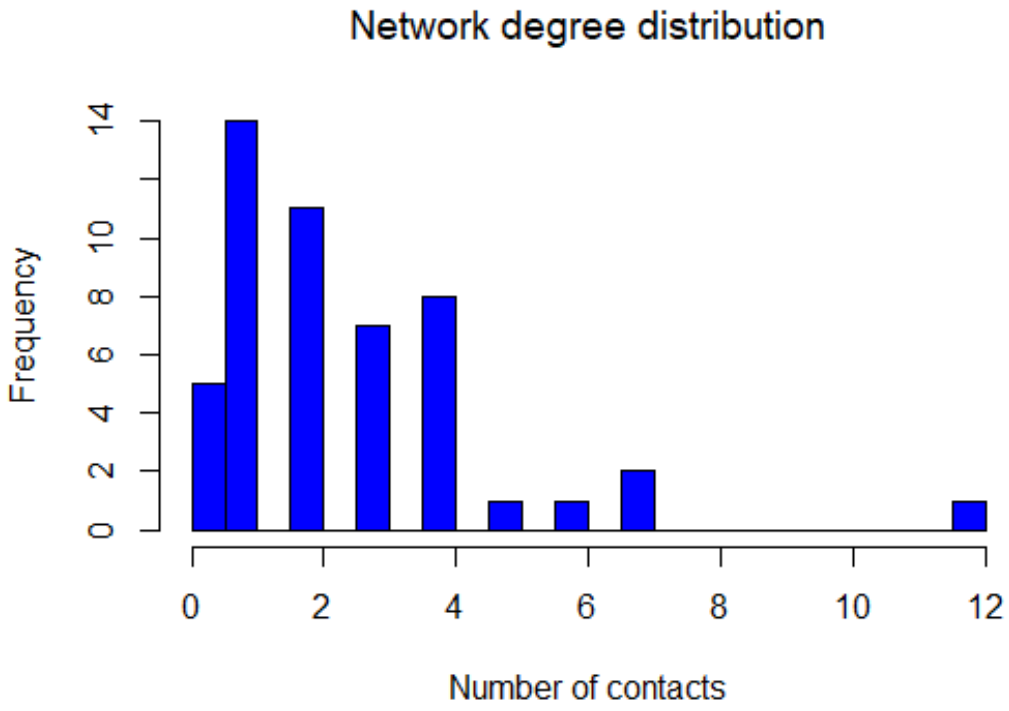

Figure 2.7: The diagram represents the network degree distribution in the cattle population

2.6 Effects of stochasticity on the model

In this section we introduce a white noise (dW_Q/dt) (that is, W(t) is a Brownian motion), where $Q = \{V_i, F_i, U_i, P_i, I_i, A_i, C_i, J_i\}$, into multiscale model system (2.2.1) which becomes

$$\begin{cases} dV_i = \left[\zeta F_i - \phi_A(t)\omega V_i + \sum_{i\neq j}^{n} \beta_{ij} V_j\right] dt + \sigma_V V_i dW_V(t), \\ dF_i = [\epsilon U_i V_i - \zeta F_i]\, dt + \sigma_F F_i dW_F(t), \\ dU_i = \left[-\kappa U_i \left(I_i - \frac{\mu}{\xi}\right)\right] dt + \sigma_U U_i dW_U(t), \\ dP_i = \left[\kappa U_i \left(I_i - \frac{\mu}{\xi}\right)\right] dt + \sigma_P P_i dW_P(t), \\ dI_i = [\mu - \xi I_i + \phi_U(U)\eta C_i]\, dt + \sigma_I I_i dW_I(t), \\ dA_i = [\phi_V(V,J)\phi_A(t)]\, dt + \sigma_A A_i dW_A(t), \\ dC_i = [\phi_A(t)\omega(V_i + J_i) - \sigma C_i]\, dt + \sigma_C C_i dW_C(t), \\ dJ_i = [\gamma\zeta F_i - \phi_A(t)\omega J_i]\, dt + \sigma_J J_i dW_J(t) \end{cases} \tag{2.6.1}$$

We set $W(t) = W_V(t), W_F(t), W_U(t), W_P(t), W_I(t), W_A(t), W_C(t), W_J(t)$ an 8-dimensional Wiener process that is defined on this probability space. Further, the constants σ_V, σ_F, σ_U, σ_P, σ_I, σ_A, σ_C, σ_J are non-negative and describe the intensities of the stochastic pertubations. Let us assume that the components of the 1-dimensional Wiener process W_i are mutually independent. It can be shown that the SDE model (2.6.1) has at least a unique global solution in order for the model to have meaning and also that the solution will always remain positive whenever the initial conditions are positive. Let us consider the following proposition.

Proposition 2.8. *For model (2.6.1) and any initial value in $\mathbb{R}^8_+$, there is a unique solution $L = (V_i, F_i, U_i, P_i, I_i, A_i, C_i, J_i)$ where $i = 1, ..., n$ of the system (2.6.1) for $t \geq 0$ which will remain in $\mathbb{R}^8_+$ with probability one.*

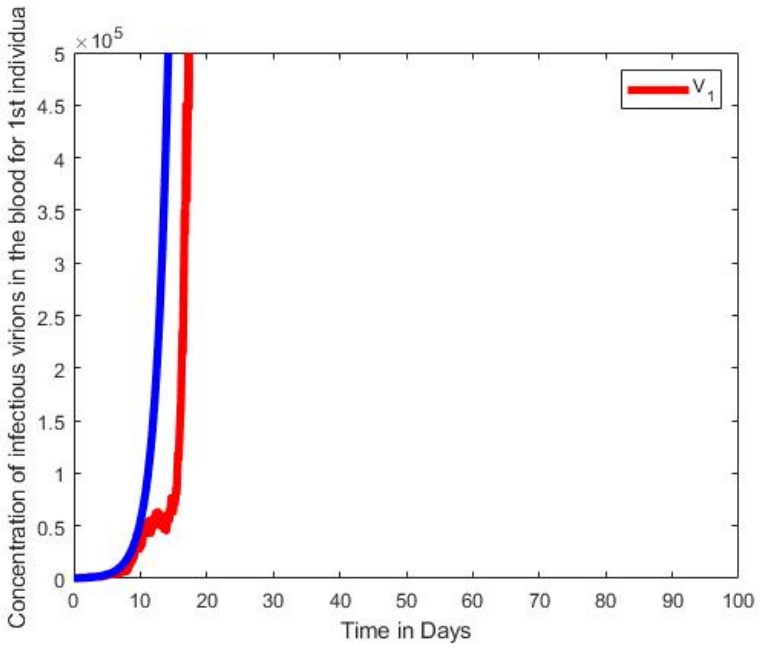

Figure 2.8: Graphs of numerical results of infectious virions in blood in the 1st individual, V_1 of the multiscale SDE model system (2.6.1) with the ODE multiscale model system (2.2.1) solutions. For the SDE $dt = 0.01$ and $\sigma = 0.3$

Figure 2.8 demonstrates the graphs of numerical results of infectious virions in blood in the 1st individual, V_1 of the multiscale SDE model system (2.6.1) with the ODE multiscale model system (2.2.1) solutions. For the SDE $dt = 0.01$ and $\sigma = 0.3$. The solution for the stochastic multiscale model is obtained using the Milsten method.

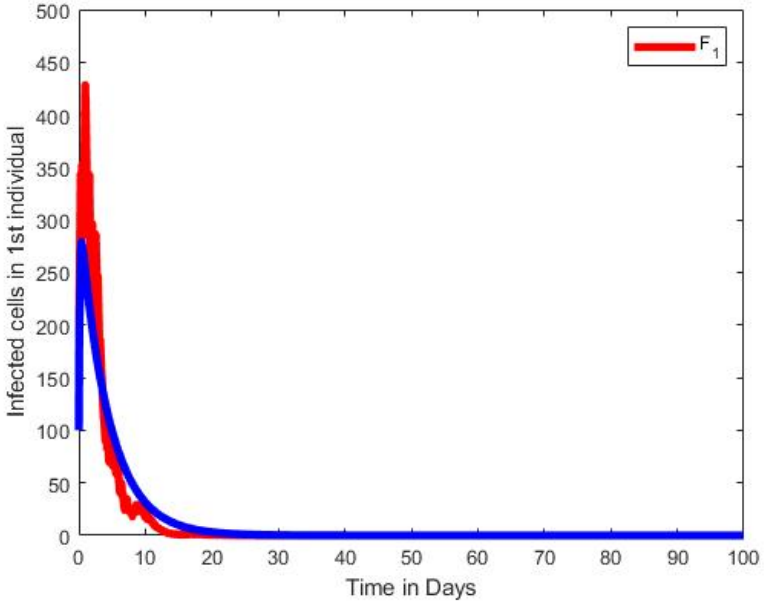

Figure 2.9: Graphs of numerical results of the infected cells in the 1st individual, F_1 of the multiscale SDE model system (2.6.1) with the ODE multiscale model system (2.2.1) solutions. For the SDE $dt = 0.01$ and $\sigma = 0.3$

Figure 2.9 demonstrates the graphs of numerical results of the infected cells in the 1st individual, F_1 of the multiscale SDE model system (2.6.1) with the ODE multiscale model system (2.2.1) solutions. For the SDE $dt = 0.01$ and $\sigma = 0.3$ The solution for the stochastic multiscale model is obtained using the Milsten method.

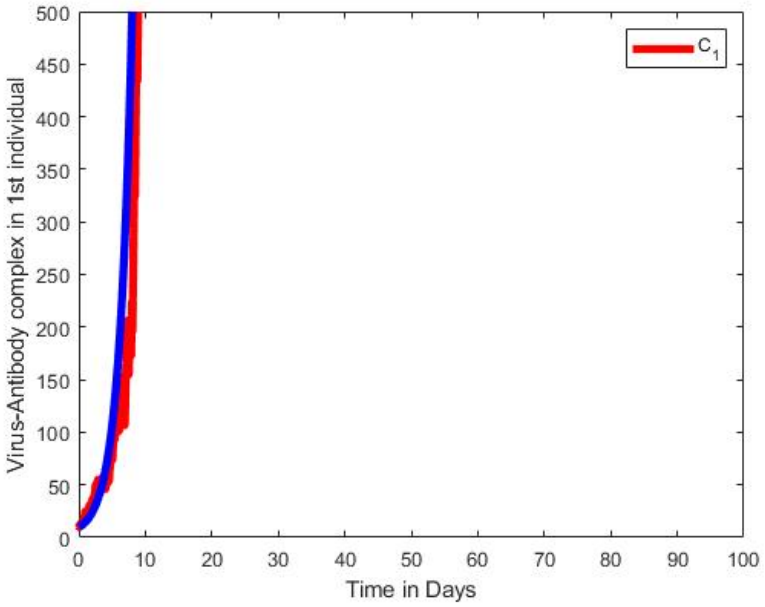

Figure 2.10: Graphs of numerical results of the Virus-antibody complex in the 1st individual, C_1 of the multiscale SDE model system (2.6.1) with the ODE multiscale model system (2.2.1) solutions. For the SDE $dt = 0.01$ and $\sigma = 0.3$

Figure 2.10 demonstrates the graphs of numerical results of the Virus-antibody complex in the 1st individual, C_1 of the multiscale SDE model system (2.6.1) with the ODE multiscale model system (2.2.1) solutions. For the SDE $dt = 0.01$ and $\sigma = 0.3$ For the SDE $dt = 0.01$ and $\sigma = 0.3$. The solution for the stochastic multiscale model is obtained using the Milsten method.

Figure 2.11 demonstrates the graphs of numerical results of the non-infectious material in the 1st individual, J_1 of the multiscale SDE model system (2.6.1) with the ODE multiscale model system (2.2.1) solutions. For the SDE $dt = 0.01$ and $\sigma = 0.3$. The solution for the stochastic multiscale model is obtained using the Milsten method.

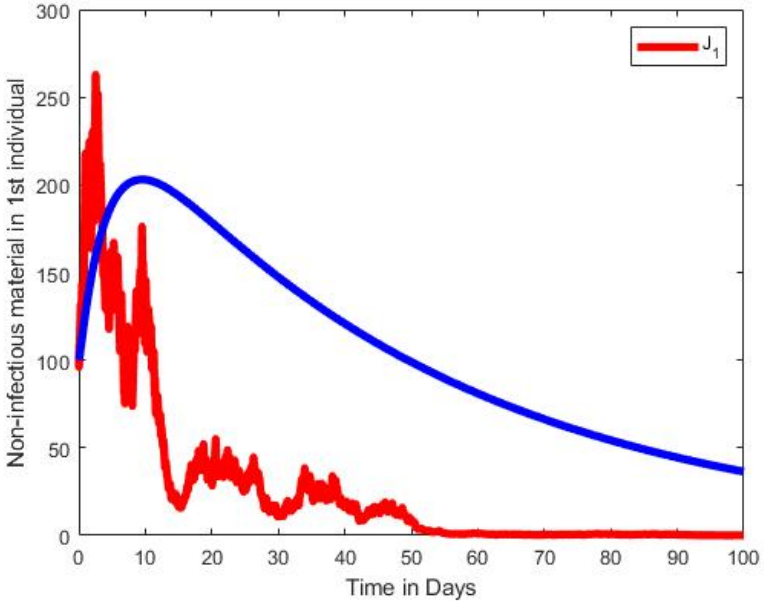

Figure 2.11: Graphs of numerical results of the non-infectious material in the 1st individual, J_1 of the multiscale SDE model system (2.6.1) with the ODE multiscale model system (2.2.1) solutions. For the SDE $dt = 0.01$ and $\sigma = 0.3$

2.7 Summary

In this chapter, we characterised an individual-based network modelling multiscale model of foot-and-mouth disease at host-level. The derivation of the model is achieved by first developing a within-cattle model and then embedding the model into a spatial network of N cattle. Thus, in order to describe the whole disease dynamics we implemented explicitly the within-cattle model. Through mathematical analysis the model was determined to be epidemiologically and mathematically sound. The analysis of sensitivity of the FMDV indicator $\mathcal{R}_0$, in relation to the variation of FMD model parameters was carried out by implementing Latin Hypercube Sampling and Partial Rank Correlation Coefficients (PRCCs). Applying the model parameter values we carried out the numerical simulations to demonstrate the impact of five FMD transmission parameters $(\beta_{ij}, U^0, \phi, \omega, \epsilon)$ on the model variables $V_i, F_i, U_i, P_i, I_i, A_i, C_i, J_i$. These parameters were only selected because they were significantly responsive to $\mathcal{R}_0$. In view of the fact that $\mathcal{R}_0$ was responsive to the transmission rate between the cattle, β_{ij} (the between-host level parameter) it implied that FMD interventions such as quarantines would be more effective to control the spread of FMD infection at the beginning of the outbreak. Furthermore, since $\mathcal{R}_0$ was significantly responsive to the rate of production of antibodies, ϕ_A and rate at which FMDV virus is cleared, ω this implied that FMD interventions such as vaccination (which increases the rate of antibody production and clearance of FMDV virus) would be more effective to control the spread of FMD infection at the beginning of outbreak. The inclusion of a stochastic model enabled us to capture randomness of disease spread. The application of this method may be relevant in managing foot-and-mouth disease and can be generalized to numerous directly transmitted diseases.

In conclusion, we established that we cannot extend the individual-based network model to a higher level of organisation using graph-theoretic method. Instead we could use different methods to extend the individual-based network modelling multiscale model to a higher level. Furthermore, we established that there is a primary level multiscale cycle of FMD dynamics.

Chapter 3

Host-level Multi-scale model of Foot-and-Mouth disease in cattle

3.1 Introduction

Infectious disease sytems have been considered as complex systems since they exhibit multilevel and multiscale nature. The use of multiscale models enables the integration of multiple scales involved in disease dynamics. In this chapter, we present a nested approach that integrates within-host and between-host scales of a disease system having a cycle for pathogen replication at the within-host scale for FMD in cattle. In other words, we characterise the host level model of FMD in cattle using the nested approach. We characterise the effect of the variation on within-cattle and between-cattle parameters on FMD dynamics. Hence, we are able to establish if the nested approach is applicable to modelling the multiscale dynamics of infectious diseases with within-cattle scale replication-cycle using FMD as a paradigm. In the case of environmentally-transmitted disease systems at host-level, the within-cattle scale and between-cattle scale are used as the key ingredients in developing multiscale models. For FMD in cattle as an environmentally-transmitted disease system, the within-cattle scale involves the interaction of FMD virus with the susceptible epithelial cells and other immune response cells within the infected cattle. The within-host scale for each individual will determine how the individual animal will transmit the virus into the environment, thus spreading the disease at cattle population-level. Transmission at this scale can be altered by interventions such as vaccination. The between-host scale involves the transmission of FMD virus between the cattle and their physical environment. This occurs through direct contact with infected animals and through fomites [90]. Transmission at the between-host scale can be altered through control measures such as movement restrictions, quarantine ,etc [94].

Numerous models in the literature have been formulated to investigate the dynamics of FMD infection in cattle with the aim of controlling, eliminating and eradicating this disease using single-scale modelling approach [7, 25]. However, to date, there is very limited literature on the modelling of FMD dynamics at multiscale. To the best of our knowledge the nested multiscale modelling approach we present is a novel method implemented in formulating the dynamics of FMD in cattle.

3.2 Derivation of the Nested Multiscale Model for the Dynamics of FMD

We consider the between-cattle scale sub-model and the within-cattle scale sub-model to formulate a multiscale model of infectious diseases at host-level. We establish a nested multiscale model that combines the between-cattle sub-model related to the dynamics of FMD disease spread and the within-cattle scale sub-model related to the replication dynamics of FMD virus within infected cattle. In section (3.2.1.1) we present the two sub-models for FMD transmission dynamics at two scales, the between-cattle scale and the within-cattle scale and then combine the two sub-models into a multiscale model in section (3.2.1.2).

3.2.1 Development of the Multiscale model for FMD transmission dynamics

3.2.1.1 The two sub-models of FMD transmission dynamics

(1) *Between-cattle scale FMDV transmission dynamics*. This submodel is demonstrated using the SI model and tracks the dynamics of two cattle populations namely suscepible cattle (S_C) and infected cattle population,I_C. The total cattle population is given by $N_C = S_C + I_C$. The following assumptions are now considered for this sub-model.

(i) Infected cattle population can naturally recover from FMD virus infection.

(ii) Transmission parameter $\hat{\beta}_C$ is a function of the number of infected cattle so that $\hat{\beta}_C = \hat{\beta}_C(I_C)$.

(iii) The dynamics of S_C and I_C are both considered to take place at slow time scale, t in comparison to the within-cattle scale FDMV transmission dynamics sub-model variables so that $S_C = S_C(t)$ and $I_C = I_C(t)$.

From these assumptions we have the following sub-model for the between-cattle scale FMDV transmission dynamics.

$$\text{Between-cattle sub-model:} \begin{cases} \dfrac{dS_C}{dt} = \Lambda_C - \hat{\beta}_C\left(I_C\right) S_C - \mu_C^{S_C} S_C + \delta_C I_C \\ \dfrac{dI_C}{dt} = \hat{\beta}_C\left(I_C\right) S_C - (\delta_C + \mu_C^{I_C}) I_C \end{cases} \tag{3.2.1}$$

The first equation in the sub-model (3.2.1) represents the susceptible cattle dynamics. This population is presumed to have increments through birth at a rate of Λ_C and at a constant rate of δ_C due to the recovered. The population decays through FMD infection of the susceptible cattle $\hat{\beta}_C\left(I_C\right)$ and natural death at a rate $\mu_C^{S_C}$. The second equation in the sub-model (3.2.1) represents the dynamics of FMDV infected cattle. The population increases when susceptible cattle are infected. The population decays through natural death rate, $\mu_C^{I_C}$ and mortality rate induced by FMD, δ_C.

(2) *Within-cattle scale FMDV dynamics*. The sub-model describes the interplay between antibody, A, virions in blood, V, interferon, I, uninfected epithelial cells, U, infected epithelial cells, F, non-infectious material denoted by J, virus-antibody complexes, C and protected cells, P. The within-cattle scale sub-model was initially developed by Howey [7]. Here we make the following assumptions:

(i) The within-cattle scale disease dynamics happen at fast time scale, s in comparison to the between-cattle scale FMDV sub-model variables so that $V = V(s)$, $F = F(s)$, $U = U(s)$, $P = P(s)$, $I = I(s)$, $A = A(s)$, $C = C(s)$ and $J = J(s)$.

(ii) The within-cattle scale viral load $V = V(s)$ is a proxy for the individual cattle infectiousness.

Below is the within-cattle scale sub-model.

$$
\begin{aligned}
\frac{dV(s)}{ds} &= \zeta F(s) - \phi_A \omega V(s), \ldots\ldots\ldots\ldots\ldots\ldots\ldots\ldots(1)\\
\frac{dF(s)}{ds} &= \epsilon U(s)V(s) - \zeta F(s), \ldots\ldots\ldots\ldots\ldots\ldots\ldots\ldots(2)\\
\frac{dU(s)}{ds} &= -\kappa U(s)\left(I(s) - \frac{\mu}{\xi}\right), \ldots\ldots\ldots\ldots\ldots\ldots\ldots\ldots(3)\\
\frac{dP(s)}{ds} &= \kappa U(s)\left(I(s) - \frac{\mu}{\xi}\right), \ldots\ldots\ldots\ldots\ldots\ldots\ldots\ldots(4)\\
\frac{dI(s)}{ds} &= \mu - \xi I(s) + \phi_U(U)\eta C(s), \ldots\ldots\ldots\ldots\ldots\ldots\ldots\ldots(5)\\
\frac{dA(s)}{ds} &= \phi_V(V,J)\phi_A, \ldots\ldots\ldots\ldots\ldots\ldots\ldots\ldots\ldots\ldots\ldots\ldots(6)\\
\frac{dC(s)}{ds} &= \phi_A \omega(V(s) + J(s)) - \sigma C(s), \ldots\ldots\ldots\ldots\ldots\ldots\ldots\ldots(7)\\
\frac{dJ(s)}{ds} &= \gamma\zeta F(s) - \phi_A \omega J(s), \ldots\ldots\ldots\ldots\ldots\ldots\ldots\ldots\ldots(8)
\end{aligned}
\tag{3.2.2}
$$

3.2.1.2 Integrating the two sub-models of FMDV transmission dynamics to form a single multi-scale model

In order to formulate the model, the individual infectiousness V, connects the within-cattle scale to the between-cattle scale whereas exposure $\hat{\beta}_C(I_C)$, connects between-catle scale to within-cattle scale, [17].

The within-cattle scale sub-model is unidirectionally coupled to the between-cattle scale FMDV transmission dynamics sub-model. In order to integrate the two sub-models shown in subsubsection (3.2.1.1) we make inferences about the association between the independent variables of the within-cattle virus population dynamics, A and V, and the parameters of the between-cattle scale viral transmission dynamics sub-model, $\hat{\beta}_C(I_C)$ and $\hat{\delta}_C$. Next we apply the concept of ecosystems to the within-cattle FMDV dynamics in which case we take into consideration FMDV infected cattle as individual microbial ecosystems that are unevenly distributed and homogeneous [104–106]. Let us consider the following derivations and assumptions.

(1) Taking FMDV into consideration, when the cattle host is taken as an ecosystem [104–106], then the cattle host death or survival can be regarded as an appropriate indicator of the emanant ecosystem property due to FMDV and antibody interplay within an infected animal. Therefore, we make the presupposition that the disease induced death rate of cattle in the between-cattle scale sub-model (3.2.1) is an emanant ecosystem property due to FMDV and is a function of the within-cattle scale FMDV and antibody dynamics such that $\hat{\delta}_C$ will become $\hat{\delta}_C = \hat{\delta}_C(V, A)$.

(2) Additionally, we make the assumption that the parameter of transmission in the between-cattle scale FMDV spread dynamics sub-model, $\hat{\beta}_C(I_C)$, is a function of the between-cattle scale infected cattle $I_C(t)$ and the within-cattle scale virus V resulting in $\hat{\beta}_C(I_C)$ being rewritten as $\hat{\beta}_C = \hat{\beta}_C(V(s)I_C(t))$. Furthermore, the quantity $V(s)I_C(t)$ is a new variable at between-cattle scale that is replaced by $V_C(t)$ to give $V_C(t) = V(s)I_C(t)$. In this case $V_C(t)$ is the total infectious resevoir of cattle in the community which we shall call CVL. With reference to CVL, the transmission parameter $\hat{\beta}_C$, for between-cattle scale FMD virus transmission dynamics sub-model becomes $\hat{\beta}_C = \hat{\beta}_C(V_C(t))$. In addition, we presume a Holling type II functional form of the function $\hat{\beta}_C(V_C)$ such that the force of infection, represented by $\lambda_C(t)$, related to FMDV infectivity to cattle at community scale is

$$\lambda_C(t) = \hat{\beta}_C(V_C(t)) = \frac{\beta_C V_C(t)}{V_0 + V_C(t)} \tag{3.2.3}$$

where β_C is the exposure to CVL per unit through contact and V_C is the CVL at the time of contact whilst

$$\lambda_C\left[V_C(t)\right] = \frac{V_C(t)}{V_0 + V_C(t)} \tag{3.2.4}$$

is probability that random contact with an animal in a community will infect the animal with FMDV in the community. From expressions (3.2.3) and (3.2.4), V_0 is the community FMD viral load that produces 50% chance of getting an individual animal infected with FMD virus after random contact in a community infected. When we look at the sub-model system (3.2.2), the differential equation of $V(s)$ is

$$\frac{dV(s)}{ds} = \zeta F(s) - \phi_A \omega V(s) \tag{3.2.5}$$

Additionally, when we apply the ecosystems concepts from [104–106] to the within-cattle population dynamics of FMD virus, we make the assumption that infected cattle in a certain community are small unevenly distributed and homogeneous habitats where FMDV survives and replicates until it becomes infectious to susceptible cattle. The rate of change of CVL V_C , in the whole commumity that is composed of $I_C(t)$ is given by

$$\frac{dV_C}{dt} = V(s)\alpha I_C(t) - \hat{\alpha}_C(V, A)V_C \tag{3.2.6}$$

where $\hat{\alpha}_C(V, A)$ is the community wide elimination rate of the total infectious reservoir of cattle V_C. The between-cattle scale FMDV transmission dynamics sub-model can be expressed as

$$\begin{cases} \dfrac{dS_C(t)}{dt} = \Lambda_C - \lambda_C(t)S_C(t) - \mu_C{}^{S_C}S_C(t) + d_C I_C(t) \\ \dfrac{dI_C(t)}{dt} = \lambda_C(t)S_C(t) - (\hat{\delta}_C(V, A) + d_C + \mu_C{}^{I_C})I_C(t) \\ \dfrac{dV_C(t)}{dt} = V(s)\alpha I_C(t) - \hat{\alpha}_C(V, A)V_C(t) \end{cases} \tag{3.2.7}$$

The complete model for FMD virus transmission dynamics from animal-to-animal is given by

$$
\begin{cases}
\dfrac{dV(s)}{ds} = \zeta F(s) - \phi_A \omega V(s), \\
\dfrac{dF(s)}{ds} = \epsilon U(s) V(s) - \zeta F(s), \\
\dfrac{dU(s)}{ds} = -\kappa U(s) \left(I(s) - \dfrac{\mu}{\xi} \right), \\
\dfrac{dP(s)}{ds} = \kappa U(s) \left(I(s) - \dfrac{\mu}{\xi} \right), \\
\dfrac{dI(s)}{ds} = \mu - \xi I(s) + \phi_U(U) \eta C(s), \\
\dfrac{dA(s)}{ds} = \phi_V(V, J) \phi_A, \\
\dfrac{dC(s)}{ds} = \phi_A \omega (V(s) + J(s)) - \sigma C(s), \\
\dfrac{dJ(s)}{ds} = \gamma \zeta F(s) - \phi_A \omega J(s) \\
\dfrac{dS_C(t)}{dt} = \Lambda_C - \lambda_C(t) S_C(t) - \mu_C{}^{S_C} S_C(t) + d_C I_C(t) \\
\dfrac{dI_C(t)}{dt} = \lambda_C(t) S_C(t) - (\hat{\delta}_C(V, A) + d_C + \mu_C{}^{I_C}) I_C(t) \\
\dfrac{dV_C(t)}{dt} = V(s) \alpha I_C(t) - \hat{\alpha}_C(V, A) V_C(t)
\end{cases}
\tag{3.2.8}
$$

The new multiscale model in (3.2.8) is called nested multiscale model [2]. This approach enables us to scale up from within-cattle FMD viral dynamics to between-cattle FMD viral spread.

Table 3.1: Description of between-host scale model variables.

Variable	Description
$S_C(t)$	Susceptible cattle
$I_C(t)$	Infectious cattle
$V_C(t)$	Community viral load

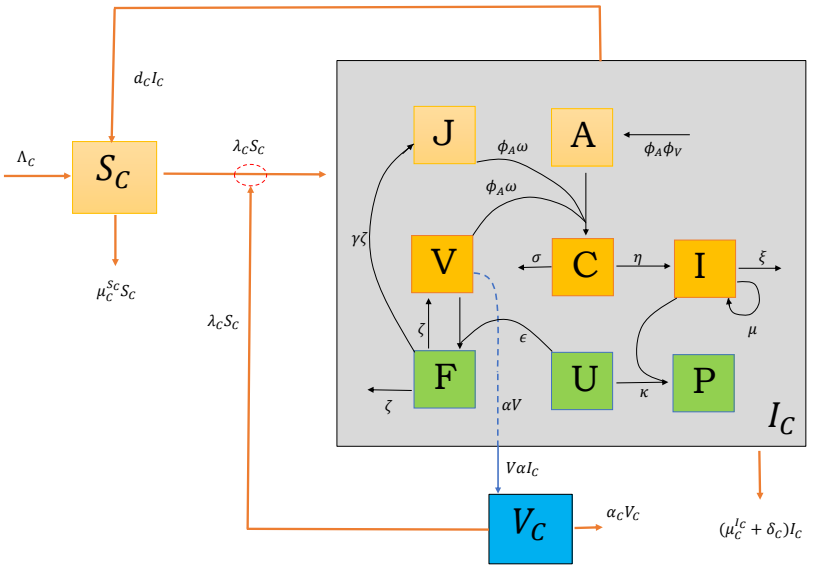

Figure 3.1: A schematic diagram of the complete multiscale model of FMDV transmission dynamics. Note that δ_C stands for $\hat{\delta}_C(V, A)$ and α_C stands for $\hat{\alpha}_C(V, A)$.

Table 3.2: Description of within-host model variables

Variable	Description	Units	Initial value
F	Infected cells	TCID_{50} ml^{-1}	0
C	Virus-antibody complexes	TCID_{50} ml^{-1} equiv.	0
P	Protected cells	Cell	0
U	Uninfected cells	Cell	1
A	Antibody	LPBE-titre	0
V	Conc. of virions in blood	TCID_{50} ml^{-1}	0
J	Non-infectious material	TCID_{50} ml^{-1} equiv.	0
I	Interferon	IU ml^{-1}	$\frac{\mu}{\xi}$

3.2.1.3 The simplified model of FMDV transmission dynamics

Due to time-scale discrepancy between the within-cattle scale submodel time-scale and the between-cattle scale submodel time-scale, we apply a slow and fast time-scale analysis. From the within-cattle sub-model (3.2.2) we can re-write the model system (3.2.2) using the slow time scale t by assuming a relation between the fast and slow time-scales to be $t = \varepsilon s$ where $0 < \varepsilon \ll 1$, so that the within-cattle scale FMD virus spread dynamics sub-model can be re-written in terms of the slow time-scale as follows:

$$
\begin{cases}
\varepsilon \dfrac{dV(t)}{dt} = \zeta F(t) - \phi_A \omega V(t), \\
\varepsilon \dfrac{dF(t)}{dt} = \epsilon U(t) V(t) - \zeta F(t), \\
\varepsilon \dfrac{dU(t)}{dt} = -\kappa U(t) \left(I(t) - \dfrac{\mu}{\xi} \right), \\
\varepsilon \dfrac{dP(t)}{dt} = \kappa U(t) \left(I(t) - \dfrac{\mu}{\xi} \right), \\
\varepsilon \dfrac{dI(t)}{dt} = \mu - \xi I(t) + \phi_U(U) \eta C(t), \\
\varepsilon \dfrac{dA(t)}{dt} = \phi_V(V, J) \phi_A, \\
\varepsilon \dfrac{dC(t)}{dt} = \phi_A \omega (V(t) + J(t)) - \sigma C(t), \\
\varepsilon \dfrac{dJ(t)}{dt} = \gamma \zeta F(t) - \phi_A \omega J(t)
\end{cases}
\tag{3.2.9}
$$

From the within-cattle scale model system (3.2.9), ε is represents the fast time-scale of the within-cattle scale submodel in comparison to the slow time-scale of the between-cattle scale FMD viral spread dynamics sub-model. Since $0 < \varepsilon \ll 1$, we let $\varepsilon = 0$ so that the within-cattle scale FMD viral spread dynamics sub-model becomes independent of time and we obtain the following result.

$$\begin{cases} \zeta\tilde{F} - \phi_A\omega\tilde{V} = 0, \\ \epsilon\tilde{U}\tilde{V} - \zeta\tilde{F} = 0, \\ -\kappa\tilde{U}\left(\tilde{I} - \dfrac{\mu}{\xi}\right) = 0, \\ \kappa\tilde{U}\left(\tilde{I} - \dfrac{\mu}{\xi}\right) = 0, \\ \mu - \xi\tilde{I} + \phi_U(U)\eta\tilde{C} = 0, \\ \phi_V(V,J)\phi_A = 0, \\ \phi_A\omega(\tilde{V} + \tilde{J}) - \sigma\tilde{C} = 0, \\ \gamma\zeta\tilde{F} - \phi_A\omega\tilde{J} = 0 \end{cases} \tag{3.2.10}$$

$$\begin{cases} \tilde{V} = \dfrac{\zeta\mathfrak{R}_0\tilde{F}}{\epsilon U^0} \\ \tilde{F} = \dfrac{\epsilon U^0}{\zeta\mathfrak{R}_0}\tilde{V} \\ \tilde{U} = U^0 \\ \tilde{I} = \dfrac{\mu}{\xi} \\ \tilde{J} = \dfrac{\gamma\epsilon U^0}{\phi_A\omega\mathfrak{R}_0}\tilde{V} \\ \tilde{C} = \dfrac{\left[\phi_A\omega\mathfrak{R}_0 + \gamma\epsilon U^0\right]}{\sigma\mathfrak{R}_0}\tilde{V} \end{cases} \tag{3.2.11}$$

where

$$\mathfrak{R}_0 = \frac{\epsilon U^0}{\phi_A\omega} \tag{3.2.12}$$

$\mathfrak{R}_0$ represents the control reproduction number of the within-cattle scale. It is defined as the number of secondary infections generated by an infected individual when introduced into a population where proportions are protected (that is, not a completely susceptible population). Therefore, the slow and fast time-scale analysis results in the within-cattle scale submodel system (3.2.2) being condensed to algebraic equations as illustrated in (3.2.10) which can be resolved to get some values as described by the expressions in equation (3.2.11) which have an effect on the variables and parameters of the between-cattle scale submodel as shown below:

$$\begin{cases} \dfrac{dS_C(t)}{dt} = \Lambda_C - \lambda_C(t)S_C(t) - {\mu_C}^{S_C}S_C(t) + d_C I_C(t) \\ \dfrac{dI_C(t)}{dt} = \lambda_C(t)S_C(t) - (\hat{\delta}_C(\tilde{V},\tilde{A}) + d_C + {\mu_C}^{I_C})I_C(t) \\ \dfrac{dV_C(t)}{dt} = \tilde{V}(s)\alpha I_C(t) - \hat{\alpha}_C(\tilde{V},\tilde{A})V_C(t) \end{cases} \tag{3.2.13}$$

Therefore

$$N = \tilde{V}, \quad \delta_C = \hat{\delta}_C(\tilde{V},\tilde{A}), \quad \alpha_C = \hat{\alpha}_C(\tilde{V},\tilde{A}). \tag{3.2.14}$$

Consequently, the full multi-scale model (3.2.8) of FMD virus transmission dynamics is simplified to become

$$\begin{cases} \dfrac{dS_C(t)}{dt} = \Lambda_C - \dfrac{\beta_C V_C(t)}{V_0 + V_C(t)}S_C(t) - {\mu_C}^{S_C}S_C(t) + d_C I_C(t) \\ \dfrac{dI_C(t)}{dt} = \dfrac{\beta_C V_C(t)}{V_0 + V_C(t)}S_C(t) - (\delta_C + d_C + {\mu_C}^{I_C})I_C(t) \\ \dfrac{dV_C(t)}{dt} = N\alpha I_C(t) - \alpha_C V_C(t) \end{cases} \tag{3.2.15}$$

where

$$N = \frac{\zeta \mathfrak{R}_0 \tilde{F}}{\epsilon U^0}, \quad \mathfrak{R}_0 = \frac{\epsilon U^0}{\phi_A \omega} \tag{3.2.16}$$

3.3 Mathematical Analysis of the Baseline multi-scale model of Foot-and-Mouth disease dynamics

3.3.1 Positivity of solutions

Theorem 3.1. *A non-negative solution* $(S_C(t), I_C(t), V_C(t))$ *exists for all* $t \geq 0$

Proof. The positivity of the solutions of the model system (3.2.15) is proved using the integrating factor technique. We consider the first equation in the multiscale model system

$$\frac{dS_C(t)}{dt} = \Lambda_C - \frac{\beta_C V_C(t)}{V_0 + V_C(t)} S_C(t) - \mu_C{}^{S_C} S_C(t) + d_C I_C(t) \tag{3.3.1}$$

We re-write equation (3.3.1) as follows

$$\frac{dS_C(t)}{dt} + \left[\frac{\beta_C V_C(t)}{V_0 + V_C(t)} + \mu_C{}^{S_C}\right] S_C(t) = \Lambda_C + d_C I_C(t) \tag{3.3.2}$$

The integrating factor for equation (3.3.2) is

$$\text{Integrating factor (IF)} = e^{\int_0^t \left[\frac{\beta_C V_C(s)}{V_0+V_C(s)} + \mu_C{}^{S_C}\right] ds} = e^{\left(\beta_C + \mu_C^{S_C}\right)t - \beta_C V_0 \ln\left|\frac{V_0+V_C(t)}{V_0+V_C(0)}\right|} \tag{3.3.3}$$

We multiple equation (3.3.2) by the integrating factor $e^{\left(\beta_C + \mu_C^{S_C}\right)t - \beta_C V_0 \ln\left|\frac{V_0+V_C(t)}{V_0+V_C(0)}\right|}$ to get

$$e^{\left(\beta_C + \mu_C^{S_C}\right)t - \beta_C V_0 \ln\left|\frac{V_0+V_C(t)}{V_0+V_C(0)}\right|}.\frac{dS_C(t)}{dt} + e^{\left(\beta_C + \mu_C^{S_C}\right)t - \beta_C V_0 \ln\left|\frac{V_0+V_C(t)}{V_0+V_C(0)}\right|}.\left[\frac{\beta_C V_C(t)}{V_0 + V_C(t)} + \mu_C{}^{S_C}\right] S_C(t)$$

$$= e^{\left(\beta_C + \mu_C^{S_C}\right)t - \beta_C V_0 \ln\left|\frac{V_0+V_C(t)}{V_0+V_C(0)}\right|}.\left[\Lambda_C + d_C I_C(t)\right] \tag{3.3.4}$$

From the product rule we obtain

$$\frac{d}{dt}\left[e^{\left(\beta_C + \mu_C^{S_C}\right)t - \beta_C V_0 \ln\left|\frac{V_0+V_C(t)}{V_0+V_C(0)}\right|}.S_C(t)\right] = e^{\left(\beta_C + \mu_C^{S_C}\right)t - \beta_C V_0 \ln\left|\frac{V_0+V_C(t)}{V_0+V_C(0)}\right|}.\left[\Lambda_C + d_C I_C(t)\right] \tag{3.3.5}$$

Dividing both sides by the integrating factor we get

$$S_C(t) = e^{-\left\{\left(\beta_C + \mu_C^{S_C}\right)t - \beta_C V_0 \ln\left|\frac{V_0+V_C(t)}{V_0+V_C(0)}\right|\right\}}.\int_0^t e^{\left(\beta_C + \mu_C^{S_C}\right)s - \beta_C V_0 \ln\left|\frac{V_0+V_C(s)}{V_0+V_C(0)}\right|}.\left[\Lambda_C + d_C I_C(s)\right] ds \geq 0 \tag{3.3.6}$$

Similarly, positivity of the other two equations of multiscale model system (3.2.15) is proved using the integrating factor technique. Consequently, $S_C(t) \geq 0, I_C(t) \geq 0, V_C(t) \geq 0$ for all time $t > 0$. □

3.3.2 Boundedness of Solutions

Letting $N_C(t)$ to represent the total number of cattle population and adding the first and second equation of the multiscale model system (3.2.15), we get

$$\frac{dN_C}{dt} = \Lambda_C - \mu_C N_C(t) - \delta_C I_C(t) \tag{3.3.1}$$

so that

$$\frac{dN_C}{dt} \leq \Lambda_C - \mu_C N_C(t) \tag{3.3.2}$$

This means that

$$\lim_{t\to\infty} \sup(N_C(t)) \leq \frac{\Lambda_C}{\mu_C} \tag{3.3.3}$$

Since $N_C(t)$ is the sum of the state variables for susceptible cattle and infected cattle then each of the individual state variables is less or equal to $\frac{\Lambda_C}{\mu_C}$. Implementing the third equation of the model system (3.2.15) we get the following inequality

$$\frac{dV_C(t)}{dt} \leq N\alpha\frac{\Lambda_C}{\mu_C} - \alpha_C V_C \tag{3.3.4}$$

since $I_C(t) \leq \frac{\Lambda_C}{\mu_C}$. Therefore, the solution of equation (3.3.4) can be obtained by using a suitable integrating factor $e^{\alpha_C t}$ to get

$$V_C(t) \leq \frac{N\alpha\Lambda_C}{\alpha_C\mu_C} + C_1 e^{-\alpha_C t} \tag{3.3.5}$$

This implies that

$$\lim_{t\to\infty} \sup(V_C(t)) \leq \frac{N\alpha\Lambda_C}{\alpha_C\mu_C} \tag{3.3.6}$$

Letting

$$\Omega = \left\{(S_C; I_C; V_C) \in \mathbb{R}^3_+ : 0 \leq S_C + I_C \leq K_1, 0 \leq V_C \leq K_2\right\} \tag{3.3.7}$$

where the constants K_1 and K_2 are such that

$$\begin{cases} K_1 = \dfrac{\Lambda_C}{\mu_C}, \\ \\ K_2 = \dfrac{N\alpha\Lambda_C}{\alpha_C\mu_C} > 0 \end{cases} \tag{3.3.8}$$

Therefore, Ω is a positively invariant and attracting region, since all the solutions that start in Ω will remain in Ω for all $t \geq 0$. Consequently, we can conclude that the multiscale model system (3.2.15) is mathematically and epidemiologically well-posed.

3.4 Determination of disease-free equilibrium and its stability

3.4.1 The disease-free equilibrium point

In this section we establish the disease-free equilibrium point of the multiscale model system by letting the right-hand side of the multi-scale model system (3.2.15) to zero and assume $I_C = V_C = 0$. When the equilibrium is disease-free, FMD virus does not exist and therefore no spread in the cattle population. Thus, the multi-scale model system (3.2.15) has a disease-free equilibrium illustrated by

$$E^0 = \left(S_C^0, I_C^0, V_C^0\right) = \left(\frac{\Lambda_C}{\mu_C{}^{S_C}}, 0, 0\right) \tag{3.4.1}$$

We now consider the reproductive number, $\mathcal{R}_0$ which is an important parameter in epidemic models.

3.4.2 The Disease-free equilibrium state and Its Stability

3.4.2.1 The model reproductive number

The multiscale model system (3.2.15) can be expressed as follows:

$$\begin{cases} \dfrac{dX}{dt} = f(X, Z), \\ \\ \dfrac{dZ}{dt} = h(X, Z), \end{cases} \tag{3.4.1}$$

where

$$X = S_C$$

$$Z = (I_C, V_C)$$

The elements of X stand for the number of susceptibles as well as other groups of non-infectious individuals. The elements of Z stand for infected individuals able to transmit the disease. Let us define $\tilde{g}(X^*, Z)$ from [101] as follows:

$$\tilde{g}(X^*, Z) = \begin{bmatrix} \frac{\beta_C V_C(t)}{V_0 + V_C(t)} S_C(t) - (\delta_C + d_C + \mu_C{}^{I_C}) I_C(t) \\ \\ N\alpha I_C(t) - \alpha_C V_C(t) \end{bmatrix} \tag{3.4.2}$$

A matrix

$$A = \begin{bmatrix} -(\delta_C + d_C + \mu_C{}^{I_C}) & \frac{\beta_C \Lambda_C}{V_0 \mu_C{}^{S_C}} \\ N\alpha & -\alpha_C \end{bmatrix} \tag{3.4.3}$$

Therefore

$$M = \begin{bmatrix} 0 & \frac{\beta_C \Lambda_C}{V_0 \mu_C{}^{S_C}} \\ N\alpha & 0 \end{bmatrix} \tag{3.4.4}$$

$$D = \begin{bmatrix} (\delta_C + d_C + \mu_C{}^{I_C}) & 0 \\ 0 & \alpha_C \end{bmatrix} \tag{3.4.5}$$

$$D^{-1} = \begin{bmatrix} \frac{1}{(\delta_C + d_C + \mu_C{}^{I_C})} & 0 \\ 0 & \frac{1}{\alpha_C} \end{bmatrix} \tag{3.4.6}$$

$$MD^{-1} = \begin{bmatrix} 0 & \frac{\beta_C \Lambda_C}{V_0 \mu_C{}^{S_C} \alpha_C} \\ \frac{N\alpha}{(\delta_C + d_C + \mu_C{}^{I_C})} & 0 \end{bmatrix} \tag{3.4.7}$$

Then $\mathcal{R}_0 = \rho\left(MD^{-1}\right)$

Hence, the basic reproduction number of the model system (3.2.15) is expressed as follows.

$$\left\{ \therefore \quad \mathcal{R}_0 = \sqrt{\frac{N\alpha\beta_C\Lambda_C}{V_0 \mu_C{}^{S_C} \alpha_C (\delta_C + d_C + \mu_C{}^{S_C})}} \right. \tag{3.4.8}$$

3.4.2.2 Local Stability of the disease-free equilibrium (DFE)

In relation to Theorem 2 of [103], $\mathcal{R}_0 < 1$, the disease-free equilibrium is locally asymptotically stable and there cannot be an outbreak. We ascertain the local stability of the disease-free-equilibrium, E^0 of the multi-scale model system (3.2.15) by establishing the Jacobian matrix of the system at the disease-free equilibrium.

(i) In the case when the community viral load is an extended state of host infectiousness the shedding of FMDV virus $(N\alpha)$ into the blood is put into the D matrix instead of the M matrix, such that the matrices M and D become:

$$M_e = \begin{bmatrix} 0 & \frac{\beta_C \Lambda_C}{V_0 {\mu_C}^{S_C}} \\ 0 & 0 \end{bmatrix} \tag{3.4.9}$$

$$D_e = \begin{bmatrix} (\delta_C + d_C + {\mu_C}^{I_C}) & 0 \\ -N\alpha & \alpha_C \end{bmatrix} \tag{3.4.10}$$

and the next generation matrix A_e is given by

$$A_e = M_e D_e^{-1} = \begin{bmatrix} \frac{N\alpha\beta_C\Lambda_C}{V_0{\mu_C}^{S_C}\alpha_C(\delta_C + d_C + {\mu_C}^{I_C})} & \frac{\beta_C\Lambda_C}{V_0{\mu_C}^{S_C}\alpha_C} \\ 0 & 0 \end{bmatrix} \tag{3.4.11}$$

Consequently, $\mathcal{R}_0^e = \rho(M_e D_e^{-1})$. Therefore, we have the following expression.

$$\begin{cases} \mathcal{R}_0^e = \dfrac{N\alpha\beta_C\Lambda_C}{V_0{\mu_C}^{S_C}\alpha_C(\delta_C + d_C + {\mu_C}^{S_C})} = R_{0Cc}.R_{0cC} \end{cases} \tag{3.4.12}$$

where R_{0Cc} is the cattle-to-community partial reproductive number and R_{0cC} is the community-to-cattle partial reproductive number.

(ii) In the case when the community is taken as a reservoir of the infective FMDV the shedding rate of FMDV into the blood $(N\alpha)$ is put into the M matrix instead of the D matrix, such that the matrices M and D become

$$M_r = \begin{bmatrix} 0 & \frac{\beta_C \Lambda_C}{V_0 {\mu_C}^{S_C}} \\ N\alpha & 0 \end{bmatrix} \tag{3.4.13}$$

$$D_r = \begin{bmatrix} (\delta_C + d_C + {\mu_C}^{I_C}) & 0 \\ 0 & \alpha_C \end{bmatrix} \tag{3.4.14}$$

and the next generation matrix A_r is given by

$$A_r = M_r D_r^{-1} = \begin{bmatrix} 0 & \frac{\beta_C \Lambda_C}{V_0 \mu_C{}^{S_C} \alpha_C} \\ \frac{N\alpha}{(\delta_C + d_C + \mu_C{}^{I_C})} & 0 \end{bmatrix} \tag{3.4.15}$$

Therefore, $\mathcal{R}_0^r = \rho(M_r D_r^{-1})$ which becomes

$$\left\{ \therefore \quad \mathcal{R}_0^r = \sqrt{\frac{N\alpha\beta_C\Lambda_C}{V_0\mu_C{}^{S_C}\alpha_C(\delta_C + d_C + \mu_C{}^{I_C})}} = \sqrt{R_{0Cc}.R_{0cC}} \right. \tag{3.4.16}$$

Wherefore, the multi-scale model system (3.2.15) has two reproductive numbers which are given by:

$$\begin{cases} \mathcal{R}_0^e = \dfrac{N\alpha\beta_C\Lambda_C}{V_0\mu_C{}^{S_C}\alpha_C(\delta_C + d_C + \mu_C{}^{I_C})} = R_{0Cc}.R_{0cC} \\ \text{and} \\ \mathcal{R}_0^r = \sqrt{\dfrac{N\alpha\beta_C\Lambda_C}{V_0\mu_C{}^{S_C}\alpha_C(\delta_C + d_C + \mu_C{}^{I_C})}} = \sqrt{R_{0Cc}.R_{0cC}} \end{cases} \tag{3.4.17}$$

The two partial basic reproductive numbers $\mathcal{R}_0^e$ and $\mathcal{R}_0^r$ given by equation (3.4.17) are explained below:

(a) Suppose that a newly infected animal invades a FMD disease-free community. The individual is still present and infectious and the expected amount of infectious reservoir contributed to the total infectious reservoir of cattle in the community (CVL) by this infected individual animal during the total period of infectiousness is approximately

$$\mathcal{R}_{0Cc} = \frac{N\alpha}{(\delta_C + d_C + \mu_C{}^{I_C})} \tag{3.4.18}$$

In the equation (3.4.18) above the quantity depends on the average FMD viral load in the individual animal's body N which is passed into the blood at a rate α of an infected individual animal, where it becomes infectious to other cattle that it comes into contact with during the individual animal's total infectiousness period. N is a parameter which is explained in this study as the endemic value of the within-cattle scale FMD viral load $\tilde{V}$ which we have already obtained from the within-cattle FMD dynamics sub-model (3.2.2) as

$$N = \frac{\zeta \mathfrak{R}_0 \tilde{F}}{\epsilon U^0}, \quad \mathfrak{R}_0 = \frac{\epsilon U^0}{\phi_A \omega} \tag{3.4.19}$$

From the equation (3.4.18) for $\mathcal{R}_{0Cc}$, $\frac{N\alpha}{(\delta_C + d_C + \mu_C{}^{I_C})}$ is elucidated as the rate illustrating the contribution of an infected individual to the CVL (the total infectious reservoir of cattle in the community) for the duration of the animal's total infectiousness period. On the other hand, $\frac{1}{(\delta_C + d_C + \mu_C{}^{I_C})}$ is the average lifespan of a FMD infected individual animal.

(b) Equivalently, we suppose that a single infectious dose of FMD virus invading FMD viral load-free community with susceptible cattle at equilibrium. This infectious dose is still present and infectious and the expected number of infected cattle coming from each infectious dose of FMD virus is approximately

$$\mathcal{R}_{0cC} = \frac{\beta_C \Lambda_C}{\mu_C^{S_C} \alpha_C V_0} \tag{3.4.20}$$

The partial reproductive number $\mathcal{R}_{0cC}$ in equation (3.4.20) above relies on susceptible cattle supply Λ, the susceptible animal's average lifespan $\frac{1}{\mu_C^{S_C}}$, the susceptible cattle contact rate with the infectious reservoir of cattle, β_C, the average time it takes to suppress the infectious reservoir of cattle in the community to below detection levels $\frac{1}{\alpha_C}$ and the susceptibility coefficient to FMDV infection in the community $\frac{1}{V_0}$ where V_0 is the CVL that leads to 50% chance for the cattle getting infected. Consequently, we can conclude that $\mathcal{R}_0$ is consisting of between-cattle scale FMD disease parameters and within-cattle scale FMD disease parameters. Due to it's straightforwardness we will use $\mathcal{R}_0 = \mathcal{R}_0^e$ as the basic reproductive number of the multiscale model system (3.2.15).

Lemma 3.2. *The matrix $(M - D)$ has a real spectrum. Moreover, if $\rho\left(MD^{-1}\right) < 1$, all eigenvalues of $(M - D)$ are negative.*

3.4.2.3 Local Stability of the Foot-and-Mouth Disease-free state

In this subsection, we establish the local stability of DFE for the multiscale model system (3.2.15) by linearizing the three equations of model system (3.2.15) to get the following Jacobian matrix given as

$$J(E_0) = \begin{bmatrix} -\mu_C & d_C & -\frac{\beta_C \Lambda_C}{V_0 \mu_C} \\ 0 & -(\delta_C + d_C + \mu_C^{I_C}) & \frac{\beta_C \Lambda_C}{V_0 \mu_C} \\ 0 & N\alpha & -\alpha_C \end{bmatrix} \tag{3.4.21}$$

We investigate stability of DFE by calculating the eigenvalues of the Jacobian matrix in (3.4.21) at the DFE. The characteristic equation for eigenvalues is given by

$$(-\mu_C - \lambda)\left[\lambda^2 + \pi_1\lambda + \pi_2\right] = 0 \tag{3.4.22}$$

where

$$\begin{cases} \pi_1 = \delta_C + d_C + \mu_C^{I_C} + \alpha_C, \\ \\ \pi_2 = \alpha_C\left(\delta_C + d_C + \mu_C^{I_C}\right)\left(1 - \mathcal{R}_0^2\right) \end{cases} \tag{3.4.23}$$

From equation (3.4.22) it can be seen that one of the eigenvalues is $\lambda = -\mu_C$. Considering the remaining eigenvalues of the polynomial

$$P(\lambda) = \lambda^2 + \pi_1\lambda + \pi_2 = 0 \tag{3.4.24}$$

we apply the Routh-Hurwitz Criterion. We define the following matrices as the coefficients (πs) of the characteristic polynomial $P(\lambda)$ in equation (3.4.24)

$$H_1 = (\pi_1)\,,\ H_2 = \begin{pmatrix} \pi_1 & 1 \\ 0 & \pi_2 \end{pmatrix} \tag{3.4.25}$$

Evaluating the determinant of H_1, we get

$$\det(H_1) = |\pi_1| = \pi_1 = \delta_C + d_C + \mu_C^{I_C} + \alpha_C > 0 \tag{3.4.26}$$

The determinant of H_2 is given by

$$\det(H_2) = \begin{vmatrix} \pi_1 & 1 \\ 0 & \pi_2 \end{vmatrix} = \pi_1\pi_2 = \phi_C\left(1 - \mathcal{R}_0^2\right) > 0 \text{ whenever } \mathcal{R}_0 < 1 \tag{3.4.27}$$

All the coefficients π_1 and π_2 of the polynomial $P(\lambda)$ in the equation (3.4.24) are greater than zero whenever $\mathcal{R}_0 < 1$. In addition, all the determinants of matrices H_1 and H_2 are positive if and only if $\mathcal{R}_0 < 1$. Therefore, all the roots of the polynomial $P(\lambda)$ are either negative or have negative real parts. Consequently, the DFE point of the model system is locally asymptotically stable if $\mathcal{R}_0 < 1$. □

Theorem 3.3. *The disease-free equilibrium point E^0 of the multi-scale model system (3.2.15) is locally asymptotically stable whenever $\mathcal{R}_0 < 1$ and unstable otherwise.*

3.4.2.4 Global Stability of the Disease-Free Equilibrium

We establish the global stability of DFE of the model system (3.2.15) by using a next generation operator [101]. We identify two conditions that warrant the global asymptotic stability of the disease-free state. The model system (3.2.15) can be written as follows:

$$\begin{cases} \dfrac{dX}{dt} = F(X,Z), \\ \\ \dfrac{dZ}{dt} = G(X,Z), \quad G(X,0) = 0 \end{cases} \tag{3.4.28}$$

where $X = S_C$ stands for all uninfected components and $Z = (I_C, V_C)$ stands for all infected and infectious components;

$$E^0 = \left(S_C^0, I_C^0, V_C^0\right) = \left(\frac{\Lambda_C}{\mu_C{}^{S_C}}, 0, 0\right) \tag{3.4.29}$$

denotes the disease-free equilibrium of the system. To warrant global asymptotic stability, the conditions $(H1)$ and $(H2)$ below must be met [101]:

(H1) For $\dfrac{dX}{dt} = F(X,0)$, X^* is globally asymptotically stable (g.a.s);

(H2) $G(X,Z) = AZ - \hat{G}(X,Z), \hat{G}(X,Z) \geq 0$ for $(X,Z) \in \Omega$,
where the Jacobian $A = \dfrac{\partial G}{\partial Z} = D_Z G(X^*, 0)$ is an M-matrix (the off diagonal elements of A are nonnegative) and Ω is the region where the model makes biological sense.

$$\frac{dX}{dt} = F(X,Z) = \Lambda_C - \frac{\beta_C V_C}{V_0 + V_C} S_C - \mu_C^{S_C} S_C + d_C I_C \tag{3.4.30}$$

At the disease-free equilibrium $Z = 0$

$$F(X,0) = \Lambda_C - \mu_C^{S_C} S_C \tag{3.4.31}$$

Since Ω is an invariant set for model system (3.2.15) and in view of Theorem 3.3, it is sufficient to show that for all $E_0 \in \Omega$

$$\lim_{t\to\infty} V_C(t) = 0, \quad \lim_{t\to\infty} I_C(t) = 0 \quad \text{and} \quad \lim_{t\to\infty} S_C(t) = S_C^0 \tag{3.4.32}$$

with S_C^0 as in (3.4.29). From the first equation of model system (3.2.15) it follows that

$$\frac{dS_C(t)}{dt} \leq \Lambda_C - \mu_C^{S_C} S_C(t) \tag{3.4.33}$$

It is easy to see that S_C^0 is a global asymptotically stable equilibrium for the comparison equation

$$\frac{dy(t)}{dt} = \Lambda_C - \mu_C^{S_C} y(t) \tag{3.4.34}$$

Then, for any $\varepsilon > 0$, there exists $\bar{t} > 0$, such that for all $t \geq \bar{t}$, it holds

$$S_C(t) \leq S_C^0 + \varepsilon \tag{3.4.35}$$

Hence

$$\lim_{t\to\infty} \sup S_C(t) \leq S_C^0 \tag{3.4.36}$$

Now, from (3.4.36) and the second and third equations of the model system (3.2.15) we have that for $t \geq \bar{t}$

$$\begin{cases} \dfrac{dI_C(t)}{dt} \leq \dfrac{\beta_C V_C(t)}{V_0 + V_C(t)} \left(S_C^0 + \varepsilon\right) - (\delta_C + d_C + \mu_C{}^{I_C}) I_C(t) \\ \dfrac{dV_C(t)}{dt} = N\alpha I_C(t) - \alpha_C V_C(t) \end{cases} \tag{3.4.37}$$

Let us now consider the comparison system

$$\begin{cases} \dfrac{dw_1(t)}{dt} = \dfrac{\beta_C w_2(t)}{V_0 + w_2(t)} \left(S_C^0 + \varepsilon\right) - (\delta_C + d_C + \mu_C{}^{I_C}) w_1(t) \\ \dfrac{dw_2(t)}{dt} = N\alpha w_1(t) - \alpha_C w_2(t), \quad w_1(\bar{t}) = I_C(\bar{t}), \quad w_2(\bar{t}) = V_C(\bar{t}) \end{cases} \tag{3.4.38}$$

that we can re-write as

$$\frac{dw(t)}{dt} = (F_\varepsilon - V_\varepsilon)\, w(t) \tag{3.4.39}$$

where $w(t) = (w_1(t), w_2(t))^T$ and $(F_\varepsilon - V_\varepsilon)$ is a matrix in (3.4.3) computed in $E_0(\varepsilon) = \left(S_C^0 + \varepsilon, 0, 0\right)$. Let us note that if $\mathcal{R}_0 = \rho\left(FV^{-1}\right) < 1$, we can choose a sufficiently small $\varepsilon > 0$ such that $\rho\left(F_\varepsilon V_\varepsilon^{-1}\right) <$

1. Then by applying Lemma 3.2 to $(F_\varepsilon - V_\varepsilon)$ we obtain that it has a real spectrum and all its eigenvalues are negative. It follows that $\lim_{t\to\infty} w(t) = 0$, whatever the initial conditions are, from which

$$\lim_{t\to\infty} I_C(t) = 0, \quad \text{and} \quad \lim_{t\to\infty} V_C(t) = 0 \tag{3.4.40}$$

Now, for any $\varepsilon > 0$, there exists $\bar{t}_1$ such that for any $t \geq \bar{t}_1$, $I_C(t) < \varepsilon$ and $V_C(t) < \varepsilon$. So, for $t \geq \bar{t}_1$ we have

$$\frac{dS_C(t)}{dt} \geq \Lambda_C - \frac{\beta_C \varepsilon}{V_0 + \varepsilon} S_C(t) - \mu_C^{S_C} S_C(t) + \varepsilon d_C \tag{3.4.41}$$

It is easy to see that $\dfrac{(\Lambda_C + \varepsilon d_C)(V_0 + \varepsilon)}{\left(\beta_C \varepsilon + \mu_C^{S_C}\right)(V_0 + \varepsilon)}$ is a global asymptotically stable equilibrium for the comparison equation

$$\frac{dy(t)}{dt} = \Lambda_C - \frac{\beta_C \varepsilon}{V_0 + \varepsilon} y(t) - \mu_C^{S_C} y(t) + \varepsilon d_C \tag{3.4.42}$$

Thus, for any $\chi > 0$, there exists $\bar{t}_2 > 0$ such that for all $t \geq \bar{t}_2$

$$S_C(t) \geq \frac{(\Lambda_C + \varepsilon d_C)(V_0 + \varepsilon)}{\left(\beta_C \varepsilon + \mu_C^{S_C}\right)(V_0 + \varepsilon)} - \chi \tag{3.4.43}$$

Then, for any $\varepsilon > 0$, we have

$$\lim_{t\to\infty} \inf S_C(t) \geq \frac{(\Lambda_C + \varepsilon d_C)(V_0 + \varepsilon)}{\left(\beta_C \varepsilon + \mu_C^{S_C}\right)(V_0 + \varepsilon)} \tag{3.4.44}$$

Letting $t \to \infty$, we have $\lim_{t\to\infty} \inf S_C(t) \geq S_C^0$ and combining this with (3.4.36) gives us

$$\lim_{t\to\infty} S_C(t) = S_C^0 \tag{3.4.45}$$

Therefore, $E^0 = \left(S_C^0, 0, 0\right)$ is a global asymptotically stable equilibrium point satisfying condition **H1**.

We now establish that condition **H2** is satisfied.

$$\frac{dZ}{dt} = G(X, Z) = \begin{bmatrix} \dfrac{\beta_C V_C}{V_0 + V_C} S_C - (\delta_C + d_C + \mu_C{}^{I_C}) I_C \\ \\ N\alpha I_C - \alpha_C V_C \end{bmatrix} \tag{3.4.46}$$

and $G(X,0)=0$

$$A = D_Z G(X_0,0) = \begin{bmatrix} -(\delta_C + d_C + \mu_C{}^{I_C}) & \dfrac{\beta_C \Lambda_C}{V_0 \mu_C{}^{S_C}} \\ N\alpha & -\alpha_C \end{bmatrix} \tag{3.4.47}$$

$$AZ = \begin{bmatrix} -(\delta_C + d_C + \mu_C{}^{I_C}) & \dfrac{\beta_C \Lambda_C}{V_0 \mu_C{}^{S_C}} \\ N\alpha & -\alpha_C \end{bmatrix} \begin{bmatrix} I_C \\ V_C \end{bmatrix} \tag{3.4.48}$$

$$= \begin{bmatrix} -(\delta_C + d_C + \mu_C{}^{I_C})I_C + \dfrac{\beta_C \Lambda_C}{V_0 \mu_C{}^{S_C}} V_C \\ N\alpha I_C - \alpha_C V_C \end{bmatrix} \tag{3.4.49}$$

$$\hat{G}(X,Z) = \begin{bmatrix} \hat{G}_1(X,Z) \\ \hat{G}_2(X,Z) \end{bmatrix} = \begin{bmatrix} \left(\dfrac{\Lambda_C}{\mu_C^{S_C} V_0} - \dfrac{S_C}{V_0 + V_C} \right) \beta_C V_C \\ 0 \end{bmatrix} \tag{3.4.50}$$

From (3.4.36) we have $S_C \leq S_C^0$ but $\dfrac{S_C}{V_0+V_C} \leq \dfrac{S_C}{V_0}$. Therefore $\dfrac{S_C}{V_0+V_C} \leq \dfrac{S_C}{V_0} \leq \dfrac{S_C^0}{V_0} = \dfrac{\Lambda_C}{\mu_C^{S_C} V_0}$

Since $\dfrac{\Lambda_C}{\mu_C^{S_C} V_0} \geq \dfrac{S_C}{V_0+V_C}$, it follows that $\hat{G}(X,Z \geq 0$ for all $(X,Z) \in \mathbb{R}^3_+$ and A is an M-matrix since the off diagonal elements of A are non-negative. Both conditions **H1** and **H2** are satisfied and hence E^0 is globally asymptotically stable for $\mathcal{R}_0 < 1$.

Theorem 3.4. *The fixed point*

$$E^0 = (X^*, 0) = \left(\frac{\Lambda_C}{\mu_C{}^{S_C}}, 0, 0 \right), \tag{3.4.51}$$

*of multi-scale model system (3.2.15) is globally asymptotically stable equilibrium if $\mathcal{R}_0 < 1$ and conditions **H1** and **H2** are satisfied.*

3.5 The endemic equilibrium and its stability

When the equilibrium is endemic then cattle population is infected by the FMD virus. The multi-scale model system (3.2.15) has an endemic equilibrium point given by

$$E^* = (S_C^*, I_C^*, V_C^*) \tag{3.5.1}$$

The three equations of the multi-scale model system (3.2.15) are set to zero on the left-hand side to give

$$\begin{cases} 0 = \Lambda_C - \lambda_C^* S_C^* - \mu_C^{S_C} S_C^* + d_C I_C^* \\ 0 = \lambda_C^* S_C^* - \left(\delta_C + d_C + \mu_C^{I_C}\right) I_C^* \\ 0 = N\alpha I_C^* - \alpha_C V_C^* \end{cases} \tag{3.5.2}$$

where

$$\lambda_C^* = \frac{\beta_C V_C^*}{V_0 + V_C^*} \tag{3.5.3}$$

Substituting (3.5.3) into (3.5.2) we get

$$\begin{cases} 0 = \Lambda_C - \dfrac{\beta_C V_C^*}{V_0 + V_C^*} S_C^* - \mu_C^{S_C} S_C^* + d_C I_C^* \\ 0 = \dfrac{\beta_C V_C^*}{V_0 + V_C^*} S_C^* - \left(\delta_C + d_C + \mu_C^{I_C}\right) I_C^* \\ 0 = N\alpha I_C^* - \alpha_C V_C^* \end{cases} \tag{3.5.4}$$

We can simplify (3.5.4) to obtain

$$\begin{cases} \left[\dfrac{\beta_C V_C^* - \mu_C^{S_C}\left(V_0 + V_C^*\right)}{V_0 + V_C^*}\right] S_C^* = \Lambda_C + d_C I_C^* \\ \dfrac{\beta_C V_C^*}{V_0 + V_C^*} S_C^* = \left(\delta_C + d_C + \mu_C^{I_C}\right) I_C^* \\ V_C^* = \dfrac{N\alpha I_C^*}{\alpha_C} \end{cases} \tag{3.5.5}$$

Substituting third equation of (3.5.5) into the first and second equation of (3.5.5) we get

$$\begin{cases} \left[\dfrac{\beta_C N\alpha I_C^* - \mu_C^{S_C}\left(V_0\alpha_C + N\alpha I_C^*\right)}{V_0\alpha_C + N\alpha I_C^*}\right] S_C^* = \Lambda_C + d_C I_C^* \\ \dfrac{\beta_C N\alpha I_C^*}{V_0\alpha_C + N\alpha I_C^*} S_C^* = \left(\delta_C + d_C + \mu_C^{I_C}\right) I_C^* \end{cases} \tag{3.5.6}$$

From (3.5.6) we equate the first and second equation to S_C^* to obtain

$$\begin{cases} S_C^* = \dfrac{\left(\Lambda_C + d_C I_C^*\right)\left(V_0\alpha_C + N\alpha I_C^*\right)}{\left[\beta_C N\alpha I_C^* - \mu_C^{S_C}\left(V_0\alpha_C + N\alpha I_C^*\right)\right]} \\ S_C^* = \dfrac{\left(\delta_C + d_C + \mu_C^{I_C}\right)\left(V_0\alpha_C + N\alpha I_C^*\right)}{\beta_C N\alpha} \end{cases} \tag{3.5.7}$$

Equating the first and second equation in (3.5.7) we get

$$\frac{\left(\Lambda_C + d_C I_C^*\right)\left(V_0\alpha_C + N\alpha I_C^*\right)}{\left[\beta_C N\alpha I_C^* - \mu_C^{S_C}\left(V_0\alpha_C + N\alpha I_C^*\right)\right]} = S_C^* = \frac{\left(\delta_C + d_C + \mu_C^{I_C}\right)\left(V_0\alpha_C + N\alpha I_C^*\right)}{\beta_C N\alpha} \tag{3.5.8}$$

Simplifying (3.5.8) we have

$$\frac{\left(\Lambda_C + d_C I_C^*\right)}{\left[\beta_C N\alpha I_C^* - \mu_C^{S_C}\left(V_0\alpha_C + N\alpha I_C^*\right)\right]} = \frac{\left(\delta_C + d_C + \mu_C^{I_C}\right)}{\beta_C N\alpha} \tag{3.5.9}$$

Further simplification of (3.5.9) gives

$$I_C^* = \frac{\Lambda_C\beta_C N\alpha - \mu_C^{S_C} V_0\alpha_C\left(\delta_C + d_C + \mu_C^{I_C}\right)}{\left[\beta_C N\alpha\left(\delta_C + d_C + \mu_C^{I_C}\right) + \mu^{S_C} N\alpha - d_C\beta_C N\alpha\right]} \tag{3.5.10}$$

Substituting (3.5.10) into (3.5.5) gives

$$\begin{cases} S_C^* = \dfrac{\alpha_C\left(\delta_C+d_C+\mu_C^{I_C}\right)\left[V_0\alpha_C\left(\left(\delta_C+d_C+\mu_C^{I_C}\right)\left(\beta_C+\mu_C^{S_C}\right)-d_C\beta_C\right)+\alpha_C\mu_C^{S_C}\left(\delta_C+d_C+\mu_C^{I_C}\right)V_0\left(\mathcal{R}_0^2-1\right)\right]}{\beta_C N\alpha\alpha_C\left[\left(\delta_C+d_C+\mu_C^{I_C}\right)\left(\beta_C+\mu_C^{S_C}\right)-d_C\beta_C\right]}, \\ I_C^* = \dfrac{\alpha_C\mu_C^{S_C}\left(\delta_C+d_C+\mu_C^{I_C}\right)V_0\left[\mathcal{R}_0^2-1\right]}{N\alpha\left[\left(\delta_C+d_C+\mu_C^{I_C}\right)\beta_C+\mu_C^{S_C}\left(\delta_C+d_C+\mu_C^{I_C}\right)-d_C\beta_C\right]} \\ V_C^* = \dfrac{\left[\alpha_C\mu_C^{S_C}\left(\delta_C+d_C+\mu_C^{I_C}\right)V_0\left[\mathcal{R}_0^2-1\right]\right]}{\alpha_C\left[\left(\delta_C+d_C+\mu_C^{I_C}\right)\beta_C+\mu_C^{S_C}\left(\delta_C+d_C+\mu_C^{I_C}\right)-d_C\beta_C\right]} \end{cases} \tag{3.5.11}$$

Furthermore, substituting the third equation of (3.5.11) into (3.5.3) gives

$$\lambda_C^* = \frac{\beta_C\left(\alpha_C\mu_C^{S_C}\left(\delta_C+d_C+\mu_C^{I_C}\right)V_0\left[\mathcal{R}_0^2-1\right]\right)}{V_0\alpha_C\left[\left(\delta_C+d_C+\mu_C^{I_C}\right)\left(\beta_C+\mu_C^{S_C}\right)-d_C\beta_C\right]+\beta_C\Lambda_C N\alpha-\alpha_C\mu_C^{S_C}\left(\delta_C+d_C+\mu_C^{I_C}\right)V_0} \tag{3.5.12}$$

Proposition 3.5. *The endemic equilibrium for the multiscale model system (3.2.15) given by equation (3.5.11) exists if* $\mathcal{R}_0 > 1$.

3.5.1 The Existence of the endemic equilibrium state

We now display some findings based on the existence of an endemic equilibrium or constant solution for model system (3.2.15) by implementing the threshold parameter, $\mathcal{R}_0$.

Theorem 3.6. *The multiscale model (3.2.15) formulated in terms of proportions has at least one endemic equilibrium solution given by*

$$E^* = (S_C^*, I_C^*, V_C^*) \tag{3.5.1}$$

with S_C^*, I_C^*, V_C^* *all non-negative, whose existence and properties are determined by the threshold parameter* $\mathcal{R}_0$ *given by*

$$\mathcal{R}_0 = \sqrt{\frac{N\alpha\beta_C\Lambda_C}{V_0\mu_C{}^{S_C}\alpha_C(\delta_C+d_C+\mu_C{}^{I_C})}} \tag{3.5.2}$$

Proof. Suppose $E^* = (S_C^*, I_C^*, V_C^*)$ is a constant solution of the multi-scale model system (3.2.15). We simply write S_C^*, I_C^* in terms of V_C^* in the form

$$\begin{cases} S_C^*(V_C^*) = \dfrac{\Lambda_C(\delta_C + d_C + \mu_C^{I_C})(V_0 + V_C^*)}{\left[\beta_C V_C^* + \mu_C^{S_C}(V_0 + V_C^*)\right](\delta_C + d_C + \mu_C^{I_C}) + d_C\beta_C V_C^*} \\ I_C^*(V_C^*) = \dfrac{\beta_C V_C^* \Lambda_C}{\left[\left[\beta_C V_C^* + \mu_C^{S_C}(V_0 + V_C^*)\right](\delta_C + d_C + \mu_C^{I_C}) + d_C\beta_C V_C^*\right]} \end{cases} \tag{3.5.3}$$

Substituting the expression in (3.5.3) in the equation for V_C in the multiscale model (3.2.15) which is given by

$$\frac{dV_C}{dt} = N\alpha I_C - \alpha_C V_C, \tag{3.5.4}$$

at the endemic equilibrium we get:

$$V_C\left[V_C A + B\right] = 0 \tag{3.5.5}$$

where

$$A = \left[\alpha_C\beta_C(\delta_C + d_C + \mu_C^{I_C}) + \alpha_C\mu_C^{I_C}(\delta_C + d_C + \mu_C^{I_C}) + \alpha_C d_C\beta_C\right]$$

and

$$B = \alpha_C\mu_C^{S_C}(\delta_C + d_C + \mu_C^{I_C})V_0 - N\alpha\beta_C\Lambda_C$$

We note that $V_C^* = 0$ matches the disease-free equilibrium. Consequently, from equation (3.5.5) we get:

$$V_C^* = \frac{V_0\mu_C^{S_C}(\delta_C + d_C + \mu_C^{I_C})\left[\mathcal{R}_0^2 - 1\right]}{\left[(\delta_C + d_C + \mu_C^{I_C})\left[\beta_C + \mu_C^{S_C}\right] + d_C\beta_C\right]} \tag{3.5.6}$$

where

$$\mathcal{R}_0 = \sqrt{\frac{N\alpha\beta_C\Lambda_C}{V_0\mu_C{}^{S_C}\alpha_C(\delta_C + d_C + \mu_C{}^{I_C})}} \tag{3.5.7}$$

Therefore, we can establish by deduction from equations (3.5.5) and (3.5.6) that only a single positive endemic equilibrium point exists for $\mathcal{R}_0 > 1$. □

Furthermore, inasmuch as $\mathcal{R}_0 > 1$ is a component of both the within-cattle scale and the between-cattle

scale parameters, the expressions from equations (3.5.3), (3.5.4) and (3.5.6) substantiate the unidirectional coupling structure of the multiscale model system (3.2.15) where the within-cattle scale submodel impact the between-cattle submodel and not vice versa.

3.5.2 Local stability of the Endemic Equilibrium

In this section we find the local asymptotic stability of the endemic steady state of the multiscale model system (3.2.15) through the implementation of the center manifold theory detailed in [101]. Therefore, by applying the theory we change variables of the multiscale model system (3.2.15). We now set $S_C = x_1, I_C = x_2$ and $V_C = x_3$. We also apply the vector notation $\mathbf{x} = (x_1, x_2, x_3)^T$ so that the multiscale model system (3.2.15) can be expressed as follows:

$$\frac{d\mathbf{x}}{dt} = \mathbf{f}(\mathbf{x}, \beta^*) \tag{3.5.1}$$

where

$$\mathbf{f} = (f_1, f_2, f_3) \tag{3.5.2}$$

Therefore, the model system (3.2.15) can be rewritten as

$$\begin{cases} \dfrac{dx_1}{dt} = \Lambda_C - \dfrac{\beta_C x_3}{V_0 + x_3} x_1 - \mu_C^{S_C} x_1 + d_C x_2 \\ \dfrac{dx_2}{dt} = \dfrac{\beta_C x_3}{V_0 + x_3} x_1 - \left(\delta_C + d_C + \mu_C^{S_C}\right) x_2 \\ \dfrac{dx_3}{dt} = N\alpha x_2 - \alpha_C x_3 \end{cases} \tag{3.5.3}$$

where

$$N = \frac{\zeta \mathfrak{R}_0 \tilde{F}}{\epsilon U^0}, \quad \mathfrak{R}_0 = \frac{\epsilon U^0}{\phi_A \omega}$$

The approach encompasses calculating the Jacobian matrix of the multiscale system (3.5.3) at the disease-free equilibrium E_0 signified by $J(E_0)$. The matrix corresponding to the multiscale system (3.5.3) established at disease-free equilibrium can be expressed as:

$$J(E^0) = \begin{bmatrix} -\mu_C^{S_C} & d_C & -\dfrac{\beta^* \Lambda_C}{\mu_C^{S_C} V_0} \\ 0 & -\left(\delta_C + d_C + \mu_C^{I_C}\right) & \dfrac{\beta^* \Lambda_C}{\mu_C^{S_C} V_0} \\ 0 & N\alpha & -\alpha_C \end{bmatrix} \tag{3.5.4}$$

By making use of an approach similar to the one in section (3.4.2.1), we can obtain the basic reproductive number of the multiscale system (3.5.3) given by

$$\mathcal{R}_0 = \frac{N\alpha\beta_C\Lambda_C}{V_0\mu_C{}^{S_C}\alpha_C(\delta_C + d_C + \mu_C{}^{I_C})} \tag{3.5.5}$$

Setting $\beta_C = \beta^*$ as the bifurcation parameter and also, letting $\mathcal{R}_0 = 1$ and determining β^* in (3.5.3), this gives

$$\beta^* = \frac{V_0\mu_C^{S_C}\alpha_C(\delta_C + d_C + \mu_C{}^{I_C})}{N\alpha\Lambda_C} \tag{3.5.6}$$

We can highlight that the linearized system of the transformed equations (3.5.3) with bifurcation point β^* has a simple zero eigenvalue. Consequently, the center manifold theory [101] can be utilized to examine the dynamics of the multiscale system (3.5.3) close to $\beta_C = \beta^*$.

Theorem 3.7. *Consider the following general system of ordinary differential equations with parameter* ϕ*:*

$$\frac{dx}{dt} = f(x, \phi) \tag{3.5.7}$$

$$f : \boldsymbol{R}^n \times \boldsymbol{R} \to \boldsymbol{R}. \quad f : \boldsymbol{C}^2\left(\boldsymbol{R}^2 \times \boldsymbol{R}\right).$$

where 0 is an equilibrium of the system, that is, $f(0, \phi) = 0$ *for all* ϕ*, and assume that*

(A1) $A = D_x f(0,0) = ((\partial f_i/\partial x_j)(0,0))$ *is a linearization matrix of the model system (3.5.3) around the equilibrium 0 with* ϕ *evaluated at 0. Zero is a simple eigenvalue of A, and other eigenvalues have negative real parts.*

(A2) matrix A has a right eigenvector u and a left eigenvector v corresponding to the zero eigenvalues.

Let f_k *be the kth component of* f *and*

$$\begin{cases} a = \sum_{k,i,j=1}^{n} u_k v_i v_j \frac{\partial^2 f_k}{\partial x_i \partial x_j}(0,0), \\ \\ b = \sum_{k,i,j=1}^{n} u_k v_i \frac{\partial^2 f_k}{\partial x_i \partial \phi}(0,0), \end{cases} \tag{3.5.8}$$

The local dynamics of model system (3.5.3) around 0 are totally governed by a and b and are summarized as follows.

(i) $a > 0$ *and* $b > 0$. *When* $\phi < 0$ *with* $|\phi| \ll 1$, *0 is locally asymptotically stable, and there exists a positive unstable equilibrium: when* $0 < \phi \ll 1$, *0 is unstable and there exists a negative and locally asymptotically stable equilibrium.*

(ii) $a < 0$ *and* $b < 0$. *When* $\phi < 0$ *with* $|\phi| \ll 1$, *0 is unstable, when* $0 < \phi \ll 1$, *0 is asymptotically stable, and there exists a positive unstable equilibrium.*

(iii) $a > 0$ *and* $b < 0$. *When* $\phi < 0$ *with* $|\phi| \ll 1$, *0 is unstable, and there exists a locally asymptotically stable negative equilibrium; when* $0 < \phi \ll 1$, *0 is stable and a positive unstable equilibrium appears.*

(iv) $a < 0$ *and* $b > 0$. *When* ϕ *changes from negative to positive, 0 changes its stability from stable to unstable. Correspondingly a negative unstable equilibrium becomes positive and locally asymptotically stable.*

To implement Theorem 3.7, the following calculations are neccessary (note that β^* is the bifurcation parameter instead of ϕ in Theorem 3.7).

When $\mathcal{R}_0 = 1$, we can demonstrate that the Jacobian matrix of the multiscale system (3.5.4) at β^* (denoted by J_{β^*}) has a right eigenvector corresponding to the zero eigenvalue expressed below:

$$\begin{bmatrix} -\mu_C^{S_C} & d_C & -\frac{\beta^* \Lambda_C}{\mu_C^{S_C} V_0} \\ 0 & -\left(\delta_C + d_C + \mu_C^{I_C}\right) & \frac{\beta^* \Lambda_C}{\mu_C^{S_C} V_0} \\ 0 & N\alpha & -\alpha_C \end{bmatrix} \begin{bmatrix} u_1 \\ u_2 \\ u_3 \end{bmatrix} = \begin{bmatrix} 0 \\ 0 \\ 0 \\ 0 \\ 0 \end{bmatrix} \tag{3.5.9}$$

with

$$\mathbf{u} = (u_1, u_2, u_3)^T \tag{3.5.10}$$

where

$$\begin{cases} u_1 = -\dfrac{\beta^* \Lambda_C \left(\delta_C + \mu_C^{I_C}\right)}{{\mu_C^{S_C}}^2 V_0 \left(\delta_C + d_C + \mu_C^{I_C}\right)} \\ u_2 = 1 \\ u_3 = 1 \end{cases} \tag{3.5.11}$$

Furthermore, the left eigenvector of the jacobian matrix in (3.5.4) corresponding to the zero eigenvalue at β^* and satisfying the condition **v.u**=1 is written as:

$$\begin{bmatrix} v_1 & v_2 & v_3 \end{bmatrix} \begin{bmatrix} -\mu_C^{S_C} & d_C & -\dfrac{\beta^* \Lambda_C}{\mu_C^{S_C} V_0} \\ 0 & -\left(\delta_C + d_C + \mu_C^{I_C}\right) & \dfrac{\beta^* \Lambda_C}{\mu_C^{S_C} V_0} \\ 0 & N\alpha & -\alpha_C \end{bmatrix} = \begin{bmatrix} 0 & 0 & 0 \end{bmatrix} \tag{3.5.12}$$

with

$$\mathbf{v} = (v_1, v_2, v_3)^T \tag{3.5.13}$$

where

$$\begin{cases} v_1 = 0, \\ v_2 = \dfrac{N\alpha\beta^* \Lambda_C}{\left[N\alpha\beta^* \Lambda_C + \mu_C^{S_C} V_0 (\delta_C + d_C + \mu_C^{I_C})\right]}, \\ v_3 = \dfrac{\mu_C^{S_C} V_0 (\delta_C + d_C + \mu_C^{I_C})}{\left[N\alpha\beta^* \Lambda_C + \mu_C^{S_C} V_0 (\delta_C + d_C + \mu_C^{I_C})\right]} \end{cases} \tag{3.5.14}$$

The condition **v.u**=1 can be verified as follows:

$$\begin{cases} v.u = \cancelto{0}{v_1.u_1} + v_2.u_2 + v_3.u_3 \\ = \left(\dfrac{N\alpha\beta^*\Lambda_C}{\left[N\alpha\beta^*\Lambda_C + \mu_C^{S_C} V_0(\delta_C + d_C + \mu_C^{I_C})\right]} \right).(1) + \left(\dfrac{\mu_C^{S_C} V_0(\delta_C + d_C + \mu_C^{I_C})}{\left[N\alpha\beta^*\Lambda_C + \mu_C^{S_C} V_0(\delta_C + d_C + \mu_C^{I_C})\right]} \right).(1) \\ = \dfrac{\left[N\alpha\beta^*\Lambda_C + \mu_C^{S_C} V_0(\delta_C + d_C + \mu_C^{I_C})\right]}{\left[N\alpha\beta^*\Lambda_C + \mu_C^{S_C} V_0(\delta_C + d_C + \mu_C^{I_C})\right]} = 1 \end{cases} \tag{3.5.15}$$

We now calculate the parameters of bifurcation a and b, by determining the value of the nonzero second-order mixed derivatives of $\mathbf{F}$ in regard to the variables and β^* to get the signs of a and b. The sign of a corresponds to, the non-vanishing partial derivatives of $\mathbf{F}$:

$$\begin{cases} \dfrac{\partial^2 f_1}{\partial x_3 \partial x_1} = \dfrac{\partial^2 f_1}{\partial x_1 \partial x_3} = -\dfrac{\beta^*}{V_0} \\ \dfrac{\partial^2 f_2}{\partial x_3 \partial x_1} = \dfrac{\partial^2 f_2}{\partial x_1 \partial x_3} = \dfrac{\beta^*}{V_0} \\ \dfrac{\partial^2 f_1}{\partial x_3^2} = \dfrac{2\beta^*\Lambda_C}{V_0^2 \mu_C^{S_C}} \\ \dfrac{\partial^2 f_2}{\partial x_3^2} = -\dfrac{2\beta^*\Lambda_C}{V_0^2 \mu_C^{S_C}} \end{cases} \tag{3.5.16}$$

Similarly, the sign of b corresponds to the non-vanishing partial derivatives of $\mathbf{F}$:

$$\begin{cases} \dfrac{\partial^2 f_1}{\partial x_3 \partial \beta^*} = -\dfrac{\Lambda_C}{\mu_C^{S_C} V_0} \\ \dfrac{\partial^2 f_2}{\partial x_3 \partial \beta^*} = \dfrac{\Lambda_C}{\mu_C^{S_C} V_0} \end{cases} \tag{3.5.17}$$

Substituting expression (3.5.11), (3.5.14) and (3.5.16) into (3.5.8), we get

$$
\begin{cases}
a = u_1 v_3^2 \dfrac{\partial^2 f_1}{\partial x_3^2} + u_2 v_3^2 \dfrac{\partial^2 f_2}{\partial x_3^2} \\
= \left(-\dfrac{\beta^* \Lambda_C \left(\delta_C + \mu_C^{I_C} \right)}{{\mu_C^{S_C}}^2 V_0 \left(\delta_C + d_C + \mu_C^{I_C} \right)} \right) \left(\dfrac{\mu_C^{S_C} V_0 (\delta_C + d_C + \mu_C^{I_C})}{\left[N\alpha\beta^* \Lambda_C + \mu_C^{S_C} V_0 (\delta_C + d_C + \mu_C^{I_C}) \right]} \right)^2 \left(\dfrac{2\beta^* \Lambda_C}{V_0^2 \mu_C^{S_C}} \right) \\
+ \left(\dfrac{\mu_C^{S_C} V_0 (\delta_C + d_C + \mu_C^{I_C})}{\left[N\alpha\beta^* \Lambda_C + \mu_C^{S_C} V_0 (\delta_C + d_C + \mu_C^{I_C}) \right]} \right)^2 \left(-\dfrac{2\beta^* \Lambda_C}{V_0^2 \mu_C^{S_C}} \right) \\
= - \left(\dfrac{\mu_C^{S_C} V_0 (\delta_C + d_C + \mu_C^{I_C})}{\left[N\alpha\beta^* \Lambda_C + \mu_C^{S_C} V_0 (\delta_C + d_C + \mu_C^{I_C}) \right]} \right)^2 \left(\dfrac{2\beta^* \Lambda_C}{V_0^2 \mu_C^{S_C}} \right) \left[\dfrac{\beta^* \Lambda_C \left(\delta_C + \mu_C^{I_C} \right) + {\mu_C^{S_C}}^2 V_0 \left(\delta_C + d_C + \mu_C^{I_C} \right)}{{\mu_C^{S_C}}^2 V_0 \left(\delta_C + d_C + \mu_C^{I_C} \right)} \right] < 0
\end{cases}
\tag{3.5.18}
$$

On the other hand, when we substitute expression (3.5.11), (3.5.14) and (3.5.17) into (3.5.8), we get

$$
\begin{cases}
b = u_1 v_3 \dfrac{\partial^2 f_1}{\partial x_3 \partial \beta^*} + u_2 v_3 \dfrac{\partial^2 f_2}{\partial x_3 \partial \beta^*} \\
= \left(-\dfrac{\beta^* \Lambda_C \left(\delta_C + \mu_C^{I_C} \right)}{{\mu_C^{S_C}}^2 V_0 \left(\delta_C + d_C + \mu_C^{I_C} \right)} \right) \left(\dfrac{\mu_C^{S_C} V_0 (\delta_C + d_C + \mu_C^{I_C})}{\left[N\alpha\beta^* \Lambda_C + \mu_C^{S_C} V_0 (\delta_C + d_C + \mu_C^{I_C}) \right]} \right) \left(-\dfrac{\Lambda_C}{\mu_C^{S_C} V_0} \right) \\
+ \left(\dfrac{\mu_C^{S_C} V_0 (\delta_C + d_C + \mu_C^{I_C})}{\left[N\alpha\beta^* \Lambda_C + \mu_C^{S_C} V_0 (\delta_C + d_C + \mu_C^{I_C}) \right]} \right) \left(\dfrac{\Lambda_C}{\mu_C^{S_C} V_0} \right) \\
= \left(\dfrac{\mu_C^{S_C} V_0 (\delta_C + d_C + \mu_C^{I_C})}{\left[N\alpha\beta^* \Lambda_C + \mu_C^{S_C} V_0 (\delta_C + d_C + \mu_C^{I_C}) \right]} \right) \left(\dfrac{\Lambda_C}{\mu_C^{S_C} V_0} \right) \left[\left(\dfrac{\beta^* \Lambda_C \left(\delta_C + \mu_C^{I_C} \right) + {\mu_C^{S_C}}^2 V_0 \left(\delta_C + d_C + \mu_C^{I_C} \right)}{{\mu_C^{S_C}}^2 V_0 \left(\delta_C + d_C + \mu_C^{I_C} \right)} \right) \right] > 0
\end{cases}
\tag{3.5.19}
$$

Consequently, $a < 0$ and $b > 0$. Implementing Theorem 3.7, item (iv), enables us to establish the following result which is only valid for $\mathcal{R}_0 > 1$ but near 1.

Theorem 3.8. *The endemic equilibrium of the multi-scale model system (3.5.3) guaranteed by Theorem 3.6 is locally asymptotically stable for $\mathcal{R}_0 > 1$ near 1.*

3.5.2.1 Bifurcation Analysis

In the Figure 3.2, we obtain a FMD infection-free steady state globally stable when $\mathcal{R}_0 < 1$ and unstable when $\mathcal{R}_0 > 1$. Furthermore, it is also clear that a unique stable endemic equilibrium arises from the bifurcation point $\mathcal{R}_0 = 1$ and increases as $\mathcal{R}_0$ increases, hence it shows that the FMD infection-free steady state exists for all $\mathcal{R}_0$, while an endemic infection only exists for $\mathcal{R}_0 > 1$. Figure 3.2 gives

forward bifucation and this is consistent with the result from section (3.5.2). This phenomenon involves a transcritical bifurcation and so we can conclude that the endemic infection only persist for $\mathcal{R}_0 > 1$.

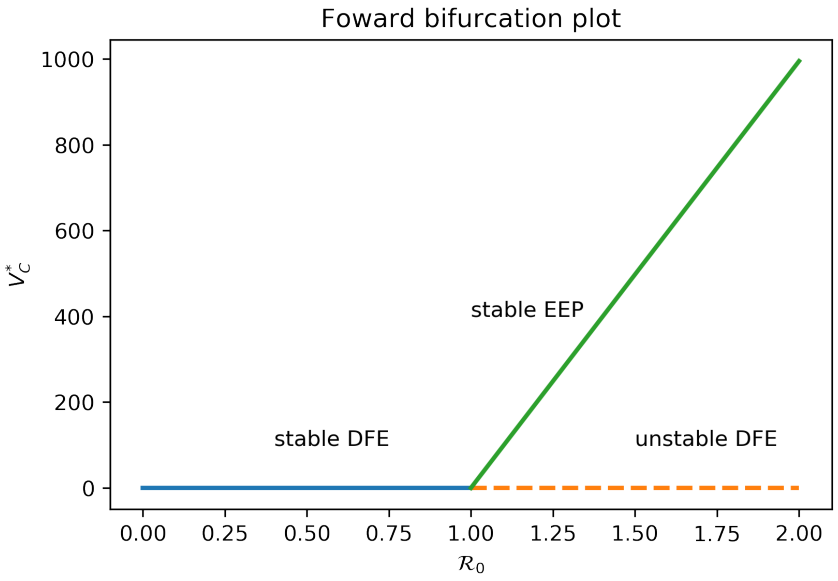

Figure 3.2: Bifurcation analysis for the FMD endemic model. Stable FMD infection-free state for $\mathcal{R}_0 < 1$; unstable FMD infection-free state and stable endemic steady state for $\mathcal{R}_0 > 1$.

3.5.3 Global stability of the Endemic Equilibrium

In order to establish that the endemic equilibrium E^* of the multiscale model (3.2.15) is globally asymptotically stable, we state the following theorem.

Theorem 3.9. *The Endemic Equilibrium E^* of the multiscale model system (3.2.15) is globally asymptotically stable whenever $\mathcal{R}_0 > 1$.*

Proof. Suppose we consider a Volterra-type Lyapunov function given by

$$\begin{aligned} \mathcal{L}_1 &= \mathcal{L}\left(S_C, I_C, V_C\right), \\ &= \kappa_1 \left[S_C - S_C^* \ln(S_C)\right] + \kappa_2 \left[I_C - I_C^* \ln(I_C)\right] + \kappa_3 \left[V_C - V_C^* \ln(V_C)\right] \end{aligned} \tag{3.5.1}$$

Derivating $\mathcal{L}_1$ gives us

$$\begin{aligned}\dot{\mathcal{L}}_1 &= \kappa_1\frac{dS_C}{dt}\left[1-\frac{S_C^*}{S_C}\right]+\kappa_2\frac{dI_C}{dt}\left[1-\frac{I_C^*}{I_C}\right]+\kappa_3\frac{dV_C}{dt}\left[1-\frac{V_C^*}{V_C}\right],\\ &= \kappa_1\left[1-\frac{S_C^*}{S_C}\right]\left[\Lambda_C-\lambda_C S_C-\mu_C^{S_C}S_C+d_C I_C\right]\\ &\quad+\kappa_2\left[1-\frac{I_C^*}{I_C}\right]\left[\lambda_C S_C-\left(\delta_C+d_C+\mu_C^{I_C}\right)I_C\right]\\ &\quad+\kappa_3\left[1-\frac{V_C^*}{V_C}\right]\left[\hat{N}\alpha I_C-\alpha_C V_C\right]\end{aligned} \tag{3.5.2}$$

Since E^* is an equilibrium point, the following relations hold,

$$\begin{cases}\Lambda_C=\lambda_C^*S_C^*+\mu_C^{S_C}S_C^*-d_C I_C^*,\left(\delta_C+d_C+\mu_C^{I_C}\right)=\dfrac{\lambda_C^*S_C^*}{I_C^*}\\ \\ \alpha_C=\dfrac{\hat{N}\alpha I_C^*}{V_C^*}\end{cases} \tag{3.5.3}$$

By implementing the relations in (3.5.3), $\dot{\mathcal{L}}_1$ becomes

$$\begin{aligned}\dot{\mathcal{L}}_1 &= \kappa_1\left[1-\frac{S_C^*}{S_C}\right]\left[\lambda_C^*S_C^*-\mu_C^{S_C}S_C^*-d_C I_C^*-\lambda_C S_C-\mu_C^{S_C}S_C+d_C I_C\right]\\ &\quad+\kappa_2\left[1-\frac{I_C^*}{I_C}\right]\left[\lambda_C S_C-\frac{\lambda_C^*S_C^*}{I_C^*}I_C\right]\\ &\quad+\kappa_3\left[1-\frac{V_C^*}{V_C}\right]\left[\hat{N}\alpha I_C-\frac{\hat{N}\alpha I_C^*}{V_C^*}V_C\right]\end{aligned} \tag{3.5.4}$$

$$\begin{aligned}\dot{\mathcal{L}}_1 &= -\frac{\kappa_1\mu_C^{S_C}}{S_C}\left[S_C-S_C^*\right]^2-\frac{\kappa_1\lambda_C^*S_C^{*2}}{S_C}-\kappa_2\lambda_C S_C\frac{I_C^*}{I_C}-\kappa_3\hat{N}\alpha I_C^*\frac{V_C}{V_C^*}\\ &\quad-\kappa_3\hat{N}\alpha I_C\frac{V_C^*}{V_C}+\left[\kappa_3\hat{N}\alpha-\kappa_2\frac{\lambda_C^*S_C^*}{I_C^*}\right]I_C+\left[\kappa_1+\kappa_2\right]\lambda_C^*S_C^*\\ &\quad+\left[\kappa_2-\kappa_1\right]\lambda_C S_C+\kappa_1\lambda_C S_C^*+\kappa_3\hat{N}\alpha I_C^*+\frac{\kappa_1 d_C}{S_C}\left[S_C-S_C^*\right]\left[I_C^*-I_C\right]\end{aligned} \tag{3.5.5}$$

We choose the value of κ_1, κ_2 and κ_3 such that

$$\begin{cases} \kappa_1 = \kappa_2 = 1 \\ \\ \kappa_3 \hat{N}\alpha - \kappa_2 \dfrac{\lambda_C^* S_C^*}{I_C^*} = 0 \end{cases} \tag{3.5.6}$$

this gives

$$\kappa_3 = \frac{\lambda_C^* S_C^*}{\hat{N}\alpha I_C^*} \tag{3.5.7}$$

We substitute the values of κ_1, κ_2 and κ_3 into equation (3.5.5)

$$\begin{aligned} \dot{\mathcal{L}}_1 &= -\frac{\mu_C^{S_C}}{S_C}[S_C - S_C^*]^2 - \frac{\lambda_C^* S_C^{*2}}{S_C} - \lambda_C S_C \frac{I_C^*}{I_C} - \lambda_C^* S_C^* \frac{V_C}{V_C^*} \\ &\quad -\lambda_C^* S_C^* \frac{V_C^* I_C}{V_C I_C^*} + 3\lambda_C^* S_C^* - \frac{d_C}{S_C}[S_C - S_C^*][I_C^* - I_C] \\ &= -\frac{\mu_C^{S_C}}{S_C}[S_C - S_C^*]^2 + \lambda_C^* S_C^* \left[3 - \frac{S_C^*}{S_C} - \frac{V_C}{V_C^*} - \frac{V_C^* I_C}{V_C I_C^*}\right] \\ &\quad +\lambda_C S_C \left[\frac{S_C^*}{S_C} - \frac{I_C^*}{I_C}\right] - \frac{d_C}{S_C}[S_C - S_C^*][I_C^* - I_C] \end{aligned} \tag{3.5.8}$$

From equation (3.5.8), we can see that $\dfrac{S_C^*}{S_C} - \dfrac{I_C^*}{I_C} \leq 0$ because $\dfrac{S_C^*}{S_C} < 1$ and $\dfrac{I_C^*}{I_C} > 1$. Therefore, by implementing the arithmetic-geometric mean equality, we obtain $\dot{\mathcal{L}}_1 \leq 0$, which implies that $\dot{\mathcal{L}}_1$ is clearly a Lyapunov function of the multiscale model system (3.2.15). Hence, we can conclude from the LaSalle's Invariance Principle that E^* is globally asymptotically stable. □

3.5.4 The Stochastic Differential Equations for the FMDV transmission dynamics

Suppose $(\Omega; \mathcal{F}; P)$ be a complete probability space with filtration $\{\mathcal{F}_t\}_{t\geq 0}$ satisfying the usual conditions (i.e. it is increasing and continuous while $\{\mathcal{F}_0\}_{t\geq 0}$ contains all P-null sets). Letting $W(t)$ be the one dimensional Wiener process or Brownian motion defined on this probability space. We also suppose $a \wedge b$ describe $\min(a, b)$ and $a \vee b$ describe $\max(a, b)$.

Theorem 3.10. *(Itô's formula): Suppose that X_t has Stochastic Differential Equation:*

$$dX_t = f(X_t, t)dt + g(X_t, t)dW_t \tag{3.5.1}$$

for $f, g \in C^{1,2}(J \times R \times R)$, assume that $F : J \times R \to R$ is continous and has $\frac{\partial F}{\partial t}, \frac{\partial F}{\partial X_t}$ and $\frac{\partial^2 F}{\partial X_t^2}$ that exist and are a continuous set $F = F(X_t, t)$, then F has the stochastic differential

$$dF = \frac{\partial F}{\partial t}dt + \frac{\partial F}{\partial X_t}dX_t + \frac{1}{2}\frac{\partial^2 F}{\partial X_t^2}g^2 dt, \tag{3.5.2}$$

$$dF(X_t, t) = \left[\frac{\partial F}{\partial t} + \frac{\partial F}{\partial X_t}f + \frac{1}{2}\frac{\partial^2 F}{\partial X_t^2}g^2\right]dt + \frac{\partial F}{\partial X_t}gdW_t \tag{3.5.3}$$

The equation (3.5.3) is called Itô's formula or Itô's chain rule.

The FMD transmission Stochastic model is given by:

$$\begin{cases} dS_C(t) = \left(\Lambda_C - \dfrac{\beta_C V_C(t)}{V_0 + V_C(t)}S_C(t) - {\mu_C}^{S_C}S_C(t) + d_C I_C(t)\right)dt + S_C(t)\sigma_S dW_S \\ dI_C(t) = \left(\dfrac{\beta_C V_C(t)}{V_0 + V_C(t)}S_C(t) - (\delta_C + d_C + {\mu_C}^{I_C})I_C(t)\right)dt + I_C(t)\sigma_I dW_I \\ dV_C(t) = (N\alpha I_C(t) - \alpha_C V_C(t))\,dt + V_C(t)\sigma_V dW_V \\ S_C(0) = S_0, I_C(0) = I_0, V_C(0) = V_0 \end{cases} \tag{3.5.4}$$

where

$$N = \frac{\zeta \mathfrak{R}_0 \tilde{F}}{\epsilon U^0}, \quad \mathfrak{R}_0 = \frac{\epsilon U^0}{\phi_A \omega} \tag{3.5.5}$$

Considering the second expression of model system (3.5.4)

$$dI_C(t) = \left(\frac{\beta_C V_C(t)}{V_0 + V_C(t)}S_C(t) - (\delta_C + d_C + {\mu_C}^{I_C})I_C(t)\right)dt + I_C(t)\sigma_I dW_I \tag{3.5.6}$$

and

$$dV_C(t) = (N\alpha I_C(t) - \alpha_C V_C(t))\,dt + V_C(t)\sigma_V dW_V \tag{3.5.7}$$

We can write equation (3.5.6) as follows

$$dI_C(t) = \left(\frac{\beta_C N\alpha I_C(t)}{\alpha_C(V_0 + V_C(t))}S_C(t) - (\delta_C + d_C + {\mu_C}^{I_C})I_C(t)\right)dt + I_C(t)\sigma_I dW_I \tag{3.5.8}$$

factoring out $I_C(t)$ on the right hand side

$$dI_C(t) = I_C(t)\left(\frac{\beta_C N\alpha}{\alpha_C(V_0+V_C(t))}S_C(t) - (\delta_C + d_C + \mu_C{}^{I_C})\right)dt + \sigma_I dW_I \tag{3.5.9}$$

this can be simplified to

$$\frac{dI_C(t)}{I_C(t)} = \left(\frac{\beta_C N\alpha}{\alpha_C(V_0+V_C(t))}S_C(t) - (\delta_C + d_C + \mu_C{}^{I_C})\right)dt + \sigma_I dW_I \tag{3.5.10}$$

Therefore, the solution of equation (3.5.10) should have the term $\ln I_C(t)$ and so we set $F(I(t),t) = \ln I_C(t)$ and applying Itô's formula (3.5.3) we obtain

$$dF(I_C(t),t)$$

$$= \left[0 + \left(\frac{\beta_C N\alpha}{\alpha_C(V_0+V_C(t))}S_C(t) - (\delta_C + d_C + \mu_C{}^{I_C})\right)I_C(t)\left(\frac{1}{I_C(t)}\right) - \frac{1}{2}\sigma_I^2 I_C(t)^2\left(\frac{1}{I_C(t)^2}\right)\right]dt$$

$$+\sigma_I I_C(t)\left(\frac{1}{I_C(t)}\right)dW_I$$

We can now write

$$d\ln I_C(t) = \left[\left(\frac{\beta_C N\alpha}{\alpha_C(V_0+V_C(t))}S_C(t) - (\delta_C + d_C + \mu_C{}^{I_C})\right) - \frac{1}{2}\sigma_I^2\right]dt + \sigma_I dW_I \tag{3.5.11}$$

When we integrate both sides we get

$$\ln I_C(t) = \ln I_C(0) = \left[\left(\frac{\beta_C N\alpha}{\alpha_C(V_0+V_C(t))}S_C(t) - (\delta_C + d_C + \mu_C{}^{I_C})\right) - \frac{1}{2}\sigma_I^2\right]t$$

$$+\sigma_I(W_t - W_0), \quad W_0 = 0$$

Evidently, the solution of the equation (3.5.10) is

$$I_C(t) = I_0 exp\left\{\left[\left(\frac{\beta_C N\alpha}{\alpha_C(V_0+V_C(t))}S_C(t) - (\delta_C + d_C + \mu_C{}^{I_C})\right) - \frac{1}{2}\sigma_I^2\right]t + \sigma_I W_t\right\} \tag{3.5.12}$$

Consequently,

$$\mathcal{R}_0^{Stoc} = \frac{N\alpha\beta_C\Lambda_C}{V_0\mu_C{}^{S_C}\alpha_C(\delta_C + d_C + \mu_C{}^{I_C})} - \frac{\sigma_I^2}{2(\delta_C + d_C + \mu_C{}^{I_C})} \tag{3.5.13}$$

The Reproductive number of the stochastic differential multi-scale model (3.5.4) is given by

$$\mathcal{R}_0^{Stoc} = \mathcal{R}_0 - \frac{\sigma_I^2}{2(\delta_C + d_C + \mu_C{}^{I_C})} \tag{3.5.14}$$

where

$$\mathcal{R}_0 = \frac{N\alpha\beta_C\Lambda_C}{V_0\mu_C{}^{S_C}\alpha_C(\delta_C + d_C + \mu_C{}^{I_C})} \tag{3.5.15}$$

3.5.5 Existence of Unique Positive Solution

Prior to exploring the dynamics of the SDE multi-scale model for FMDV transmission (3.5.4), it is essential to prove that the multi-scale SDE model only has a unique global solution and also that the solution will stay in $(0, N_C)$ whenever it starts from there. The general existence-and-uniqueness theorem on SDEs (see example [107–109]) currently does not relate to this particular stochastic differential equation. Therefore, it is important to set up a novel theory.

Theorem 3.11. *For any given initial value $I_C(0) = I_0 \in (0, N_C)$, the SDE (3.5.4) has a unique global positive solution $I_C(t) \in (0, N_C)$ for all $t \geq 0$ with probability one, namely*

$$\mathbb{P}\{I_C(t) \in (0, N_C) \text{ for all } t \geq 0\} = 1. \tag{3.5.1}$$

Proof. Pertaining to the expression (3.5.4) as a stochastic differential equation on $\mathbb{R}$, we can observe that its coefficients are locally Lipschitz continuous. It has been established (see example [107–109]) that for any given initial value $S_0 \in (0, N_C)$ there exists a unique maximal local solution $I_C(t)$ on $t \in [0, \tau_e)$, where τ_e is the explosion time. We set $k_0 > 0$ to be sufficiently large for $1/k_0 < I_0 < N_C - (1/k_0)$. For each integer $k \geq k_0$, define the stopping time

$$\tau_k = \inf\{t \in [0, \tau_e) : I_C \notin (1/k, N_C - (1/k))\} \tag{3.5.2}$$

where for the duration of this chapter we let $\inf \emptyset = \infty$, i.e. $\emptyset$ is the empty set. Evidently, τ_k is increasing as $k \to \infty$. Set $\tau_\infty = \lim_{k\to\infty}$, consequently $\tau_\infty \leq \tau_e$ a.s. If we can establish that $\tau_\infty = \infty$ a.s., then $\tau_e = \infty$ a.s. and $I_C(t) \in (0, N_C)$ a.s. for all $t \geq 0$. To put it another way, in order to finish the proof we establish that $\tau_\infty = \infty$ a.s. If this statement is false, then there exists a pair of constants $T > 0$ and $\varepsilon \in (0, 1)$ such that

$$\mathbb{P}\{\tau_\infty \leq T\} > \varepsilon. \tag{3.5.3}$$

Therefore there is an integer $k_1 \geq k_0$ such that

$$\mathbb{P}\{\tau_\infty \leq T\} > \varepsilon \text{ for all } k \geq k_1. \tag{3.5.4}$$

Let us define a function $V : (0, N_C) \in \mathbb{R}_+$ by

$$V(x) = \frac{1}{x} + \frac{1}{N_C - x} \tag{3.5.5}$$

Using the Itô's formula (3.5.3) we have, for all $t \in [0, T]$ and $k \geq k_1$,

$$\mathbb{E}\left(I_C\left(t \wedge \tau_k\right)\right) = \mathbb{E}\int_0^{t\wedge\tau_k} LV(I(s)d_s), \tag{3.5.6}$$

where $LV : (0, N_C) \to \mathbb{R}_+$ is defined by

$$V(x) = \frac{1}{x} + \frac{1}{N_C - x}, \tag{3.5.7}$$

By making use of the Itô's formula we have, for any $t \in [0.T]$ and $k \geq k_1$,

$$\mathbb{E}V(I_C(t \wedge \tau_k)) = V(I_0) + \mathbb{E}\int_0^{t\wedge\tau_k} LV(I_C(s))d_s, \tag{3.5.8}$$

where $LV : (0, N_C) \to \mathbb{R}$ is defined by

$$LV(x) = x\left(-\frac{1}{x^2} + \frac{1}{(N_C - x)^2}\right)\left[\frac{\beta_C N\alpha}{\alpha_C V_0}(N_C - x) - (\delta_C + d_C + \mu_C^{I_C})\right] + \sigma_I^2\left(\frac{1}{x^3} + \frac{1}{(N_C - x)^3}\right) \tag{3.5.9}$$

It can be surely established that

$$\frac{(\delta_C + d_C + \mu_C^{I_C})}{x} + \frac{\beta_C N\alpha}{\alpha_C V_0}.\frac{N_C}{N_C - x} + \sigma_I^2\left(\frac{1}{x} + \frac{1}{N_C - x}\right) \leq GV(x) \tag{3.5.10}$$

where

$G = \delta_C + d_C + \mu_C^{I_C} \vee \frac{\beta_C N\alpha}{\alpha_C V_0} N_C + \sigma_I^2.$

Substituting equation (3.5.9) into equation (3.5.8), we obtain

$$\mathbb{E}V(I_C(t \wedge \tau_k)) \leq V(I_0) + \mathbb{E}\int_0^{t\wedge\tau_k} GV(I_C(s))d_s \leq V(I_0) + G\int_0^t \mathbb{E}V(I_C(s \wedge \tau_k))ds. \tag{3.5.11}$$

The Gronwall inequality yields that

$$\mathbb{E}V(I_C(T \wedge \tau_k)) \leq V(I_0)e^{GT} \tag{3.5.12}$$

Setting $\Omega_k = \{\tau_k \leq T\}$ for $k \geq k_1$ and, according to (3.5.3), $\mathbb{P}(\Omega_k) \geq \varepsilon$. Note that for each $\omega \in \Omega_k, I_C(\tau_k, \omega)$ equal either to $1/k$ or $N_C - (1/k)$, therefore $V(I_C(\tau_k, \omega)) \geq k$. Hence, it follows from (3.5.12) that $V(I_0)e^{GT} \geq \mathbb{E}[I_{\Omega_k}(\omega)V(I_C(\tau_k, \omega))] \geq k\mathbb{P}(\Omega_k) \geq \varepsilon k$. As $k \to \infty$ we have the contradiction

$$\infty \geq V(I_0)e^{GT} = \infty \tag{3.5.13}$$

Consequently, we must have $\tau_\infty = \infty$ a.s., hence completing the proof. □

3.6 Numerical analysis

This section presents computer simulations for the multiscale model system (3.2.15)'s behaviour using Python program version 3.6 on the Windows 10 operation system.

Table 3.3: Description of between-host and within-host model parameters.

Symbol	Description	Value	Source
Λ_C	Birth rate of susceptible cattle	0.3 day^{-1}	[110]
β_C	Rate of infection of susceptible cattle	0.05 day^{-1}	[111]
$\mu_C^{S_C}$	Natural mortality rate of susceptible cattle	0.05 year^{-1}	[112]
$\mu_C^{I_C}$	Natural mortality rate of infected cattle	0.05 year^{-1}	[112]
α	Excretion of infectious virions from cells and tissues of cattle into the blood plasma	0.02 day^{-1}	Estimate
d_C	Per ca-pita rate of loss of immunity	0.001 day^{-1}	[113]
α_C	Community elimination of total infectious reservoir	0.03 day^{-1}	Estimate
δ_C	Mortality rate of animals due to FMD.	0.055 day^{-1}	[114]
N	Number of FMD virus available for excretion	1000 day^{-1}	Assumed
V_0	Half saturation constant	2×10^8virions day^{-1}	Estimate

The numerical simulations of the multiscale model system (3.2.15) were carried out to explain some of the mathematical results that we obtained. We used the estimated parameter values presented in Table 3.3 for sensitivity and numerical analysis. A certain amount of the parameter values implemented in the simulations are results from publications and the others are estimates. The following are initial conditions implemented for these simulations: $S_C(0) = \dfrac{\Lambda_C}{\mu_C^{S_C}}, I_C(0) = 0, V_C(0) = 0.$

3.6.1 Sensitivity Analysis

This section presents the sensitivity analysis for the FMDV transmission indicators obtained from the multiscale model to the model parameters. The transmission indicator we consider is the basic reproductive number, $\mathcal{R}_0$ that generally describes the dynamics for a disease at the beginning of an infection and the endemic value of the community viral load V_C^*. For any particular epidemic model that illustrates the disease dynamics within a particular population, a sensitivity analysis study is important to perform since it enables us to establish model parameters which can be marked for control, elimination as well as eradication of disease. Therefore, the analysis of sensitivity of the FMDV metric $\mathcal{R}_0$ and the endemic value of the community viral load V_C^*, in relation to the variation of FMD multiscale model parameters is carried out by implementing Latin Hypercube Sampling (LHS) and Partial Rank Correlation Coefficients (PRCCs). In order to explore the influence of each model parameter on the basic reproduction number, $\mathcal{R}_0$ and the endemic value of the community viral load V_C^*, we perfomed 1000 simulations per run. The results of sensitivity of $\mathcal{R}_0$ and V_C^* to the model parameters are presented by the Tornado plots, Figure 3.3 and Figure 3.4 respectively. From the sensitivity analysis results of $\mathcal{R}_0$ and V_C^* to the multiscale model system (3.2.15)'s parameters in Figure 3.3 and Figure 3.4, the following deductions are listed below:

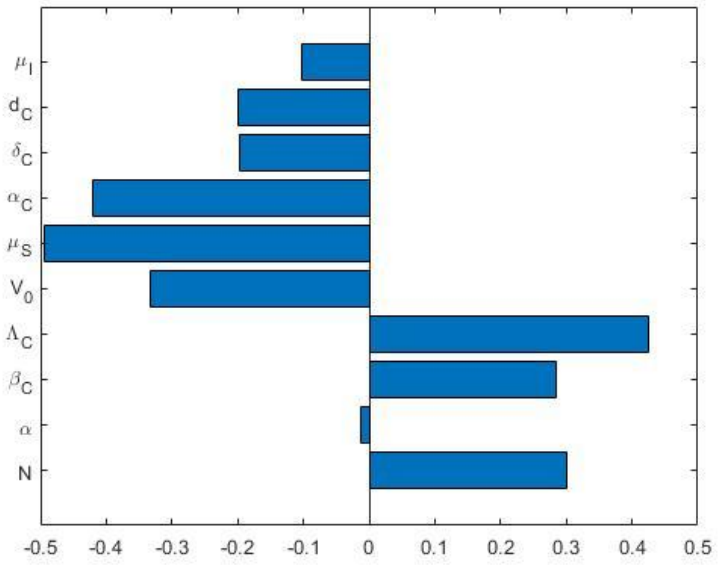

Figure 3.3: *Tornado plot of partial rank correlation coefficients (PRCCs) of the model parameters that impact the FMD spread indicator* $\mathcal{R}_0$

(a) The multiscale model system (3.2.15)'s parameters have both positive PRCCs and negative PRCCs.

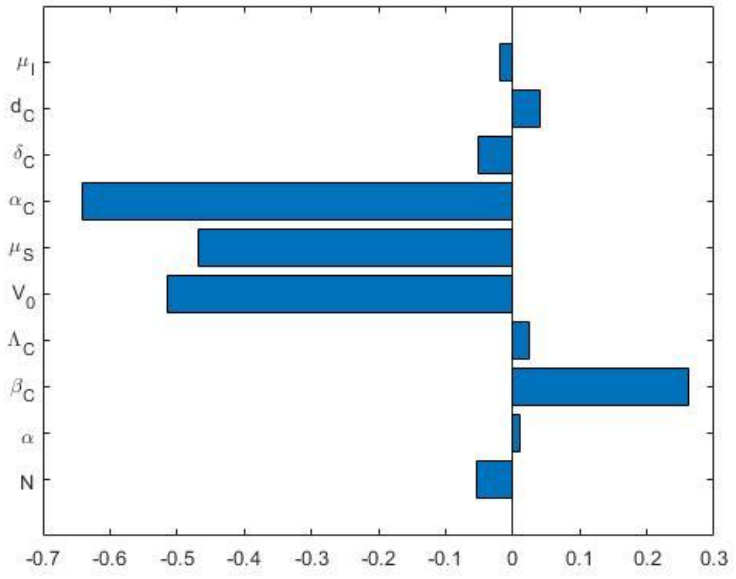

Figure 3.4: *Tornado plot of partial rank correlation coefficients (PRCCs) of the model parameters that influence the FMD transmission metric* V_C^*

This implies that parameters with positive PRCCs will increase the value of $\mathcal{R}_0$ as they are increased, where as parameters with negative PRCCs will decrease the value for $\mathcal{R}_0$ as they are increased. For example, an increase in a parameter like rate of infection of susceptible cattle, β_C will consequently increase the value of $\mathcal{R}_0$, and also increasing a parameter like the natural mortality rate of susceptible cattle, $\mu_C^{S_C}$ leads to a decrease in the value of $\mathcal{R}_0$.

(b) The FMD transmission metrics $\mathcal{R}_0$ and V_C^* are extremely sensitive to five of the disease parameters of the multiscale model system (3.2.15), $(\beta_C, \mu_C^{S_C}, V_0, \alpha_C, \Lambda_C)$ characterizes transmission of FMD at the beginning of the epidemic. Listed below are deductions based on the sensitivity of $\mathcal{R}_0$ to the FMD multiscale model system (3.2.15)'s parameters.

(i) Since $\mathcal{R}_0$ is significantly sensitive to $(\beta_C, \mu_C^{S_C}, V_0, \alpha_C, \Lambda_C)$, this implies that caution must be applied on the accuracy of these five FMD multiscale model system (3.2.15)'s parameters during the collection of data if the effectiveness and usefulness of the FMD multiscale model system (3.2.15) is to be intensified.

(ii) In view of the fact that $\mathcal{R}_0$ is responsive to the rate of infection of susceptible cattle, β_C and birth rate of susceptibles, Λ_C this implies that FMD interventions such as vaccination would be more effective in preventing the spread of FMD infection at the beginning of the outbreak.

(iii) Since $\mathcal{R}_0$ is significantly sensitive to the community elimination of total infectious reservoir, α_C, the Half saturation constant, V_0 and the natural mortality rate of susceptible cattle, $\mu_C^{S_C}$

this implies that FMD interventions such as vaccination and quarantine would be more effective to manage the spread of FMD infection at the beginning of the outbreak.

3.6.2 Numerical simulations of the multiscale model of FMD transmission dynamics

This section enables us to implement numerical simulations to substantiate some outcomes obtained from the sensitivity analysis for $\mathcal{R}_0$ and analytical results of the multiscale model. Applying the multiscale model parameter values obtained from Table 3.3 we conducted numerical simulations. We demonstrated the impact of five FMD disease transmission parameters $(\beta_C, \mu_C^{S_C}, V_0, \alpha_C, \Lambda_C)$ on the multiscale model variables $S_C(t), I_C(t), V_C(t)$. These parameters were only selected because they are significantly sensitive to $\mathcal{R}_0$ and V_C^*.

3.6.2.1 The influence of initial inoculum on the between-host scale of FMD infection dynamics

We investigate by implementing numerical simulations of the nested multiscale model system (3.2.15) the influence of initial inoculum on the between-cattle scale variables for FMD infection dynamics. We can establish this by varying the initial condition of the infective inoculum $V(0)$ that susceptible cattle can get through interaction with FMD virus in contaminated environment for different values and determine its effect on the dynamics of all the three between-cattle variables: S_C, I_C and V_C. The following are the results of the influence of initial inoculum on the between-cattle scale variables for the FMD infection dynamics:

(a) Figure 3.5 demonstrates the impact of varying $V(0)$ for different values of the initial value of the within-cattle FMD viral load $V(0)$: $V(0) = 10, V(0) = 1000$ and $V(0) = 10000$ on the between-cattle variables (S_C, I_C, V_C).

(b) Figure 3.6 demonstrates the impact of varying $V(0)$ for different values of the initial value of the within-cattle FMD viral load $V(0)$: $V(0) = 1000, V(0) = 100000$ and $V(0) = 1000000$ on the between-cattle variables (S_C, I_C, V_C).

(c) Figure 3.7 demonstrates the impact of varying $V(0)$ for different values of the initial value of the within-cattle FMD viral load $V(0)$: $V(0) = 100000, V(0) = 10000000$ and $V(0) = 100000000$ on the between-cattle variables (S_C, I_C, V_C).

We can observe from the numerical results of all the three Figure 3.5, Figure 3.6 and Figure 3.7 that there is a similar trend in which as the initial inoculum $V(0)$ increases beyond the minimum infectious dose, there is a remarkable but minimal changes in the dynamics of the between-cattle scale variables S_C, I_C, V_C.

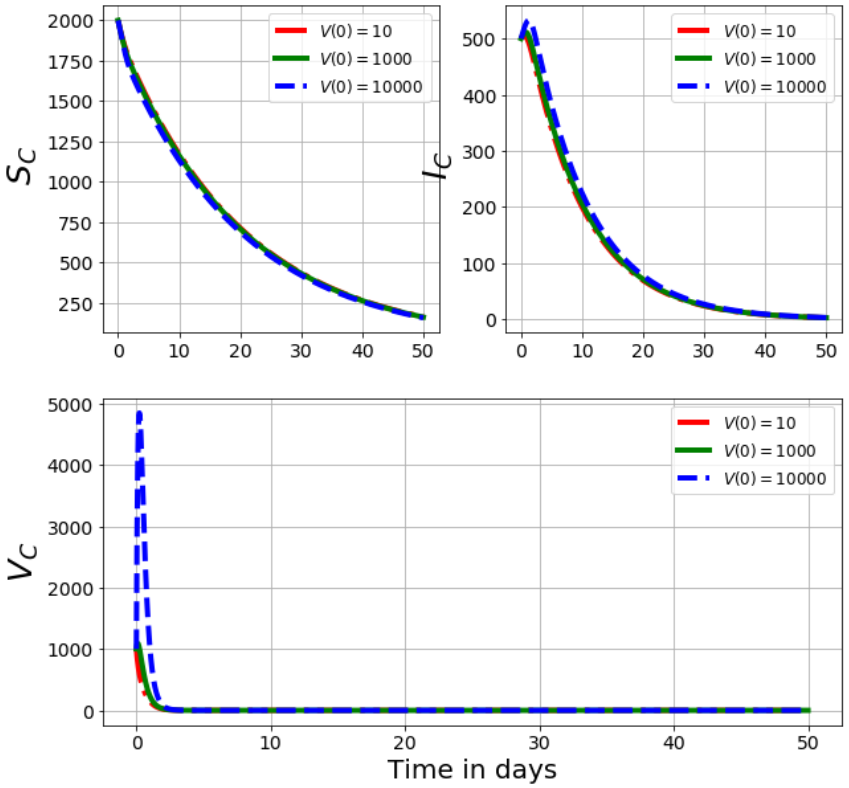

Figure 3.5: *Graphs of numerical solutions of the multiscale model system (3.2.15) showing propagation of (a) susceptible cattle population (S_C), (b) infected cattle population (I_C) and (c) between-cattle community viral load (V_C) for different values of the initial value of the within-cattle FMD viral load $V(0)$:* $V(0) = 10, V(0) = 1000$ *and* $V(0) = 10000$

Figure 3.5 demonstrates graphs of numerical solutions of the multiscale model system (3.2.15) showing dynamics of (a) susceptible cattle population (S_C), (b) infected cattle population (I_C) and (c) between-cattle community viral load (V_C) for different values of the initial value of the within-cattle FMD viral load $V(0)$: $V(0) = 10, V(0) = 1000$ and $V(0) = 10000$. Results in Figure 3.5 indicate that an increase in the initial inoculum from $V(0) = 10, V(0) = 1000$ and $V(0) = 10000$ makes a small difference in the transmission dynamics at the between-cattle scale as the between-cattle scale variables S_C, I_C, V_C change slightly as the initial inoculum changes.

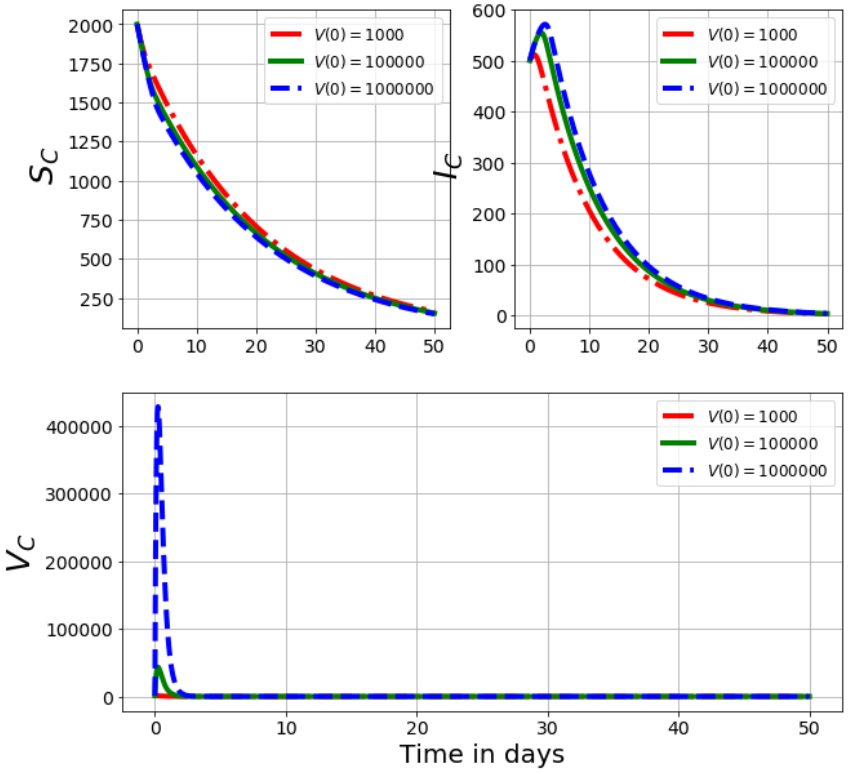

Figure 3.6: *Graphs of numerical solutions of the multiscale model system (3.2.15) showing propagation of (a) susceptible cattle population (S_C), (b) infected cattle population (I_C) and (c) between-cattle community viral load (V_C) for different values of the initial value of the within-cattle FMD viral load $V(0)$:* $V(0) = 1000, V(0) = 100000$ *and* $V(0) = 1000000$

Figure 3.6 shows graphs of numerical solutions of the multiscale model system (3.2.15) showing dynamics of (a) susceptible cattle population (S_C), (b) infected cattle population (I_C) and (c) between-cattle community viral load (V_C) for different values of the initial value of the within-cattle FMD viral load $V(0)$: $V(0) = 1000, V(0) = 100000$ and $V(0) = 1000000$. Results in Figure 3.6 indicate that an increase in the initial inoculum from $V(0) = 1000, V(0) = 100000$ and $V(0) = 1000000$ makes a significant difference in the transmission dynamics at the between-cattle scale as the between-cattle scale variables S_C, I_C, V_C change significantly as the initial inoculum changes.

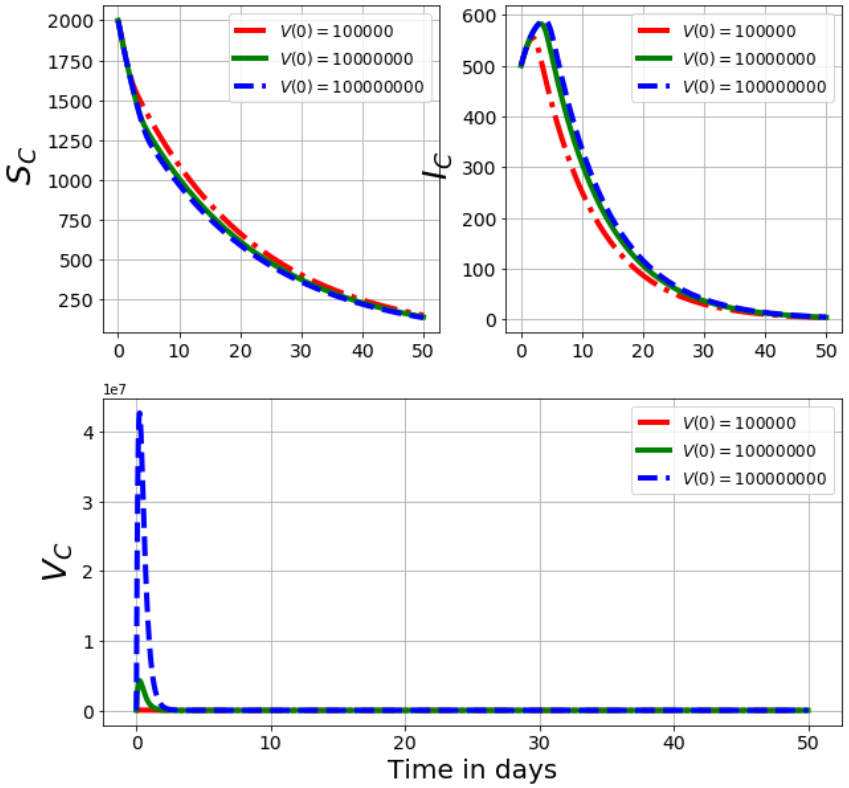

Figure 3.7: *Graphs of numerical solutions of the multiscale model system (3.2.15) showing propagation of (a) susceptible cattle population (S_C), (b) infected cattle population (I_C) and (c) between-cattle community viral load (V_C) for different values of the initial value of the within-cattle FMD viral load $V(0)$:* $V(0) = 100000, V(0) = 10000000$ *and* $V(0) = 100000000$

Figure 3.7 shows graphs of numerical solutions of the multiscale model system (3.2.15) showing dynamics of (a) susceptible cattle population (S_C), (b) infected cattle population (I_C) and (c) between-cattle community viral load (V_C) for different values of the initial value of the within-cattle FMD viral load $V(0)$: $V(0) = 100000, V(0) = 10000000$ and $V(0) = 100000000$. Results in Figure 3.7 indicate that an increase in the initial inoculum from $V(0) = 100000, V(0) = 10000000$ and $V(0) = 100000000$ makes a significant difference in the transmission dynamics at the between-cattle scale as the between-cattle scale variables S_C, I_C, V_C change significantly as the initial inoculum changes.

3.6.3 Influence of the between-host parameters on the FMD model

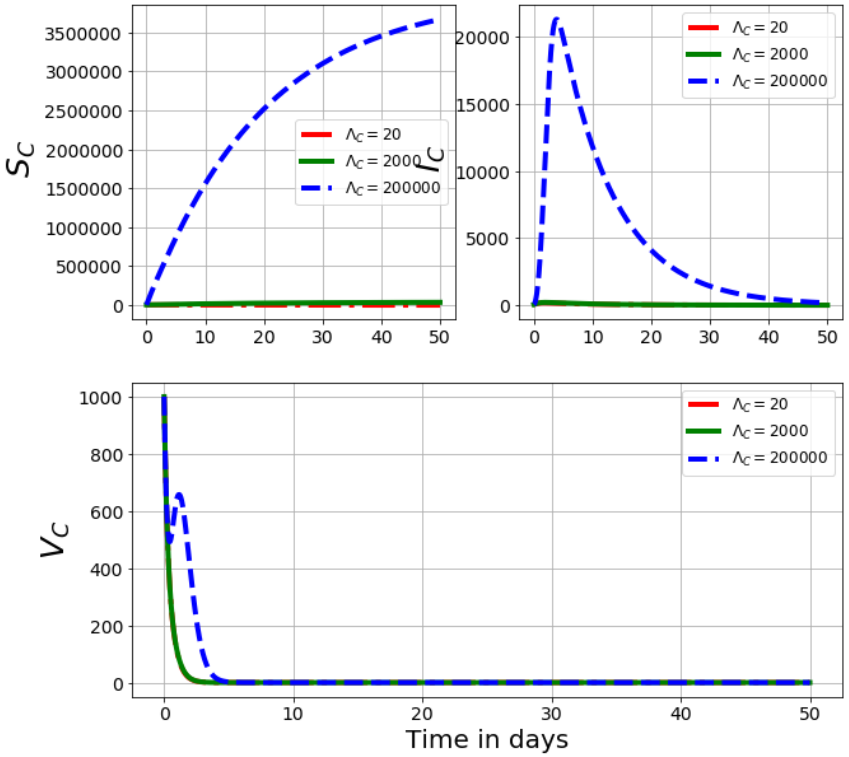

Figure 3.8: Graphs of numerical results of the model system (3.2.15) demonstrating the advancement with time of (a) Susceptible cattle population, S_C, (b) Infected cattle population, I_C, (c) Community viral load, V_C for variant values of the birth rate of susceptible cattle, $\Lambda_C : \Lambda_C = 20, \Lambda_C = 2000$ and $\Lambda_C = 200000$

Figure 3.8 demonstrates the impact of variation of the birth rate of susceptible cattle, $\Lambda_C : \Lambda_C = 20, \Lambda_C = 2000$ and $\Lambda_C = 200000$ on the between-host scale variables (S_C, I_C, V_C). The outcomes demonstrate that an increase in Λ_C is related to an increment in the susceptible cattle population and infected cattle population.

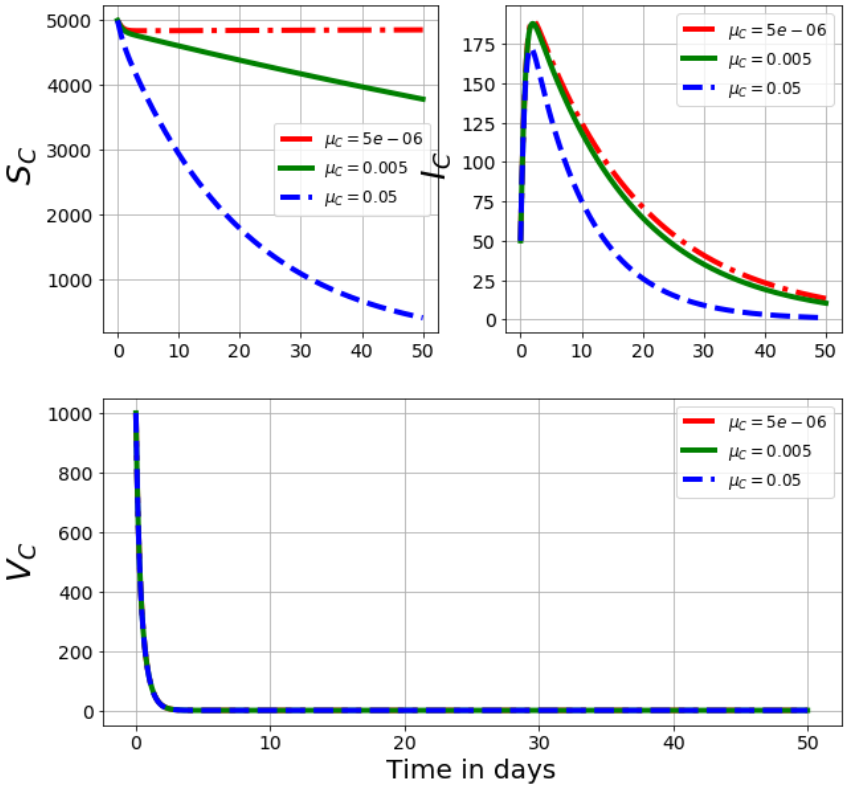

Figure 3.9: Graphs of numerical results of the model system (3.2.15) demonstrating the advancement with time of (a) Susceptible cattle population, S_C, (b) Infected cattle population, I_C, (c) Community viral load, V_C for variant values of the natural mortality rate of susceptible cattle, $\mu_C^{S_C}$: $\mu_C^{S_C} = 0.000005, \mu_C^{S_C} = 0.005$ and $\mu_C^{S_C} = 0.05$

Figure 3.9 demonstrates the impact of variation of the natural mortality rate of susceptible cattle, $\mu_C^{S_C}$: $\mu_C^{S_C} = 0.000005, \mu_C^{S_C} = 0.005$ and $\mu_C^{S_C} = 0.05$ on the between-host scale variables (S_C, I_C, V_C). The outcomes demonstrate that an increase in $\mu_C^{S_C}$ is related to a reduction in the susceptible cattle population and infected cattle population. There is no change in the community viral load.

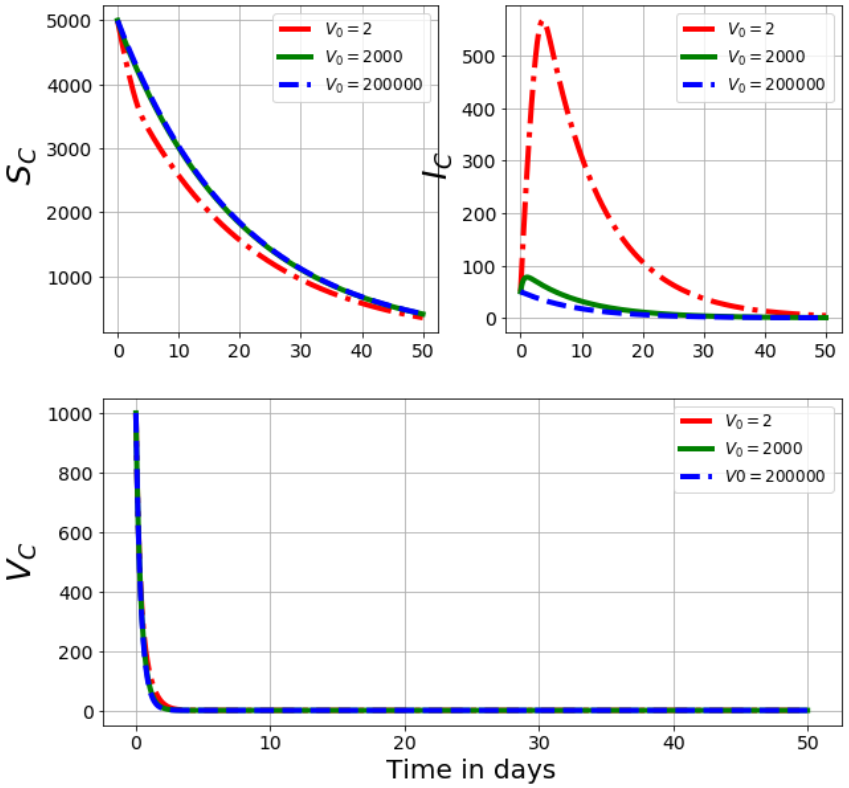

Figure 3.10: Graphs of numerical results of the model system (3.2.15) demonstrating the advancement with time of (a) Susceptible cattle population, S_C, (b) Infected cattle population, I_C, (c) Community viral load, V_C for variant values of the half saturation constant, $V_0 : V_0 = 2, V_0 = 2000$ and $V_0 = 200000$

Figure 3.10 demonstrates the impact of variation of the half saturation constant, $V_0 : V_0 = 2, V_0 = 2000$ and $V_0 = 200000$ on the between-host scale variables (S_C, I_C, V_C). The outcomes demonstrate that increments in V_0 result in an increase in the susceptible cattle population and reduction in the infected cattle population. There is no change in the community viral load.

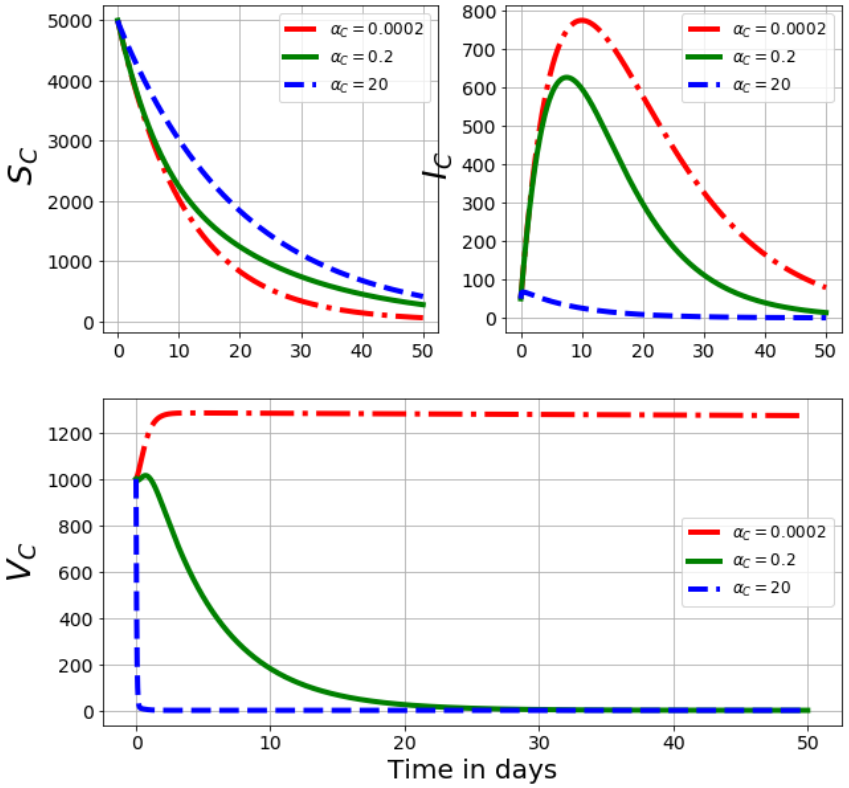

Figure 3.11: Graphs of numerical results of the model system (3.2.15) demonstrating the advancement with time of (a) Susceptible cattle population, S_C, (b) Infected cattle population, I_C, (c) Community viral load, V_C for variant values of the community elimination of total infectious reservoir, α_C: $\alpha_C = 0.0002$, $\alpha_C = 0.2$ and $\alpha_C = 20$.

Figure 3.11 demonstrates the impact of variation of the community elimination of total infectious reservoir, α_C: $\alpha_C = 0.0002$, $\alpha_C = 0.2$ and $\alpha_C = 20$ on the between-host scale variables (S_C, I_C, V_C). The outcomes demonstrate that increments in α_C result in an increase in the susceptible cattle population. Furthermore, there is reduction in the infected cattle population and community viral load.

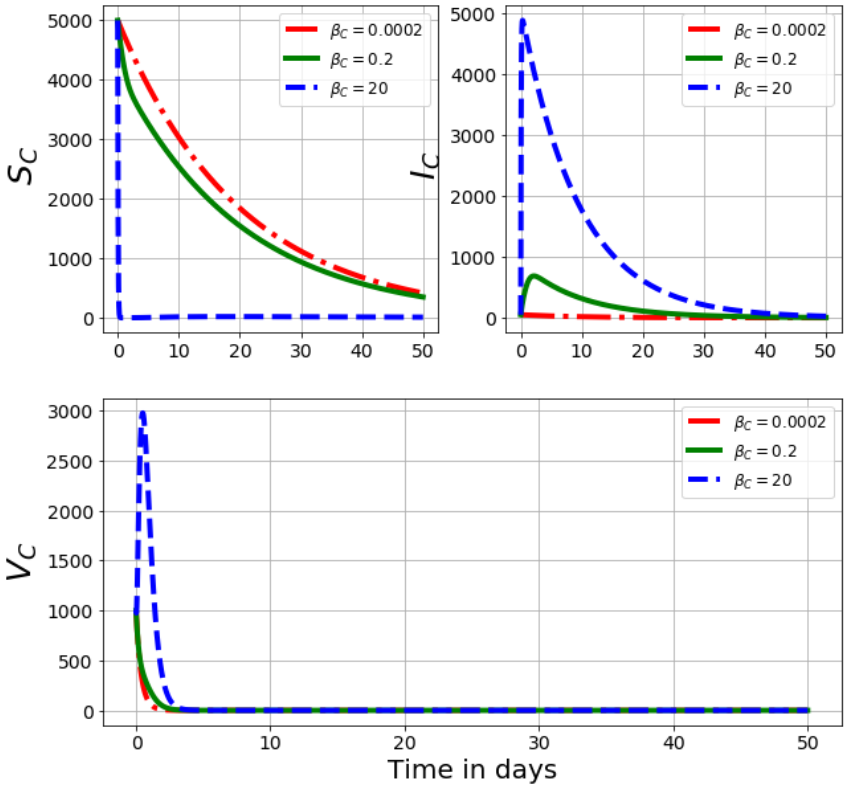

Figure 3.12: Graphs of numerical results of the model system (3.2.15) demonstrating the advancement with time of (a) Susceptible cattle population, S_C, (b) Infected cattle population, I_C, (c) Community viral load, V_C for variant values of the infection rate of susceptible cattle, $\beta_C : \beta_C = 0.0002, \beta_C = 0.2$ and $\beta_C = 20$

Figure 3.12 demonstrates the impact of variation of the infection rate of susceptible cattle, $\beta_C : \beta_C = 0.0002, \beta_C = 0.2$ and $\beta_C = 20$ on the between-host scale variables (S_C, I_C, V_C). The outcomes demonstrate that increments in α_C result in an increase in the susceptible cattle population. Furthermore, there is reduction in the infected cattle population and community viral load.

3.6.4 Effects of sochasticity on the FMD model

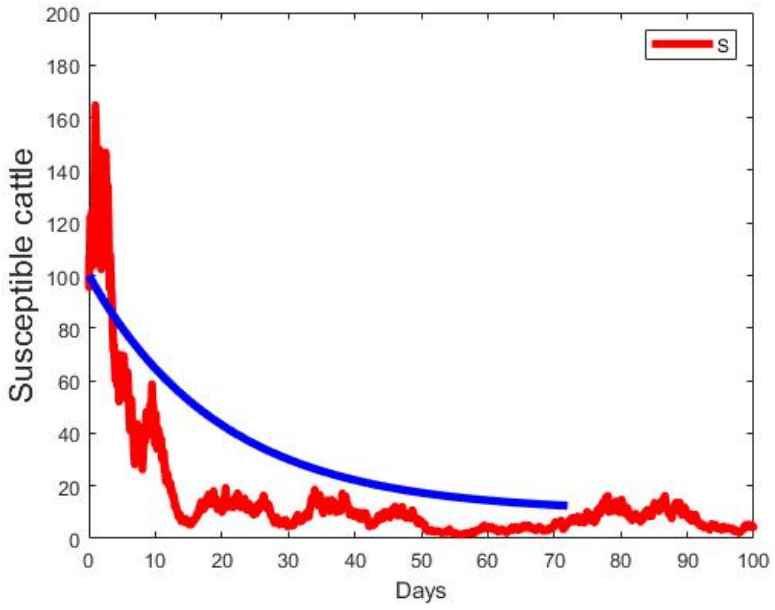

Figure 3.13: Graphs of numerical results of the Susceptible cattle, S_C of the multiscale SDE model system (3.5.4) with the ODE multiscale model system (3.2.15) solutions.

Figure 3.13 demonstrates the graphs of numerical results of the Susceptible cattle, S_C of the multiscale SDE model system (3.5.4) with the ODE multiscale model system (3.2.15) solutions. The solution for the stochastic multiscale model is obtained using the Milsten method.

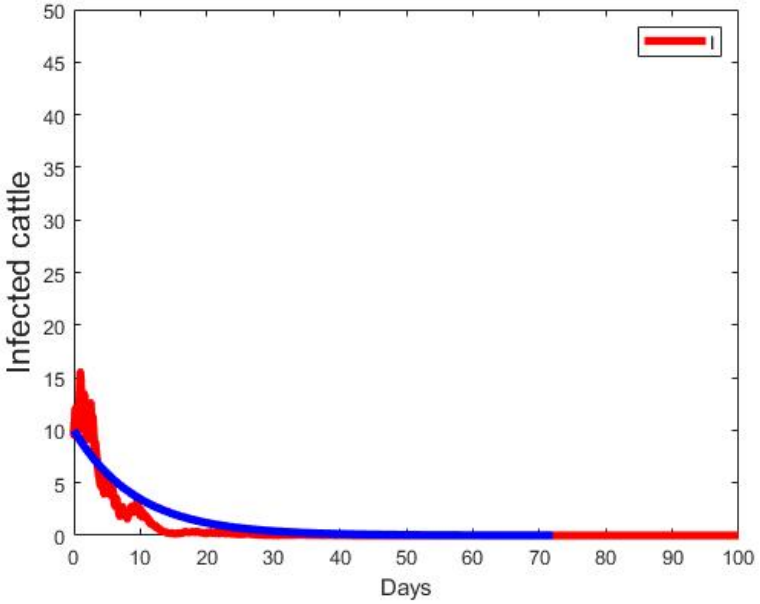

Figure 3.14: Graphs of numerical solutions of the Infected cattle, I_C of the multiscale SDE model system (3.5.4) with the ODE multiscale model system (3.2.15) solutions

Figure 3.14 demonstrates the graphs of numerical results of the Infected cattle, I_C of the multiscale SDE model system (3.5.4) with the ODE multiscale model system (3.2.15) solutions. The solution for the stochastic multiscale model is obtained using the Milsten method.

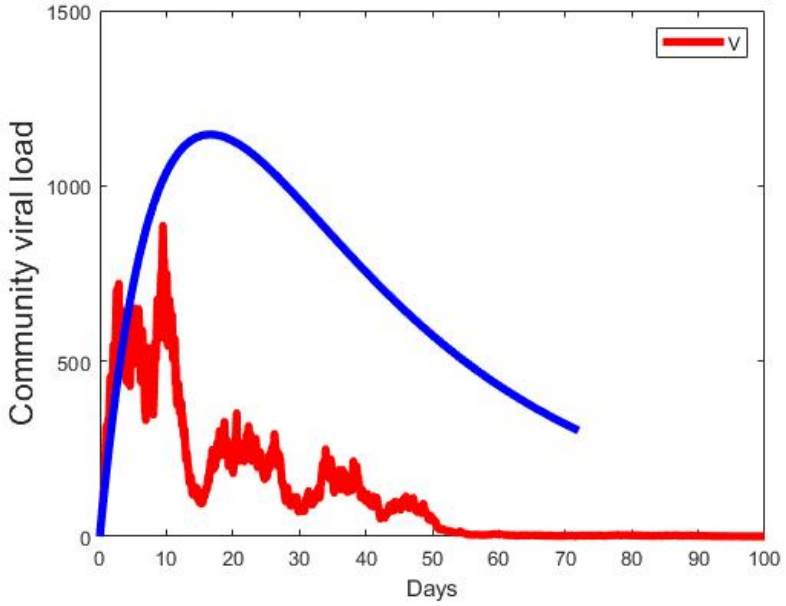

Figure 3.15: Graphs of numerical solutions of the Community viral load, V_C of the multiscale SDE model system (3.5.4) with the ODE multiscale model system (3.2.15) solutions.

Figure 3.15 demonstrates the graphs of numerical solutions of the Community viral load, V_C of the multiscale SDE model system (3.5.4) with the ODE multiscale model system (3.2.15) solutions. The solution for the stochastic multiscale model is obtained using the Milsten method.

3.7 Summary

In this chapter, we characterised a model centred on combining two sub-models namely: (i) the within-cattle scale and (ii) between-cattle scale sub-models for FMDV dynamics. Hence, we established a uni-directionally coupled multiscale model in which the within-cattle scale submodel is uni-directionally coupled to the between-cattle scale FMDV transmission dynamics submodel. By performing mathematical analysis the model was determined to be epidemiologically and mathematically sound. Therefore, the analysis of sensitivity of the FMDV metric $\mathcal{R}_0$ and the endemic value of the community viral load V_C^*, in relation to the variation of FMD multiscale model parameters was carried out by implementing Latin Hypercube Sampling (LHS) and Partial Rank Correlation Coefficients (PRCCs). Applying the model parameter values we conducted the numerical simulations to demonstrate the impact of five FMD disease transmission parameters $(\beta_C, \mu_C^{S_C}, V_0, \alpha_C, \Lambda_C)$ on the model variables $S_C(t), I_C(t), V_C(t)$. These parameters were only selected because they were significantly responsive to $\mathcal{R}_0$ and V_C^*. In view of the fact that $\mathcal{R}_0$ was responsive to the rate of infection of susceptible cattle, β_C and birth rate of susceptibles, Λ_C this

implied that FMD interventions such as vaccination would be more effective in preventing the spread of FMD disease infection at the beginning of the outbreak. Randomness of disease dynamics was highlighted by implementing a stochastic model.

In conclusion, we established that the nested multiscale model of FMD can be extended to higher levels of organisation using graph-theoretic methods. Furthermore, the nested model has a primary level multiscale cycle with only local exchange of pathogen.

Chapter 4

Community-level Multiscale model for Foot-and-Mouth disease in cattle

4.1 Introduction

In this chapter, we characterise a multiscale model for FMD at community level using graph-theoretic method. However, the major challenge is whether we can extend the models in chapter 2 and chapter 3 to community level in order to characterise the multiscale model which incorporates both local transmission and global transmission. Therefore, based on the characterisation of the multiscale models we established that the graph theoretic model in chapter 2 can not be extended to a higher level using the graph-theoretic method. Thus, we extend the nested multiscale model in chapter 3 to a community level multiscale model. We seek to characterise the spread of FMDV taking into account both the dynamics of FMD at within-community scale and the interactions at between-community scale.

At community level, within the community there is direct transmission of FMDV when infected cells/tissues/hosts come into direct contact with susceptible cells/tissues/hosts or environmental transmission when FMDV comes in contact with susceptible cells/tissues/hosts. This is local transmission that can be represented by ordinary differential equations. At between-community there is movement of infected individuals between communities. This movement is global transmission and can be represented using graph theoretic approach. This is a new aspect that is characterised in this chapter.

Mathematical models are fundamental tools to acquire better understanding into various aspects of environmentally transmitted diseases, particularly FMD. These insights have the potential to assist us in implementing interventions. Presently, the modelling frameworks based on compartmentalization of animals (cattle) into SIRS (and their variations) have been used to give insights of local transmission mechanisms

or global transmission mechanisms of FMD separately [7, 78, 79, 83, 93, 111, 115–128]. Furthermore, various mathematical models have been formulated giving insights of transmission mechanisms of FMD disease at single scale using graph theoretic methods [122, 129, 130] however, to the best of my knowledge there is no model that characterises local transmission and global transmission of pathogen at macrocommunity level using both ordinary differential equations and graph theoretic methods. The latest work that has been done which is more appropriate in modelling the progression of infectious disease systems based on replication-transmission relativity theory is the multiscale modelling appproach [1]. The multiscale modelling of global transmission mechanisms of infectious diseases is better achieved through the use of graph theoretic methods while the standard SIR models address the local transmission mechanisms. In this study, the main ideas are centred on developing a multiscale modelling approach in tandem with graph theoretic methods at macrocommunity level, and nodes represent communities (patches) with possible transmission represented by edges.

4.2 The mathematical model

The model we formulate is derived from the model in chapter 3 developed using the nested approach in section (3.2.1.3). To formulate the multi-scale model, assume that the environment under consideration is divided into n patches, which may be cities, geographic regions or communities. We assume that there is homogeneity within each patch. We divide the cattle population in patch i into compartments of susceptible and infective individuals with the number in each compartment represented by S_{Ci} and I_{Ci}, respectively, for $i = 1, ..., n$. Let the total number of individuals in patch i be represented by $N_{Ci} = S_{Ci} + I_{Ci}$. Assume that the rates of cattle migration between patches hinges on disease status, and that the infection status of individuals does not change during migration. The rate of migration of cattle from patch j to patch i is represented by $\psi^S_{j,i}$ and $\psi^I_{j,i}$ for susceptible and infective individuals, respectively, where $\psi^S_{i,i} = \psi^I_{i,i} = 0$. This framework illustrates a multi-digraph where nodes represent patches and links represent the rates of migration, described by the nonnegative matrices $\Psi^S = [\psi^S_{j,i}]$ and $\Psi^I = [\psi^I_{j,i}]$. These matrices are presumed to be irreducible. We assume the birth rate in patch i for the susceptible class to be Λ_{Ci} individuals per unit time. We also assume that the natural death rate is independent of disease status with $\mu_{C_i}^{S_C} > 0$ and $\mu_{C_i}^{I_C} > 0$ for susceptible and infected populations. Once infected, a susceptible individual (S_{C_i}) in patch i harbors FMDV, develops clinical infection and progresses into the infectious compartment I_{C_i} at the rate α_{C_i} . Upon recovery, an individual moves to the susceptible compartment as disease immunity fades at a rate δ_{C_i}. The death rate induced by FMD is denoted by d_{Ci}. V_{Ci} is the total infectious reservoir of cattle in a particular community defined here as community viral load (CVL).

$$\begin{cases} \dfrac{dS_{Ci}}{dt} = \Lambda_{Ci} - \dfrac{\beta_{Ci}V_{Ci}}{V_{0i}+V_{Ci}}S_{Ci} - \mu_{C_i}^{S_C}S_{Ci} + \delta_{Ci}I_{Ci} + \sum_{j=1,j\neq i}^{n}\psi_{j,i}^{S_C}S_{Cj} - \sum_{j=1,j\neq i}^{n}\psi_{i,j}^{S_C}S_{Ci} \\ \dfrac{dI_{Ci}}{dt} = \dfrac{\beta_{Ci}V_{Ci}}{V_{0i}+V_{Ci}}S_{Ci} - (\delta_{Ci} + d_{Ci}(V,A) + \mu_{C_i}^{I_C})I_{Ci} + \sum_{j=1,j\neq i}^{n}\psi_{j,i}^{I_C}I_{Cj} - \sum_{j=1,j\neq i}^{n}\psi_{i,j}^{I_C}I_{Ci} \\ \dfrac{dV_{Ci}}{dt} = N_i\alpha_i I_{Ci}(t) - \alpha_{Ci}(V,A)V_{Ci} \end{cases} \quad (4.2.1)$$

where

$$N_i = \frac{\zeta\tilde{F}\mathfrak{R}_0}{\epsilon U^0}$$

is a composite constant parameter

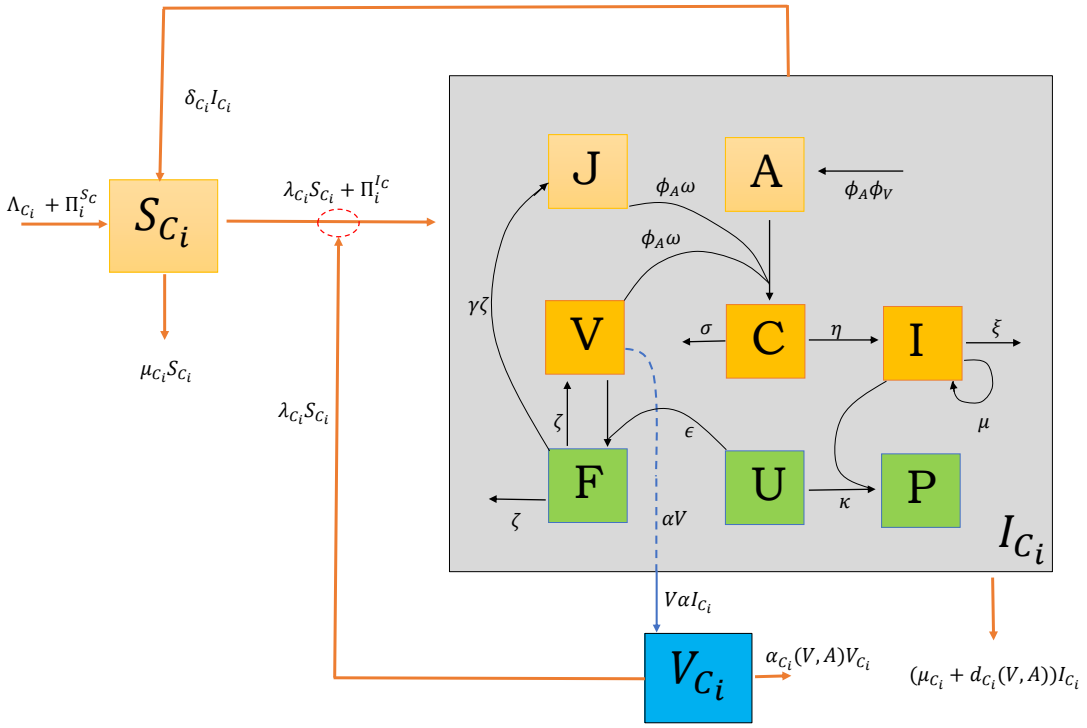

Figure 4.1: Multiscale Schematic diagram of a multiscale model system (4.2.1) of FMD for the cattle population in province i, where $\Pi_i^Q = \sum_{j=1,j\neq i}^{n}\psi_{j,i}^{Q}Q_j - \sum_{j=1,j\neq i}^{n}\psi_{i,j}^{Q}Q_i$, represents the cattle migration between provinces, with $Q \in \{S_C, I_C\}$

We presume that the parameters implemented in the model are all positive and the initial conditions for

the multiscale model system (4.2.1) are $S_{Ci}(0) \geq 0$, $I_{Ci}(0) \geq 0$, $V_{Ci}(0) \geq 0$.

Table 4.1: Description of between-host scale model variables for ith individual.

Variable	Description
$S_{C_i}(t)$	Susceptible cattle
$I_{C_i}(t)$	Infectious cattle
$V_{C_i}(t)$	Community viral load

Table 4.2: Description of within-host model variables in (3.2.2).

Variable	Description	Units	Initial value
F	Infected cells	TCID_{50} ml^{-1}	0
C	Virus-antibody complexes	TCID_{50} ml^{-1} equiv.	0
P	Protected cells	Cell	0
U	Uninfected cells	Cell	1
A	Antibody	LPBE-titre	0
V	Conc. of virions in blood	TCID_{50} ml^{-1}	0
J	Non-infectious material	TCID_{50} ml^{-1} equiv.	0
I	Interferon	IU ml^{-1}	$\frac{\mu}{\xi}$

4.2.1 Feasibe region of the model

The model that we formulate has to be biologically meaningful. Therefore, we establish the non-negativity and boundedness of all the state variables as well as their solutions, respectively, in the region Φ, where

$$\Phi = \left\{(S_{C_i}, I_{C_i}, V_{C_i}) \in \mathbb{R}^{3n}_{+}\right\}, i = 1, ..., n \tag{4.2.1}$$

4.2.1.1 Positivity of solutions

Theorem 4.1. *A non-negative solution* $(S_{C_i}(t), I_{C_i}(t), V_{C_i}(t))$ *exists for all* $t \geq 0$

Proof. The positivity of the solutions of the multiscale model system (4.2.1) can be proved using the integrating factor technique. Considering the first equation in the multiscale model system

$$\frac{dS_{Ci}}{dt} = \Lambda_{Ci} - \frac{\beta_{Ci} V_{Ci}}{V_{0i} + V_{Ci}} S_{Ci} - \mu_{C_i}^{S_C} S_{Ci} + \delta_{Ci} I_{Ci} + \sum_{j=1, j\neq i}^{n} \psi_{j,i}^{S_C} S_{Cj} - \sum_{j=1, j\neq i}^{n} \psi_{i,j}^{S_C} S_{Ci} \tag{4.2.2}$$

We re-write equation (4.2.2) as follows

$$\frac{dS_{Ci}}{dt}+\left[\frac{\beta_{Ci}V_{Ci}}{V_{0i}+V_{Ci}}+\mu_{C_i}^{S_C}+\sum_{j=1,j\neq i}^{n}\psi_{i,j}^{S_C}\right]S_{Ci}=\Lambda_{Ci}+\delta_{Ci}I_{Ci}+\sum_{j=1,j\neq i}^{n}\psi_{j,i}^{S_C}S_{Cj} \tag{4.2.3}$$

The integrating factor for equation (4.2.3) is

$$\text{Integrating factor (IF)}=e^{\int_0^t\left[\frac{\beta_{C_i}V_{C_i}(s)}{V_{0i}+V_{C_i}(s)}+{\mu_{C_i}}^{S_C}+\sum_{j=1,j\neq i}^{n}\psi_{i,j}^{S_C}\right]ds}$$

$$=e^{\left(\beta_{C_i}+\mu_{C_i}^{S_C}+\sum_{j=1,j\neq i}^{n}\psi_{i,j}^{S_C}\right)t-\beta_{C_i}V_{0i}\ln\left|\frac{V_{0i}+V_{C_i}(t)}{V_{0i}+V_{C_i}(0)}\right|} \tag{4.2.4}$$

Multiplying equation (4.2.3) by the integrating factor $e^{\left(\beta_{C_i}+\mu_{C_i}^{S_C}+\sum_{j=1,j\neq i}^{n}\psi_{i,j}^{S_C}\right)t-\beta_{C_i}V_{0i}\ln\left|\frac{V_{0i}+V_{C_i}(t)}{V_{0i}+V_{C_i}(0)}\right|}$ to get

$$e^{\left(\beta_{C_i}+\mu_{C_i}^{S_C}+\sum_{j=1,j\neq i}^{n}\psi_{i,j}^{S_C}\right)t-\beta_{C_i}V_{0i}\ln\left|\frac{V_{0i}+V_{C_i}(t)}{V_{0i}+V_{C_i}(0)}\right|}.\frac{dS_{Ci}}{dt}$$

$$+e^{\left(\beta_{C_i}+\mu_{C_i}^{S_C}+\sum_{j=1,j\neq i}^{n}\psi_{i,j}^{S_C}\right)t-\beta_{C_i}V_{0i}\ln\left|\frac{V_{0i}+V_{C_i}(t)}{V_{0i}+V_{C_i}(0)}\right|}.\left[\frac{\beta_{Ci}V_{Ci}}{V_{0i}+V_{Ci}}+\mu_{C_i}^{S_C}+\sum_{j=1,j\neq i}^{n}\psi_{i,j}^{S_C}\right]S_{Ci}$$

$$=e^{\left(\beta_{C_i}+\mu_{C_i}^{S_C}+\sum_{j=1,j\neq i}^{n}\psi_{i,j}^{S_C}\right)t-\beta_{C_i}V_{0i}\ln\left|\frac{V_{0i}+V_{C_i}(t)}{V_{0i}+V_{C_i}(0)}\right|}.\left[\Lambda_{Ci}+\delta_{Ci}I_{Ci}+\sum_{j=1,j\neq i}^{n}\psi_{j,i}^{S_C}S_{Cj}\right] \tag{4.2.5}$$

From the product rule we obtain

$$\frac{d}{dt}\left[e^{\left(\beta_{C_i}+\mu_{C_i}^{S_C}+\sum_{j=1,j\neq i}^{n}\psi_{i,j}^{S_C}\right)t-\beta_{C_i}V_{0i}\ln\left|\frac{V_{0i}+V_{C_i}(t)}{V_{0i}+V_{C_i}(0)}\right|}.S_{C_i}\right]$$

$$=e^{\left(\beta_{C_i}+\mu_{C_i}^{S_C}+\sum_{j=1,j\neq i}^{n}\psi_{i,j}^{S_C}\right)t-\beta_{C_i}V_{0i}\ln\left|\frac{V_{0i}+V_{C_i}(t)}{V_{0i}+V_{C_i}(0)}\right|}.\left[\Lambda_{Ci}+\delta_{Ci}I_{Ci}+\sum_{j=1,j\neq i}^{n}\psi_{j,i}^{S_C}S_{Cj}\right] \tag{4.2.6}$$

Dividing both sides by the integrating factor we get

$$S_{C_i}(t)=e^{-\left\{\left(\beta_{C_i}+\mu_{C_i}^{S_C}+\sum_{j=1,j\neq i}^{n}\psi_{i,j}^{S_C}\right)s-\beta_{C_i}V_{0i}\ln\left|\frac{V_{0i}+V_{C_i}(t)}{V_{0i}+V_{C_i}(0)}\right|\right\}}\times$$

$$\int_0^t e^{\left(\beta_{C_i}+\mu_{C_i}^{S_C}+\sum_{j=1,j\neq i}^{n}\psi_{i,j}^{S_C}\right)t-\beta_{C_i}V_{0i}\ln\left|\frac{V_{0i}+V_{C_i}(s)}{V_{0i}+V_{C_i}(0)}\right|}.\left[\Lambda_{Ci}+\delta_{Ci}I_{Ci}(s)+\sum_{j=1,j\neq i}^{n}\psi_{j,i}^{S_C}S_{Cj}(s)\right]ds\geq 0 \tag{4.2.7}$$

Similarly, positivity of the other two equations of multiscale model system (4.2.1) is proved using the integrating factor technique. Consequently, $S_{C_i}(t)\geq 0, I_{C_i}(t)\geq 0, V_{C_i}(t)\geq 0$ for all time $t>0$. □

4.2.2 Boundedness of Solutions

Letting $N_{C_i}(t)$ to represent the total number of cattle population and adding the first and second equation of the multiscale model system (4.2.1) and letting $N_C(t)=N_{C_1}(t)+N_{C_2}(t)+...+N_{C_n}(t)$, we get

$$\frac{dN_C(t)}{dt}=\Lambda_{C_i}-\mu_{C_i}^{S_C}N_{C_i}(t)-\delta_{C_i}I_{C_i}(t)+\sum_{j=1,j\neq i}^{n}\psi_{j,i}^{S_C}S_{Cj}-\sum_{j=1,j\neq i}^{n}\psi_{i,j}^{S_C}S_{Ci}+\sum_{j=1,j\neq i}^{n}\psi_{j,i}^{I_C}I_{Cj}$$

$$-\sum_{j=1,j\neq i}^{n}\psi_{i,j}^{I_C}I_{Ci}\leq\sum_{i=1}^{n}\Lambda_{C_i}-\min\left\{\mu_{C_1}^{S_C},\mu_{C_2}^{S_C},...,\mu_{C_n}^{S_C}\right\}N_C(t) \tag{4.2.1}$$

Because $dN_C(t)/dt\leq\sum_{i}^{n}\Lambda_{C_i}-\min\left\{\mu_{C_1}^{S_C},\mu_{C_2}^{S_C},...,\mu_{C_n}^{S_C}\right\}N_C(t)$, it follows that $dN_C(t)/dt\leq 0$ if $N_C(t)\geq\dfrac{\sum_{i=1}^{n}\Lambda_{C_i}}{\min\left\{\mu_{C_1}^{S_C},\mu_{C_2}^{S_C},...,\mu_{C_n}^{S_C}\right\}}$.

We implement the integrating factor method to (4.2.1). When we re-write (4.2.1) we get

$$\frac{dN_C(t)}{dt}+\min\left\{\mu_{C_1}^{S_C},\mu_{C_2}^{S_C},...,\mu_{C_n}^{S_C}\right\}N(t)\leq\sum_{i=1}^{n}\Lambda_{C_i} \tag{4.2.2}$$

The integrating factor (IF) is

$$e^{\int_0^t\min\left\{\mu_{C_1}^{S_C},\mu_{C_2}^{S_C},...,\mu_{C_n}^{S_C}\right\}ds}=e^{\min\left\{\mu_{C_1}^{S_C},\mu_{C_2}^{S_C},...,\mu_{C_n}^{S_C}\right\}t} \tag{4.2.3}$$

We multiply $e^{\min\left\{\mu_{C_1}^{S_C},\mu_{C_2}^{S_C},...,\mu_{C_n}^{S_C}\right\}t}$ into (4.2.2) to obtain

$$e^{\min\left\{\mu_{C_1}^{S_C},\mu_{C_2}^{S_C},...,\mu_{C_n}^{S_C}\right\}t}.\frac{dN_C(t)}{dt}+e^{\min\left\{\mu_{C_1}^{S_C},\mu_{C_2}^{S_C},...,\mu_{C_n}^{S_C}\right\}t}.\min\left\{\mu_{C_1}^{S_C},\mu_{C_2}^{S_C},...,\mu_{C_n}^{S_C}\right\}N(t)$$

$$\leq e^{\min\left\{\mu_{C_1}^{S_C},\mu_{C_2}^{S_C},...,\mu_{C_n}^{S_C}\right\}t}.\sum_{i=1}^{n}\Lambda_{C_i} \tag{4.2.4}$$

From the product rule we have

$$\frac{d}{dt}\left[e^{\min\left\{\mu_{C_1}^{S_C},\mu_{C_2}^{S_C},...,\mu_{C_n}^{S_C}\right\}t}.N_C(t)\right] \leq e^{\min\left\{\mu_{C_1}^{S_C},\mu_{C_2}^{S_C},...,\mu_{C_n}^{S_C}\right\}t}.\sum_{i=1}^{n}\Lambda_{C_i} \tag{4.2.5}$$

$$e^{\min\left\{\mu_{C_1}^{S_C},\mu_{C_2}^{S_C},...,\mu_{C_n}^{S_C}\right\}t}.N_C(t) \leq N_C(0) + \frac{\left[e^{\min\left\{\mu_{C_1}^{S_C},\mu_{C_2}^{S_C},...,\mu_{C_n}^{S_C}\right\}t}-1\right].\sum_{i=1}^{n}\Lambda_{C_i}}{\min\left\{\mu_{C_1}^{S_C},\mu_{C_2}^{S_C},...,\mu_{C_n}^{S_C}\right\}} \tag{4.2.6}$$

$$N_C(t) \leq e^{-\min\left\{\mu_{C_1}^{S_C},\mu_{C_2}^{S_C},...,\mu_{C_n}^{S_C}\right\}t}.N_C(0) + e^{-\min\left\{\mu_{C_1}^{S_C},\mu_{C_2}^{S_C},...,\mu_{C_n}^{S_C}\right\}t}.\frac{\left[e^{\min\left\{\mu_{C_1}^{S_C},\mu_{C_2}^{S_C},...,\mu_{C_n}^{S_C}\right\}t}-1\right].\sum_{i=1}^{n}\Lambda_{C_i}}{\min\left\{\mu_{C_1}^{S_C},\mu_{C_2}^{S_C},...,\mu_{C_n}^{S_C}\right\}} \tag{4.2.7}$$

$$N_C(t) \leq e^{-\min\left\{\mu_{C_1}^{S_C},\mu_{C_2}^{S_C},...,\mu_{C_n}^{S_C}\right\}t}.N_C(0) + \frac{\left[1-e^{-\min\left\{\mu_{C_1}^{S_C},\mu_{C_2}^{S_C},...,\mu_{C_n}^{S_C}\right\}t}\right].\sum_{i=1}^{n}\Lambda_{C_i}}{\min\left\{\mu_{C_1}^{S_C},\mu_{C_2}^{S_C},...,\mu_{C_n}^{S_C}\right\}} \tag{4.2.8}$$

This implies that

$$\lim_{t\to\infty}\sup(N_C(t)) \leq \frac{\sum_{i=1}^{n}\Lambda_{C_i}}{\min\left\{\mu_{C_1}^{S_C},\mu_{C_2}^{S_C},...,\mu_{C_n}^{S_C}\right\}} \tag{4.2.9}$$

Similarly, we let $V_C = \sum_{i=1}^{n} V_{C_i}$ and $I_C = \sum_{i=1}^{n} I_{C_i}$. Then from the third equation of model system (4.2.1) we obtain

$$\frac{dV_C}{dt} = \min\left\{N_1\alpha_1,...,N_n\alpha_n\right\}I_C - \min\left\{\alpha_{C_1},...,\alpha_{C_n}\right\}V_C \tag{4.2.10}$$

$$\frac{dV_C}{dt} \leq \min\left\{N_1\alpha_1,...,N_n\alpha_n\right\}\frac{\sum_{i=1}^{n}\Lambda_{C_i}}{\min\left\{\mu_{C_1}^{S_C},\mu_{C_2}^{S_C},...,\mu_{C_n}^{S_C}\right\}} - \min\left\{\alpha_{C_1},...,\alpha_{C_n}\right\}V_C \tag{4.2.11}$$

We re-write (4.2.11) to get

$$\frac{dV_C}{dt} + \min\left\{\alpha_{C_1},...,\alpha_{C_n}\right\}V_C \leq \min\left\{N_1\alpha_1,...,N_n\alpha_n\right\}\frac{\sum_{i=1}^{n}\Lambda_{C_i}}{\min\left\{\mu_{C_1}^{S_C},\mu_{C_2}^{S_C},...,\mu_{C_n}^{S_C}\right\}} \tag{4.2.12}$$

The integrating factor (IF) is $e^{\min\left\{\alpha_{C_1},...,\alpha_{C_n}\right\}t}$. Multipying (4.2.12) with the integrating factor $e^{\min\left\{\alpha_{C_1},...,\alpha_{C_n}\right\}t}$ we obtain

$$e^{\min\{\alpha_{C_1},...,\alpha_{C_n}\}t}.\frac{dV_C}{dt}+e^{\min\{\alpha_{C_1},...,\alpha_{C_n}\}t}.\min\{\alpha_{C_1},...,\alpha_{C_n}\}V_C$$

$$\leq e^{\min\{\alpha_{C_1},...,\alpha_{C_n}\}t}.\min\{N_1\alpha_1,...,N_n\alpha_n\}\frac{\sum_{i=1}^{n}\Lambda_{C_i}}{\min\left\{\mu_{C_1}^{S_C},\mu_{C_2}^{S_C},...,\mu_{C_n}^{S_C}\right\}} \tag{4.2.13}$$

From the product rule we have

$$\frac{d}{dt}\left[e^{\min\{\alpha_{C_1},...,\alpha_{C_n}\}t}.V_C\right]\leq e^{\min\{\alpha_{C_1},...,\alpha_{C_n}\}t}.\min\{N_1\alpha_1,...,N_n\alpha_n\}\frac{\sum_{i=1}^{n}\Lambda_{C_i}}{\min\left\{\mu_{C_1}^{S_C},\mu_{C_2}^{S_C},...,\mu_{C_n}^{S_C}\right\}} \tag{4.2.14}$$

When integrate (4.2.14) we get

$$e^{\min\{\alpha_{C_1},...,\alpha_{C_n}\}t}.V_C\leq V_C(0)+\frac{\left[e^{\min\{\alpha_{C_1},...,\alpha_{C_n}\}t}-1\right]}{\min\{\alpha_{C_1},...,\alpha_{C_n}\}}.\min\{N_1\alpha_1,...,N_n\alpha_n\}.\frac{\sum_{i=1}^{n}\Lambda_{C_i}}{\min\left\{\mu_{C_1}^{S_C},\mu_{C_2}^{S_C},...,\mu_{C_n}^{S_C}\right\}} \tag{4.2.15}$$

Dividing both sides by the integrating factor gives

$$V_C\leq e^{-\min\{\alpha_{C_1},...,\alpha_{C_n}\}t}.V_C(0)+\frac{\left[1-e^{-\min\{\alpha_{C_1},...,\alpha_{C_n}\}t}\right]}{\min\{\alpha_{C_1},...,\alpha_{C_n}\}}.\frac{\sum_{i=1}^{n}\Lambda_{C_i}.\min\{N_1\alpha_1,...,N_n\alpha_n\}}{\min\left\{\mu_{C_1}^{S_C},\mu_{C_2}^{S_C},...,\mu_{C_n}^{S_C}\right\}} \tag{4.2.16}$$

This implies

$$\lim_{t\to\infty}\sup(V_C(t))\leq\frac{\sum_{i=1}^{n}\Lambda_{C_i}.\min\{N_1\alpha_1,...,N_n\alpha_n\}}{\min\left\{\alpha_{C_1}\mu_{C_1}^{S_C},\alpha_{C_2}\mu_{C_2}^{S_C},...,\alpha_{C_n}\mu_{C_n}^{S_C}\right\}} \tag{4.2.17}$$

Letting

$$\Phi=\left\{(S_{C_i};I_{C_i};V_{C_i})\in\mathbb{R}_+^3:0\leq N_C\leq K_1,0\leq V_C\leq K_2\right\} \tag{4.2.18}$$

where the constants K_1 and K_2 are such that

$$\begin{cases}K_1=\dfrac{\sum_{i=1}^{n}\Lambda_{C_i}}{\min\left\{\mu_{C_1}^{S_C},\mu_{C_2}^{S_C},...,\mu_{C_n}^{S_C}\right\}},\\[2ex] K_2=\dfrac{\sum_{i=1}^{n}\Lambda_{C_i}.\min\{N_1\alpha_1,...,N_n\alpha_n\}}{\min\left\{\alpha_{C_1}\mu_{C_1}^{S_C},\alpha_{C_2}\mu_{C_2}^{S_C},...,\alpha_{C_n}\mu_{C_n}^{S_C}\right\}}>0\end{cases} \tag{4.2.19}$$

Therefore, Φ is a positively invariant and attracting region, since all the solutions that start in Φ will remain in Φ for all $t \geq 0$. Therefore, the results confirm the non-negativity and boundedness of all the state variables respectively, in the region Φ. Consequently, we can conclude that the multiscale model system (4.2.1) is mathematically and epidemiologically well-posed. □

Theorem 4.2. *The region* $\Phi = \left\{(S_{C_i}, I_{C_i}, V_{C_i}) \in \mathbb{R}_+^{3n}\right\}, i = 1, ..., n$ *is positively invariant for the multiscale model system (4.2.1) with nonnegative initial conditions in* $\mathbb{R}_+^{3n}$.

4.3 Determination of disease free equilibrium and its stability

From the multiscale model (4.2.1), we have

$$\Lambda_{Ci} - \mu_{C_i}^{S_C} S_{Ci} + \sum_{j\neq i=1}^{n} \psi_{j,i}^{S_C} S_{Cj} - \sum_{j\neq i=1}^{n} \psi_{i,j}^{S_C} S_{Ci} = 0, \quad i = i, 1, 2, ..., n, \tag{4.3.1}$$

Infact, expressing equation (4.3.1) in the form of matrix system we have,

$$\begin{aligned}
\Lambda_{Ci} - \frac{\beta_{Ci} V_{Ci}}{V_{0i} + V_{Ci}}^{0} S_{Ci} - \mu_{C_i}^{S_C} S_{Ci} + \delta_{Ci}{}^{0} I_{Ci} + \sum_{j\neq i=1}^{n} \psi_{j,i}^{S_C} S_{Cj} - \sum_{j\neq i=1}^{n} \psi_{i,j}^{S_C} S_{Ci} = 0, \\
\Lambda_{Ci} - \mu_{C_i}^{S_C} S_{Ci} + \sum_{j\neq i=1}^{n} \psi_{j,i}^{S_C} S_{Cj} - \sum_{j\neq i=1}^{n} \psi_{i,j}^{S_C} S_{Ci} = 0, \\
\Lambda_{Ci} - \left(\mu_{C_i}^{S_C} + \sum_{j\neq i=1}^{n} \psi_{i,j}^{S_C}\right) S_{Ci} + \sum_{j\neq i=1}^{n} \psi_{j,i}^{S_C} S_{Cj} = 0
\end{aligned} \tag{4.3.2}$$

From (4.3.2) we obtain the solution

$$\sum_{j=1}^{n} \varphi_{i,j}^{S} S_{Cj} = \Lambda_{Ci} \tag{4.3.3}$$

where

$$\begin{cases}
\varphi_{i,j}^{S_C} = -\psi_{i,j}^{S_C} \quad \text{for} \quad j = 1; 2; ...; n; j \neq i \\
\varphi_{i,j}^{S_C} = \mu_{C_i}^{S_C} + \sum_{j\neq i=1}^{n} \psi_{i,j}^{S_C} \quad \text{for} \quad j = i
\end{cases} \tag{4.3.4}$$

By the matricial form we have

$$\varphi^{S_C} S_C = \Lambda_C, \tag{4.3.5}$$

where $\varphi^{S_C} = \left(\varphi_{i,j}^{S_C}\right)_{1\leq i,j\leq n}$; $S_C = (S_{C1}; S_{C2}; ...; S_{Cn})$ and $\Lambda_C = (\Lambda_{C1}; \Lambda_{C2}; ...; \Lambda_{Cn})^T$

We can demonstrate that the positivity of the disease-free equilibrium, which results in the multiscale model system (4.2.1) having a unique positive solution $S_C = S_C^0 = (\varphi^{S_C})^{-1}\Lambda_C > 0$.

In the case of cattle hosts:

$$\Lambda_{Ci} - \left(\mu_{C_i}^{S_C} + \sum_{i=1, j\neq i}^{n} \psi_{i,j}^{S_C}\right) S_{Ci} + \sum_{i=1, j\neq i}^{n} \psi_{j,i}^{S_C} S_{Cj} = 0 \tag{4.3.6}$$

$$\left(\mu_{C_i}^{S_C} + \sum_{i=1, j\neq i}^{n} \psi_{i,j}^{S_C}\right) S_{Ci} - \sum_{i=1, j\neq i}^{n} \psi_{j,i}^{S_C} S_{Cj} = \Lambda_{Ci} \tag{4.3.7}$$

$$\begin{bmatrix} \mu_{C_1} + \sum_{j\neq i=1}^{n} \psi_{1j}^{S} & -\psi_{12}^{S} & \cdots & -\psi_{1n}^{S} \\ -\psi_{21}^{S} & \ddots & \cdots & -\psi_{2n}^{S} \\ \vdots & \vdots & \ddots & \vdots \\ -\psi_{n1}^{S} & -\psi_{n2}^{S} & \cdots & \mu_{C_n} + \sum_{j=n} \psi_{jn} \end{bmatrix} \begin{bmatrix} S_{C_1}^0 \\ S_{C_2}^0 \\ \vdots \\ S_{C_n}^0 \end{bmatrix} = \begin{bmatrix} \Lambda_{C_1} \\ \Lambda_{C_2} \\ \vdots \\ \Lambda_{C_n} \end{bmatrix} \tag{4.3.8}$$

i.e. $DS_C^0 = \Lambda_C$ where $D = diag\left(\mu_{C_i}^{S_C} + \sum_{i=1, j\neq i}^{n} \psi_{i,j}^{S_C}\right) - M^{S_C}$;

$$M^{S_C} = \begin{bmatrix} 0 & \psi_{1,2}^{S_C} & \cdots & \psi_{1,n}^{S_C} \\ \psi_{2,1}^{S_C} & 0 & \cdots & \psi_{2,n}^{S_C} \\ \vdots & \vdots & \ddots & \vdots \\ \psi_{n,1}^{S_C} & \psi_{n,2}^{S_C} & \cdots & 0 \end{bmatrix} \tag{4.3.9}$$

$\Lambda_C = (\Lambda_{C_1}, \Lambda_{C_2}, ..., \Lambda_{C_n})^T$, $S_C^0 = \left(S_{C1}^0; S_{C2}^0; ...; S_{Cn}^0\right)^T$

From (4.3.8) all the off-diagonal entries of φ^{S_C} are non-positive and the total of all the entries in every column of φ^S is positive. Furthermore, φ^{S_C} is an irreducible non-singular M-matrix and so φ^{S_C} must have positive inverse, that is, $\left(\varphi^{S_C}\right)^{-1} > 0$, [131]. Consequently, this implies uniqueness of a positive solution $S_C^0 = \left(\varphi^{S_C}\right)^{-1}\Lambda_C > 0$. Therefore, the results demonstrate the existence of a unique positive disease-free equilibrium

$$E_0 = \left(S_C^0, \mathbf{0}, \mathbf{0}, \right) \tag{4.3.10}$$

where $\mathbf{0} = \underbrace{(0, ..., 0)}_{n \quad times}$, $S_C^0 = \left(\varphi^{S_C}\right)^{-1} \Lambda_C$ □

Theorem 4.3. *The multiscale model system (4.2.1) always has a unique disease-free equilibrium point* E_0.

4.3.1 The model reproduction number, $\mathcal{R}_0$

In order to evaluate the basic reproductive number we implement the next generation operator approach [101]. The multiscale model system (4.2.1) can be expressed as follows:

$$\begin{aligned} \frac{dX}{dt} &= f(X, Z), \\ \frac{dZ}{dt} &= h(X, Z), \end{aligned} \tag{4.3.1}$$

where

$$X = (S_{C_i}) \tag{4.3.2}$$

$$Z = (I_{C_i}, V_{C_i}) \tag{4.3.3}$$

The elements of X stand for the number of susceptibles as well as other groups of non-infectious individuals. The elements of Z stand for infected individuals able to transmit the disease.

The compartments of the disease can be given as I_{C_i} and V_{C_i}. The infected case can be expressed as follows:

$(I_{C_1}, I_{C_2}, ..., I_{C_n}, V_{C_1}, V_{C_2}, ..., V_{C_n})$ as

$$\begin{cases} \dfrac{dI_{Ci}}{dt} = \dfrac{\beta_{Ci} V_{Ci}}{V_{0i} + V_{Ci}} S_{Ci} - (\delta_{Ci} + d_{Ci}(V, A) + \mu_{C_i}^{I_C}) I_{Ci} + \displaystyle\sum_{i=1, j \neq i}^{n} \psi_{j,i}^{I_C} I_{Cj} - \sum_{i=1, j \neq i}^{n} \psi_{i,j}^{I_C} I_{Ci} \\ \dfrac{dV_{Ci}}{dt} = N_i \alpha_i I_{Ci}(t) - \alpha_{Ci}(V, A) V_{Ci} \end{cases} \tag{4.3.4}$$

$$\begin{cases} \dfrac{dI_{Ci}}{dt} = \dfrac{\beta_{Ci}V_{Ci}}{V_{0i}+V_{Ci}}S_{Ci} - \left(\delta_{Ci} + d_{Ci}(V,A) + \mu_{C_i}^{I_C}\right)\displaystyle\sum_{i=1,j\neq i}^{n}\psi_{i,j}^{I_C}\right) I_{Ci} + \sum_{i=1,j\neq i}^{n}\psi_{j,i}^{I_C} I_{Cj} \\ \dfrac{dV_{Ci}}{dt} = N_i\alpha_i I_{Ci}(t) - \alpha_{Ci}(V,A)V_{Ci} \end{cases} \tag{4.3.5}$$

$$\begin{cases} \dfrac{dI_{Ci}}{dt} = \dfrac{\beta_{Ci}V_{Ci}}{V_{0i}+V_{Ci}}S_{Ci} - \displaystyle\sum_{i=1,j\neq i}^{n}\varphi_{i,j}^{I_C} I_{Cj} \\ \dfrac{dV_{Ci}}{dt} = N_i\alpha_i I_{Ci}(t) - \alpha_{Ci}(V,A)V_{Ci} \end{cases} \tag{4.3.6}$$

where

$$\begin{cases} \varphi_{i,j}^{I_C} = -\psi_{i,j}^{I_C} \quad \text{for} \quad j = 1,...,n, j \neq i \\ \varphi_{i,j}^{I_C} = \delta_{Ci} + d_{Ci}(V,A) + \mu_{C_i}^{I_C} + \displaystyle\sum_{i=1,j\neq i}^{n}\psi_{i,j}^{I_C}, j = i \end{cases} \tag{4.3.7}$$

The vector of the rates of new infections and the vector of the rates of other transfers between disease states from (4.3.6) are respectively represented by

$$\mathbf{F} = \begin{bmatrix} \left[\dfrac{\beta_{Ci}V_{Ci}}{V_{0i}+V_{Ci}}S_{Ci}\right]_{i=1,...,n} \\ 0_n \end{bmatrix} \text{ and } \quad \mathbf{V} = \begin{bmatrix} \left[\displaystyle\sum_{j=1}^{n}\varphi_{i,j}^{I_C} I_{C_j}\right]_{i=1,..,n} \\ \left[-N_i\alpha_i I_{Ci} + \alpha_{Ci}(V,A)V_{Ci}\right]_{i=1,...,n} \end{bmatrix} \tag{4.3.8}$$

With respect to the infected classes (I_{Ci} and V_{Ci}) evaluated at the disease-free equilibrium point $\mathcal{E}_0$, the Jacobian matrices of $\mathbf{F}$ and $\mathbf{V}$ are respectively described as

$$\mathcal{F} = \begin{bmatrix} \mathbb{O} & \dfrac{\beta_{C_i}\Lambda_{C_i}}{V_{0i}\mu_{C_i}^{S_C}} \\ \mathbb{O} & \mathbb{O} \end{bmatrix} \tag{4.3.9}$$

$$\mathcal{F} = \begin{bmatrix} \mathbb{O} & F_{1,2} \\ \mathbb{O} & \mathbb{O} \end{bmatrix} \tag{4.3.10}$$

where

$$F_{1,2} = diag\left\{ \frac{\beta_{C_1}\Lambda_{C_1}}{V_{01}\mu_{C_1}^{S_C}}, ..., \frac{\beta_{C_n}\Lambda_{C_n}}{V_{0n}\mu_{C_n}^{S_C}} \right\} \tag{4.3.11}$$

On the other hand,

$$\mathcal{V} = \begin{bmatrix} V_{1,1} & \mathbb{O} \\ V_{2.1} & V_{2,2} \end{bmatrix} \tag{4.3.12}$$

$$\begin{cases} V_{1,1} = \left(\varphi_{i,j}^{I_C}\right)_{1\leq i,j\leq n} \\ V_{2,1} = diag(-N_1\alpha_1, -N_2\alpha_2, ..., -N_n\alpha_n) \\ V_{2,2} = diag(\alpha_{C_1}, ..., \alpha_{C_n}) \end{cases} \tag{4.3.13}$$

We define $\mathbb{O}$ as the $n \times n$ matrix with all entries being zero. Furthermore, we define the matrix $\mathcal{F}$ to be non-negative of rank one and that can be written as the product of vectors. The matrices $V_{1,1}$ and $V_{2,2}$ are non-singular irreducible M-matrices and can be inverted. We now determine the inverse of matrix $\mathcal{V}$.

$$\mathcal{V}^{-1} = \begin{bmatrix} V_{1,1}^{-1} & \mathbb{O} \\ -V_{2,1}v_{1,1}^{-1}V_{2,2}^{-1} & V_{2,2}^{-1} \end{bmatrix} \tag{4.3.14}$$

The Next Generation Matrix is given by:

$$M = \mathcal{F}\mathcal{V}^{-1} = \begin{bmatrix} \mathbb{O} & F_{1,2} \\ \mathbb{O} & \mathbb{O} \end{bmatrix} \begin{bmatrix} V_{1,1}^{-1} & \mathbb{O} \\ -V_{2,1}V_{1,1}^{-1}V_{2,2}^{-1} & V_{2,2}^{-1} \end{bmatrix} \tag{4.3.15}$$

$$M = \mathcal{F}\mathcal{V}^{-1} = \begin{bmatrix} -F_{1,2}V_{2,1}V_{1,1}^{-1}V_{2,2}^{-1} & F_{1,2}V_{2,2}^{-1} \\ \mathbb{O} & \mathbb{O} \end{bmatrix} \tag{4.3.16}$$

Therefore, $\mathcal{R}_0$ defined by the spectral radius of $\mathcal{F}\mathcal{V}^{-1}$, is

$\mathcal{R}_0 = \rho(\mathcal{B})$

where $\mathcal{B}$ represents an $n \times n$ positive matrix illustrated by

$\mathcal{B} = -F_{1,2}V_{2,1}V_{1,1}^{-1}V_{2,2}^{-1}$

$\mathcal{B} = -diag\left\{\frac{\beta_{C_1}\Lambda_{C_1}}{V_{01}\mu_{C_1}^{S_C}\alpha_{C_1}}, ..., \frac{\beta_{C_n}\Lambda_{C_n}}{V_{0n}\mu_{C_n}^{S_C}\alpha_{C_n}}\right\} diag\left\{-N_1\alpha_1, ..., -N_n\alpha_n\right\}\left(\varphi^{I_C}\right)^{-1}$

We now consider some particular situations:

(i) **Situation 1:** Suppose there is no migration between patches, hence, $\psi_{i,j}^{I_C} = \psi_{j,i}^{I_C} = 0$ for $j = i = 1, ..., n$ $j \neq i$ and we get

$$\begin{cases} \varphi_{i,j}^{I_C} = 0 \quad \text{for} \quad j = 1, ..., n \quad j \neq i \\ \\ \varphi_{i,i}^{I_C} = \delta_{Ci} + d_{Ci}(V, A) + \mu_{C_i}^{I_C} \end{cases} \tag{4.3.17}$$

Then $-F_{1,2}V_{2,1}V_{1,1}^{-1}V_{2,2}^{-1} = diag\left\{\frac{\beta_{C_1}\Lambda_{C_1}N_1\alpha_1}{V_{01}\mu_{C_1}^{S_C}\alpha_{C_1}(\delta_{C1} + d_{C1}(V, A) + \mu_{C_1}^{I_C})}, ..., \frac{\beta_{C_n}\Lambda_{C_n}N_n\alpha_n}{V_{0n}\mu_{C_n}^{S_C}\alpha_{C_n}(\delta_{Cn} + d_{Cn}(V, A) + \mu_{C_n}^{I_C})}\right\}$

Therefore

$$\mathcal{B} = diag\left\{\frac{\beta_{C_1}\Lambda_{C_1}N_1\alpha_1}{V_{01}\mu_{C_1}^{S_C}\alpha_{C_1}(\delta_{C1} + d_{C1}(V, A) + \mu_{C_1}^{I_C})}, ..., \frac{\beta_{C_n}\Lambda_{C_n}N_n\alpha_n}{V_{0n}\mu_{C_n}^{S_C}\alpha_{C_n}(\delta_{Cn} + d_{Cn}(V, A) + \mu_{C_n}^{I_C})}\right\} \tag{4.3.18}$$

and

$$\mathcal{R}_{0i} = \rho\left(\mathcal{B}\right) \tag{4.3.19}$$

Hence

$\mathcal{R}_0 = \max \mathcal{R}_{0i}$

where

$$\mathcal{R}_{0i} = \frac{\beta_{C_i}\Lambda_{C_i}N_i\alpha_i}{V_{0i}\mu_{C_i}^{S_C}\alpha_{C_i}(\delta_{Ci} + d_{Ci}(V, A) + \mu_{C_i}^{I_C})} \tag{4.3.20}$$

Accordingly, when $\mathcal{R}_{0i} > 1$ for all i, the disease-free equilibrium is unstable resulting in FMD invading the cattle population. This is verified by proving the global stability of the endemic equilibrium of FMD in section (4.4). However, when $\mathcal{R}_{0i} < 1$ for all i, the disease-free equilibrium is asymptotically stable

and FMD may be eliminated. Therefore, it is essential to diminish $\mathcal{R}_{0i}$ in each patch i in order to control FMD. This is verified by proving the global stability of the disease-free equilibrium in section (4.3.3).

(ii) **Situation 2:** Suppose there is migration in a model with two patches where the migration rates of the animal populations are nonzero.

$$F_{1,2} = diag\left\{\frac{\beta_{C_1}\Lambda_{C_1}}{V_{01}\mu_{C_1}^{S_C}}, \frac{\beta_{C_2}\Lambda_{C_2}}{V_{02}\mu_{C_2}^{S_C}}\right\} \tag{4.3.21}$$

and

$$\begin{cases} V_{1,1} = \left(\varphi_{i,j}^{I_C}\right)_{1\leq i,j\leq 2} \\ V_{2,1} = diag(-N_1\alpha_1, -N_2\alpha_2) \\ V_{2,2} = diag(\alpha_{C_1}, \alpha_{C_2}) \end{cases} \tag{4.3.22}$$

Then

$$\mathcal{B} = -F_{1,2}V_{2,1}V_{1,1}^{-1}V_{2,2}^{-1} = \begin{bmatrix} B_{11} & B_{12} \\ B_{21} & B_{22} \end{bmatrix}$$

$$\begin{cases} F_{1,2} = \begin{bmatrix} \frac{\beta_{C_1}\Lambda_{C_1}}{V_{01}\mu_{C_1}^{S_C}} & 0 \\ 0 & \frac{\beta_{C_2}\Lambda_{C_2}}{V_{02}\mu_{C_2}^{S_C}} \end{bmatrix} \\ V_{2,1} = \begin{bmatrix} -N_1\alpha_1 & 0 \\ 0 & -N_2\alpha_2 \end{bmatrix} \\ V_{1,1}^{-1} = \frac{1}{\varphi_{11}^{I_C}\varphi_{22}^{I_C} - \varphi_{12}^{I_C}\varphi_{21}^{I_C}} \begin{bmatrix} \varphi_{22}^{I_C} & -\varphi_{12}^{I_C} \\ -\varphi_{21}^{I_C} & \varphi_{11}^{I_C} \end{bmatrix} \\ V_{2,2}^{-1} = \frac{1}{\alpha_{C_1}\alpha_{C_2}} \begin{bmatrix} \alpha_{C_2} & 0 \\ 0 & \alpha_{C_1} \end{bmatrix} \end{cases} \tag{4.3.23}$$

$$\mathcal{B} = \frac{1}{\alpha_{C_1}\alpha_{C_2}\left(\varphi_{11}^{I_C}\varphi_{22}^{I_C} - \varphi_{12}^{I_C}\varphi_{21}^{I_C}\right)} \begin{bmatrix} \dfrac{\beta_{C_1}\Lambda_{C_1}N_1\alpha_1\alpha_{C_2}\varphi_{22}^{I_C}}{V_{01}\mu_{C_1}^{S_C}} & -\dfrac{\beta_{C_1}\Lambda_{C_1}N_1\alpha_1\alpha_{C_1}\varphi_{12}^{I_C}}{V_{01}\mu_{C_1}^{S_C}} \\ -\dfrac{\beta_{C_2}\Lambda_{C_2}N_2\alpha_2\alpha_{C_2}\varphi_{21}^{I_C}}{V_{02}\mu_{C_2}^{S_C}} & \dfrac{\beta_{C_2}\Lambda_{C_2}N_2\alpha_2\alpha_{C_1}\varphi_{11}^{I_C}}{V_{02}\mu_{C_2}^{S_C}} \end{bmatrix}$$

$$\begin{cases} B_{11} = \dfrac{\beta_{C_1}\Lambda_{C_1}N_1\alpha_1\alpha_{C_2}\varphi_{22}^{I_C}}{\alpha_{C_1}\alpha_{C_2}V_{01}\mu_{C_1}^{S_C}\left(\varphi_{11}^{I_C}\varphi_{22}^{I_C} - \varphi_{12}^{I_C}\varphi_{21}^{I_C}\right)} \\ B_{12} = -\dfrac{\beta_{C_1}\Lambda_{C_1}N_1\alpha_1\alpha_{C_1}\varphi_{12}^{I_C}}{\alpha_{C_1}\alpha_{C_2}V_{01}\mu_{C_1}^{S_C}\left(\varphi_{11}^{I_C}\varphi_{22}^{I_C} - \varphi_{12}^{I_C}\varphi_{21}^{I_C}\right)} \\ B_{21} = -\dfrac{\beta_{C_2}\Lambda_{C_2}N_2\alpha_2\alpha_{C_2}\varphi_{21}^{I_C}}{\alpha_{C_1}\alpha_{C_2}V_{02}\mu_{C_2}^{S_C}\left(\varphi_{11}^{I_C}\varphi_{22}^{I_C} - \varphi_{12}^{I_C}\varphi_{21}^{I_C}\right)} \\ B_{22} = \dfrac{\beta_{C_2}\Lambda_{C_2}N_2\alpha_2\alpha_{C_1}\varphi_{11}^{I_C}}{\alpha_{C_1}\alpha_{C_2}V_{02}\mu_{C_2}^{S_C}\left(\varphi_{11}^{I_C}\varphi_{22}^{I_C} - \varphi_{12}^{I_C}\varphi_{21}^{I_C}\right)} \end{cases} \tag{4.3.24}$$

Taking the characteristic polynomial

$$\begin{vmatrix} B_{11} - \Lambda & B_{12} \\ B_{21} & B_{22} - \Lambda \end{vmatrix} = 0 \tag{4.3.25}$$

$$(B_{11} - \Lambda)(B_{22} - \Lambda) - B_{12}B_{21} = 0$$

$$\Lambda^2 - B_{11}\Lambda - B_{22}\Lambda + B_{11}B_{22} - B_{12}B_{21} = 0$$

Applying the quadratic formula

$$\Lambda = \frac{1}{2}\left[(B_{11} + B_{22}) \pm \sqrt{B_{11}^2 + 2B_{11}B_{22} + B_{22}^2 - 4B_{11}B_{22} + 4B_{12}B_{21}}\right]$$

$$\Lambda = \frac{1}{2}\left[(B_{11} + B_{22}) \pm \sqrt{B_{11}^2 - 2B_{11}B_{22} + B_{22}^2 + 4B_{12}B_{21}}\right]$$

$$\Lambda = \frac{1}{2}\left[(B_{11}+B_{22}) \pm \sqrt{(B_{11}-B_{22})^2+4B_{12}B_{21}}\right]$$

Take

$$\Lambda = \frac{1}{2}\left[(B_{11}+B_{22}) + \sqrt{(B_{11}-B_{22})^2+4B_{12}B_{21}}\right]$$

Hence

$$\mathcal{R}_0 = \frac{1}{2}\left[(B_{11}+B_{22}) + \sqrt{(B_{11}-B_{22})^2+4B_{12}B_{21}}\right] \tag{4.3.26}$$

The basic reproduction number in patch i when there is no movement between patch i and other patches (in otherwords, patch i is isolated from the other patches) is given by

$$\mathcal{R}_{0i} = \frac{\beta_{C_i}\Lambda_{C_i}N_i\alpha_i}{V_{0i}\mu_{C_i}^{S_C}\alpha_{C_i}(\delta_{Ci}+d_{Ci}(V,A)+\mu_{C_i}^{I_C})} \tag{4.3.27}$$

where β_{C_i} is the contact rate in patch i. When the microscale and macroscale parameters of the patches differ only in their contact rates, we obtain a result of bounds on $\mathcal{R}_0$ in terms of $\mathcal{R}_{0i}$.

Theorem 4.4. *Suppose* $\Lambda_{C_i} = \Lambda_C$, $N_i = N$, $\alpha_i = \alpha$, $V_{0i} = V_0$, $\mu_{C_i}^{S_C} = \mu_C^{S_C}$, $\alpha_{C_i} = \alpha_C$, $\delta_{C_i} = \delta_C$,$d_{C_i}(V,A) = d_C(V,A)$, $\alpha_{C_i}^{I_C} = \alpha_C^{I_C}$ *for all* $i = 1,...,n$.

Then

$$\min_i \mathcal{R}_{0i} \leq \mathcal{R}_0 \leq \max_i \mathcal{R}_{0i} \tag{4.3.28}$$

Proof Without the loss of generality we take

$$\beta_{C_1} \leq \beta_{C_2} \leq ... \leq \beta_{C_n} \tag{4.3.29}$$

Thus

$$\min_{i=1,...,n} \mathcal{R}_{0i} = \mathcal{R}_{01} = \frac{\beta_{C_1}\Lambda_C N\alpha}{V_0\mu_C^{S_C}\alpha_C(\delta_C+d_C(V,A)+\mu_C{}^{I_C})} \leq ... \leq \frac{\beta_{C_n}\Lambda_C N\alpha}{V_0\mu_C^{S_C}\alpha_C(\delta_C+d_C(V,A)+\mu_C{}^{I_C})} = \mathcal{R}_{0n} = \max_{i=1,...,n} \mathcal{R}_{0i} \tag{4.3.30}$$

Let $V_{1,1}^{-1} = X = [x_{ij}]$ and $V_{2,2}^{-1} = Y = [y_{ij}]$. We can write $diag\{N\alpha, ..., N\alpha\}$ as $diag(N\alpha)$, $diag\left\{\frac{\Lambda_C}{V_0\mu_C^{S_C}}, ..., \frac{\Lambda_C}{V_0\mu_C^{S_C}}\right\}$ as $diag\left(\frac{\Lambda_C}{V_0\mu_C^{S_C}}\right)$

From (4.3.19) we have

$$\mathcal{R}_0 = \rho\left(diag(\beta_{C_1}, ..., \beta_{C_n})Y diag\left(\frac{\Lambda_C}{V_0\mu_C^{S_C}}\right) diag(N\alpha)X\right) \tag{4.3.31}$$

Taking $W = diag(\beta_{C_1}, ..., \beta_{C_n})Y diag\left(\frac{\Lambda_C}{V_0\mu_C^{S_C}}\right) diag(N\alpha)X$, which can be written as

$$W = \begin{bmatrix} \frac{\beta_{C_1}\Lambda_C N\alpha}{V_0\mu_C^{S_C}}(y_{11}x_{11} + ... + y_{1n}x_{n1}) & ... & \frac{\beta_{C_1}\Lambda_C N\alpha}{V_0\mu_C^{S_C}}(y_{11}x_{1n} + ... + y_{1n}x_{nn}) \\ ... & ... & ... \\ \frac{\beta_{C_n}\Lambda_C N\alpha}{V_0\mu_C^{S_C}}(y_{n1}x_{11} + ... + y_{nn}x_{n1}) & ... & \frac{\beta_{C_n}\Lambda_C N\alpha}{V_0\mu_C^{S_C}}(y_{n1}x_{1n} + ... + y_{nn}x_{nn}) \end{bmatrix} \tag{4.3.32}$$

Now we let $\left[\mathbb{I}^T W\right]_1$ define the total of the entries in the first column of W, as $\mathbb{I}^T = (1, ..., 1)$. Then

$$\left[\mathbb{I}^T W\right]_1 = \frac{\beta_{C_1}\Lambda_C N\alpha}{V_0\mu_C^{S_C}} y_{11}x_{11} + ... + \frac{\beta_{C_1}\Lambda_C N\alpha}{V_0\mu_C^{S_C}} y_{1n}x_{n1}$$

$$+\frac{\beta_{C_2}\Lambda_C N\alpha}{V_0\mu_C^{S_C}} y_{21}x_{11} + ... + \frac{\beta_{C_2}\Lambda_C N\alpha}{V_0\mu_C^{S_C}} y_{2n}x_{n1} + ...$$

$$+... + \frac{\beta_{C_n}\Lambda_C N\alpha}{V_0\mu_C^{S_C}} y_{n1}x_{11} + ... + \frac{\beta_{C_n}\Lambda_C N\alpha}{V_0\mu_C^{S_C}} y_{nn}x_{n1}$$

$$\leq \frac{\beta_{C_n}\Lambda_C N\alpha}{V_0\mu_C^{S_C}} \sum_{i=1}^{n} x_{i1}(y_{1i} + ... + y_{ni})$$

$$= \frac{\beta_{C_n}}{\alpha_C} \frac{\Lambda_C N\alpha}{V_0\mu_C^{S_C}} \sum_{i=1}^{n} x_{i1} \tag{4.3.33}$$

where the inequality comes from (4.3.29), and the final equality comes from the reason that $V_{2,2}$ has column sum α_C, hence $\mathbb{I}^T V_{2,2} = \alpha_C \mathbb{I}^T$, which means $\mathbb{I}^T Y = (1/\alpha_C)\mathbb{I}^T$. The column sum of $V_{1,1}$ is $\delta_C + d_C(V, A) + \mu_C^{I_C}$ from (4.3.30) and (4.3.33)

$$\left[\mathbb{I}^T W\right]_1 \leq \frac{\beta_{C_n}\Lambda_C N\alpha}{V_0\mu_C^{S_C}\alpha_C\left(\delta_C + d_C(V, A) + \mu_C^{I_C}\right)} = \mathcal{R}_{0n} = \max_{i=1,...,n} \mathcal{R}_{0i} \tag{4.3.34}$$

Similarly

$$\min_{i=1,\ldots,n} \mathcal{R}_{0i} = \mathcal{R}_{01} = \frac{\beta_{C_1}\Lambda_C N\alpha}{V_0\mu_C^{S_C}\alpha_C\left(\delta_C + d_C(V,A) + \mu_C^{I_C}\right)} \leq \left[\mathbb{I}^T W\right]_1 \tag{4.3.35}$$

By using similar arguments we show that these inequalities remain valid for every column for W. Since the spectral radius of a nonnegative matrix is between the minimum column sum and maximum column sum, therefore

$$\min_{i=1,\ldots,n} \mathcal{R}_{0i} \leq \rho\left(diag(\beta_{C_1},...,\beta_{C_n})Y diag(N\alpha) diag\left(\frac{\Lambda_C}{V_0\mu_C^{S_C}}\right)X\right) \leq \max_{i=1,\ldots,n} \mathcal{R}_{0i} \tag{4.3.36}$$

Therefore, the proof is completed □

4.3.2 Local Stability of the FMD disease free equilibrium (DFE)

From Theorem 4.2 of van den Driessche and Watmough [103], if $\mathcal{R}_0 < 1$ then the FMD disease free equilibrium is locally asymptotically stable and the disease cannot persist in the cattle population. We summarize this result below.

Theorem 4.5. *The disease-free equilibrium point E^0 of the multi-scale model system (4.2.1) is locally asymptotically stable whenever $\mathcal{R}_0 < 1$ and unstable otherwise.*

Proof Let J_{12} be the matrix of the partial derivatives evaluated at the disease-free equilibrium. The Jacobian matrix for the linearization of the system about the disease free equilibrium is obtained as the block structure.

$$J = \begin{bmatrix} -\varphi^{S_C} & J_{12} \\ 0 & F - V \end{bmatrix} \tag{4.3.1}$$

The matrix J is triangular. Therefore, the eigenvalues of J are those of the partition matrices φ^{S_C} and $F - V$ where φ^{S_C} is an irreducible non-singular M-matrix as defined in (section 4.3). Hence, special abcissa, $s(-\varphi^{S_C})$ has negative real parts. Therefore, the matrix J will has eigenvalues all with negative real parts if the matrix $F - V$ has all eigenvalues with negative real parts. In addition, F is non-negative matrix and V is a non-singular M-matrix. Thus, the eigenvalues of $F - V$ will have negative real parts if and only if $\rho(FV^{-1}) < 1$, that is, the disease-free equilibrium is locally asymptotically stable if and only if the basic reproduction number $\mathcal{R}_0 = \rho(FV^{-1}) < 1$. If $\mathcal{R}_0 > 1$, then $s(F - V) > 0$. This shows that at least one eigenvalue lies in the right half plane. So, the disease-free equilibrium is unstable if $\mathcal{R}_0 > 1$. □

Lemma 4.6. *The matrix* $(F-V)$ *has a real spectrum. Moreover, if* $\rho\left(FV^{-1}\right)<1$*, all eigenvalues of* $(F-V)$ *are negative.*

4.3.3 Global Stability of the disease-free equilibrium

For the purpose of establishing the global stability of DFE of the model system (4.2.1), we implement Theorem 2 in van den Driessche and Watmough [103] to establish that the disease-free equilibrium is globally asymptotically stable whenever $\mathcal{R}_0<1$ and unstable when $\mathcal{R}_0>1$. We identify two conditions that warrant the global asymptotic stability of the disease-free state. The model system (4.2.1) can be written as follows:

$$\begin{cases} \dfrac{dX}{dt}=F(X,Z), \\ \\ \dfrac{dZ}{dt}=G(X,Z), \quad G(X,0)=0 \end{cases} \tag{4.3.1}$$

where $X=S_{C_i}$ denotes all uninfected components and $Z=(I_{C_i},V_{C_i})$ denotes all infected and infectious components;

$$E_0=\left(S_C^0,\mathbf{0},\mathbf{0}\right) \tag{4.3.2}$$

where $\mathbf{0}=\underbrace{(0,...,0)}_{n\quad times}$, $S_C^0=\left(\varphi^{S_C}\right)^{-1}\Lambda_C$

denotes the disease-free equilibrium of the system. To warrant global asymptotic stability, the conditions $(H1)$ and $(H2)$ below must be met [101]:

(H1) For $\dfrac{dX}{dt}=F(X,0)$, X^* is globally asymptotically stable (g.a.s);

(H2) $G(X,Z)=AZ-\hat{G}(X,Z),\hat{G}(X,Z)\geq 0$ for $(X,Z)\in\mathbb{R}^3_+$, where the Jacobian $A=\dfrac{\partial G}{\partial Z}=D_ZG(X^*,0)$ is an M-matrix (the off diagonal elements of A are nonnegative) and $\mathbb{R}^3_+$ is the region where the model makes biological sense.

$$\frac{dX}{dt}=F(X,Z)=\Lambda_{Ci}-\frac{\beta_{Ci}V_{Ci}}{V_{0i}+V_{Ci}}S_{Ci}-\mu_{C_i}^{S_C}S_{Ci}+\delta_{Ci}I_{Ci}+\sum_{j=1,j\neq i}^{n}\psi_{j,i}^{S_C}S_{Cj}-\sum_{j=1,j\neq i}^{n}\psi_{i,j}^{S_C}S_{Ci}, \tag{4.3.3}$$

At the disease-free equilibrium $Z=0$

$$F(X,0) = \Lambda_{Ci} - \mu_{C_i}^{S_C} S_{Ci} \tag{4.3.4}$$

Hence, since Φ is an invariant set for model system (4.2.1) and in view of Theorem (4.5), it is sufficient to show that for all $E_0 \in \Phi$

$$\lim_{t\to\infty} S_{C_i}(t) = S_{C_i}^0, \lim_{t\to\infty} I_{C_i}(t) = 0, \lim_{t\to\infty} V_{C_i}(t) = 0, \tag{4.3.5}$$

where $S_{C_i}^0$ is as in (4.3.2) , it follows that

$$\frac{dS_{C_i}(t)}{dt} \leq \Lambda_{C_i} - \mu_{C_i}^{S_C} S_{C_i}(t) \tag{4.3.6}$$

It is easy to see that $S_{C_i}^0$ is globally asymptotically stable equilibrium for the comparison equations

$$\frac{dy_1(t)}{dt} \leq \Lambda_{C_i} - \mu_{C_i}^{S_C} y_1(t) \tag{4.3.7}$$

Therefore, for any $\varepsilon > 0$, there exists $\bar{t} > 0$, such that for all $t \geq \bar{t}$, it holds $S_{C_i}(t) \leq S_{C_i}^0 + \varepsilon$

$$\lim_{t\to\infty} \sup S_{C_i}(t) \leq S_{C_i}^0 \tag{4.3.8}$$

From (4.3.8) and the equations (2) and (3) of the model system (4.2.1) we have that for $t \geq \bar{t}$

$$\begin{aligned}
\frac{dS_{C_i}(t)}{dt} &\leq \Lambda_{C_i} - \left(\lambda_{C_i}(t) + \mu_{C_i}^{S_C}\right)\left(S_{C_i}^0 + \varepsilon\right) + \delta_{C_i} I_{C_i}(t) + \sum_{j\neq i=1}^{n} \psi_{j,i}^{S_C} S_{C_j} - \sum_{j\neq i=1}^{n} \psi_{i,j}^{S_C} S_{C_i}, \\
\frac{dI_{C_i}(t)}{dt} &\leq \lambda_{C_i}(t)\left(S_{C_i}^0 + \varepsilon\right) - (\delta_{C_i} + d_{C_i} + \mu_{C_i}^{S_C}) I_{C_i} + \sum_{j\neq i=1}^{n} \psi_{j,i}^{I_C} I_{C_j} - \sum_{j\neq i=1}^{n} \psi_{i,j}^{I_C} I_{C_i} \\
\frac{dV_{C_i}(t)}{dt} &= N_i \alpha_i I_{C_i}(t) - \alpha_{C_i} V_{C_i}(t)
\end{aligned} \tag{4.3.9}$$

Let us consider the comparison system

$$\begin{aligned}
\frac{dw_1(t)}{dt} &\leq \Lambda_{C_i} - \left(\lambda_{C_i}(t) + \mu_{C_i}^{S_C}\right)\left(S_{C_i}^0 + \varepsilon\right) + \delta_{C_i} w_2(t) + \sum_{j\neq i=1}^{n} \psi_{j,i}^{S_C} S_{C_j} - \sum_{j\neq i=1}^{n} \psi_{i,j}^{S_C} S_{C_i}, \\
\frac{dw_2(t)}{dt} &\leq \lambda_{C_i}(t)\left(S_{C_i}^0 + \varepsilon\right) - (\delta_{C_i} + d_{C_i} + \mu_{C_i}^{S_C}) w_2 + \sum_{j\neq i=1}^{n} \psi_{j,i}^{I_C} I_{C_j} - \sum_{j\neq i=1}^{n} \psi_{i,j}^{I_C} I_{C_i} \\
\frac{dw_3(t)}{dt} &= N_i \alpha_i I_{C_i}(t) - \alpha_{C_i} w_3(t), \quad w_1(\bar{t}) = S_{C_i}(\bar{t}), w_2(\bar{t}) = I_{C_i}(\bar{t}), w_3(\bar{t}) = V_{C_i}(\bar{t})
\end{aligned} \tag{4.3.10}$$

that we can re-write as

$$\frac{dw(t)}{dt} = (F_\varepsilon - V_\varepsilon)\, w(t) \tag{4.3.11}$$

where $w(t) = (w_1(t), w_2(t), w_3(t))^T$ and $(F_\varepsilon - V_\varepsilon)$ is a matrix in (4.3.8) computed in $E_0(\varepsilon) = \left(S^0_{C_i} + \varepsilon, 0, 0\right)$. Let us note that if $\mathcal{R}_0 = \rho\left(FV^{-1}\right) < 1$, we can choose a sufficiently small $\varepsilon > 0$ such that $\rho\left(F_\varepsilon V_\varepsilon^{-1}\right) < 1$. Then by applying Lemma 4.6 to $(F_\varepsilon - V_\varepsilon)$ we obtain that it has a real spectrum and all its eigenvalues are negative. It follows that $\lim_{t\to\infty} w(t) = 0$, whatever the initial conditions are, from which

$$\lim_{t\to\infty} I_{C_i}(t) = 0, \lim_{t\to\infty} V_{C_i}(t) = 0 \tag{4.3.12}$$

Now, for any $\varepsilon > 0$, there exists $\bar{t}_1$ such that for any $t \geq \bar{t}_1$, $I_{C_i}(t) < \varepsilon$, $V_{C_i}(t) < \varepsilon$. So, for $t \geq \bar{t}_1$ we have

$$\frac{dS_{C_i}(t)}{dt} \geq \Lambda_{C_i} - \frac{\beta_{C_i}\varepsilon}{V_{0i}+\varepsilon} S_{C_i} - \mu^{S_C}_{C_i} S_{C_i}(t), \tag{4.3.13}$$

It is easy to see that $\dfrac{\Lambda_{C_i}}{\left[\frac{\beta_{C_i}\varepsilon}{V_{0i}+\varepsilon} + \mu^{S_C}_{C_i}\right]}$ is a global asymptotically stable equilibrium for the comparison equation

$$\frac{dy(t)}{dt} \geq \Lambda_{C_i} - \frac{\beta_{C_i}\varepsilon}{V_{0i}+\varepsilon} y(t) - \mu^{S_C}_{C_i} y(t), \tag{4.3.14}$$

Thus, for any $\chi > 0$, there exists $\bar{t}_2 > 0$ such that for all $t \geq \bar{t}_2$

$$S_{C_i}(t) \geq \frac{\Lambda_{C_i}}{\left[\frac{\beta_{C_i}\varepsilon}{V_{0i}+\varepsilon} + \mu^{S_C}_{C_i}\right]} - \chi \tag{4.3.15}$$

Therefore, for any $\varepsilon > 0$, we have

$$\lim_{t\to\infty} \inf S_{C_i}(t) \geq \frac{\Lambda_{C_i}}{\left[\frac{\beta_{C_i}\varepsilon}{V_{0i}+\varepsilon} + \mu^{S_C}_{C_i}\right]} \tag{4.3.16}$$

Letting $t \to \infty$, we get $\lim_{t\to\infty} \inf S^H_i(t) \geq S^H_{0i}$ and combining this with (4.3.8) gives us

$$\lim_{t\to\infty} S_{C_i}(t) = S^0_{C_i} \tag{4.3.17}$$

Therefore, $E_0 = \left(\dfrac{\Lambda_{C_i}}{\mu^{S_C}_{C_i}}, 0, 0\right), i = 1, .., n$ is a global asymptotically stable equilibrium point satisfying condition **H1**.

Since $S_{C_i} \leq S^0_{C_i}$, we can obtain from the multiscale model system (4.2.1).

$$\begin{cases} \dfrac{dI_{C_i}(t)}{dt} \leq \lambda_{C_i}(t)S^0_{C_i}(t) - (\delta_{C_i} + d_{C_i} + \mu^{S_C}_{C_i})I^H_i(t) + \displaystyle\sum_{j\neq i=1}^{n} \psi^{I_C}_{j,i} I_{C_j}(t) - \sum_{j\neq i=1}^{n} \psi^{I_C}_{i,j} I_{C_i}(t) \\ \dfrac{dV_{C_i}(t)}{dt} \leq N_i\alpha_i I_{C_i}(t) - \alpha_{C_i} V_{C_i}(t) \end{cases} \tag{4.3.18}$$

We consider the linear system

$$\begin{cases} \dfrac{dI_{C_i}(t)}{dt} \leq \lambda_{C_i}(t)S^0_{C_i}(t) - (\delta_{C_i} + d_{C_i} + \mu^{S_C}_{C_i})I^H_i(t) + \displaystyle\sum_{j\neq i=1}^{n} \psi^{I_C}_{j,i} I_{C_j}(t) - \sum_{j\neq i=1}^{n} \psi^{I_C}_{i,j} I_{C_i}(t) \\ \dfrac{dV_{C_i}(t)}{dt} \leq N_i\alpha_i I_{C_i}(t) - \alpha_{C_i} V_{C_i}(t) \end{cases} \tag{4.3.19}$$

Therefore, the system of equations (4.3.19) can be written as

$$\frac{d\mathbf{u}}{dt} = \mathbf{A}\mathbf{u} \tag{4.3.20}$$

where, $\mathbf{u} = [I_{C_1}, I_{C_2}, ..., I_{C_n}, V_{C_1}, V_{C_2}, ..., V_{C_n}]^T$, $\mathbf{A} = \mathbf{F} - \mathbf{V}$. In this case, $\mathbf{F}$ is a non-negative matrix (from 4.3.9) and $\mathbf{V}$ is a non-negative M-matrix (from 4.3.12). Hence,

$$s(\mathbf{F} - \mathbf{V}) < 0 \iff \rho\left\{\mathbf{F}\mathbf{V}^{-1}\right\} < 1 \tag{4.3.21}$$

In other words, the eigenvalues of $\mathbf{F} - \mathbf{V}$ lie on the left half plane if $\mathcal{R}_0 < 1$. Therefore, each positive solution of (4.3.20) satisfies

$$\lim_{t\to\infty} \mathbf{u} = 0 \tag{4.3.22}$$

that is, $\lim\limits_{t\to\infty} I_{C_i} = 0, \lim\limits_{t\to\infty} V_{C_i} = 0 \quad \text{for all} \quad i = 1, 2, ..., n$

Since all the variables of the multiscale model system (4.2.1) are non-negative, then the use of Comparison theorem [132, 133]

$$\lim_{t\to\infty}\lim_{t\to\infty} I_{C_i} = 0, \lim_{t\to\infty} V_{C_i} = 0 \quad \text{for all} \quad i = 1, 2, ..., n \tag{4.3.23}$$

Furthermore, as $t \to \infty$

$$\frac{dS_{C_i}}{dt} = \Lambda_{C_i} - \mu_{C_i}^{S_C} S_{C_i} + \sum_{j\neq i=1}^{n} \psi_{j,i}^{S_C} S_{C_j} - \sum_{j\neq i=1}^{n} \psi_{i,j}^{S_C} S_{C_i} \tag{4.3.24}$$

In the matrix form

$$\frac{d}{dt}\left[S_C\right] = \Lambda_C - \varphi^{S_C} S_C, \tag{4.3.25}$$

Therefore, the matrices φ^{S_C} is non-singular M-matrix, where all their eigenvalues lie in the left half plane. Consequently, if S_C^h is the homogeneous solutions of system equations (4.3.24) and (4.3.25) respectively, then we have

$$\lim_{t\to\infty} S_C^h = 0 \tag{4.3.26}$$

From section (4.3) matrix φ^{S_C} is an irreducible, non-singular M-matrix. Therefore, the matrix φ^{S_C} has a positive inverse. $S_C^0 = \left(\varphi^{S_C}\right)^{-1} \Lambda_C$ is a particular solution and $S_C = S_C^h + S_C^0$ is the general solution of (4.3.25). In addition,

$$\lim_{t\to\infty} S_{C_i} = S_{C_i}^0, \lim_{t\to\infty} I_{C_i} = 0, \lim_{t\to\infty} V_{C_i} = 0, \tag{4.3.27}$$

for all $i = 1, 2, ..., n$

Therefore, as $t \to \infty$, we obtain the equilibrium point

$$E_0 = \left(S_C^0, \mathbf{0}, \mathbf{0}\right) \tag{4.3.28}$$

where $\mathbf{0} = \underbrace{(0, ..., 0)}_{n \quad times}$, $S_C^0 = \left(\varphi^{S_C}\right)^{-1} \Lambda_C$ Therefore, the disease-free equilibrium is globally asymptotically stable if $\mathcal{R}_0 < 1$ and unstable if $\mathcal{R}_0 > 1$ □

Theorem 4.7. *If $\mathcal{R}_0 < 1$, then the disease-free equilibrium is globally asymptotically stable and unstable if $\mathcal{R}_0 > 1$*

Proposition 4.8. *Suppose that $\Psi^I = \left(\psi_{ij}^I\right)$ is irreducible. If $\mathcal{R}_0 > 1$, then the model system (4.2.1) is uniformly persistent and there exists an endemic equilibrium E^* in $\hat{\Omega}$.*

4.4 Global stability of endemic equilibria and uniqueness

We now establish the sufficient conditions which ensure global stability and uniqueness of the endemic equilibrium. We assume that $\mathcal{R}_0 > 1$. We deduce global stability and uniqueness of the endemic equilibrium by implementing graph-theoretic method [134–136]

Theorem 4.9. *Assume that* $\mathcal{R}_0 > 1$ *and claim that an endemic equilibrium* $E^* = (S^*_{C_1}, I^*_{C_1}, V^*_{C_1}, S^*_{C_2}, I^*_{C_2}, V^*_{C_2}, ..., S^*_{C_n}, I^*_{C_n}, V^*_{C_n})$ *exists. Suppose that one of the following assumptions is satisfied.*

(1) $\Psi^S = 0$ *and* Ψ^I *is irreducible;*

(2) $\Psi^I = 0$ *and* Ψ^S *is irreducible;*

(3) Ψ^S *and* Ψ^I *are irreducible, and there exists* $\lambda > 0$ *such that* $\psi^S_{j,i} S^*_{C_j} = \lambda \psi^I_{j,i} I^*_{C_j}$ *for all* $1 \leq i, j \leq n$.

where $\Psi^S = \left(\psi^S_{ij}\right)$ *and* $\Psi^I = \left(\psi^I_{ij}\right)$ *are migration matrices for susceptible and infected humans respectively. Then* E^* *is unique and asymptotically stable in* $\hat{\Omega}$.

By Proposition (4.8), the existence of a endemic equilibrium E^* is ensured if the assumption (1) or assumption (3) is satisfied.

Proof. This proof is completed through the implementation of the approach by [137]. In the proof we consider assumption (3) is fulfilled and then the remaining assumptions can be proved the same way. We now deduce the global asymptotic stability of E^* in $\hat{\Omega}$ which implies that E^* is necessarily unique.

$$\begin{cases} \dfrac{dS_{Ci}}{dt} = \Lambda_{Ci} - \lambda_{C_i} S_{Ci} - \mu_{C_i}^{S_C} S_{Ci} + \delta_{Ci} I_{Ci} + \displaystyle\sum_{j \neq i=1}^{n} \psi_{j,i}^{S_C} S_{Cj} - \sum_{j \neq i=1}^{n} \psi_{i,j}^{S_C} S_{Ci} \\ \dfrac{dI_{Ci}}{dt} = \lambda_{C_i} S_{Ci} - (\delta_{Ci} + d_{Ci} + \mu_{C_i}^{I_C}) I_{Ci} + \displaystyle\sum_{j \neq i=1}^{n} \psi_{j,i}^{I_C} I_{Cj} - \sum_{j \neq i=1}^{n} \psi_{i,j}^{I_C} I_{Ci} \\ \dfrac{dV_{Ci}}{dt} = N_i \alpha_i I_{Ci}(t) - \alpha_{C_i} V_{Ci} \end{cases} \tag{4.4.1}$$

Set

$$V_i\left(S_{C_i}, I_{C_i}\right) = S_{C_i} - S^*_{C_i} - S^*_{C_i} \ln \frac{S_{C_i}}{S^*_{C_i}} + I_{C_i} - I^*_{C_i} - I^*_{C_i} \ln \frac{I_{C_i}}{I^*_{C_i}} \tag{4.4.2}$$

From equilibrium equations of (4.4.1), we obtain

$$0 = \Lambda_{C_i} - \lambda_{C_i}(t) S_{C_i}(t) - \mu_{C_i}^{S_C} S_{C_i} + \delta_{C_i} I_{C_i}(t) + \sum_{j \neq i=1}^{n} \psi_{j,i}^{S_C} S_{C_j} - \sum_{j \neq i=1}^{n} \psi_{i,j}^{S_C} S_{C_i}, \tag{4.4.3}$$

$$\mu_{C_i}^{S_C} S_{C_i} = \Lambda_{C_i} - \lambda_{C_i}(t) S_{C_i}(t) + \delta_{C_i} I_{C_i}(t) + \sum_{j \neq i=1}^{n} \psi_{j,i}^{S_C} S_{C_j} - \sum_{j \neq i=1}^{n} \psi_{i,j}^{S_C} S_{C_i} \tag{4.4.4}$$

$$\mu_{C_i}^{S_C} S_{C_i}^* = \Lambda_{C_i} - \lambda_{C_i}^*(t) S_{C_i}^*(t) + \delta_{C_i} I_{C_i}^*(t) + \sum_{j \neq i=1}^{n} \psi_{j,i}^{S_C} S_{C_j}^* - \sum_{j \neq i=1}^{n} \psi_{i,j}^{S_C} S_{C_i}^* \tag{4.4.5}$$

$$0 = \lambda_{C_i} S_{Ci} - (\delta_{Ci} + d_{Ci} + \mu_{C_i}^{I_C}) I_{Ci} + \sum_{j \neq i=1}^{n} \psi_{j,i}^{I_C} I_{Cj} - \sum_{j \neq i=1}^{n} \psi_{i,j}^{I_C} I_{Ci} \tag{4.4.6}$$

$$(\delta_{Ci} + d_{Ci} + \mu_{C_i}^{I_C}) I_{Ci} = \lambda_{C_i} S_{Ci} + \sum_{j \neq i=1}^{n} \psi_{j,i}^{I_C} I_{Cj} - \sum_{j \neq i=1}^{n} \psi_{i,j}^{I_C} I_{Ci} \tag{4.4.7}$$

$$(\delta_{Ci} + d_{Ci} + \mu_{C_i}^{I_C}) I_{Ci}^* = \lambda_{C_i}^* S_{Ci}^* + \sum_{j \neq i=1}^{n} \psi_{j,i}^{I_C} I_{Cj}^* - \sum_{j \neq i=1}^{n} \psi_{i,j}^{I_C} I_{Ci}^* \tag{4.4.8}$$

We can highlight that $1 - x + \ln x \leq 0$ for $x > 0$ and equality holds if and only if $x = 1$. When we differentiate V_i along the solution of system (4.4.1), gives

$$\frac{dV_i}{dt} = \frac{\partial V_i}{\partial S_{C_i}} . \frac{dS_{C_i}}{dt} + \frac{\partial V_i}{\partial I_{C_i}} . \frac{dI_{C_i}}{dt} \tag{4.4.9}$$

$$\frac{dV_i}{dt} = \left(1 - \frac{S_{C_i}^*}{S_{C_i}}\right) . \frac{dS_{C_i}}{dt} + \left(1 - \frac{I_{C_i}^*}{I_{C_i}}\right) . \frac{dI_{C_i}}{dt} \tag{4.4.10}$$

Substituting equations in (4.4.1) into (4.4.10) we get

$$\frac{dV_i}{dt} = \left(1 - \frac{S_i^*}{S_{C_i}}\right) . \left(\Lambda_{C_i} - \lambda_{C_i}(t) S_{C_i}(t) - \mu_{C_i}^{S_C} S_{C_i} + \delta_{C_i} I_{C_i}(t) + \sum_{j \neq i=1}^{n} \psi_{j,i}^{S_C} S_{C_j} - \sum_{j \neq i=1}^{n} \psi_{i,j}^{S_C} S_{C_i}\right)$$

$$+ \left(1 - \frac{I_{C_i}^*}{I_{C_i}}\right) . \left(\lambda_{C_i} S_{Ci} - (\delta_{Ci} + d_{Ci} + \mu_{C_i}^{I_C}) I_{Ci} + \sum_{j \neq i=1}^{n} \psi_{j,i}^{I_C} I_{Cj} - \sum_{j \neq i=1}^{n} \psi_{i,j}^{I_C} I_{Ci}\right) \tag{4.4.11}$$

$$\frac{dV_i}{dt} = \Lambda_{C_i} - \lambda_{C_i}(t) S_{C_i}(t) - \mu_{C_i}^{S_C} S_{C_i} + \delta_{C_i} I_{C_i}(t) + \sum_{j \neq i=1}^{n} \psi_{j,i}^{S_C} S_{C_j} - \sum_{j \neq i=1}^{n} \psi_{i,j}^{S_C} S_{C_i} - \frac{S_{C_i}^*}{S_{C_i}} \Lambda_{C_i} + \frac{S_{C_i}^*}{S_{C_i}} \lambda_{C_i} S_{C_i}$$

$$+\frac{S^*_{C_i}}{S_{C_i}}\mu_i^{S_C}S_{C_i}-\frac{S^*_{C_i}}{S_{C_i}}\delta_{C_i}I_{C_i}-\frac{S^*_{C_i}}{S_{C_i}}\sum_{j=1}^{n}\psi_{ji}^{S_C}S_{C_j}+\frac{S^*_{C_i}}{S_{C_i}}\sum_{j=1}^{n}\psi_{ij}^{S_C}S_{C_i}+\lambda_{C_i}(t)S_{C_i}(t)-(\delta_{Ci}+d_{Ci}+\mu_{C}{}_i^{I_C})I_{Ci}$$

$$+\sum_{j\neq i=1}^{n}\psi_{j,i}^{I_C}I_{Cj}-\sum_{j\neq i=1}^{n}\psi_{i,j}^{I_C}I_{Ci}-\frac{I^*_{C_i}}{I_{C_i}}\lambda_{C_i}S_{C_i}+\frac{I^*_{C_i}}{I_{C_i}}(\delta_{Ci}+d_{Ci}+\mu_{C}{}_i^{I_C})I_{Ci}-\frac{I^*_{C_i}}{I_{C_i}}\sum_{j=1}^{n}\psi_{ji}^{I_C}I_{C_j}+\frac{I^*_{C_i}}{I_{C_i}}\sum_{j=1}^{n}\psi_{ij}^{I_C}I_{C_i} \tag{4.4.12}$$

$$\frac{dV_i}{dt}=\Lambda_{C_i}-\lambda_{C_i}(t)S_{C_i}(t)-\mu_i^{S_C}S_{C_i}+\delta_{C_i}I_{C_i}(t)+\sum_{j\neq i=1}^{n}\psi_{j,i}^{S_C}S_{C_j}-\sum_{j\neq i=1}^{n}\psi_{i,j}^{S_C}S_{C_i}-\Lambda_{C_i}\frac{S^*_{C_i}}{S_{C_i}}+\lambda_{C_i}S^*_{C_i}+\mu_i^{S_C}S^*_{C_i}$$

$$-\delta_{C_i}\frac{S^*_{C_i}}{S_{C_i}}I_{C_i}-\sum_{j=1}^{n}\psi_{ji}^{S_C}S_{C_j}\frac{S^*_{C_i}}{S_{C_i}}+\sum_{j=1}^{n}\psi_{ij}^{S_C}S^*_{C_i}+\lambda_{C_i}(t)S_{C_i}(t)-(\delta_{Ci}+d_{Ci}+\mu_{C}{}_i^{I_C})I_{Ci}+\sum_{j\neq i=1}^{n}\psi_{j,i}^{I_C}I_{C_j}$$

$$-\sum_{j\neq i=1}^{n}\psi_{i,j}^{I_C}I_{C_i}-\lambda_{C_i}\frac{I^*_{C_i}}{I_{C_i}}S_{C_i}+(\delta_{Ci}+d_{Ci}+\mu_{C}{}_i^{I_C})I^*_{Ci}-\sum_{j=1}^{n}\psi_{ji}^{I_C}I_{C_j}\frac{I^*_{C_i}}{I_{C_i}}+\sum_{j=1}^{n}\psi_{ij}^{I_C}I^*_{C_i} \tag{4.4.13}$$

$$\begin{cases}\mu_{C_i}^{S_C}S^*_{C_i}=\Lambda_{C_i}-\lambda^*_{C_i}S^*_{C_i}+\delta_{C_i}I^*_{C_i}+\sum_{j\neq i=1}^{n}\psi_{ji}^{S_C}S^*_{C_j}-\sum_{j\neq i=1}^{n}\psi_{ij}^{S_C}S^*_{C_i}\\ \mu_{C_i}^{S_C}S_{C_i}=\Lambda_{C_i}\frac{S_{C_i}}{S^*_{C_i}}-\lambda^*_{C_i}S_{C_i}+\delta_{C_i}I^*_{C_i}\frac{S_{C_i}}{S^*_{C_i}}+\sum_{j\neq i=1}^{n}\psi_{ji}^{S_C}S^*_{C_j}\frac{S_{C_i}}{S^*_{C_i}}-\sum_{j\neq i=1}^{n}\psi_{ij}^{S_C}S_{C_i}\\ \left(\delta_{C_i}+d_{C_i}(V,A)+\mu_{C_i}^{I_C}\right)I^*_{C_i}=\lambda^*_{C_i}S^*_{C_i}+\sum_{j\neq i=1}^{n}\psi_{ji}^{I_C}I^*_{C_j}-\sum_{j\neq i=1}^{n}\psi_{ij}^{I_C}I^*_{C_i}\\ \left(\delta_{C_i}+d_{C_i}(V,A)+\mu_{C_i}^{I_C}\right)I_{C_i}=\lambda^*_{C_i}S^*_{C_i}\frac{I_{C_i}}{I^*_{C_i}}+\sum_{j\neq i=1}^{n}\psi_{ji}^{I_C}I^*_{C_j}\frac{I_{C_i}}{I^*_{C_i}}-\sum_{j\neq i=1}^{n}\psi_{ij}^{I_C}I_{C_i}\end{cases} \tag{4.4.14}$$

Substituting equations in (4.4.14) into (4.4.13) we get

$$\frac{dV_i}{dt}=\Lambda_{C_i}-\lambda_{C_i}(t)S_{C_i}(t)-\left(\Lambda_{C_i}\frac{S_{C_i}}{S^*_{C_i}}-\lambda^*_{C_i}(t)S_{C_i}(t)+\delta_{C_i}I^*_{C_i}(t)\frac{S_{C_i}}{S^*_{C_i}}+\sum_{j=1}^{n}\psi_{ji}^{S_C}S^*_{C_j}\frac{S_{C_i}}{S^*_{C_i}}-\sum_{j=1}^{n}\psi_{ij}^{S_C}S_{C_i}\right)$$

$$+\delta_{C_i} I_{C_i}(t) + \sum_{j\neq i=1}^{n} \psi_{j,i}^{S_C} S_{C_j} - \sum_{j\neq i=1}^{n} \psi_{i,j}^{S_C} S_{C_i} - \Lambda_{C_i} \frac{S_{C_i}^*}{S_{C_i}} + \lambda_{C_i} S_{C_i}^*$$

$$+ \left(\Lambda_{C_i} - \lambda_{C_i}^*(t) S_{C_i}^*(t) + \delta_{C_i} I_{C_i}^*(t) + \sum_{j\neq i=1}^{n} \psi_{j,i}^{S_C} S_{C_j}^* - \sum_{j\neq i=1}^{n} \psi_{i,j}^{S_C} S_{C_i}^* \right)$$

$$-\delta_{C_i} \frac{S_{C_i}^*}{S_{C_i}} I_{C_i} - \sum_{j=1}^{n} \psi_{ji}^{S_C} S_{C_j} \frac{S_{C_i}^*}{S_{C_i}} + \sum_{j=1}^{n} \psi_{ij}^{S_C} S_{C_i}^* + \lambda_{C_i}(t) S_{C_i}(t)$$

$$- \left(\lambda_{C_i}^*(t) S_{C_i}^*(t) \frac{I_{C_i}}{I_{C_i}^*} + \sum_{j\neq i=1}^{n} \psi_{j,i}^{I_C} I_{C_j}^* \frac{I_{C_i}}{I_{C_i}^*} - \sum_{j\neq i=1}^{n} \psi_{i,j}^{I_C} I_{C_i} \right) + \sum_{j\neq i=1}^{n} \psi_{j,i}^{I_C} I_{C_j} - \sum_{j\neq i=1}^{n} \psi_{i,j}^{I_C} I_{C_i} - \lambda_{C_i} \frac{I_{C_i}^*}{I_{C_i}} S_{C_i}$$

$$+ \left(\lambda_{C_i}^*(t) S_i^*(t) + \sum_{j\neq i=1}^{n} \psi_{j,i}^{I_C} I_{C_j}^* - \sum_{j\neq i=1}^{n} \psi_{i,j}^{I_C} I_{C_i}^* \right) - \sum_{j=1}^{n} \psi_{ji}^{I_C} I_{C_j} \frac{I_{C_i}^*}{I_{C_i}} + \sum_{j=1}^{n} \psi_{ij}^{I_C} I_{C_i}^* \tag{4.4.15}$$

Simplifying (4.4.15) we obtain

$$\frac{dV_i}{dt} = \Lambda_{C_i} - \lambda_{C_i}(t) S_{C_i}(t) - \Lambda_{C_i} \frac{S_{C_i}}{S_{C_i}^*} + \lambda_{C_i}^*(t) S_{C_i}(t) - \delta_{C_i} I_{C_i}^*(t) \frac{S_{C_i}}{S_{C_i}^*} - \sum_{j=1}^{n} \psi_{ji}^{S_C} S_{C_j}^* \frac{S_{C_i}}{S_{C_i}^*} + \sum_{j=1}^{n} \psi_{ij}^{S_C} S_{C_i}$$

$$+\delta_{C_i} I_{C_i}(t) + \sum_{j\neq i=1}^{n} \psi_{j,i}^{S_C} S_{C_j} - \sum_{j\neq i=1}^{n} \psi_{i,j}^{S_C} S_{C_i} - \Lambda_{C_i} \frac{S_{C_i}^*}{S_{C_i}} + \lambda_{C_i} S_{C_i}^*$$

$$+\Lambda_{C_i} - \lambda_{C_i}^*(t) S_{C_i}^*(t) + \delta_{C_i} I_{C_i}^*(t) + \sum_{j\neq i=1}^{n} \psi_{j,i}^{S_C} S_{C_j}^* - \sum_{j\neq i=1}^{n} \psi_{i,j}^{S_C} S_{C_i}^*$$

$$-\delta_{C_i} \frac{S_{C_i}^*}{S_{C_i}} I_{C_i} - \sum_{j=1}^{n} \psi_{ji}^{S_C} S_{C_j} \frac{S_{C_i}^*}{S_{C_i}} + \sum_{j=1}^{n} \psi_{ij}^{S_C} S_{C_i}^* + \lambda_{C_i}(t) S_{C_i}(t)$$

$$-\lambda_{C_i}^*(t) S_i^*(t) \frac{I_{C_i}}{I_{C_i}^*} - \sum_{j\neq i=1}^{n} \psi_{j,i}^{I_C} I_{C_j}^* \frac{I_{C_i}}{I_{C_i}^*} + \sum_{j\neq i=1}^{n} \psi_{i,j}^{I_C} I_{C_i} + \sum_{j\neq i=1}^{n} \psi_{j,i}^{I_C} I_{C_j} - \sum_{j\neq i=1}^{n} \psi_{i,j}^{I_C} I_{C_i}$$

$$- \lambda_{C_i} \frac{I_{C_i}^*}{I_{C_i}} S_{C_i} + \lambda_{C_i}^*(t) S_{C_i}^*(t) + \sum_{j\neq i=1}^{n} \psi_{j,i}^{I_C} I_{C_j}^* - \sum_{j\neq i=1}^{n} \psi_{i,j}^{I_C} I_{C_i}^* - \sum_{j=1}^{n} \psi_{ji}^{I_C} I_{C_j} \frac{I_{C_i}^*}{I_{C_i}} + \sum_{j=1}^{n} \psi_{ij}^{I_C} I_{C_i}^* \tag{4.4.16}$$

$$\frac{dV_i}{dt} = \Lambda_{C_i} - \cancelto{0}{\lambda_{C_i}(t)S_{C_i}(t)} - \Lambda_{C_i}\frac{S_{C_i}}{S^*_{C_i}} + \lambda^*_{C_i}(t)S_{C_i}(t) - \delta_{C_i}I^*_{C_i}(t)\frac{S_{C_i}}{S^*_{C_i}} - \sum_{j=1}^{n}\psi^{S_C}_{ji}S^*_{C_j}\frac{S_{C_i}}{S^*_{C_i}} + \sum_{j=1}^{n}\cancelto{0}{\psi^{S_C}_{ij}S_{C_i}}$$

$$+\delta_{C_i}I_{C_i}(t) + \sum_{j\neq i=1}^{n}\psi^{S_C}_{j,i}S_{C_j} - \sum_{j\neq i=1}^{n}\cancelto{0}{\psi^{S_C}_{i,j}S_{C_i}} - \Lambda_{C_i}\frac{S^*_{C_i}}{S_{C_i}} + \lambda_{C_i}S^*_{C_i}$$

$$+\Lambda_{C_i} - \cancelto{0}{\lambda^*_{C_i}(t)S^*_{C_i}(t)} + \delta_{C_i}I^*_{C_i}(t) + \sum_{j\neq i=1}^{n}\psi^{S_C}_{j,i}S^*_{C_j} - \sum_{j\neq i=1}^{n}\cancelto{0}{\psi^{S_C}_{i,j}S^*_{C_i}}$$

$$-\delta_{C_i}\frac{S^*_{C_i}}{S_{C_i}}I_{C_i} - \sum_{j=1}^{n}\psi^{S_C}_{ji}S_{C_j}\frac{S^*_{C_i}}{S_{C_i}} + \sum_{j=1}^{n}\cancelto{0}{\psi^{S_C}_{ij}S^*_{C_i}} + \cancelto{0}{\lambda_{C_i}(t)S_{C_i}(t)}$$

$$-\lambda^*_{C_i}(t)S^*_{C_i}(t)\frac{I_{C_i}}{I^*_{C_i}} - \sum_{j\neq i=1}^{n}\psi^{I_C}_{j,i}I^*_{C_j}\frac{I_{C_i}}{I^*_{C_i}} + \sum_{j\neq i=1}^{n}\cancelto{0}{\psi^{I_C}_{i,j}I_{C_i}} + \sum_{j\neq i=1}^{n}\psi^{I_C}_{j,i}I_{C_j} - \sum_{j\neq i=1}^{n}\cancelto{0}{\psi^{I_C}_{i,j}I_{C_i}}$$

$$-\lambda_{C_i}\frac{I^*_{C_i}}{I_{C_i}}S_{C_i} + \cancelto{0}{\lambda^*_{C_i}(t)S^*_{C_i}(t)} + \sum_{j\neq i=1}^{n}\psi^{I_C}_{j,i}I^*_{C_j} - \sum_{j\neq i=1}^{n}\cancelto{0}{\psi^{I_C}_{i,j}I^*_{C_i}} - \sum_{j=1}^{n}\psi^{I_C}_{ji}I_{C_j}\frac{I^*_{C_i}}{I_{C_i}} + \sum_{j=1}^{n}\cancelto{0}{\psi^{I_C}_{ij}I^*_{C_i}} \quad (4.4.17)$$

$$\frac{dV_i}{dt} = \Lambda_{C_i} - \Lambda_{C_i}\frac{S_{C_i}}{S^*_{C_i}} + \Lambda_{C_i} - \Lambda_{C_i}\frac{S^*_{C_i}}{S_{C_i}}$$

$$+\lambda^*_{C_i}S_{C_i} + \lambda_{C_i}S^*_{C_i} - \lambda_{C_i}\frac{I^*_{C_i}}{I_{C_i}}S_{C_i} - \lambda^*_{C_i}(t)S^*_{C_i}(t)\frac{I_{C_i}}{I^*_{C_i}}$$

$$+\delta_{C_i}I_{C_i}(t) - \delta_{C_i}\frac{S^*_{C_i}}{S_{C_i}}I_{C_i} - \delta_{C_i}I^*_{C_i}(t)\frac{S_{C_i}}{S^*_{C_i}} + \delta_{C_i}I^*_{C_i}(t)$$

$$-\sum_{j=1}^{n}\psi^{S_C}_{ji}S^*_{C_j}\frac{S_{C_i}}{S^*_{C_i}} - \sum_{j=1}^{n}\psi^{S_C}_{ji}S_{C_j}\frac{S^*_{C_i}}{S_{C_i}} + \sum_{j\neq i=1}^{n}\psi^{S_C}_{j,i}S_{C_j} + \sum_{j\neq i=1}^{n}\psi^{S_C}_{j,i}S^*_{C_j}$$

$$-\sum_{j\neq i=1}^{n}\psi^{I_C}_{j,i}I^*_{C_j}\frac{I_{C_i}}{I^*_{C_i}} + \sum_{j\neq i=1}^{n}\psi^{I_C}_{j,i}I_{C_j} + \sum_{j\neq i=1}^{n}\psi^{I_C}_{j,i}I^*_{C_j} - \sum_{j=1}^{n}\psi^{I_C}_{ji}I_{C_j}\frac{I^*_{C_i}}{I_{C_i}} \quad (4.4.18)$$

Therefore

$$\frac{dV_i}{dt} = \Lambda_{C_i} - \Lambda_{C_i}\frac{S_{C_i}}{S^*_{C_i}} + \Lambda_{C_i} - \Lambda_{C_i}\frac{S^*_{C_i}}{S_{C_i}} + \Lambda_{C_i}\ln\frac{S_{C_i}}{S^*_{C_i}} - \Lambda_{C_i}\ln\frac{S_{C_i}}{S^*_{C_i}}$$

$$+\lambda^*_{C_i} S_{C_i}\left[1-\frac{S^*_{C_i}I_{C_i}}{S_{C_i}I^*_{C_i}}+\ln\frac{S^*_{C_i}I_{C_i}}{S_{C_i}I^*_{C_i}}-\ln\frac{S^*_{C_i}I_{C_i}}{S_{C_i}I^*_{C_i}}\right]+\lambda_{C_i}S^*_{C_i}\left[1-\frac{S_{C_i}I^*_{C_i}}{S^*_{C_i}I_{C_i}}+\ln\frac{S_{C_i}I^*_{C_i}}{S^*_{C_i}I_{C_i}}-\ln\frac{S_{C_i}I^*_{C_i}}{S^*_{C_i}I_{C_i}}\right]$$

$$+\delta_{C_i}I_{C_i}(t)\left[1-\frac{S^*_{C_i}}{S_{C_i}}+\ln\frac{S^*_{C_i}}{S_{C_i}}-\ln\frac{S^*_{C_i}}{S_{C_i}}\right]+\delta_{C_i}I^*_{C_i}(t)\left[1-\frac{S_{C_i}}{S^*_{C_i}}+\ln\frac{S_{C_i}}{S^*_{C_i}}-\ln\frac{S_{C_i}}{S^*_{C_i}}\right]$$

$$+\sum_{j\neq i=1}^{n}\psi^{S_C}_{j,i}S^*_{C_j}\left[1-\frac{S_{C_i}}{S^*_{C_i}}+\frac{S_{C_j}}{S^*_{C_j}}-\frac{S_{C_j}S^*_{C_i}}{S^*_{C_j}S_{C_i}}+\ln\frac{S_{C_j}S^*_{C_i}}{S^*_{C_j}S_{C_i}}-\ln\frac{S_{C_j}S^*_{C_i}}{S^*_{C_j}S_{C_i}}\right]$$

$$+\sum_{j\neq i=1}^{n}\psi^{I_C}_{j,i}I^*_{C_j}\left[1-\frac{I_{C_i}}{I^*_{C_i}}+\frac{I_{C_j}}{I^*_{C_j}}-\frac{I_{C_j}I^*_{C_i}}{I^*_{C_j}I_{C_i}}+\ln\frac{I_{C_j}I^*_{C_i}}{I^*_{C_j}I_{C_i}}-\ln\frac{I_{C_j}I^*_{C_i}}{I^*_{C_j}I_{C_i}}\right] \tag{4.4.19}$$

$$\frac{dV_i}{dt}=\Lambda_{C_i}\left[1-\frac{S_{C_i}}{S^*_{C_i}}+1-\frac{S^*_{C_i}}{S_{C_i}}+\ln\frac{S_{C_i}}{S^*_{C_i}}-\ln\frac{S_{C_i}}{S^*_{C_i}}\right]$$

$$+\lambda^*_{C_i}S_{C_i}\left[1-\frac{S^*_{C_i}I_{C_i}}{S_{C_i}I^*_{C_i}}+\ln\frac{S^*_{C_i}I_{C_i}}{S_{C_i}I^*_{C_i}}\right]-\lambda^*_{C_i}S_{C_i}\ln\frac{S^*_{C_i}I_{C_i}}{S_{C_i}I^*_{C_i}}+\lambda_{C_i}S^*_{C_i}\left[1-\frac{S_{C_i}I^*_{C_i}}{S^*_{C_i}I_{C_i}}+\ln\frac{S_{C_i}I^*_{C_i}}{S^*_{C_i}I_{C_i}}\right]$$

$$-\lambda_{C_i}S^*_{C_i}\ln\frac{S_{C_i}I^*_{C_i}}{S^*_{C_i}I_{C_i}}+\delta_{C_i}I_{C_i}(t)\left[1-\frac{S^*_{C_i}}{S_{C_i}}+\ln\frac{S^*_{C_i}}{S_{C_i}}\right]-\delta_{C_i}I_{C_i}(t)\ln\frac{S^*_{C_i}}{S_{C_i}}+\delta_{C_i}I^*_{C_i}(t)\left[1-\frac{S_{C_i}}{S^*_{C_i}}+\ln\frac{S_{C_i}}{S^*_{C_i}}\right]$$

$$-\delta_{C_i}I^*_{C_i}(t)\ln\frac{S_{C_i}}{S^*_{C_i}}+\sum_{j\neq i=1}^{n}\psi^{S_C}_{j,i}S^*_{C_j}\left[1-\frac{S_{C_i}}{S^*_{C_i}}+\frac{S_{C_j}}{S^*_{C_j}}-\frac{S_{C_j}S^*_{C_i}}{S^*_{C_j}S_{C_i}}+\ln\frac{S_{C_j}S^*_{C_i}}{S^*_{C_j}S_{C_i}}-\ln\frac{S_{C_j}S^*_{C_i}}{S^*_{C_j}S_{C_i}}\right]$$

$$+\sum_{j\neq i=1}^{n}\psi^{I_C}_{j,i}I^*_{C_j}\left[1-\frac{I_{C_i}}{I^*_{C_i}}+\frac{I_{C_j}}{I^*_{C_j}}-\frac{I_{C_j}I^*_{C_i}}{I^*_{C_j}I_{C_i}}+\ln\frac{I_{C_j}I^*_{C_i}}{I^*_{C_j}I_{C_i}}-\ln\frac{I_{C_j}I^*_{C_i}}{I^*_{C_j}I_{C_i}}\right] \tag{4.4.20}$$

$$\frac{dV_i}{dt}=\Lambda_{C_i}\left[1-\frac{S_{C_i}}{S^*_{C_i}}+1-\frac{S^*_{C_i}}{S_{C_i}}+\ln\frac{S_{C_i}}{S^*_{C_i}}-\ln\frac{S_{C_i}}{S^*_{C_i}}\right]$$

$$+\lambda^*_{C_i}S_{C_i}\left[1-\frac{S^*_{C_i}I_{C_i}}{S_{C_i}I^*_{C_i}}+\ln\frac{S^*_{C_i}I_{C_i}}{S_{C_i}I^*_{C_i}}\right]+\lambda_{C_i}S^*_{C_i}\left[1-\frac{S_{C_i}I^*_{C_i}}{S^*_{C_i}I_{C_i}}+\ln\frac{S_{C_i}I^*_{C_i}}{S^*_{C_i}I_{C_i}}\right]+\ln\frac{S^*_{C_i}I_{C_i}}{S_{C_i}I^*_{C_i}}\left(\lambda_{C_i}S^*_{C_i}-\lambda^*_{C_i}S_{C_i}\right)$$

$$+\delta_{C_i} I_{C_i}(t)\left[1-\frac{S^*_{C_i}}{S_{C_i}}+\ln\frac{S^*_{C_i}}{S_{C_i}}\right]+\delta_{C_i} I^*_{C_i}(t)\left[1-\frac{S_{C_i}}{S^*_{C_i}}+\ln\frac{S_{C_i}}{S^*_{C_i}}\right]+\delta_{C_i}\ln\frac{S_{C_i}}{S^*_{C_i}}\left(I_{C_i}(t)-I^*_{C_i}(t)\right)$$

$$+\sum_{j\neq i=1}^{n}\psi^{S_C}_{j,i}S^*_j\left[1-\frac{S_{C_j}S^*_{C_i}}{S^*_{C_j}S_{C_i}}+\ln\frac{S_{C_j}S^*_{C_i}}{S^*_{C_j}S_{C_i}}\right]+\sum_{j\neq i=1}^{n}\psi^{S_C}_{j,i}S^*_{C_j}\left[-\frac{S_{C_i}}{S^*_{C_i}}+\frac{S_{C_j}}{S^*_{C_j}}-\ln\frac{S_{C_j}}{S^*_{C_j}}-\ln\frac{S^*_{C_i}}{S_{C_i}}\right]$$

$$+\sum_{j\neq i=1}^{n}\psi^{I_C}_{j,i}I^*_{C_j}\left[1-\frac{I_{C_j}I^*_{C_i}}{I^*_{C_j}I_{C_i}}+\ln\frac{I_{C_j}I^*_{C_i}}{I^*_{C_j}I_{C_i}}\right]+\sum_{j\neq i=1}^{n}\psi^{I_C}_{j,i}I^*_{C_j}\left[-\frac{I_{C_i}}{I^*_{C_i}}+\frac{I_{C_j}}{I^*_{C_j}}-\ln\frac{I_{C_j}}{I^*_{C_j}}-\ln\frac{I^*_{C_i}}{I_{C_i}}\right] \quad (4.4.21)$$

where $\lambda_{C_i}S^*_{C_i}\leq\lambda^*_{C_i}S_{C_i}$ and $I_{C_i}(t)\leq I^*_{C_i}(t)$

$$\frac{dV_i}{dt}=\Lambda_{C_i}\left[1-\frac{S_{C_i}}{S^*_{C_i}}+1-\frac{S^*_{C_i}}{S_{C_i}}+\ln\frac{S_{C_i}}{S^*_{C_i}}-\ln\frac{S_{C_i}}{S^*_{C_i}}\right]$$

$$+\lambda^*_{C_i}S_{C_i}\left[1-\frac{S^*_{C_i}I_{C_i}}{S_{C_i}I^*_{C_i}}+\ln\frac{S^*_{C_i}I_{C_i}}{S_{C_i}I^*_{C_i}}\right]+\lambda_{C_i}S^*_{C_i}\left[1-\frac{S_{C_i}I^*_{C_i}}{S^*_{C_i}I_{C_i}}+\ln\frac{S_{C_i}I^*_{C_i}}{S^*_{C_i}I_{C_i}}\right]+\ln\frac{S^*_{C_i}I_{C_i}}{S_{C_i}I^*_{C_i}}\left(\lambda_{C_i}S^*_{C_i}-\lambda^*_{C_i}S_{C_i}\right)$$

$$+\delta_{C_i} I_{C_i}(t)\left[1-\frac{S^*_{C_i}}{S_{C_i}}+\ln\frac{S^*_{C_i}}{S_{C_i}}\right]+\delta_{C_i} I^*_{C_i}(t)\left[1-\frac{S_{C_i}}{S^*_{C_i}}+\ln\frac{S_{C_i}}{S^*_{C_i}}\right]+\delta_{C_i}\ln\frac{S_{C_i}}{S^*_{C_i}}\left(I_{C_i}(t)-I^*_{C_i}(t)\right)$$

$$+\sum_{j\neq i=1}^{n}\psi^{S_C}_{j,i}S^*_{C_j}\left[1-\frac{S_{C_j}S^*_{C_i}}{S^*_{C_j}S_{C_i}}+\ln\frac{S_{C_j}S^*_{C_i}}{S^*_{C_j}S_{C_i}}\right]+\sum_{j\neq i=1}^{n}\psi^{S_C}_{j,i}S^*_{C_j}\left[\frac{S_{C_j}}{S^*_{C_j}}+\ln\frac{S^*_{C_j}}{S_{C_j}}-\frac{S_{C_i}}{S^*_{C_i}}-\ln\frac{S^*_{C_i}}{S_{C_i}}\right]$$

$$+\sum_{j\neq i=1}^{n}\psi^{I_C}_{j,i}I^*_{C_j}\left[1-\frac{I_{C_j}I^*_{C_i}}{I^*_{C_j}I_{C_i}}+\ln\frac{I_{C_j}I^*_{C_i}}{I^*_{C_j}I_{C_i}}\right]+\sum_{j\neq i=1}^{n}\psi^{I_C}_{j,i}I^*_{C_j}\left[\frac{I_{C_j}}{I^*_{C_j}}+\ln\frac{I^*_{C_j}}{I_{C_j}}-\frac{I_{C_i}}{I^*_{C_i}}-\ln\frac{I^*_{C_i}}{I_{C_i}}\right] \quad (4.4.22)$$

$$\leq\sum_{j\neq i=1}^{n}\psi^{S_C}_{j,i}S^*_{C_j}\left[\frac{S_{C_j}}{S^{H*}_j}+\ln\frac{S^{H*}_j}{S^H_j}-\frac{S_{C_i}}{S^*_{C_i}}-\ln\frac{S^*_{C_i}}{S_{C_i}}\right]+\sum_{j\neq i=1}^{n}\psi^{I_C}_{j,i}I^*_{C_j}\left[\frac{I_{C_j}}{I^*_{C_j}}+\ln\frac{I^*_{C_j}}{I_{C_j}}-\frac{I_{C_i}}{I^*_{C_i}}-\ln\frac{I^*_{C_i}}{I_{C_i}}\right] \quad (4.4.23)$$

$$= \sum_{j\neq i=1}^{n} \lambda \psi_{j,i}^{I_C} I_j^* \left[\frac{S_{C_j}}{S_{C_j}^*} + \ln \frac{S_{C_j}^*}{S_{C_j}} - \frac{S_{C_i}}{S_{C_i}^*} - \ln \frac{S_{C_i}^*}{S_{C_i}} \right] + \sum_{j\neq i=1}^{n} \psi_{j,i}^{I_C} I_{C_j}^* \left[\frac{I_{C_j}}{I_{C_j}^*} + \ln \frac{I_{C_j}^*}{I_{C_j}} - \frac{I_{C_i}}{I_{C_i}^*} - \ln \frac{I_{C_i}^*}{I_{C_i}} \right] \tag{4.4.24}$$

$$= \sum_{j\neq i=1}^{n} \psi_{j,i}^{I_C} I_{C_j}^* \left[\left(\lambda \frac{S_{C_j}}{S_{C_j}^*} + \lambda \ln \frac{S_{C_j}^*}{S_{C_j}} + \frac{I_{C_j}}{I_{C_j}^*} + \ln \frac{I_{C_j}^*}{I_{C_j}} \right) - \left(\lambda \frac{S_{C_i}}{S_{C_i}^*} + \lambda \ln \frac{S_{C_i}^*}{S_{C_i}} + \frac{I_{C_i}}{I_{C_i}^*} + \ln \frac{I_{C_i}^*}{I_{C_i}} \right) \right] \tag{4.4.25}$$

$$= \sum_{j=1}^{n} \psi_{j,i}^{I_C} I_{C_j}^* \left[H_j(S_{C_j}, I_{C_j}) - H_i(S_{C_i}, I_{C_i}) \right] \tag{4.4.26}$$

where

$$H_i(S_{C_i}, I_{C_i}) = \lambda \frac{S_{C_i}}{S_{C_i}^*} + \lambda \ln \frac{S_{C_i}^*}{S_{C_i}} + \frac{I_{C_i}}{I_{C_i}^*} + \ln \frac{I_{C_i}^*}{I_{C_i}} \tag{4.4.27}$$

We consider a weight matrix $\mathcal{W} = (w_{ij})$ with entry $w_{ij} = \psi_{j,i}^{I_C} I_{C_j}^*$ and indicate the corresponding weighted digraph as $(\mathcal{H}, \mathcal{W})$. Letting $c_i = \sum_{\mathcal{T}\in\mathbb{T}_i} w(\mathcal{T}) \geq 0$ be defined in (B.1) in Appendix 7.3 with $(\mathcal{H}, \mathcal{W})$. Therefore, implementing (B.2) in Appendix 7.3, the identity below is satisfied

$$\sum_{i=1}^{n} c_i \sum_{j=1}^{n} \psi_{j,i}^{I_C} I_{C_j}^* \left[H_j(S_{C_j}, I_{C_j}) - H_i(S_{C_i}, I_{C_i}) \right] = 0 \tag{4.4.28}$$

Setting

$$V(S_{C_1}, I_{C_1}, S_{C_2}, I_{C_2}, ..., S_{C_n} I_{C_n}) = \sum_{i=1}^{n} c_i V_i(S_{C_i}, I_{C_i}) \tag{4.4.29}$$

Taking (4.4.26) and (4.4.29) we get

$$\frac{dV}{dt} = c_i \frac{dV_i}{dt} \leq \sum_{i=1}^{n} c_i \sum_{j=1}^{n} \psi_{j,i}^{I_C} I_{C_j}^* \left[H_j(S_{C_j}, I_{C_j}) - H_i(S_{C_i}, I_{C_i}) \right] = 0 \tag{4.4.30}$$

for all $(S_{C_1}, I_{C_1}, ..., S_{C_n} I_{C_n}) \in \tilde{\Omega}$. Consequently, V is a Lyapunov function for the system (4.2.1). In view of the fact that $\Psi^I = \left(\psi_{ij}^{I_C}\right)$ is irreducible, we know that $c_i > 0 \ \forall i$ (see the Appendix 7.3), and therefore $dV_i/dt = 0$ implies that $S_{C_i} = S_{C_i}^*$ for all i. From the first equation of system (4.2.1), get

$$0 = \frac{dS_{C_i}(t)}{dt} = \Lambda_{C_i} - \lambda_{C_i}(t) S_{C_i}(t) - \mu_i^{S_C} S_{C_i} + \delta_{C_i} I_{C_i}(t) + \sum_{j\neq i=1}^{n} \psi_{j,i}^{S_C} S_{C_j} - \sum_{j\neq i=1}^{n} \psi_{i,j}^{S_C} S_{C_i} \tag{4.4.31}$$

$i = 1, 2, ..., n$, which implies that $I_{C_i} = I^*_{C_i}$ for all i. The only invariant set on which $dV_i/dt = 0$ is the singleton $\{P^*\}$. Hence, by LaSalle Invariance Principle [138], P^* is globally asymptotically stable in $\tilde{\Omega}$. □

4.5 Numerical analysis

This section presents computer simulations for the multiscale model system (4.2.1)'s behaviour performed using Python program version 3.6 on the Windows 10 operation system.

Table 4.3: Description of within-host and between-host model parameters for the i^{th} individual.

Symbol	Description	Value	Source
Λ_{C_i}	Birth rate of susceptible cattle	0.3 day^{-1}	[110]
β_{C_i}	Rate of infection of susceptible animals via direct contact	0.05 day^{-1}	[111]
$\mu_{C_i}^{S_C}$	Natural mortality rate of susceptible cattle	0.05 year^{-1}	[112]
$\mu_{C_i}^{I_C}$	Natural mortality rate of infected cattle	0.05 year^{-1}	[112]
α_i	Excretion of infectious virions from cells and tissues of cattle into the blood plasma	0.02 day^{-1}	Estimate
d_{C_i}	Per ca-pita rate of loss of immunity	0.001 day^{-1}	[113]
α_{C_i}	Community elimination of total infectious reservoir	0.03 day^{-1}	Estimate
δ_{C_i}	Mortality rate of animals due to FMD.	0.055 day^{-1}	[114]
N_i	Number of FMD virus available for excretion	1000 day^{-1}	Assumed
V_{0i}	Half saturation constant	2×10^8 virions day^{-1}	Estimate

We performed some numerical simulations of the multiscale model system (4.2.1) using estimated parameter values presented in Table 4.3 for sensitivity and numerical analysis. The initial conditions implemented for these simulations are listed below: $S_{C_i}(0) = \dfrac{\Lambda_{C_i}}{\mu_{C_i}^{S_C}}, I_{C_i}(0) = 0, V_{C_i}(0) = 0.$

4.5.1 Numerical simulations of the multiscale model of FMD transmission dynamics

This section enables us to implement numerical simulations to substantiate some outcomes obtained from the sensitivity analysis for $\mathcal{R}_0$ and analytical results of the multiscale model. Applying the multiscale model parameter values obtained from Table 4.3 we carried out the numerical simulations. We demonstrated the impact of six FMD transmission parameters (N_2, $\mu_{C_2}^{S_C}$, V_{02}, α_{C_2}, α_2, ψ_{12}^I) on the multiscale model variables $S_{C_i}(t), I_{C_i}(t), V_{C_i}(t)$. These parameters were only selected because they are significantly sensitive to $\mathcal{R}_0$ and V_C^*.

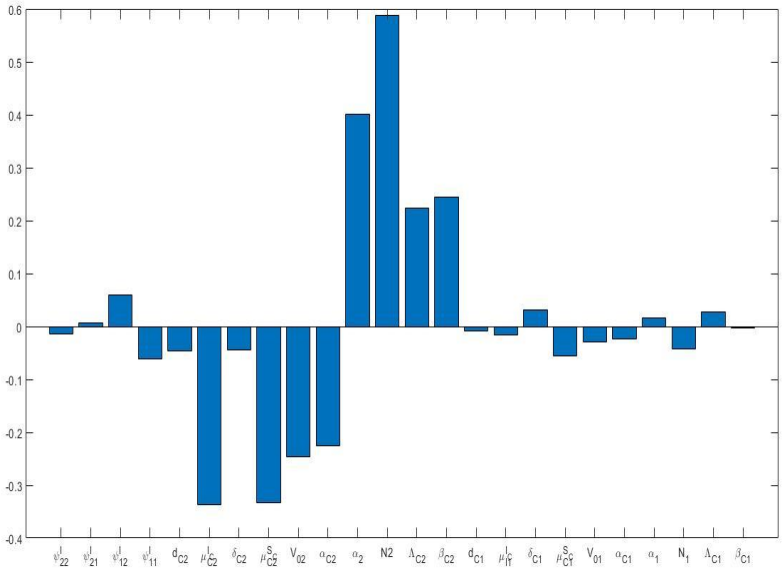

Figure 4.2: *Tornado plot of PRCCs of the model parameters that impact the FMD transmission metric* $\mathcal{R}_0$

4.5.1.1 Influence of within-host scale parameters of the FMD multiscale model dynamics

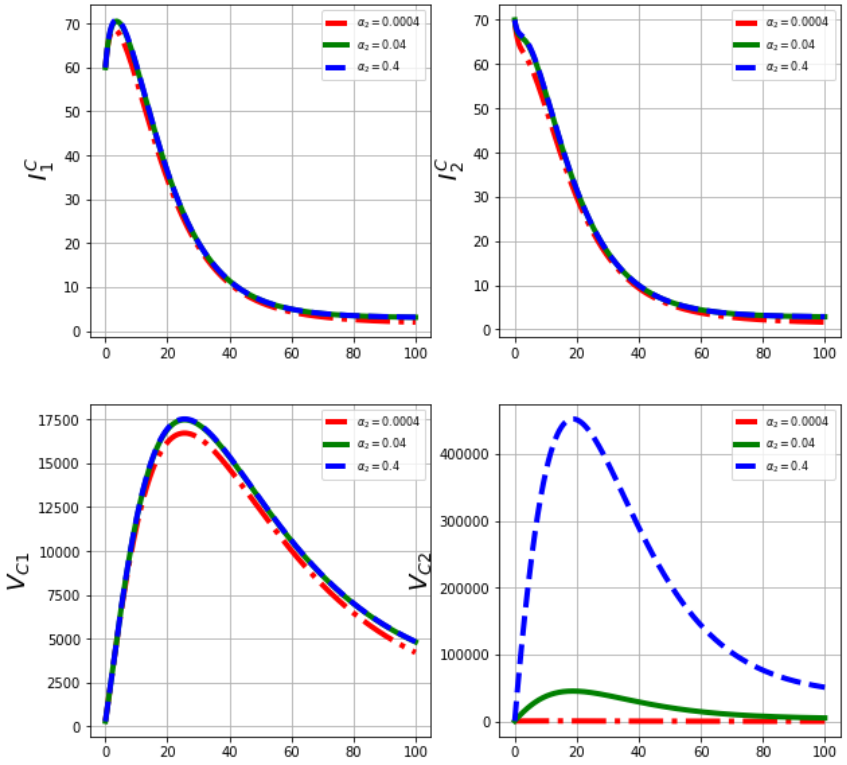

Figure 4.3: Graphs of numerical results of the model system 4.2.1 demonstrating the advancement in time of (a) Infected cattle in patch 1, I_{C_1}, (b) Infected cattle in patch 2, I_{C_2}, (c) Community viral load in patch 1, V_{C_1}, (d) Community viral load in patch 2, V_{C_2} for variant values of the excretion of infectious virions from cells and tissues of cattle into blood plasma in patch 2, $\alpha_2 : \alpha_2 = 0.0004, \alpha_2 = 0.04$ and $\alpha_2 = 0.4$.

Figure (4.3) represents the graphs of numerical results of the model system (4.2.1) demonstrating the progression in time of (a) Infected cattle in patch 1, I_{C_1}, (b) Infected cattle in patch 2, I_{C_2}, (c) Community viral load in patch 1, V_{C_1}, (d) Community viral load in patch 2, V_{C_2} for variant values of the excretion of infectious virions from cells and tissues of cattle into blood plasma in patch 2, $\alpha_2 : \alpha_2 = 0.0004, \alpha_2 = 0.04$ and $\alpha_2 = 0.4$. From these results we can observe that as the excretion of infectious virions from cells and tissues of cattle into blood plasma increases, there is a noticeable increase in the community viral load in patch 2.

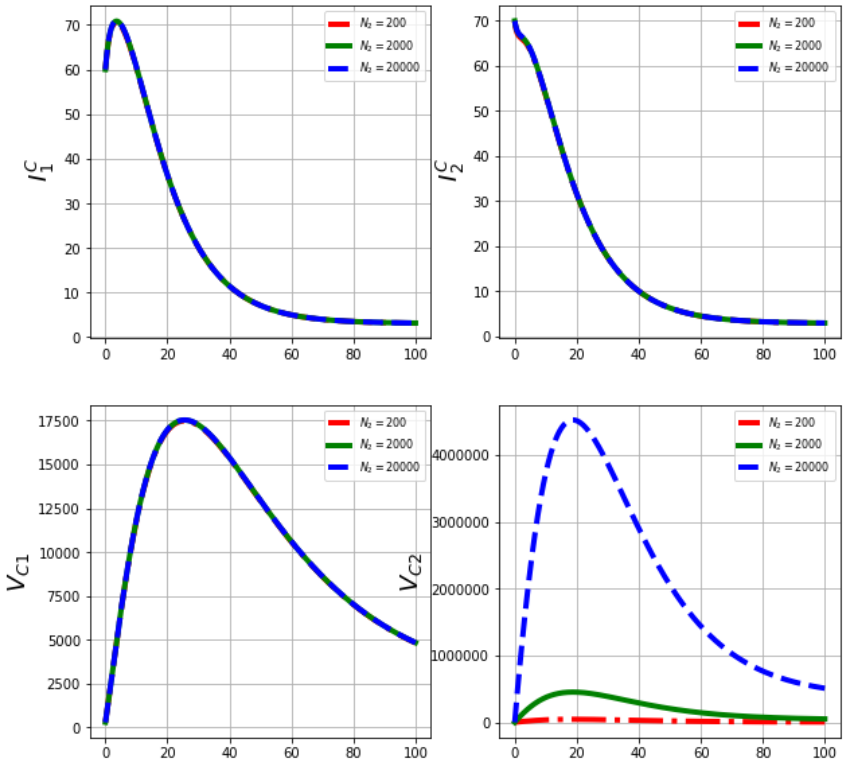

Figure 4.4: Graphs of numerical results of the model system 4.2.1 demonstrating the advancement in time of (a) Infected cattle in patch 1, I_{C_1}, (b) Infected cattle in patch 2, I_{C_2}, (c) Community viral load in patch 1, V_{C_1}, (d) Community viral load in patch 2, V_{C_2} for variant values of the number of FMD virus available for excretion in patch 2, $N_2 : N_2 = 200, N_2 = 2000$ and $N_2 = 20000$.

Figure (4.4) represents the graphs of numerical results of the model system (4.2.1) demonstrating the progression in time of (a) Infected cattle in patch 1, I_{C_1}, (b) Infected cattle in patch 2, I_{C_2}, (c) Community viral load in patch 1, V_{C_1}, (d) Community viral load in patch 2, V_{C_2} for variant values of the number of FMD virus available for excretion in patch 2, $N_2 : N_2 = 200, N_2 = 2000$ and $N_2 = 20000$. From these results we can observe that as the number of FMD virus available for excretion increases, there is a noticeable increase in the community viral load in patch 2.

4.5.1.2 Influence of between-host scale parameters of the FMD multiscale model dynamics

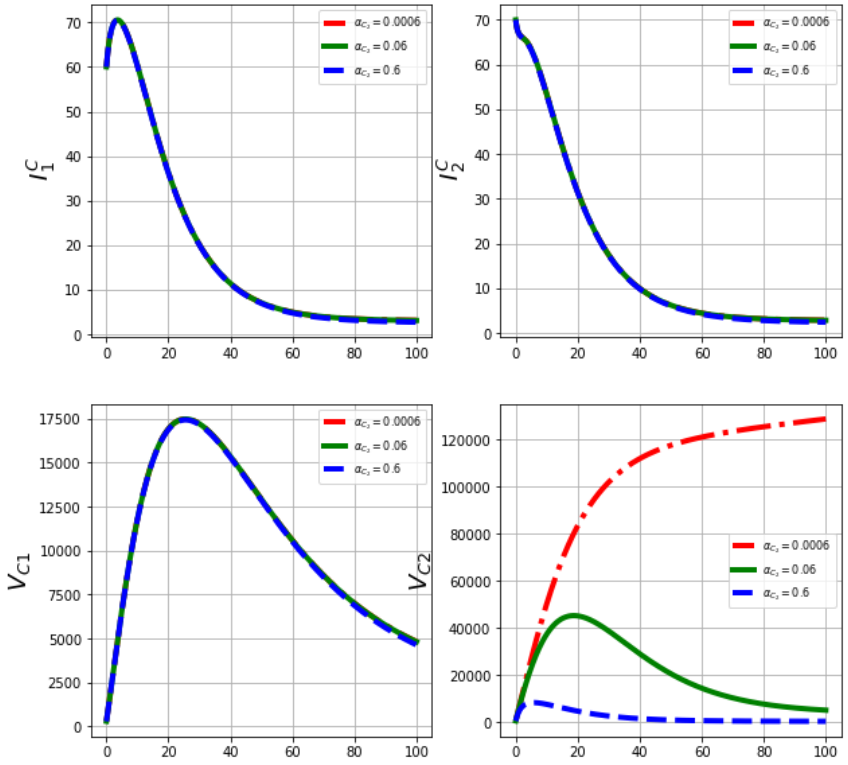

Figure 4.5: Graphs of numerical results of the model system (4.2.1) demonstrating the advancement in time of (a) Infected cattle in patch 1, I_{C_1}, (b) Infected cattle in patch 2, I_{C_2}, (c) Community viral load in patch 1, V_{C_1}, (d) Community viral load in patch 2, V_{C_2} for variant values of the community elimination of total infectious reservior in patch 2, α_{C_2} : $\alpha_{C_2} = 0.0006, \alpha_{C_2} = 0.06$ and $\alpha_{C_2} = 0.6$.

Figure (4.5) represents the graphs of numerical results of the model system (4.2.1) demonstrating the progression in time of (a) Infected cattle in patch 1, I_{C_1}, (b) Infected cattle in patch 2, I_{C_2}, (c) Community viral load in patch 1, V_{C_1}, (d) Community viral load in patch 2, V_{C_2} for variant values of the community elimination of total infectious reservior in patch 2, α_{C_2} : $\alpha_{C_2} = 0.0006, \alpha_{C_2} = 0.06$ and $\alpha_{C_2} = 0.6$. From these results we can observe that as the community elimination of total infectious reservior increases, there is a noticeable decrease in the community viral load in patch 2.

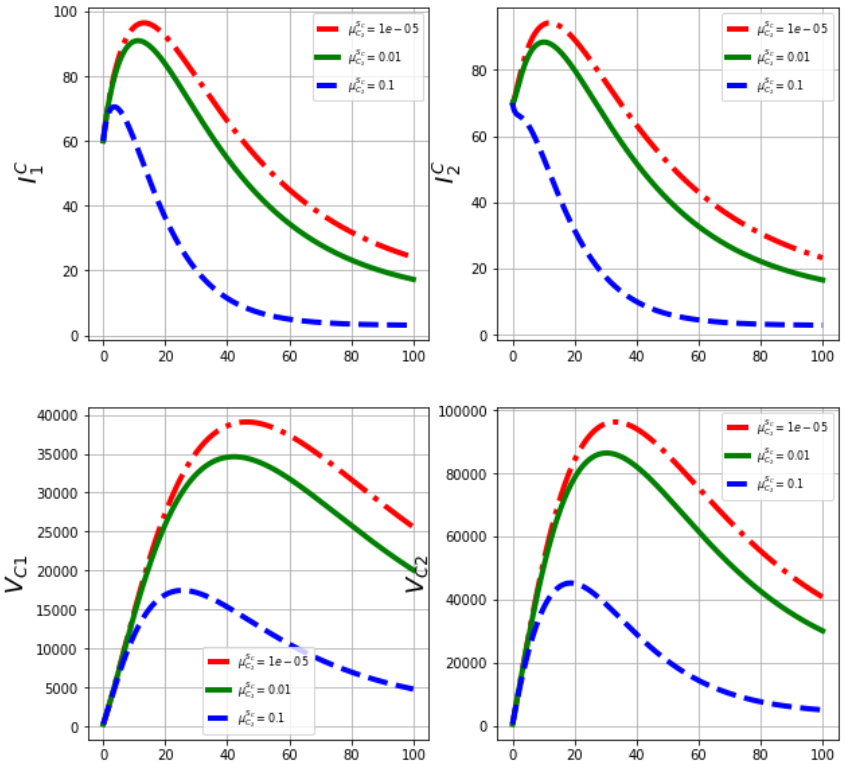

Figure 4.6: Graphs of numerical results of the model system (4.2.1) demonstrating the advancement in time of (a) Infected cattle in patch 1, I_{C_1}, (b) Infected cattle in patch 2, I_{C_2}, (c) Community viral load in patch 1, V_{C_1}, (d) Community viral load in patch 2, V_{C_2} for variant values of the natural mortality rate of susceptible cattle in patch 2, $\mu_{C_2}^{SC} : \mu_{C_2}^{SC} = 1e-05, \mu_{C_2}^{SC} = 0.01$ and $\mu_{C_2}^{SC} = 0.1$.

Figure (4.6) represents the graphs of numerical results of the model system (4.2.1) demonstrating the progression in time of (a) Infected cattle in patch 1, I_{C_1}, (b) Infected cattle in patch 2, I_{C_2}, (c) Community viral load in patch 1, V_{C_1}, (d) Community viral load in patch 2, V_{C_2} for variant values of the natural mortality rate of susceptible cattle in patch 2, $\mu_{C_2}^{SC} : \mu_{C_2}^{SC} = 1e-05, \mu_{C_2}^{SC} = 0.01$ and $\mu_{C_2}^{SC} = 0.1$. From these results we can observe that as the natural mortality rate of susceptible cattle increases, there is a noticeable decrease in infected cattle in patch 1, in infected cattle in patch 2, in community viral load in patch 1, and in the community viral load in patch 2.

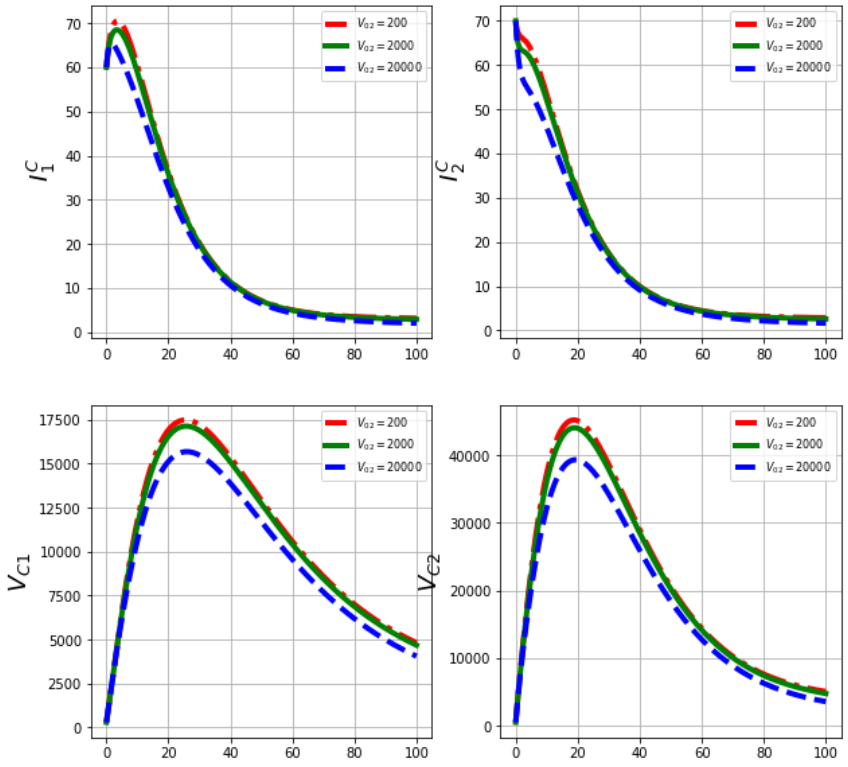

Figure 4.7: Graphs of numerical results of the model system (4.2.1) demonstrating the advancement in time of (a) Infected cattle in patch 1, I_{C_1}, (b) Infected cattle in patch 2, I_{C_2}, (c) Community viral load in patch 1, V_{C_1}, (d) Community viral load in patch 2, V_{C_2} for variant values of the half saturation constant in patch 2, V_{02} : $V_{02} = 200, V_{02} = 2000$ and $V_{02} = 20000$.

Figure (4.7) represents the graphs of numerical results of the model system (4.2.1) demonstrating the progression in time of (a) Infected cattle in patch 1, I_{C_1}, (b) Infected cattle in patch 2, I_{C_2}, (c) Community viral load in patch 1, V_{C_1}, (d) Community viral load in patch 2, V_{C_2} for variant values of the half saturation constant in patch 2, V_{02} : $V_{02} = 200, V_{02} = 2000$ and $V_{02} = 20000$. From these results we can observe that as the half saturation constant increases, there is a noticeable decrease in infected cattle in patch 1, in infected cattle in patch 2, in community viral load in patch 1, and in the community viral load in patch 2.

4.5.1.3 Influence of between-community scale parameters of the FMD multiscale model dynamics

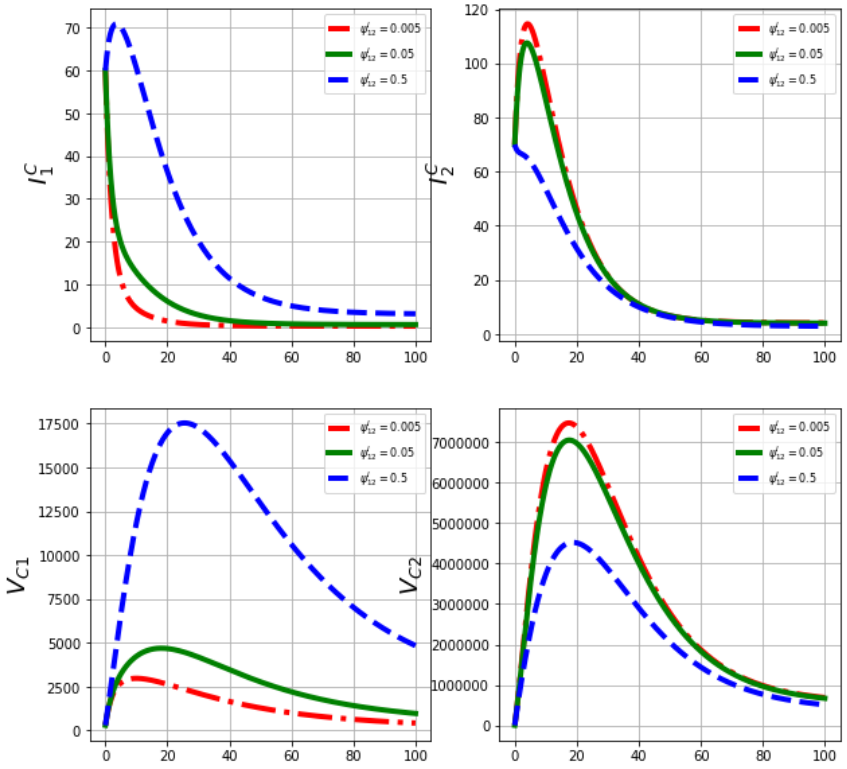

Figure 4.8: Graphs of numerical results of the model system (4.2.1) demonstrating the advancement in time of (a) Infected cattle in patch 1, I_{C_1}, (b) Infected cattle in patch 2, I_{C_2}, (c) Community viral load in patch 1, V_{C_1}, (d) Community viral load in patch 2, V_{C_2} for variant values of the migration rate of cattle from patch 2 to patch 1, $\psi_{12}^I : \psi_{12}^I = 0.005, \psi_{12}^I = 0.05$ and $\psi_{12}^I = 0.5$.

Figure (4.8) represents the graphs of numerical results of the model system (4.2.1) demonstrating the progression in time of (a) Infected cattle in patch 1, I_{C_1}, (b) Infected cattle in patch 2, I_{C_2}, (c) Community viral load in patch 1, V_{C_1}, (d) Community viral load in patch 2, V_{C_2} for variant values of the migration rate of cattle from patch 2 to patch 1, $\psi_{12}^I : \psi_{12}^I = 0.005, \psi_{12}^I = 0.05$ and $\psi_{12}^I = 0.5$. From these results we can observe that as the migration rate of cattle from patch 2 to patch 1 increases, there is a noticeable increase in infected cattle in patch 1 and in community viral load in patch 1. Furthermore, there is a decrease in infected cattle in patch 2 and in the community viral load in patch 2.

4.5.2 Effects of sochasticity on the model

We consider a stochastic model adopted from section (3.5.4) of chapter 3

$$\begin{cases} dS_{C_i}(t) = \left(\Lambda_{C_i} - \dfrac{\beta_{C_i} V_{C_i}(t)}{V_{0i} + V_{C_i}(t)} S_{C_i}(t) - \mu_{C_i}{}^{S_C} S_{C_i}(t) + d_{C_i} I_{C_i}(t)\right) dt + S_{C_i}(t)\sigma_S dW_{S_i} \\ dI_{C_i}(t) = \left(\dfrac{\beta_{C_i} V_{C_i}(t)}{V_{0i} + V_{C_i}(t)} S_{C_i}(t) - (\delta_{C_i} + d_{C_i} + \mu_{C_i}{}^{I_C}) I_{C_i}(t)\right) dt + I_{C_i}(t)\sigma_I dW_{I_i} \\ dV_{C_i}(t) = (N_i \alpha I_{C_i}(t) - \alpha_{C_i} V_{C_i}(t))\, dt + V_{C_i}(t)\sigma_V dW_{V_i} \\ S_{C_i}(0) = S_{0i}, I_{C_i}(0) = I_{0i}, V_{C_i}(0) = V_{0i} \end{cases} \tag{4.5.1}$$

where

$$N = \frac{\zeta \mathfrak{R}_0 \tilde{F}}{\epsilon U^0}, \quad \mathfrak{R}_0 = \frac{\epsilon U^0}{\phi_A \omega} \tag{4.5.2}$$

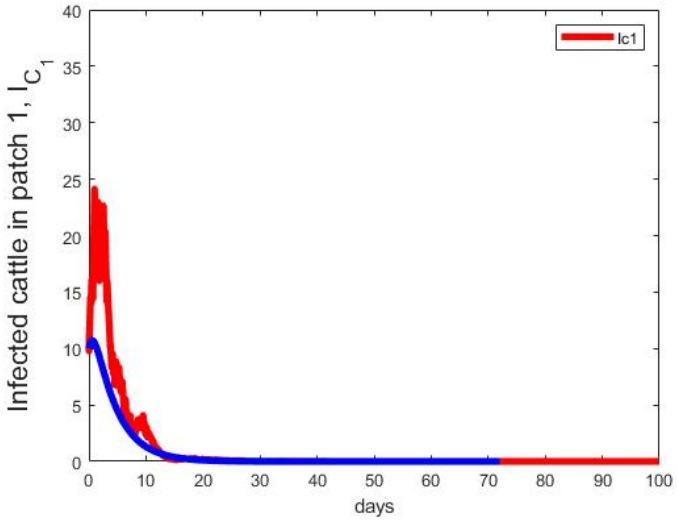

Figure 4.9: Graphs of numerical results of the Infected cattle in pacth 1, I_{C_1} of the multiscale SDE model system (4.5.1) with the ODE multiscale model system (4.2.1) solutions.

Figure 4.9 demonstrates the graphs of numerical results of the Infected cattle, I_{C_1} of the multiscale SDE model system (4.5.1) with the ODE multiscale model system (4.2.1) solutions. The solution for the stochastic multiscale model is obtained using the Milsten method.

Figure 4.10 demonstrates the graphs of numerical results of the Infected cattle, I_{C_2} of the multiscale SDE model system (4.5.1) with the ODE multiscale model system (4.2.1) solutions. The solution for the stochastic multiscale model is obtained using the Milsten method.

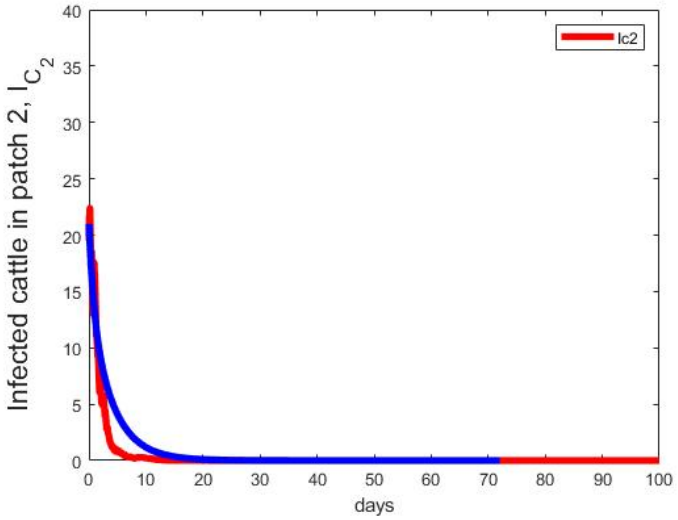

Figure 4.10: Graphs of numerical results of the Infected cattle in pacth 2, I_{C_2} of the multiscale SDE model system (4.5.1) with the ODE multiscale model system (4.2.1) solutions.

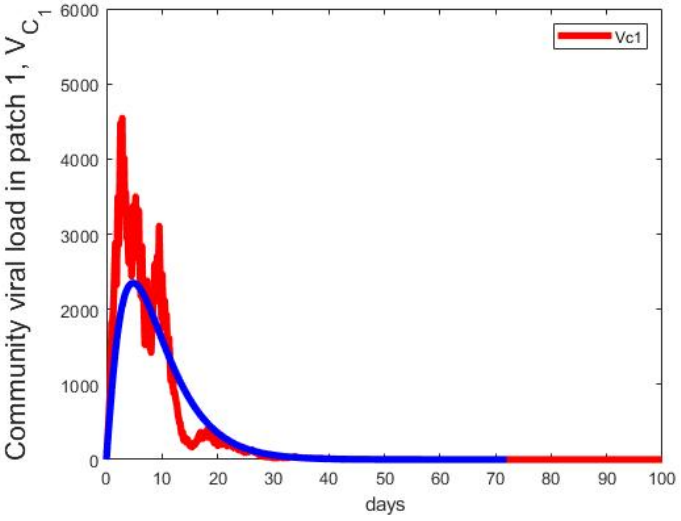

Figure 4.11: Graphs of numerical results of the Community viral load in patch 1, V_{C_1} of the multiscale SDE model system (4.5.1) with the ODE multiscale model system (4.2.1) solutions.

Figure 4.11 demonstrates the graphs of numerical results of the community viral load in patch 1, V_{C_1} of the multiscale SDE model system (4.5.1) with the ODE multiscale model system (4.2.1) solutions. The solution for the stochastic multiscale model is obtained using the Milsten method.

Figure 4.12 demonstrates the graphs of numerical results of the community viral load in patch 2, V_{C_2} of the multiscale SDE model system (4.5.1) with the ODE multiscale model system (4.2.1) solutions. The solution for the stochastic multiscale model is obtained using the Milsten method.

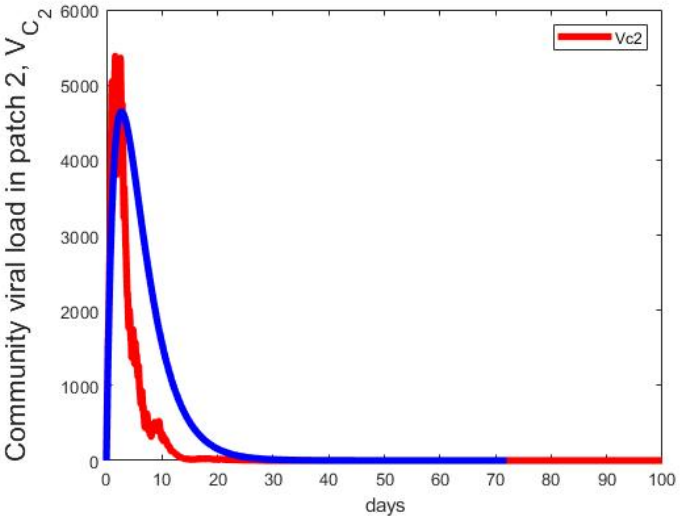

Figure 4.12: Graphs of numerical results of the Community viral load in patch 2, V_{C_2} of the multiscale SDE model system (4.5.1) with the ODE multiscale model system (4.2.1) solutions.

4.5.3 Effects of migration on the model

Fiigure 4.13-Figure 4.15 demonstrate the variation in the rate of migration of infected cattle population from patch 1 to patch 2. Results show that an increase in the rate of migration lead to an increase of infected cattle population in the receiving patch 2. Therefore, interventions such as movement restrictions can help to control the spread of FMD infection at global scale.

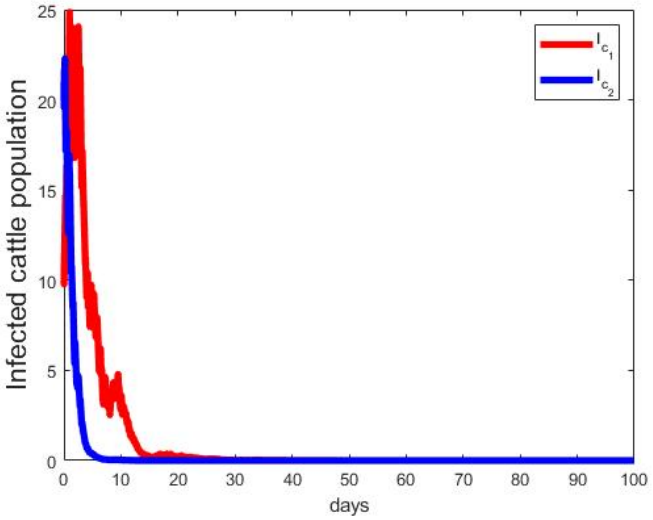

Figure 4.13: Migration rate of infected cattle from patch 1 to patch 2, $\psi_{12}^{I} = 0.005$

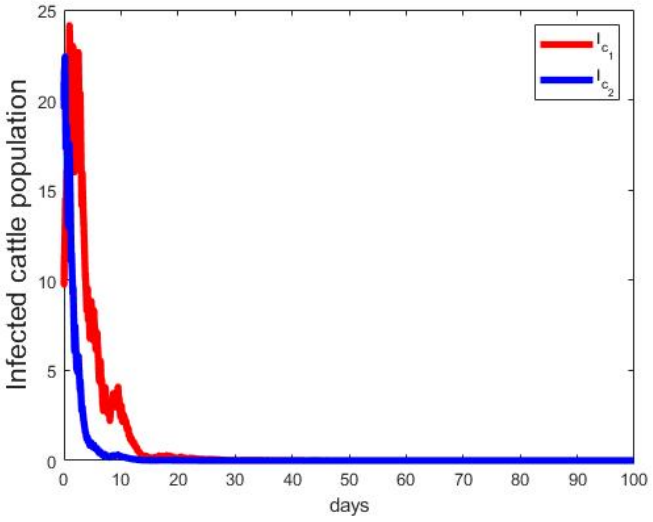

Figure 4.14: Migration rate of infected cattle from patch 1 to patch 2, $\psi_{12}^{I} = 0.05$

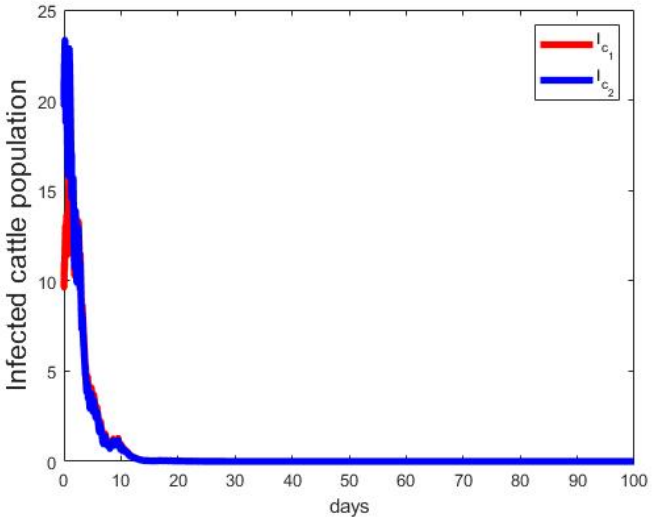

Figure 4.15: Migration rate of infected cattle from patch 1 to patch 2, $\psi_{12}^{I} = 0.5$

4.6 Summary

In this chapter, characterised a nested multiscale model of FMD at community-level, with the main objective of investigating the role of migration on the multiscale dynamics of FMD in cattle. Through mathematical analysis the model was determined to be epidemiologically and mathematically sound. The analysis of sensitivity of the FMDV indicator $\mathcal{R}_0$, in relation to the variation of FMD model parameters was carried out by implementing Latin Hypercube Sampling (LHS) and Partial Rank Correlation Coefficients (PRCCs). Applying the model parameter values we conducted the numerical simulations

to demonstrate the impact of six FMD transmission parameters (N_2, $\mu_{C_2}^{S_C}$, V_{02}, α_{C_2}, α_2, ψ_{12}^I) on the multiscale model variables $S_{C_i}(t), I_{C_i}(t), V_{C_i}(t)$. These parameters were only selected because they are significantly sensitive to $\mathcal{R}_0$. The results from analysis of sensitivity of $\mathcal{R}_0$ indicated that the variation of the within-community scale parameters in particular the amount of FMD virus available for excretion in patch 2, N_2 have a huge impact on the transmission risk of FMD in cattle at community-level and this was confirmed by the Tornado plot in Figure 4.2. Results from Tornado plot in Figure 4.2 also confirmed that the migration rate of infected cattle from patch 1 from patch 2, ψ_{12}^I has an impact on $\mathcal{R}_0$. Figure (4.8) and Figure 4.13-Figure 4.15 demonstrate the variation in the rate of migration of infected cattle population from patch 1 to patch 2. Results show that an increase in the rate of migration lead to an increase of infected cattle population in the receiving patch 2. Furthermore, Figure 4.3 - Figure 4.7 showed the impact in the variation of the parameter values ($\alpha_2, \mu_{C_2}^{S_C}, V_{02}, \alpha_{C_2}, N_2$) on the model variables ($S_{C_1}, I_{C_i}, V_{C_i}$). In addition, Figure 4.9- Figure 4.12 described the graphs of the stochastic models in comparison to the ODE multiscale models.

In conclusion, we established that the model we characterised in this chapter can not be extended to macroecosystem level using graph-theoretic approach. Furthermore, we established that the global transmission of FMD can be described using graph-theoretic approach. In addition, we established that this distinction of local transmission and global transmission of infectious diseases informs us on the appropriate interventions at community level from calculations of the reproduction number. Finally, the model presented has a secondary level multiscale cycle with both local exchange and global exchange of pathogen.

Chapter 5

Multiscale modelling of vector-borne diseases with Malaria as paradigm at Whole organism level

5.1 Introduction

In this chapter, we characterise an individual-based network modelling multiscale model of Malaria disease at whole organism-level. We aim to characterise the spread of Malaria disease taking into account both the dynamics of plasmodium parasite at within- whole organism scale (microscale) and the interactions (direct contact) between whole organism at between-whole organism scale (macroscale). Infection disease systems are considered to be complex systems that can be studied at multilevel and multiscale. Recently, a new multiscale modelling approach called the replication-transmission relativity theory has offered a framework in which both the dynamics of pathogen replication and transmission can be studied together [1]. Among these infectious diseases is Malaria which has been serious public health concern. Malaria is a disease (vector-borne) caused by a parasite called *Plasmodium falciparum* (Pf) transmitted through blood feeding of infectious *Anopheles* mosquitoes and mainly affects vascular blood flow by invading red blood cells (RBCs) [5]. The infection process starts when the infected mosquito injects sporozoites into the skin of a host while feeding. Once the sporozoites gain entry into the blood stream they are carried to the liver where they infect liver cells. When liver cells have burst they release merozoites into the bloodstream which leads to infection and destruction of red blood cells, resulting in fever, anaemia, cerebral Malaria and death if the disease is untreated [139]. Malaria symptoms can develop soon after being bitten by an infected mosquito (6-8 days), or several months after leaving a Malaria region. Once a human

host has been infected by Malaria parasites the individual normally experiences fever, cough, shivering, joint pains, respiratory distress, headache, water diarrhea, vomiting and convulsions. The host–parasite interactions are complex and as a result the development of an effective prophylactic vaccine is extremely challenging. Laboratory diagnosis of Malaria can be made through several approaches including Malaria antigen rapid diagnostic test (RDT). Malaria is a central global health concern that has resulted in over 40% of the world's popualtion being at risk of contracting the disease and according to World Health Organization (WHO) reports, the number of Malaria related mortalities worldwide has been approximated to be over one million per year [6, 140].

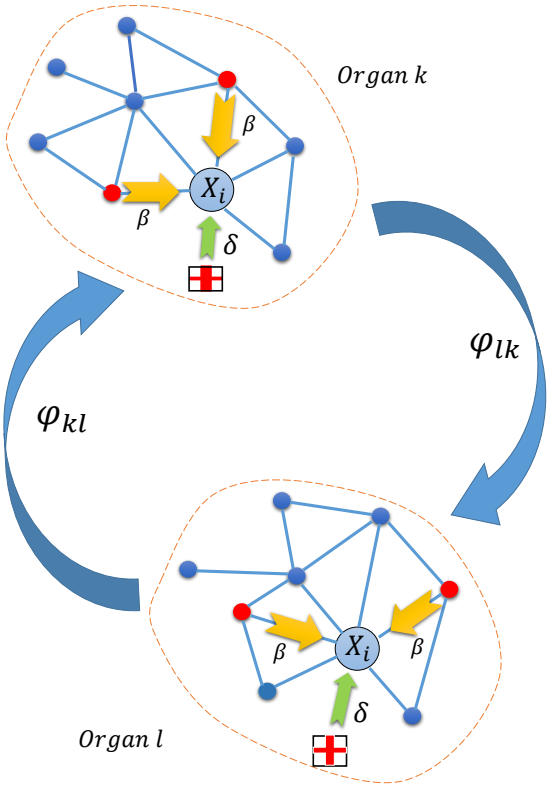

Figure 5.1: The diagram represents the local transmission within-organ and global transmission between-organs.

The whole organism-level constitutes the cell-level, the tissue-level and the organ-level. The transmission of the plasmodium parasite at cell-level occurs by direct contact of infected cell with a susceptible cell or contact of susceptible cell with the plasmodium parasite. This direct transmission of pathogen is local transmission. At organ-level the infected organ such as the liver which is infected by sporozoites will release merozoites into the blood stream leading to the transportation of the pathogen to other parts of the body. Once the pathogen arrives at another organ then direct contact of pathogen or infected cells with susceptible cells results in local transmission represented by ODEs. The transportation of pathogen

between organs through the blood stream is global transmission represented by graph theoretic approach. This aspect is new idea that has not been investigated before and we address it in this chapter.

Present modelling frameworks established from compartmentalizing hosts into SIRS type models (and their variations) have been used to give insights of local transmission mechanisms or global transmission mechanisms of Malaria separately [5, 8, 26, 140–142]. Furthermore, various mathematical models have been developed giving insights of transmission mechanisms of Malaria disease at single scale using graph theoretic methods however, to the best of my knowledge there is no model that addresses pathogen transmission mechanisms at different scales (local transmission and global transmission) at whole organism-level using graph theoretic methods. The latest work that has been done which is more appropriate in modelling the progression of infectious disease systems based on replication-transmission relativity theory is the multiscale modelling appproach. The multiscale modelling of global transmission mechanisms of infectious diseases is better achieved through the use of graph theoretic methods while the standard SIR models address the local transmission mechanisms. The mathematical framework we propose models the local transmission and global transmission mechanisms of Malaria thereby enabling us to explore the multiscale character of infectious disease systems. The framework we formulate separates between-organ transmission dynamics (inflow and outflow) and the within-organs infection dynamics (replication) for the whole transmission-replication loop. In this study, the main ideas are centred on developing a multiscale modelling approach in tandem with graph theoretic methods at whole organism-level. Furthermore, nodes represent communities (organs) and possible transmission is represented by edges. We also seek to establish if the model we have developed can be extended to higher levels of organisation using graph-theoretic methods.

5.2 The Multiscale model for Malaria

The mathematical model we develop consists of within-mosquito Malaria parasite population dynamics as well as the within-human Malaria parasite population dynamics where the human population is connected by a spatial network of n individuals and the mosquito population is connected by a network of m individuals. We consider the human host, mosquito vector and environment as temporary or pesistent patches of the pathogen (malaria parasite) such that the pathogen migrates and replicates or dies. The transmission between-organ is characterized by pathogen migration from its initial organ (patch) i to the final organ (patch) j through the bloodstream. The infection at within-organ is characterized by the replication of pathogen. The model demonstrates the time progression of within infected mosquito host as well as within the infected human host. The populations in the infected human host include the erythrocytes infected by gametocytes G_i^h, free merozoites in blood M_i^h, susceptible erythrocytes R_i^h, erythrocytes infected by merozoites R_i^m. In addition, the populations in the infected mosquito include the sporozoites, P_i^v, gametes, G_i^m, infected erythrocytes, G_i^v, oocysts, O_i^v, zygotes Z_i^v.

Therefore the multiscale model we propose is as follows:

$$
\begin{aligned}
\frac{dR_i^h(t)}{dt} &= \Lambda_i^h - \beta_i^h R_i^h(t) M_i^h(t) - \mu_i^b R_i^h(t), \ldots \quad (1)\\
\frac{dR_i^m(t)}{dt} &= (1-\pi_i)\beta_i^h R_i^h(t) M_i^h(t) - \alpha_i^m R_i^m(t), \ldots \quad (2)\\
\frac{dM_i^h(t)}{dt} &= N_i^m \alpha_i^m R_i^m(t) - \mu_i^m M_i^h(t) + \sum_{i\neq j=1}^{n} \beta_{ij}^v M_j^h(t) - \sum_{i\neq j=1}^{n} \beta_{ji}^h M_i^h(t), \ldots \quad (3)\\
\frac{dG_i^h(t)}{dt} &= \pi_i \beta_i^h R_i^h(t) M_i^h(t) - \left[\alpha_i^h + \mu_i^h\right] G_i^h(t), \ldots \quad (4)\\
\frac{dG_i^v(t)}{dt} &= \Lambda_i^v - \left[\alpha_i^g + \mu_i^g\right] G_i^v(t) + \sum_{i\neq j=1}^{m} \beta_{ij}^h G_j^v(t) - \sum_{i\neq j=1}^{m} \beta_{ji}^v G_i^v(t), \ldots \quad (5)\\
\frac{dG_i^m(t)}{dt} &= N_i^g \alpha_i^g G_i^v(t) - \left[\alpha_i^s + \mu_i^s\right] G_i^m(t), \ldots \quad (6)\\
\frac{dZ_i^v(t)}{dt} &= \frac{1}{2}\alpha_i^s G_i^m(t) - \left[\alpha_i^z + \mu_i^z\right] Z_i^v(t), \ldots \quad (7)\\
\frac{dO_i^v(t)}{dt} &= \alpha_i^z Z_i^v(t) - \left[\alpha_i^k + \mu_i^k\right] O_i^v(t), \ldots \quad (8)\\
\frac{dP_i^v(t)}{dt} &= N_i^k \alpha_i^k O_i^v(t) - \left[\alpha_i^v + \mu_i^v\right] P_i^v(t), \ldots \quad (9)
\end{aligned}
\tag{5.2.1}
$$

where

$$\beta_{ij} = \beta\left(1-\delta_{ij}\right) e^{-\alpha|i-j|},$$

δ_{ij} is Kronecker's delta , α and β are non-negative constants. Small values of α implies a widespread influence of infection while bigger values of α implies local spread. The elements β_{ji} of the transmission matrix **B**, representing the strength of transmission from j to i depend on spatial factors. β represents the overfall strength of transmission [100].

In the multiscale model system (5.2.1) equation (1) represents the susceptible erythrocytes dynamics. Susceptible red blood cells are presumed to accumulate since they are produced from the bone marrow at rate Λ_i [143] and declines through the contagion. The rate at which erythrocytes are infected by free merozoites is given by $\beta_i^h R_i^h M_i^h$. The natural decay rate of susceptible erythrocytes is μ_i^b.

Equation (2) of the multiscale model system (5.2.1) represents merozoite infected erythrocytes dynamics. From equation (2) of multiscale model system (5.2.1) we assume that merozoite infected erythrocytes R_i^m, after rupture increases merozoites by a ratio $(1-\pi_i)$ of all the erythrocytes infected by merozoite. Consequently, the first part of equation (2) of the multiscale model system (5.2.1) models the rate of growth of the ratio of erythrocytes infected by merozoites. The second term of the multiscale model system (5.2.1) models the reduction rate of the ratio of erythrocytes infected by merozoites via rupture releasing merozoites. In the multiscale model system (5.2.1), equation (3) represents the merozoites dynamics in the human blood. We make the assumption that infected erythrocyte that bursts to release merozoites produces an average of N_i^m merozoites after lysis. Consequently, $N_i^m \alpha_i^m R_i^m$ represents the growth rate of merozoites in the human blood via rupture of infected erythrocytes. Merozoites are presumed to reduce from natural decay. The last term in equation (3) represents the rate of growth of merozoites as a result

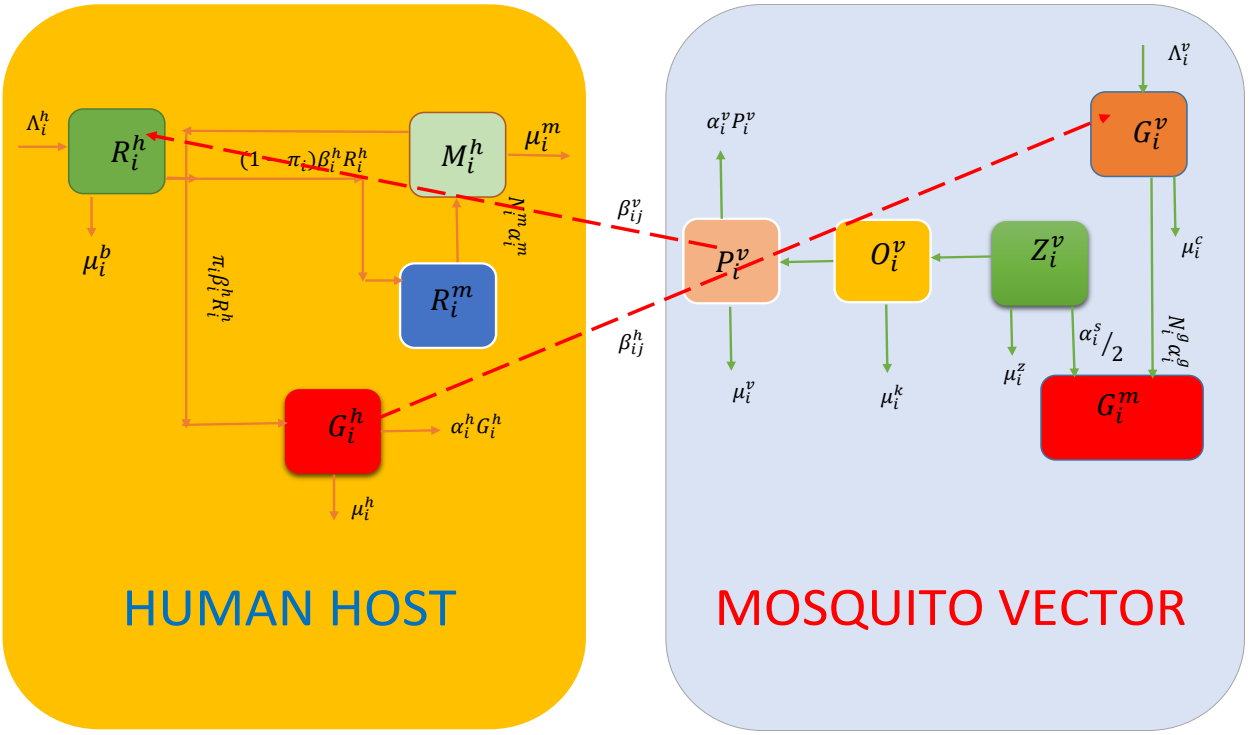

Figure 5.2: Schematic diagram of an microcommunity level multiscale model of Malaria in the human population

of injection of sporozoites by m mosquitoes in contact with the i^{th} individual. (Here there is no explicit model for the developmental stages from injection of sporozoites to the development of merozoites). Equation (4) of the multiscale model system (5.2.1) represents the dynamics of the excess proportion, π_i, of all erythrocytes infected by merozoite, G_i^h. Equation (4) of the multiscale model system (5.2.1) represents growth rate of erythrocytes infected by gametocytes. Looking at the equation α_i^g defines the mature rate of gametocytes in the erythrocytes becoming contagious to mosquitoes. Erythrocytes infected by gametocytes are presumed to decrease at a rate μ_i^G by natural decay. Equation (5) of the multiscale model (5.2.1) represents the gametocyte infected erythrocytes dynamics in an infected mosquito when a mosquito has consumed a blood-meal. Super-infection of the infected mosquito is described by the first part, Λ_i^v. α_i^g represents the bursting rate of gametocyte infected erythrocytes producing sex cells called gametes. μ_i^g is the natural death rate of erythrocytes infected by gametocytes inside a mosquito. Equation (6) of the multiscale model system (5.2.1) represents the gamete population dynamics inside an infected mosquito. The bursting gametocyte infected erythrocytes are presumed to produce an average of N_i^g gametes after rupture. Hence, $N_i^g \alpha_i^g G_i^v$ models the growth rate of gametes inside a mosquito. Gametes are presumed to die at a rate μ_i^s. In addition, male and female gametes fuse to produce zygotes at a rate α_i^s, contributing to the depletion of gametes. Equation (7) of the multiscale model system (5.2.1) represents

the zygote dynamics. The average zygote population Z_i^v, inside a mosquito is produced at rate $\alpha_i^s/2$. We presume that the natural death of zygotes is μ_i^z. Equation (8) in the multiscale model system (5.2.1) represents the oocysts population dynamics. The average oocyst population is produced at a rate α_i^z. The first part of equation (8) represents the growth rate of the oocyst population. The second part represents the reduction of the population from natural death rate μ_i^k or via bursting rate of oocysts to release sporozoites at presumed rate of α_i^k. Equation (9) of the multiscale model system (5.2.1) represents the sporozoite dynamics. Oocyst are presumed to burst at a rate of α_i^k producing an average of N_i^k sporozoites after rupture. Hence, $N_i^k \alpha_i^k O_i^v$ describes growth rate of sporozoites inside mosquito. The rate of excretion' of sporozoites into salivary glands is α_i^v. The last term in equation (9) describes the rate of growth of sporozoites as a result of ingestions of blood-meals from n humans in the network. (Here there is no explicit model for the developmental stages until sporozoites are formed).

5.2.1 Mathematical Analysis of the Multiscale model of Malaria Dynamics

In this section, we determine that multiscale model system (5.2.1) makes biological sense. In other words, we demonstrate non-negativity and boundedness of all the state variables and their solutions, respectively.

5.2.1.1 Positivity of solutions

Theorem 5.1. *A non-negative solution of* $R_i^h(t), R_i^m(t), M_i^h(t), G_i^h(t), G_i^v(t), G_i^m(t), Z_i^v(t), O_i^v(t), P_i^v(t)$ *exists for all* $t \geq 0$.

Proof. The positivity of the solutions of the model system (5.2.1) is proved by implementing the integrating factor technique. Let us consider (1) in model system (5.2.1)

$$\frac{dR_i^h(t)}{dt} = \Lambda_i^h - \beta_i^h R_i^h(t) M_i^h(t) - \mu_i^b R_i^h(t) \tag{5.2.1}$$

We re-write (5.2.1) to obtain

$$\frac{dR_i^h(t)}{dt} + \left(\beta_i^h M_i^h(t) + \mu_i^b\right) R_i^h(t) = \Lambda_i^h \tag{5.2.2}$$

The integrating factor (IF) of (5.2.2) is given by

$$IF = e^{\int_0^t \left(\beta_i^h M_i^h(s) + \mu_i^b\right) ds} \tag{5.2.3}$$

We multiple the integrating factor $e^{\int_0^t \left(\beta_i^h M_i^h(s) + \mu_i^b\right) ds}$ into (5.2.2) to get

$$e^{\int_0^t \left(\beta_i^h M_i^h(s)+\mu_i^b\right)ds}.\frac{dR_i^h(t)}{dt} + e^{\int_0^t \left(\beta_i^h M_i^h(s)+\mu_i^b\right)ds}.\left(\beta_i^h M_i^h(t)+\mu_i^b\right)R_i^h(t) = e^{\int_0^t \left(\beta_i^h M_i^h(s)+\mu_i^b\right)ds}.\Lambda_i^h \tag{5.2.4}$$

From the product rule we obtain

$$\frac{d}{dt}\left[e^{\int_0^t \left(\beta_i^h M_i^h(s)+\mu_i^b\right)ds}.R_i^h(t)\right] = e^{\int_0^t \left(\beta_i^h M_i^h(s)+\mu_i^b\right)ds}.\Lambda_i^h \tag{5.2.5}$$

Integrating both sides of (5.2.5) with respect to t we obtain

$$e^{\int_0^t \left(\beta_i^h M_i^h(s)+\mu_i^b\right)ds}.R_i^h(t) = R_i^h(0) + \int_0^t e^{\int_0^t \left(\beta_i^h M_i^h(s)+\mu_i^b\right)ds}.\Lambda_i^h \tag{5.2.6}$$

We divide both sides of (5.2.6) by the integrating factor $e^{\int_0^t \left(\beta_i^h M_i^h(s)+\mu_i^b\right)ds}$ to get

$$R_i^h(t) = e^{-\int_0^t \left(\beta_i^h M_i^h(s)+\mu_i^b\right)ds}.\left[R_i^h(0) + \int_0^t e^{\int_0^t \left(\beta_i^h M_i^h(s)+\mu_i^b\right)ds}.\Lambda_i^h\right] \geq 0 \tag{5.2.7}$$

Similarly, the remaining solutions for equations (2) - (9) of multiscale model system (5.2.1) can also be obtained using the integrating factor technique. Consequently, $R_i^h(t) \geq 0, R_i^m(t) \geq 0, M_i^h(t) \geq 0, G_i^h(t) \geq 0, G_i^v(t) \geq 0, G_i^m(t) \geq 0, Z_i^v(t) \geq 0, O_i^v(t) \geq 0$ and $P_i^v(t)$ for all time $t > 0$. □

5.2.1.2 Boundedness of solutions

The multiscale model system (5.2.1) represents the populations of the mosquito parasite and the human parasite. Therefore, the entire collection of parameters in the multiscale model (5.2.1) have to be non-negative. Given that the initial values of the parameters are non-negative, we can demonstrate that the solutions of the multiscale model system (5.2.1) are also non-negative. The model can be explored by separating it into mosquito population Ω_V and human population Ω_H. We define the feasible region by

$$\Omega = \left\{\Omega_H \times \Omega_V \subset \mathbb{R}_+^4 \times \mathbb{R}_+^5\right\} \tag{5.2.8}$$

where

$$\begin{cases} \Omega_H = \left\{(R_i^h, R_i^m, M_i^h, G_i^h) | 0 \leq R_i^h + R_i^m + G_i^h \leq K_1, 0 \leq M_i^h(t) \leq K_2\right\} \\ \Omega_V = \left\{(G_i^v, G_i^m, Z^v, O^v, P^v) | 0 \leq N_i^V \leq \frac{\Lambda_i^v}{\mu_i^g}\right\} \end{cases} \tag{5.2.9}$$

where N_i^V denotes the total number of infected cells in the mosquito host.

Letting $N_i^H(t)$ denote the total number of erythrocytes (both susceptible and infected) in the human host and adding equations (1), (2) and (4) of multiscale model system (5.2.1), we obtain

$$\frac{dN_i^H(t)}{dt} = \Lambda_i^h - \mu_i^b R_i^h - \alpha_i^m R_i^m - \mu_i^h G_i^h - \alpha_i^h G_i^h, \tag{5.2.10}$$

so that

$$\frac{dN_i^H(t)}{dt} \leq \Lambda_i^h - \mu_i^b N_i^H(t) - \alpha_i^h G_i^h, \tag{5.2.11}$$

therefore

$$\frac{dN_i^H(t)}{dt} \leq \Lambda_i^h - \mu_i^b N_i^H(t), \tag{5.2.12}$$

This implies that

$$\lim_{t\to\infty} \sup(N_i^H(t)) \leq \frac{\Lambda_i^h}{\mu_i^b}. \tag{5.2.13}$$

Since N_i^H is the sum of the state variables for the susceptible erythrocytes and infected erythrocytes in the humans, then each of the individual state variables is less or equal to $\frac{\Lambda_i^h}{\mu_i^b}$. Therefore, applying equation (2) of the multiscale model system (5.2.1) we get the following inequality

$$\frac{dM_i^h}{dt} \leq N_i^m \alpha_i^m R_i^m - \mu_i^m M_i^h, \tag{5.2.14}$$

$$\frac{dM_i^h}{dt} \leq N_i^m \alpha_i^m \frac{\Lambda_i^h}{\mu_i^b} - \mu_i^m M_i^h, \tag{5.2.15}$$

since $R_i^m(t) \leq \frac{\Lambda_i^h}{\mu_i^b}$. Hence, the solution of the equation (5.2.15) can be obtained by using a suitable integrating factor $(e^{-\mu_i^m t})$, to obtain

$$M_i^h \leq \frac{N_i^m \alpha_i^m \Lambda_i^h}{\mu_i^m \mu_i^b} + D_1 e^{-\mu_i^m t}, \tag{5.2.16}$$

This implies that

$$\lim_{t\to\infty} \sup(M_i^h(t)) \leq \frac{N_i^m \alpha_i^m \Lambda_i^h}{\mu_i^m \mu_i^b}, \tag{5.2.17}$$

We let

$$\Omega_H = \left\{(R_i^h, R_i^m, M_i^h, G_i^h)|0 \leq R_i^h + R_i^m + G_i^h \leq K_1, 0 \leq M_i^h(t) \leq K_2\right\}, \tag{5.2.18}$$

be an invariant region of the model system (5.2.1), where

$$\begin{cases} K_1 = \dfrac{\Lambda_i^h}{\mu_i^b} \\ \\ K_2 = \dfrac{N_i^m \alpha_i^m \Lambda_i^h}{\mu_i^m \mu_i^b} > 0 \end{cases} \tag{5.2.19}$$

Similarly, letting $N^V = G_i^v + G_i^m + Z^v + O^v + P^v$ we get

$$\Omega_V = \left\{(G_i^v, G_i^m, Z^v, O^v, P^v)|0 \leq N_i^V \leq \frac{\Lambda_i^v}{\mu_i^g}\right\} \tag{5.2.20}$$

We let

$$\Omega = \left\{\Omega_H \times \Omega_V \in \mathbb{R}_+^4 \times \mathbb{R}_+^5\right\} \tag{5.2.21}$$

$$\begin{cases} 1. \dfrac{dN_i^H(t)}{dt} \leq \Lambda_i^h - \mu_i^b N_i^H(t), \\ \\ 2. \dfrac{dM_i^h}{dt} \leq N_i^m \alpha_i^m \dfrac{\Lambda_i^h}{\mu_i^b} - \mu_i^m M_i^h \\ \\ 3. \dfrac{dN_i^V(t)}{dt} \leq \Lambda_i^v - \mu_i^g N_i^V(t) \end{cases} \tag{5.2.22}$$

From this we get

$$\begin{cases} 1. N_i^H(t) \leq N_i^H(0) e^{-\mu_i^m t} + \dfrac{\Lambda_i^h}{\mu_i^b}\left[1 - e^{-\mu_i^m t}\right], \\ \\ 2. M_i^h(t) \leq M_i^h(0) e^{-\mu_i^m t} + \dfrac{N_i^m \alpha_i^m \Lambda_i^h}{\mu_i^m \mu_i^b}\left[1 - e^{-\mu_i^m t}\right] \\ \\ 3. N_i^V(t) \leq N_i^V(0) e^{-\mu_i^v t} + \dfrac{\Lambda_i^v}{\mu_i^g}\left[1 - e^{-\mu_i^v t}\right] \end{cases} \tag{5.2.23}$$

where $N_i^H(0), M_i^h(0), N_i^V(0)$ represent the total population of erythrocytes in human host, total parasite population in mosquito host and total parasite population in human host calculated at the initial values of the corresponding variables. We consider the limit when time increases giving the expressions below.

$$\begin{cases} 1.\ \lim\limits_{t\to\infty} \sup(N_i^H(t)) \leq \dfrac{\Lambda_i^h}{\mu_i^b}., \\ 2.\ \lim\limits_{t\to\infty} \sup(M_i^h(t)) \leq \dfrac{N_i^m \alpha_i^m \Lambda_i^h}{\mu_i^m \mu_i^b} \\ 3.\ \lim\limits_{t\to\infty} \sup(N_i^V(t)) \leq \dfrac{\Lambda_i^v}{\mu_i^g} \end{cases} \tag{5.2.24}$$

Thus, Ω is positively invariant and attracting region, since all the solutions or trajectories that begin in Ω will remain in Ω for all $t \geq 0$. Consequently, we can deduce that the multiscale model system (5.2.1) is well-posed (epidemiologically and mathematically) [144]. This outcome is summarized in Theorem 5.2.

Theorem 5.2. *The region* $\Omega = \left\{\Omega_H \times \Omega_V \subset \mathbb{R}_+^4 \times \mathbb{R}_+^5\right\}$ *is positively invariant for the multiscale model system (5.2.1) with non-negative initial conditions in* $\mathbb{R}_+^9$.

5.3 Determination of the disease free equilibrium and its stability

5.3.1 The disease free equilibrium point

We set the right-hand side of the multiscale system (5.2.1) to zero in order to obtain the disease-free equilibrium point. When the equilibrium is disease-free, there are no merozoites in the bloodstream of an individual and therefore, no Malaria infection in humans. Consequently, the disease-free equilibrium of the multiscale model system (5.2.1) is

$$E^0 = \left(R_i^h, R_i^m, M_i^h, G_i^h, G_i^v, G_i^m, Z_i^v, O_i^v, P_i^v\right) = \left(\frac{\Lambda_i^h}{\mu_i^b}, 0, 0, 0, \frac{\Lambda_i^v}{\mu_i^g}, 0, 0, 0, 0\right), i = 1, .., n \tag{5.3.1}$$

5.3.2 The model Reproductive number

The multiscale model system (5.2.1) can be expressed as follows:

$$\begin{aligned} \frac{dX}{dt} &= f(X,Z), \\ \frac{dZ}{dt} &= h(X,Z), \end{aligned} \tag{5.3.1}$$

where

$$X = R_i^h$$

$$Z = (R_i^m, M_i^h, G_i^h)$$

The elements of X stand for the number of susceptibles as well as other groups of non-infectious individuals. The elements of Z stand for the number of infected individuals able to transmit the disease. Define $\tilde{g}(X^*, Z)$ from [101] by

$$\tilde{g}(X^*,Z) = \begin{bmatrix} (1-\pi_i)\beta_i^h R_i^h(t) M_i^h(t) - \alpha_i^m R_i^m(t) \\ N_i^m \alpha_i^m R_i^m(t) - \mu_i^m M_i^h(t) + \sum_{i\neq j=1}^{n} \beta_{ij}^v M_j^h(t) - \sum_{i\neq j=1}^{n} \beta_{ji}^h M_i^h(t) \\ \pi_i \beta_i^h R_i^h(t) M_i^h(t) - \left[\alpha_i^h + \mu_i^h\right] G_i^h(t) \end{bmatrix}_{i=1,2,\ldots,n} \tag{5.3.2}$$

A matrix

$$A = \begin{bmatrix} -\alpha_i^m & \frac{(1-\pi_i)\,\beta_i^h \Lambda_i^h}{\mu_i^b} & 0 \\ N_i^m \alpha_i^m & -\mu_i^m + \sum_{i\neq j=1}^{n} \beta_{ij}^v - \sum_{i\neq j=1}^{n} \beta_{ji}^h & 0 \\ 0 & \frac{\pi_i \beta_i^h \Lambda_i^h}{\mu_i^b} & -\left(\alpha_i^h + \mu_i^h\right) \end{bmatrix}_{i=1,2,\ldots,n} \tag{5.3.3}$$

may be expressed as $A = M - D$, so that

$$M = \begin{bmatrix} 0 & \frac{(1-\pi_i)\,\beta_i^h \Lambda_i^h}{\mu_i^b} & 0 \\ 0 & \sum_{i\neq j=1}^{n} \beta_{ij}^v - \sum_{i\neq j=1}^{n} \beta_{ji}^h & 0 \\ 0 & \frac{\pi_i \beta_i^h \Lambda_i^h}{\mu_i^b} & 0 \end{bmatrix} \tag{5.3.4}$$

$$D = \begin{bmatrix} \alpha_i^m & 0 & 0 \\ -N_i^m \alpha_i^m & \mu_i^m & 0 \\ 0 & 0 & \left(\alpha_i^h + \mu_i^h\right) \end{bmatrix} \tag{5.3.5}$$

$$D^{-1} = \begin{bmatrix} \frac{1}{\alpha_i^m} & 0 & 0 \\ \frac{N_i^m}{\mu_i^m} & \frac{1}{\mu_i^m} & 0 \\ 0 & 0 & \frac{1}{\left(\alpha_i^h + \mu_i^h\right)} \end{bmatrix} \tag{5.3.6}$$

$$MD^{-1} = \begin{bmatrix} 0 & \frac{(1-\pi_i)\,\beta_i^h \Lambda_i}{\mu_i^b \mu_i^m} & 0 \\ 0 & \frac{(1-\pi_i)\,\beta_i^h \Lambda_i N_i^m + \mu_i^b \left(\sum_{i\neq j=1}^{n} \beta_{ij}^v - \sum_{i\neq j=1}^{n} \beta_{ji}^h\right)}{\mu_i^b \mu_i^m} & 0 \\ 0 & \frac{\pi_i \beta_i^h \Lambda_i^h}{\mu_i^b \mu_i^m} & 0 \end{bmatrix}_{i=1,2,\ldots,n} \tag{5.3.7}$$

Then $\mathcal{R}_0 = \rho\left(MD^{-1}\right)$

Hence, the basic reproduction number of the multi-scale model system (5.2.1) for each individual i is expressed by the following quantity.

$$\mathcal{R}_{0i} = \frac{(1-\pi_i)\,\beta_i^h \Lambda_i N_i^m + \mu_i^b \left(\sum_{i\neq j=1}^{n} \beta_{ij}^v - \sum_{i\neq j=1}^{n} \beta_{ji}^h\right)}{\mu_i^b \mu_i^m},\ i = 1, 2, ..., n \tag{5.3.8}$$

5.3.3 Local Stability of the Malaria disease free equilibrium (DFE)

In this subsection, we establish the local stability of DFE of the multiscale model system (5.2.1) by linearizing all the equations of the model system (5.2.1) to get a Jacobian matrix. Then we evaluate the Jacobian matrix of the system at the disease-free equilibrium

$$E^0 = \left(\frac{\Lambda_i^h}{\mu_i^b}, 0, 0, 0, \frac{\Lambda_i^v}{\mu_i^g}, 0, 0, 0, 0\right), i = 1, .., n \tag{5.3.1}$$

Evaluating the Jacobian matrix of the multiscale model system (5.2.1) at the disease-free equilibrium (DFE), we get

$$J(E^0) = \begin{bmatrix} -\mu_i^b & 0 & -\beta_i^h \frac{\Lambda_i^h}{\mu_i^b} & 0 & 0 & 0 & 0 & 0 & 0 \\ 0 & -\alpha_i^m & (1-\pi_i)\beta_i^h \frac{\Lambda_i^h}{\mu_i^b} & 0 & 0 & 0 & 0 & 0 & 0 \\ 0 & N_i^m \alpha_i^m & a_1 & 0 & 0 & 0 & 0 & 0 & 0 \\ 0 & 0 & \pi_i \beta_i^h \frac{\Lambda_i^h}{\mu_i^b} & -\left(\alpha_i^h + \mu_i^h\right) & 0 & 0 & 0 & 0 & 0 \\ 0 & 0 & 0 & 0 & a_2 & 0 & 0 & 0 & \\ 0 & 0 & 0 & 0 & N_i^g \alpha_i^g & -(\alpha_i^s + \mu_i^s) & 0 & 0 & 0 \\ 0 & 0 & 0 & 0 & 0 & \frac{1}{2}\alpha_i^s & -(\alpha_i^z + \mu_i^z) & 0 & 0 \\ 0 & 0 & 0 & 0 & 0 & 0 & \alpha_i^z & -\left(\alpha_i^k + \mu_i^k\right) & 0 \\ 0 & 0 & 0 & 0 & 0 & 0 & 0 & N_i^k \alpha_i^k & -(\alpha_i^v + \mu_i^v) \end{bmatrix} \tag{5.3.2}$$

$$\begin{cases} a_1 = -\mu_i^m + \sum_{i=1, i\neq j}^{n} \beta_{ij}^v - \sum_{i=1, i\neq j}^{n} \beta_{ji}^h = -(1-\pi_i)\beta_i^h N_i^m \frac{\Lambda_i^h}{\mu_i^b} + (\mathcal{R}_{0i} - 1)\mu_i^m \\ a_2 = -(\alpha_i^g + \mu_i^g) + \sum_{i=1, i\neq j}^{n} \beta_{ij}^h - \sum_{i=1, i\neq j}^{n} \beta_{ji}^v \end{cases} \tag{5.3.3}$$

We now consider stability of DFE by calculating the eigenvalues (λ_s) of the Jacobian matrix given by (5.3.2), the characteristic equation for the eigenvalues is given by

$$\Phi_0 \left[-\left(\alpha_i^h + \mu_i^h\right) - \lambda\right] \left[-(\alpha_i^s + \mu_i^s) - \lambda\right] \left[-(\alpha_i^z + \mu_i^z) - \lambda\right] \left[-\left(\alpha_i^k + \mu_i^k\right) - \lambda\right] \left[-(\alpha_i^v + \mu_i^v) - \lambda\right] = 0 \tag{5.3.4}$$

where

$$\Phi_0 = \left(-\mu_i^b - \lambda\right)(-\alpha_i^m - \lambda)(a_1 - \lambda)(a_2 - \lambda) \tag{5.3.5}$$

Since all the eigenvalues from the characteristic equation (5.3.4) are negative then the disease-free equilibrium point E^0 of the multiscale model system (5.2.1) is locally asymptotically stable.

Theorem 5.3. *The disease-free equilibrium point E^0 of the multi-scale model system 5.2.1 is locally asymptotically stable whenever $\mathcal{R}_0 < 1$ and unstable otherwise.*

Lemma 5.4. *The matrix $(M - D)$ has a real spectrum. Moreover, if $\rho\left(MD^{-1}\right) < 1$, all eigenvalues of $(M - D)$ are negative.*

5.3.4 Global Stability of the disease free equilibrium

In order to establish the global stability of DFE of the model system (5.2.1), we implement Theorem 2 in van den Driessche and Watmough [103] to establish that the disease-free equilibrium is globally asymptotically stable whenever $\mathcal{R}_0 < 1$ and unstable when $\mathcal{R}_0 > 1$. We identify two conditions that

warrant the global asymptotic stability of the disease-free state. The model system (5.2.1) can be written as follows:

$$\begin{cases} \dfrac{dX}{dt} = F(X,Z), \\ \\ \dfrac{dZ}{dt} = G(X,Z), \quad G(X,0) = 0 \end{cases} \tag{5.3.1}$$

where $X = \left(R_i^h\right)$ denotes all uninfected components and $Z = (R_i^m, M_i^h, G_i^h, G_i^v, G_i^m, Z_i^v, O_i^v, P_i^v)$ denotes all infected and infectious components;

$$E^0 = \left(R_{0i}^h, R_{0i}^m, M_{0i}^h, G_{0i}^h, G_{0i}^v, G_{0i}^m, Z_{0i}^v, O_{0i}^v, P_{0i}^v\right) = \left(\frac{\Lambda_i^h}{\mu_i^b}, 0, 0, 0, \frac{\Lambda_i^v}{\mu_i^g}, 0, 0, 0, 0\right), i = 1, .., n \tag{5.3.2}$$

represents the disease-free equilibrium of the system. The conditions $(H1)$ and $(H2)$ below must be satisfied in order to assure global asymptotic stability [101]:

(H1) For $\dfrac{dX}{dt} = F(X,0), X^*$ is globally asymptotically stable (g.a.s);

(H2) $G(X,Z) = AZ - \hat{G}(X,Z), \hat{G}(X,Z) \geq 0$ for $(X,Z) \in \mathbb{R}_+^3$,
where the Jacobian $A = \dfrac{\partial G}{\partial Z} = D_Z G(X^*, 0)$ is an M-matrix (the off diagonal elements of A are nonnegative) and Φ is the region where the model makes biological sense.

$$\frac{dX}{dt} = F(X,Z) = \Lambda_i^h - \beta_i^m R_i^h(t) M_i^h(t) - \mu_i^h R_i^h(t) \tag{5.3.3}$$

At the disease-free equilibrium $Z = 0$

$$F(X,0) = \Lambda_i^h - \mu_i^h R_i^h \tag{5.3.4}$$

Hence, in regard of the fact that Φ is an invariant set for model system (5.2.1) and in view of Theorem (5.3), it is sufficient to show that for all $E^0 \in \Phi$

$$\lim_{t\to\infty} P_i^v(t) = 0, \lim_{t\to\infty} O_i^v(t) = 0, \lim_{t\to\infty} Z_i^v(t) = 0, \lim_{t\to\infty} G_i^m(t) = 0, \lim_{t\to\infty} G_i^v(t) = G_{0i}^v,$$

$$\lim_{t\to\infty} G_i^h(t) = 0, \lim_{t\to\infty} M_i^h(t) = 0, \lim_{t\to\infty} R_i^m(t) = 0, \lim_{t\to\infty} R_i^h(t) = R_{0i}^h \tag{5.3.5}$$

where R_{0i}^h and G_{0i}^v are as in (5.3.2) , it follows that

$$\frac{dR_i^h(t)}{dt} \leq \Lambda_i^h - \mu_i^b R_i^h(t) \tag{5.3.6}$$

and

$$\frac{dG_i^v(t)}{dt} \leq \Lambda_i^v - \mu_i^g G_i^v(t) \tag{5.3.7}$$

It is easy to see that R_{0i}^h and G_{0i}^v are globally asymptotically stable equilibria for the comparison equations

$$\frac{dy_1(t)}{dt} \leq \Lambda_i^h - \mu_i^b y_1(t) \tag{5.3.8}$$

and

$$\frac{dy_2(t)}{dt} \leq \Lambda_i^v - \mu_i^g y_2(t) \tag{5.3.9}$$

Therefore, for any $\varepsilon > 0$, there exists $\bar{t} > 0$, such that for all $t \geq \bar{t}$, it holds $R_i^h(t) \leq R_{0i}^h + \varepsilon$ and $G_i^v(t) \leq G_{0i}^v + \varepsilon$

$$\limsup_{t\to\infty} R_i^h(t) \leq R_{0i}^h \text{ and } \limsup_{t\to\infty} G_i^v(t) \leq G_{0i}^v \tag{5.3.10}$$

From (5.3.10) and the equations (2)-(4) and (6)-(9) of the model system (5.2.1) we have that for $t \geq \bar{t}$

$$\begin{aligned}
\frac{dR_i^m(t)}{dt} &\leq (1-\pi_i)\beta_i^h M_i^h(t)\left(R_{0i}^h + \varepsilon\right) - \alpha_i^m R_i^m(t),\\
\frac{dM_i^h(t)}{dt} &= N_i^m \alpha_i^m R_i^m(t) - \mu_i^m M_i^h(t) + \sum_{i\neq j=1}^{n} \beta_{ij}^v M_j^h(t) - \sum_{i\neq j=1}^{n} \beta_{ji}^h M_i^h(t),\\
\frac{dG_i^h(t)}{dt} &\leq \pi_i \beta_i^h M_i^h(t)\left(R_{0i}^h + \varepsilon\right) - \left[\alpha_i^h + \mu_i^h\right] G_i^h(t),\\
\frac{dG_i^m(t)}{dt} &\leq N_i^g \alpha_i^g \left(G_{0i}^v + \varepsilon\right) - \left[\alpha_i^s + \mu_i^s\right] G_i^m(t),\\
\frac{dZ_i^v(t)}{dt} &= \frac{1}{2}\alpha_i^s G_i^m(t) - \left[\alpha_i^z + \mu_i^z\right] Z_i^v(t),\\
\frac{dO_i^v(t)}{dt} &= \alpha_i^z Z_i^v(t) - \left[\alpha_i^k + \mu_i^k\right] O_i^v(t),\\
\frac{dP_i^v(t)}{dt} &= N_i^k \alpha_i^k O_i^v(t) - \left[\alpha_i^v + \mu_i^v\right] P_i^v(t),
\end{aligned} \tag{5.3.11}$$

Let us consider the comparison system

$$
\begin{aligned}
\frac{dw_1(t)}{dt} &\leq (1-\pi_i)\beta_i^h w_2(t)\left(R_{0i}^h+\varepsilon\right)-\alpha_i^m w_1(t),\\
\frac{dw_2(t)}{dt} &= N_i^m\alpha_i^m w_1(t)-\mu_i^m w_2(t)+\sum_{i\neq j=1}^{n}\beta_{ij}^v w_2(t)-\sum_{i\neq j=1}^{n}\beta_{ji}^h w_2(t),\\
\frac{dw_3(t)}{dt} &\leq \pi_i\beta_i^h w_2(t)\left(R_{0i}^h+\varepsilon\right)-\left[\alpha_i^h+\mu_i^h\right]w_3(t),\\
\frac{dw_4(t)}{dt} &\leq N_i^g\alpha_i^g\left(G_{0i}^v+\varepsilon\right)-\left[\alpha_i^s+\mu_i^s\right]w_4(t),\\
\frac{dw_5(t)}{dt} &= \frac{1}{2}\alpha_i^s w_4(t)-\left[\alpha_i^z+\mu_i^z\right]w_5(t),\\
\frac{dw_6(t)}{dt} &= \alpha_i^z w_5(t)-\left[\alpha_i^k+\mu_i^k\right]w_6(t),\\
\frac{dw_7(t)}{dt} &= N_i^k\alpha_i^k w_6(t)-\left[\alpha_i^v+\mu_i^v\right]w_7(t),\ w_1(\bar{t})=R_i^m(\bar{t}),w_2(\bar{t})=M_i^h(\bar{t}),\\
&\quad w_3(\bar{t})=G_i^h(\bar{t}),w_4(\bar{t})=G_i^m(\bar{t}),w_5(\bar{t})=Z_i^v(\bar{t}),w_6(\bar{t})=O_i^v(\bar{t}),w_7(\bar{t})=P_i^v(\bar{t})
\end{aligned}
\tag{5.3.12}
$$

that we can re-write as

$$
\frac{dw(t)}{dt}=\left(F_\varepsilon-V_\varepsilon\right)w(t) \tag{5.3.13}
$$

where $w(t)=(w_1(t),w_2(t),w_3(t),w_4(t),w_5(t),w_6(t),w_7(t))^T$ and $(F_\varepsilon-V_\varepsilon)$ is a matrix in (5.3.3) computed in $E^0(\varepsilon)=\left(R_i^h+\varepsilon,0,0,0,G_i^v+\varepsilon,0,0,0,0\right)$. Let us note that if $\mathcal{R}_0=\rho\left(FV^{-1}\right)<1$, we can choose a sufficiently small $\varepsilon>0$ such that $\rho\left(F_\varepsilon V_\varepsilon^{-1}\right)<1$. Then by applying Lemma 5.4 to $(F_\varepsilon-V_\varepsilon)$ we obtain that it has a real spectrum and all its eigenvalues are negative. It follows that $\lim_{t\to\infty}w(t)=0$, whatever the initial conditions are, from which

$$
\lim_{t\to\infty}R_i^m(t)=0,\lim_{t\to\infty}M_i^h(t)=0,\lim_{t\to\infty}G_i^h(t)=0,\lim_{t\to\infty}G_i^m(t)=0,\lim_{t\to\infty}Z_i^v(t)=0,\lim_{t\to\infty}O_i^v(t)=0,\lim_{t\to\infty}P_i^v(t)=0 \tag{5.3.14}
$$

Now, for any $\varepsilon>0$, there exists $\bar{t}_1$ such that for any $t\geq\bar{t}_1$, $R_i^m(t)<\varepsilon$, $M_i^h(t)<\varepsilon$, $G_i^h(t)<\varepsilon$, $G_i^m(t)<\varepsilon$, $Z_i^v(t)<\varepsilon$, $O_i^v(t)<\varepsilon$, $P_i^v(t)<\varepsilon$. So, for $t\geq\bar{t}_1$ we have

$$
\frac{dR_i^h(t)}{dt}\geq\Lambda_i^h-\beta_i^h R_i^h(t)\varepsilon-\mu_i^b R_i^h(t), \tag{5.3.15}
$$

It is easy to see that $\dfrac{\Lambda_i^h}{\beta_i^h\varepsilon+\mu_i^b}$ is a global asymptotically stable equilibrium for the comparison equation

$$
\frac{dy(t)}{dt}\geq\Lambda_i^h-\beta_i^h y(t)\varepsilon-\mu_i^b y(t), \tag{5.3.16}
$$

Thus, for any $\chi>0$, there exists $\bar{t}_2>0$ such that for all $t\geq\bar{t}_2$

$$R_i^h(t) \geq \frac{\Lambda_i^h}{\beta_i^h \varepsilon + \mu_i^b} - \chi \tag{5.3.17}$$

Therefore, for any $\varepsilon > 0$, we have

$$\liminf_{t\to\infty} R_i^h(t) \geq \frac{\Lambda_i^h}{\beta_i^h \varepsilon + \mu_i^b} \tag{5.3.18}$$

Letting $t \to \infty$, we get $\liminf_{t\to\infty} R_i^h(t) \geq R_{0i}^h$ and combining this with (5.3.10) gives us

$$\lim_{t\to\infty} R_i^h(t) = R_{0i}^h \tag{5.3.19}$$

A similar argument ensures that

$$\lim_{t\to\infty} G_i^v(t) = G_{0i}^v \tag{5.3.20}$$

Therefore, $E^0 = \left(\frac{\Lambda_i^h}{\mu_i^b}, 0, 0, 0, \frac{\Lambda_i^v}{\mu_i^g}, 0, 0, 0, 0\right), i = 1, .., n$ is a global asymptotically stable equilibrium point satisfying condition **H1**.

We can now establish that condition **H2** is satisfied.

$$\frac{dZ}{dt} = G^H(X, Z) = \begin{bmatrix} (1-\pi_i)\beta_i^h R_i^h(t) M_i^h(t) - \alpha_i^m R_i^m(t) \\ (1-\pi_j)\beta_j^h R_j^h(t) M_j^h(t) - \alpha_j^m R_j^m(t) \\ N_i^m \alpha_i^m R_i^m(t) - \mu_i^m M_i^h(t) + \beta_{ij}^v M_j^h(t) - \beta_{ji}^h M_i^h(t) \\ N_j^m \alpha_j^m R_j^m(t) - \mu_j^m M_j^h(t) + \beta_{ji}^h M_i^h(t) - \beta_{ij}^v M_j^h(t) \\ \pi_i \beta_i^h R_i^h(t) M_i^h(t) - \left[\alpha_i^h + \mu_i^h\right] G_i^h(t) \\ \pi_j \beta_j^h R_j^h(t) M_j^h(t) - \left[\alpha_j^h + \mu_j^h\right] G_j^h(t) \end{bmatrix} \tag{5.3.21}$$

$$\frac{dZ}{dt} = G^V(X, Z) = \begin{bmatrix} \Lambda_i^v - \left[\alpha_i^g + \mu_i^g\right] G_i^v(t) + \beta_{ij}^h G_j^v(t) - \beta_{ji}^v G_i^v(t) \\ \Lambda_j^v - \left[\alpha_j^g + \mu_j^g\right] G_j^v(t) + \beta_{ji}^v G_i^v(t) - \beta_{ij}^h G_j^v(t) \\ N_i^g \alpha_i^g G_i^v(t) - \left[\alpha_i^s + \mu_i^s\right] G_i^m(t) \\ N_j^g \alpha_j^g G_j^v(t) - \left[\alpha_j^s + \mu_j^s\right] G_j^m(t) \\ \frac{1}{2}\alpha_i^s G_i^m(t) - \left[\alpha_i^z + \mu_i^z\right] Z_i^v(t) \\ \frac{1}{2}\alpha_j^s G_j^m(t) - \left[\alpha_j^z + \mu_j^z\right] Z_j^v(t) \\ \alpha_i^z Z_i^v(t) - \left[\alpha_i^k + \mu_i^k\right] O_i^v(t) \\ \alpha_j^z Z_j^v(t) - \left[\alpha_j^k + \mu_j^k\right] O_j^v(t) \\ N_i^k \alpha_i^k O_i^v(t) - \left[\alpha_i^v + \mu_i^v\right] P_i^v(t) \\ N_j^k \alpha_j^k O_j^v(t) - \left[\alpha_j^v + \mu_j^v\right] P_j^v(t), \end{bmatrix} \tag{5.3.22}$$

and $G(X,0)=0$

$$A^H Z = \begin{bmatrix} -\alpha_i^m R_i^m(t) + \dfrac{(1-\pi_i)\beta_i^h \Lambda_i^h(t)}{\mu_i^b} M_i^h(t) \\ -\alpha_j^m R_j^m(t) + \dfrac{(1-\pi_j)\beta_j^h \Lambda_j^h(t)}{\mu_j^b} M_j^h(t) \\ N_i^m \alpha_i^m R_i^m(t) - \mu_i^m M_i^h(t) + \beta_{ij}^v M_j^h(t) - \beta_{ji}^h M_i^h(t) \\ N_j^m \alpha_j^m R_j^m(t) - \mu_j^m M_j^h(t) + \beta_{ji}^h M_i^h(t) - \beta_{ij}^v M_j^h(t) \\ \dfrac{\pi_i \beta_i^h \Lambda_i^h(t)}{\mu_i^b} M_i^h(t) - \left[\alpha_i^h + \mu_i^h\right] G_i^h(t) \\ \dfrac{\pi_j \beta_j^h \Lambda_j^h(t)}{\mu_j^b} M_j^h(t) - \left[\alpha_j^h + \mu_j^h\right] G_j^h(t) \end{bmatrix} \tag{5.3.23}$$

$$A^H = \begin{bmatrix} -\alpha_i^m & 0 & \dfrac{(1-\pi_i)\,\beta_i^h \Lambda_i^h}{\mu_i^b} & 0 & 0 & 0 \\ 0 & -\alpha_j^m & 0 & \dfrac{(1-\pi_i)\,\beta_i^h \Lambda_i^h}{\mu_j^b} & 0 & 0 \\ N_i^m \alpha_i^m & 0 & -\left(\mu_i^m + \beta_{ji}^h\right) & \beta_{ij}^v & 0 & 0 \\ 0 & N_j^m \alpha_j^m & \beta_{ji}^h & -\left(\mu_j^m + \beta_{ij}^v\right) & 0 & 0 \\ 0 & 0 & \dfrac{\pi_i \beta_i^h \Lambda_i^h}{\mu_i^b} & 0 & -\left(\alpha_i^h + \mu_i^h\right) & 0 \\ 0 & 0 & 0 & \dfrac{\pi_j \beta_j^h \Lambda_j^h}{\mu_j^b} & 0 & -\left(\alpha_j^h + \mu_j^h\right) \end{bmatrix} \tag{5.3.24}$$

$$A^V Z = \begin{bmatrix} \Lambda_i^v - \left[\alpha_i^g + \mu_i^g\right] G_i^v(t) + \beta_{ij}^h G_j^v(t) - \beta_{ji}^v G_i^v(t) \\ \Lambda_j^v - \left[\alpha_j^g + \mu_j^g\right] G_j^v(t) + \beta_{ji}^v G_i^v(t) - \beta_{ij}^h G_j^v(t) \\ N_i^g \alpha_i^g G_i^v(t) - \left[\alpha_i^s + \mu_i^s\right] G_i^m(t) \\ N_j^g \alpha_j^g G_j^v(t) - \left[\alpha_j^s + \mu_j^s\right] G_j^m(t) \\ \dfrac{1}{2}\alpha_i^s G_i^m(t) - \left[\alpha_i^z + \mu_i^z\right] Z_i^v(t) \\ \dfrac{1}{2}\alpha_j^s G_j^m(t) - \left[\alpha_j^z + \mu_j^z\right] Z_j^v(t) \\ \alpha_i^z Z_i^v(t) - \left[\alpha_i^k + \mu_i^k\right] O_i^v(t) \\ \alpha_j^z Z_j^v(t) - \left[\alpha_j^k + \mu_j^k\right] O_j^v(t) \\ N_i^k \alpha_i^k O_i^v(t) - \left[\alpha_i^v + \mu_i^v\right] P_i^v(t) \\ N_j^k \alpha_j^k O_j^v(t) - \left[\alpha_j^v + \mu_j^v\right] P_j^v(t), \end{bmatrix} \tag{5.3.25}$$

$$A^V = \begin{bmatrix} a_1 & 0 & 0 & 0 & 0 & 0 & 0 & 0 & 0 & 0 \\ 0 & a_2 & 0 & 0 & 0 & 0 & 0 & 0 & 0 & 0 \\ N_i^g \alpha_i^g & 0 & a_3 & 0 & 0 & 0 & 0 & 0 & 0 & 0 \\ 0 & N_j^g \alpha_j^g & 0 & a_4 & 0 & 0 & 0 & 0 & 0 & 0 \\ 0 & 0 & \frac{1}{2}\alpha_i^s & 0 & a_5 & 0 & 0 & 0 & 0 & 0 \\ 0 & 0 & 0 & \frac{1}{2}\alpha_j^s & 0 & a_6 & 0 & 0 & 0 & 0 \\ 0 & 0 & 0 & 0 & \alpha_i^z & 0 & a_7 & 0 & 0 & 0 \\ 0 & 0 & 0 & 0 & 0 & \alpha_j^z & 0 & a_8 & 0 & 0 \\ 0 & 0 & 0 & 0 & 0 & 0 & N_i^k \alpha_i^k & 0 & a_9 & 0 \\ 0 & 0 & 0 & 0 & 0 & 0 & 0 & N_j^k \alpha_j^k & 0 & a_{10} \end{bmatrix} \tag{5.3.26}$$

where

$$\begin{cases} a_1 = -\left(\alpha_i^g + \mu_i^g + \beta_{ji}^v\right) \\ a_2 = -\left(\alpha_j^g + \mu_j^g + \beta_{ij}^h\right) \\ a_3 = -\left(\alpha_i^s + \mu_i^s\right) \\ a_4 = -\left(\alpha_j^s + \mu_j^s\right) \\ a_5 = -\left(\alpha_i^z + \mu_i^z\right) \\ a_6 = -\left(\alpha_j^z + \mu_j^z\right) \\ a_7 = -\left(\alpha_i^k + \mu_i^k\right) \\ a_8 = -\left(\alpha_j^k + \mu_j^k\right) \\ a_9 = -\left(\alpha_i^v + \mu_i^v\right) \\ a_{10} = -\left(\alpha_j^v + \mu_j^v\right) \end{cases} \tag{5.3.27}$$

From (5.3.24) and (5.3.26) we can easily see that A^H and A^V have non negative off-diagonal entries. Therefore A^H and A^V are M-matrices.

Furthermore,

$$\hat{G}^H(X,Z) = \begin{bmatrix} \hat{G}_1(X,Z) \\ \hat{G}_2(X,Z) \\ \hat{G}_3(X,Z) \\ \hat{G}_4(X,Z) \\ \hat{G}_5(X,Z) \\ \hat{G}_6(X,Z) \end{bmatrix} = \begin{bmatrix} [1-\pi_i]\left(\frac{\Lambda_i^h}{\mu_i^b} - R_i^h\right)\beta_i^h M_i^h \\ [1-\pi_j]\left(\frac{\Lambda_j^h}{\mu_j^b} - R_j^h\right)\beta_j^h M_j^h \\ 0 \\ 0 \\ \pi_i\left(\frac{\Lambda_i^h}{\mu_i^h} - R_i^h\right)\beta_i^h M_i^h \\ \pi_j\left(\frac{\Lambda_j^h}{\mu_j^h} - R_j^h\right)\beta_j^h M_j^h \end{bmatrix} \tag{5.3.28}$$

and

$$\hat{G}^V(X,Z) = \begin{bmatrix} \hat{G}_1(X,Z) \\ \hat{G}_2(X,Z) \\ \hat{G}_3(X,Z) \\ \hat{G}_4(X,Z) \\ \hat{G}_5(X,Z) \\ \hat{G}_6(X,Z) \\ \hat{G}_7(X,Z) \\ \hat{G}_8(X,Z) \\ \hat{G}_9(X,Z) \\ \hat{G}_{10}(X,Z) \end{bmatrix} = \begin{bmatrix} \left(\Lambda_i^v + \beta_{ij}^h G_j^v\right) \\ \left(\Lambda_j^v + \beta_{ji}^v G_i^v\right) \\ 0 \\ 0 \\ 0 \\ 0 \\ 0 \\ 0 \\ 0 \\ 0 \end{bmatrix} \tag{5.3.29}$$

From (5.3.10) we can deduce that $\frac{\Lambda_i^h}{\mu_i^b} \geq R_i^h$ for $i = 1, ..., n$, $\frac{\Lambda_j^h}{\mu_j^b} \geq R_j^h$ for $j = 1, ..., n$ where $i \neq j$, it is clear that $\hat{G}^H(X,Z) \geq 0$ and $\hat{G}^V(X,Z) \geq 0$ for all $(X,Z) \in \mathbb{R}_+^{9n}$ and A is an M-matrix because the off diagonal elements of A are non-negative. Conditions **H1** and **H2** are satisfied and therefore E^0 is Globally Asymptotically Stable (GAS) for $\mathcal{R}_0 < 1$.

Theorem 5.5. *The disease-free equilibrium of the multiscale model system (5.2.1) is globally asymptotically stable if $\mathcal{R}_0 \leq 1$ and the assumptions (H1) and (H2) are satisfied.*

5.4 The endemic equilibrium and its stability

5.4.1 The endemic equilibrium

At the endemic equilibrium the human population is infected by Malaria. The endemic equilibrium point of the multiscale model system (5.2.1) is given by

$$E^* = \left(R_i^{h*}, R_i^{m*}, M_i^{h*}, G_i^{h*}, G_i^{v*}, G_i^{m*}, Z_i^{v*}, O_i^{v*}, P_i^{v*}\right), i = 1, .., n \tag{5.4.1}$$

We set the left-hand side of the multiscale model system (5.2.1) to zero and obtain:

$$\begin{aligned}
0 &= \Lambda_i^h - \beta_i^h R_i^{h*} M_i^{h*} - \mu_i^b R_i^{h*}, \\
0 &= (1-\pi_i)\beta_i^h R_i^{h*} M_i^{h*} - \alpha_i^m R_i^{m*}, \\
0 &= N_i^m \alpha_i^m R_i^{m*} - \mu_i^m M_i^{h*} + \sum_{i\neq j=1}^{n} \beta_{ij}^v M_j^{h*} - \sum_{i\neq j=1}^{n} \beta_{ji}^h M_i^{h*}, \\
0 &= \pi_i \beta_i^h R_i^{h*} M_i^{h*} - \left[\alpha_i^h + \mu_i^h\right] G_i^{h*}, \\
0 &= \Lambda_i^v - \left[\alpha_i^g + \mu_i^g\right] G_i^{v*} + \sum_{i\neq j=1}^{m} \beta_{ij}^h G_j^{v*} - \sum_{i\neq j=1}^{m} \beta_{ji}^v G_i^{v*}, \\
0 &= N_i^g \alpha_i^g G_i^{v*} - \left[\alpha_i^s + \mu_i^s\right] G_i^{m*}, \\
0 &= \frac{1}{2}\alpha_i^s G_i^{m*} - \left[\alpha_i^z + \mu_i^z\right] Z_i^{v*}, \\
0 &= \alpha_i^z Z_i^{v*} - \left[\alpha_i^k + \mu_i^k\right] O_i^{v*}, \\
0 &= N_i^k \alpha_i^k O_i^{v*} - \left[\alpha_i^v + \mu_i^v\right] P_i^{v*}, \; i = 1, ..., n
\end{aligned} \tag{5.4.2}$$

where

$$\beta_{ij} = \beta\left(1 - \delta_{ij}\right) e^{-\alpha|i-j|},$$

$$
\begin{cases}
R_i^{h*} = \dfrac{\Lambda_i^h}{\left[\beta_i^h M_i^{h*} + \mu_i^b\right]} \\
R_i^{m*} = \dfrac{(1-\pi_i)\beta_i^h R_i^{h*} M_i^{h*}}{\alpha_i^m} \\
M_i^{h*} = \dfrac{\sum_{i\neq j=1}^{n} \beta_{ij}^v M_j^{h*}}{\left[\sum_{i\neq j=1}^{n} \beta_{ji}^h + \mu_i^m - N_i^m(1-\pi_i)\beta_i^h R_i^{h*}\right]} \\
M_j^{h*} = \dfrac{\sum_{i=1,i\neq j}^{n} \beta_{ji}^h M_i^h + \mu_i^m M_i^h - N_i^m \alpha_i^m R_i^m}{\sum_{i=1,i\neq j}^{n} \beta_{ij}^v} \\
G_i^{h*} = \dfrac{\pi_i \beta_i^h R_i^{h*} M_i^{h*}}{\left[\alpha_i^h + \mu_i^h\right]} \\
G_i^{v*} = \dfrac{\Lambda_i^v + \sum_{i\neq j=1}^{m} \beta_{ij}^h G_j^{v*}}{\left[\alpha_i^g + \mu_i^g + \sum_{i\neq j=1}^{m} \beta_{ji}^v\right]} \\
G^{m*} = \dfrac{N_i^g \alpha_i^g G_i^{v*}}{\left[\alpha_i^s + \mu_i^s\right]} \\
Z^{v*} = \dfrac{\alpha_i^s G_i^{m*}}{2\left[\alpha_i^z + \mu_i^z\right]} \\
O^{v*} = \dfrac{\alpha_i^z Z_i^{v*}}{\left[\alpha_i^k + \mu_i^k\right]} \\
P^{v*} = \dfrac{N_i^k \alpha_i^k O_i^{v*}}{\left[\alpha_i^v + \mu_i^v\right]}
\end{cases}
\tag{5.4.3}
$$

We represent the endemic equilibrium by $E^* = \left(R_i^{h*}, R_i^{m*}, M_i^{h*}, G_i^{h*}, G_i^{v*}, G_i^{m*}, Z_i^{v*}, O_i^{v*}, P_i^{v*}\right)$. The endemic value of susceptible erythrocytes is represented by

$$
R_i^{h*} = \frac{\Lambda_i^h}{\left[\beta_i^h M_i^{h*} + \mu_i^b\right]} \tag{5.4.4}
$$

We deduce from equation (5.4.4) the endemic value of the susceptible erythrocytes corresponds to the average period spent in the susceptible compartment and the supply rate of new susceptible red blood cells from the bone marrow. The susceptible red blood cells leaves this compartment either through death or infection. The endemic value of merozoite infected erythrocytes is represented by

$$R_i^{m*} = \frac{(1-\pi_i)\beta_i^h R_i^{h*} M_i^{h*}}{\alpha_i^m} \tag{5.4.5}$$

We deduce from equation (5.4.5) the endemic value of the merozoite infected erythrocytes is in proportion to the number of merozoites produced upon erythrocytes bursting and the bursting rate of erythrocytes to produce merozoites. The endemic value of merozoites in the blood stream is given by:

$$M_i^{h*} = \frac{\sum_{i\neq j=1}^{n} \beta_{ij}^v M_j^{h*}}{\left[\sum_{i\neq j=1}^{n} \beta_{ji}^h + \mu_i^m - N_i^m(1-\pi_i)\beta_i^h R_i^{h*}\right]} \tag{5.4.6}$$

We deduce from equation (5.4.6) the endemic value of the merozoites in the blood stream corresponds to the mean life-span of each merozoite, number of merozoites produced upon bursting of erythrocytes and the rate of intrinsic growth of merozoites due to infected mosquitoes in contact with the i^{th} individual. The endemic value of gametocyte infected erythrocytes within the individual human is given by

$$G_i^{h*} = \frac{\pi_i \beta_i^h R_i^{h*} M_i^{h*}}{\left[\alpha_i^h + \mu_i^h\right]} \tag{5.4.7}$$

We deduce from equation (5.4.7) the endemic value of the gametocyte infected erythrocytes within the humans is proportional to the rate at which gametocytes inside erythrocytes mature and become contagious to mosquitoes and the mean life-span of each gametocyte infected erythrocyte. The endemic value of the erythrocytes infected by gametocyte within the mosquito is given by

$$G_i^{v*} = \frac{\Lambda_i^v + \sum_{i\neq j=1}^{m} \beta_{ij}^h G_j^{v*}(t)}{\left[\alpha_i^g + \mu_i^g + \sum_{i\neq j=1}^{m} \beta_{ji}^v\right]} \tag{5.4.8}$$

We deduce from equation (5.4.8) the endemic value of the gametocyte infected erythrocytes inside the mosquito is proportional to the bursting rate of gametocyte infected erythrocytes to produce gametes, the life-span of erythrocytes infected by gametocytes inside the mosquito and super-infection rate of the mosquito. The endemic value of the population of gametes is given by

$$G^{m*} = \frac{N_i^g \alpha_i^g G_i^{v*}}{\left[\alpha_i^s + \mu_i^s\right]} \tag{5.4.9}$$

We deduce from equation (5.4.9) the endemic value of the population of gametes corresponds to the growth rate of gametes within an infected mosquito, to mean life-span of the gametes and rate of fusion of male and female gametes to form zygotes. The endemic value of the population of zygotes is given by

$$Z^{v*} = \frac{\alpha_i^s G_i^{m*}}{2\left[\alpha_i^z + \mu_i^z\right]} \tag{5.4.10}$$

We deduce from equation (5.4.10) the endemic value of the zygote population corresponds to the mean

life-span of zygotes and rate at which ookinetes become oocysts. The endemic value of the population of oocysts is given by

$$O^{v*} = \frac{\alpha_i^z Z_i^{v*}}{\left[\alpha_i^k + \mu_i^k\right]} \tag{5.4.11}$$

We deduce from equation (5.4.11) the endemic value of the population of oocysts corresponds to the mean life-span of oocysts and bursting rate of oocysts releasing sporozoites. The endemic value of the population of sporozoites is represented by

$$P^{v*} = \frac{N_i^k \alpha_i^k O_i^{v*}}{\left[\alpha_i^v + \mu_i^v\right]} \tag{5.4.12}$$

We deduce from equation (5.4.12) the endemic value of the sporozoite population is in proportion to the average number of sporozoites released upon bursting of oocysts, to the average life-span of sporozoites, to the rate of excretion of mature sporozoites into the salivary glands of the mosquito and the rate of intrinsic growth of pathogen due to infected individuals in contact with the vector (mosquito). We now look at the conditions at which the endemic state exists.

5.4.2 Existence of the Endemic Equilibrium State

We present results relating to existence of an endemic state for Malaria as conditions on a solution for the multiscale model system (5.2.1). In order to achieve this we implement the reproductive number, $\mathcal{R}_0$.

Theorem 5.6. *The multiscale model system (5.2.1) has a unique endemic equilibrium solution given by*

$$E^* = \left(R_i^{h*}, R_i^{m*}, M_i^{h*}, G_i^{h*}, G_i^{v*}, G_i^{m*}, Z_i^{v*}, O_i^{v*}, P_i^{v*}\right), i = 1, .., n \tag{5.4.1}$$

with $R_i^{h*}, R_i^{m*}, M_i^{h*}, G_i^{h*}, G_i^{v*}, G_i^{m*}, Z_i^{v*}, O_i^{v*}, P_i^{v*}$ all non-negative, whose existence and properties are determined by the threshold parameter $\mathcal{R}_0$ where

$$\mathcal{R}_{0i} = \frac{\left(1-\pi_i\right)\beta_i^h \Lambda_i N_i^m + \mu_i^b \left(\sum_{i\neq j=1}^n \beta_{ij}^v - \sum_{i\neq j=1}^n \beta_{ji}^h\right)}{\mu_i^b \mu_i^m}, \; i = 1, 2, ..., n \tag{5.4.2}$$

Proof. Let $E^* = \left(R_i^{h*}, R_i^{m*}, M_i^{h*}, G_i^{h*}, G_i^{v*}, G_i^{m*}, Z_i^{v*}, O_i^{v*}, P_i^{v*}\right)$ be a constant solution of the multiscale model system (5.2.1). We can simply present $R_i^{h*}, R_i^{m*}, G_i^{h*}$ in terms of M_i^{h*} in the form

$$\begin{cases} R_i^{h*}(M_i^{h*}) = \dfrac{\Lambda_i^h}{\left[\beta_i^h M_i^{h*} + \mu_i^b\right]} \\ R_i^{m*}(M_i^{h*}) = \dfrac{(1-\pi_i)\beta_i^h M_i^{h*}\Lambda_i^h}{\alpha_i^m\left[\beta_i^h M_i^{h*} + \mu_i^b\right]} \\ G_i^{h*}(M_i^{h*}) = \dfrac{\pi_i\beta_i^h\Lambda_i^h M_i^{h*}}{\left[\beta_i^h M_i^{h*} + \mu_i^b\right]\left[\alpha_i^h + \mu_i^h\right]} \end{cases} \tag{5.4.3}$$

Substituting the expressions in equation (5.4.3) into equation (3) from the multiscale model (5.2.1) given by

$$\frac{dM_i^h(t)}{dt} = N_i^m\alpha_i^m R_i^m(t) - \mu_i^m M_i^h(t) + \sum_{i\neq j=1}^{n}\beta_{ij}^v M_j^h(t) - \sum_{i\neq j=1}^{n}\beta_{ji}^h M_i^h(t) \tag{5.4.4}$$

at the endemic equilibrium we get

$$\left[\sum_{i\neq j}^{n}\beta_{ij}^v - \sum_{i\neq j=1}^{n}\beta_{ji}^h - \mu_i^m\right]\beta_i^h M_i^{h*2} + \mu_i^m\mu_i^h\left[\frac{N_i^h(1-\pi_i)\beta_i^h\Lambda_i^h + \mu_i^h\left(\sum_{i\neq j=1}^{n}\beta_{ij}^v - \sum_{i\neq j=1}^{n}\beta_{ji}^h\right)}{\mu_i^n\mu_i^h} - 1\right]M_i^{h*} = 0 \tag{5.4.5}$$

$M_i^{h*} = 0$ coincides with the disease free equilibrium.

$$\left[\sum_{i\neq j}^{n}\beta_{ij}^v - \sum_{i\neq j=1}^{n}\beta_{ji}^h - \mu_i^m\right]\beta_i^h M_i^{h*} + \mu_i^m\mu_i^h\left[\mathcal{R}_{0i} - 1\right] = 0 \tag{5.4.6}$$

Therefore at the endemic equilibrium for each individual i we obtain:

$$M_i^{*h} = \frac{\mu_i^m\mu_i^b\left[\mathcal{R}_{0i} - 1\right]}{\left(\mu_i^m - \left(\sum_{i\neq j}^{n}\beta_{ij}^v - \sum_{i\neq j=1}^{n}\beta_{ji}^h\right)\right)\beta_i^h} \tag{5.4.7}$$

From the expression (5.4.7) we can deduce that there exists one unique endemic equilibrium for multiscale model system (5.2.1) whenever $\mathcal{R}_0 > 1$ and $\sum_{i\neq j}^{n}\beta_{ij}^v < \mu_i^m + \sum_{i\neq j=1}^{n}\beta_{ji}^h$. □

5.4.3 Local Stability of the Malaria Endemic Equilibrium

We now establish the local asymptotic stability of the multiscale model system (5.2.1) by implementing the Center Manifold Theory explained in [101]. In order to effectively manipulate the Center Manifold Theory, we change variables of the multiscale model system (5.2.1) as follows. Let $R_i^h = x_1$, $R_i^m = x_2$,

$M_i^h = x_3$, $G_i^h = x_4$, $G_i^v = x_5$, $G_i^m = x_6$, $Z_i^v = x_7$, $O_i^v = x_8$ and $P_i^v = x_9$. In addition, we also implement the vector notation

$\mathbf{x} = (x_1, x_2, x_3, x_4, x_5, x_6, x_7, x_8, x_9)^T$ resulting in the multiscale model system (5.2.1) being written as

$$\frac{d\mathbf{x}}{dt} = \mathbf{F}(\mathbf{x}, \beta^*) \tag{5.4.1}$$

where

$$\mathbf{F} = (f_1, f_2, f_3, f_4, f_5, f_6, f_7, f_8, f_9) \tag{5.4.2}$$

such that

$$\begin{aligned}
1.\frac{dx_1(t)}{dt} &= \Lambda_i^h - \beta_i^h x_1(t)x_3(t) - \mu_i^b x_1(t),\\
2.\frac{dx_2(t)}{dt} &= (1-\pi_i)\beta_i^h x_1(t)x_3(t) - \alpha_i^m x_2(t),\\
3.\frac{dx_3(t)}{dt} &= N_i^m \alpha_i^m x_2(t) - \mu_i^m x_3(t) + \sum_{i\neq j=1}^{n} \beta_{ij}^v x_3(t) - \sum_{i\neq j=1}^{n} \beta_{ji}^h x_3(t),\\
4.\frac{x_4(t)}{dt} &= \pi_i \beta_i^h x_1(t)x_3(t) - \left[\alpha_i^h + \mu_i^h\right] x_4(t),\\
5.\frac{dx_5(t)}{dt} &= \Lambda_i^v - \left[\alpha_i^g + \mu_i^g\right] x_5(t) + \sum_{i\neq j=1}^{n} \beta_{ij}^h x_5(t) - \sum_{i\neq j=1}^{n} \beta_{ji}^v x_5(t),\\
6.\frac{dx_6(t)}{dt} &= N_i^g \alpha_i^g x_5(t) - \left[\alpha_i^s + \mu_i^s\right] x_6(t),\\
7.\frac{dx_7(t)}{dt} &= \frac{1}{2}\alpha_i^s x_6(t) - \left[\alpha_i^z + \mu_i^z\right] x_7(t),\\
8.\frac{dx_8(t)}{dt} &= \alpha_i^z x_7(t) - \left[\alpha_i^k + \mu_i^k\right] x_8(t),\\
9.\frac{dx_9(t)}{dt} &= N_i^k \alpha_i^k x_8(t) - \left[\alpha_i^v + \mu_i^v\right] x_9(t),\ i = 1, 2, ..., n
\end{aligned} \tag{5.4.3}$$

where

$$\beta_{ij} = \beta\,(1-\delta_{ij})\,e^{-\alpha|i-j|},$$

The approach encompasses calculating the Jacobian matrix of the multiscale system (5.4.3) at the disease-free equilibrium E_0 signified by $J(E_0)$. The matrix corresponding to the multiscale system (5.4.3) evaluated at the disease-free equilibrium is denoted by

$$J(E^0) = \begin{bmatrix} a_0 & 0 & -a_1 & 0 & 0 & 0 & 0 & 0 & 0 \\ 0 & -\alpha_i^m & a_2 & 0 & 0 & 0 & 0 & 0 & 0 \\ 0 & a_3 & a_4 & 0 & 0 & 0 & 0 & 0 & 0 \\ 0 & 0 & a_5 & -a_6 & 0 & 0 & 0 & 0 & 0 \\ 0 & 0 & 0 & 0 & -a_7 & 0 & 0 & 0 & 0 \\ 0 & 0 & 0 & 0 & a_8 & -a_9 & 0 & 0 & 0 \\ 0 & 0 & 0 & 0 & 0 & -\frac{1}{2}\alpha_i^s & -a_{10} & 0 & 0 \\ 0 & 0 & 0 & 0 & 0 & 0 & \alpha_i^z & -a_{11} & 0 \\ 0 & 0 & 0 & 0 & 0 & 0 & 0 & 0 & a_{12} \end{bmatrix} \tag{5.4.4}$$

$$
\begin{cases}
a_0 = -\mu_i^b \\
a_1 = \dfrac{\beta_i^* \Lambda_i^h}{\mu_i^b} \\
a_2 = (1-\pi_i)\dfrac{\beta_i^* \Lambda_i^h}{\mu_i^b} \\
a_3 = N_i^m \alpha_i^m \\
a_4 = \displaystyle\sum_{i\neq j}^{n} \beta_{ij}^v - \sum_{i\neq j}^{n} \beta_{ji}^h - \mu_i^m \\
a_5 = \pi_i \dfrac{\beta_i^* \Lambda_i^h}{\mu_i^b} \\
a_6 = \left[\alpha_i^h + \mu_i^h\right] \\
a_7 = [\alpha_i^g + \mu_i^g] + \displaystyle\sum_{i\neq j}^{n} \beta_{ij}^v - \sum_{i\neq j}^{n} \beta_{ji}^h \\
a_8 = N_i^g \alpha_i^g \\
a_9 = [\alpha_i^s + \mu_i^s] \\
a_{10} = [\alpha_i^z + \mu_i^z] \\
a_{11} = \left[\alpha_i^k + \mu_i^k\right] \\
a_{12} = -[\alpha_i^v + \mu_i^v]
\end{cases}
\tag{5.4.5}
$$

By making the use of an approach similar to the one in section (5.3.2), we can obtain the basic reproductive number of the multiscale system (5.4.3) as

$$
\mathcal{R}_{0i} = \frac{(1-\pi_i)\,\beta_i^h \Lambda_i N_i^m + \mu_i^b \left(\sum_{i\neq j=1}^{n} \beta_{ij}^v - \sum_{i\neq j=1}^{n} \beta_{ji}^h\right)}{\mu_i^b \mu_i^m},\ i = 1, 2, ..., n \tag{5.4.6}
$$

Let us consider $\beta_i^h = k\beta_{ij}^v$, even if $k \in (0,1)$ or $k \geq 1$. Taking $\beta_{ij}^v = \beta^*$ as the parameter of bifurcation and also letting $\mathcal{R}_{0i} = 1$, we determine β^* to get

$$\beta^* = \frac{\mu_i^b \left[\mu_i^m + \sum_{i=1, i\neq j}^{n} \beta_{ji}^h\right]}{\left[(1-\pi_i)k\Lambda_i^h N_i^m + \mu_i^b.n\right]} \tag{5.4.7}$$

We can highlight that the linearized system of the transformed equations (5.4.3) with bifurcation point β^* has a simple zero eigenvalue. Consequently, the center manifold theory [101] can be utilized to examine the dynamics of the multiscale system (5.4.3) close to $\beta_{ij}^v = \beta^*$.

To implement Theorem 7.2, the following calculations are neccessary (note that β^* is the bifurcation parameter instead of ϕ in Theorem 7.2).

When $\mathcal{R}_0 = 1$, we can demonstrate that the Jacobian matrix of the multiscale system (5.4.3) at β^* (denoted by J_{β^*}) has a right eigenvector corresponding to the zero eigenvalue expressed below:

$$\begin{bmatrix} a_0 & 0 & -a_1 & 0 & 0 & 0 & 0 & 0 & 0 \\ 0 & -\alpha_i^m & a_2 & 0 & 0 & 0 & 0 & 0 & 0 \\ 0 & a_3 & a_4 & 0 & 0 & 0 & 0 & 0 & 0 \\ 0 & 0 & a_5 & -a_6 & 0 & 0 & 0 & 0 & 0 \\ 0 & 0 & 0 & 0 & -a_7 & 0 & 0 & 0 & 0 \\ 0 & 0 & 0 & 0 & a_8 & -a_9 & 0 & 0 & 0 \\ 0 & 0 & 0 & 0 & 0 & -\frac{1}{2}\alpha_i^s & -a_{10} & 0 & 0 \\ 0 & 0 & 0 & 0 & 0 & 0 & \alpha_i^z & -a_{11} & 0 \\ 0 & 0 & 0 & 0 & 0 & 0 & 0 & 0 & a_{12} \end{bmatrix} \begin{bmatrix} u_1 \\ u_2 \\ u_3 \\ u_4 \\ u_5 \\ u_6 \\ u_7 \\ u_8 \\ u_9 \end{bmatrix} = \begin{bmatrix} 0 \\ 0 \\ 0 \\ 0 \\ 0 \\ 0 \\ 0 \\ 0 \\ 0 \end{bmatrix} \tag{5.4.8}$$

$$\mathbf{u} = (u_1, u_2, u_3, u_4, u_5, u_6, u_7, u_8, u_9)^T \tag{5.4.9}$$

where

$$\begin{cases} u_1 = -\dfrac{k\beta^*\Lambda_i^h}{\mu_i^{b2}} \\ u_2 = 1 \\ u_3 = 1 \\ u_4 = \dfrac{\pi_i k\beta^*\Lambda_i^h}{\mu_i^b\left[\alpha_i^h + \mu_i^h\right]} \\ u_5 = 0 \\ u_6 = 0 \\ u_7 = 0 \\ u_8 = 0 \\ u_9 = 0 \end{cases} \tag{5.4.10}$$

Furthermore, the left eigenvector of the jacobian matrix in (5.4.4) corresponding to the zero eigenvalue at β^* and satisfying the condition $\mathbf{v.u} = 1$ is written as:

$$\begin{bmatrix} v_1 & v_2 & v_3 & v_4 & v_5 & v_6 & v_7 & v_8 & v_9 \end{bmatrix} \begin{bmatrix} a_0 & 0 & -a_1 & 0 & 0 & 0 & 0 & 0 & 0 \\ 0 & -\alpha_i^m & a_2 & 0 & 0 & 0 & 0 & 0 & 0 \\ 0 & a_3 & a_4 & 0 & 0 & 0 & 0 & 0 & 0 \\ 0 & 0 & a_5 & -a_6 & 0 & 0 & 0 & 0 & 0 \\ 0 & 0 & 0 & 0 & -a_7 & 0 & 0 & 0 & 0 \\ 0 & 0 & 0 & 0 & a_8 & -a_9 & 0 & 0 & 0 \\ 0 & 0 & 0 & 0 & 0 & -\frac{1}{2}\alpha_i^s & -a_{10} & 0 & 0 \\ 0 & 0 & 0 & 0 & 0 & 0 & \alpha_i^z & -a_{11} & 0 \\ 0 & 0 & 0 & 0 & 0 & 0 & 0 & 0 & a_{12} \end{bmatrix} = \begin{bmatrix} 0 & 0 & 0 & 0 & 0 & 0 & 0 & 0 & 0 \end{bmatrix} \tag{5.4.11}$$

$$\mathbf{v} = (v_1, v_2, v_3, v_4, v_5, v_6, v_7, v_8, v_9)^T \tag{5.4.12}$$

where

$$\begin{cases} v_1 = 0, \\ v_2 = \dfrac{(1-\pi_i)\, k\beta_i^{*I}\Lambda_i^h N_i^m}{\left[(1-\pi_i)\, k\beta_i^*\Lambda_i^h N_i^m + \alpha_i^m \mu_i^b\right]}, \\ v_3 = \dfrac{\alpha_i^m \mu_i^b}{\left[(1-\pi_i)\, k\beta_i^*\Lambda_i^h N_i^m + \alpha_i^m \mu_i^b\right]} \\ v_4 = 0 \\ v_5 = 0 \\ v_6 = 0 \\ v_7 = 0 \\ v_8 = 0 \\ v_9 = 0 \end{cases} \tag{5.4.13}$$

We can verify the condition **v.u** $= 1$ as shown below:

$$\begin{cases} v.u = v_2.u_2 + v_3.u_3 \\ = \left(\dfrac{(1-\pi_i)\, k\beta_i^*\Lambda_i^h N_i^m}{\left[(1-\pi_i)\, k\beta_i^*\Lambda_i^h N_i^m + \alpha_i^m \mu_i^b\right]}\right).(1) + \left(\dfrac{\alpha_i^m \mu_i^b}{\left[(1-\pi_i)\, k\beta_i^*\Lambda_i^h N_i^m + \alpha_i^m \mu_i^b\right]}\right).(1) \\ = \dfrac{(1-\pi_i)\, k\beta_i^*\Lambda_i^h N_i^m + \alpha_i^m \mu_i^b}{\left[(1-\pi_i)\, k\beta_i^*\Lambda_i^h N_i^m + \alpha_i^m \mu_i^b\right]} = 1 \end{cases} \tag{5.4.14}$$

We now calculate the parameters of bifurcation a and b, by determining the value of the nonzero second-order mixed derivatives of **F** in regard to the variables and β^* to get the signs of a and b. The sign of a corresponds to, the following nonvanishing partial derivatives of **F**:

$$\begin{cases} \dfrac{\partial^2 f_1}{\partial x_1 \partial x_3} = -k\beta^* = \dfrac{\partial^2 f_1}{\partial x_3 \partial x_1} \\ \dfrac{\partial^2 f_2}{\partial x_1 \partial x_3} = (1-\pi_i)k\beta^* = \dfrac{\partial^2 f_2}{\partial x_3 \partial x_1} \\ \dfrac{\partial^2 f_4}{\partial x_1 \partial x_3} = \pi_i k\beta^* = \dfrac{\partial^2 f_4}{\partial x_3 \partial x_1} \end{cases} \tag{5.4.15}$$

$$\begin{cases} \dfrac{\partial^2 f_1}{\partial \beta^* \partial x_3} = -\dfrac{k\beta^* \Lambda_i^h}{\mu_i^b} \\ \dfrac{\partial^2 f_2}{\partial \beta^* \partial x_3} = (1-\pi_i)k\dfrac{\beta^* \Lambda_i^h}{\mu_i^b} \\ \dfrac{\partial^2 f_4}{\partial \beta^* \partial x_3} = \pi_i \dfrac{k\beta^* \Lambda_i^h}{\mu_i^b} \end{cases} \tag{5.4.16}$$

Substituting equation (5.4.10), (5.4.13) and (5.4.15) into the equation (7.4.6) we obtain:

$$\begin{cases} a = 2v_1 u_1 u_3 \dfrac{\partial^2 f_1}{\partial x_1 \partial x_3} + 2v_2 u_1 u_3 \dfrac{\partial^2 f_2}{\partial x_1 \partial x_3} + 2v_4 u_1 u_3 \dfrac{\partial^2 f_4}{\partial x_1 \partial x_3} \\ a = -2. \left(\dfrac{(1-\pi_i)\, k\beta_i^* \Lambda_i^h N_i^m}{\left[(1-\pi_i)\, k\beta_i^* \Lambda_i^h N_i^m + \alpha_i^m \mu_i^b\right]} \right) \left(\dfrac{k\beta^* \Lambda_i^h}{\mu_i^{b2}} \right) .(1-\pi_i)k\beta^* \\ a = -2. \left(\dfrac{(1-\pi_i)^2\, k^2 \beta_i^{*2} \Lambda_i^h N_i^m}{\left[(1-\pi_i)\, k\beta_i^* \Lambda_i^h N_i^m + \alpha_i^m \mu_i^b\right]} \right) \left(\dfrac{k\beta^* \Lambda_i^h}{\mu_i^{b2}} \right) < 0 \end{cases} \tag{5.4.17}$$

On the other hand, substituting equation (5.4.10), (5.4.13) and (5.4.16) into the equation (7.4.6) we obtain:

$$
\begin{cases}
b = u_1 v_3 \dfrac{\partial^2 f_1}{\partial \beta^* \partial x_3} + u_2 v_3 \dfrac{\partial^2 f_2}{\partial \beta^* \partial x_3} + u_4 v_3 \dfrac{\partial^2 f_4}{\partial \beta^* \partial x_3} \\
= \left(-\dfrac{k\beta^* \Lambda_i^h}{\mu_i^{b2}} \right) \cdot \left(\dfrac{\alpha_i^m \mu_i^b}{\left[(1-\pi_i)\, k\beta_i^* \Lambda_i^h N_i^m + \alpha_i^m \mu_i^b \right]} \right) \left(-k\beta^* \dfrac{\Lambda_i^h}{\mu_i^b} \right) \\
+ \left(\dfrac{\alpha_i^m \mu_i^b}{\left[(1-\pi_i)\, k\beta_i^* \Lambda_i^h N_i^m + \alpha_i^m \mu_i^b \right]} \right) . (1-\pi_i) \dfrac{k\beta^* \Lambda_i^h}{\mu_i^b} \\
+ \left[\dfrac{\pi_i \beta^* \Lambda_i^h}{\mu_i^b \left[\alpha_i^h + \mu_i^h \right]} \right] \cdot \left(\left(\dfrac{\alpha_i^m \mu_i^b}{\left[(1-\pi_i)\, k\beta_i^* \Lambda_i^h N_i^m + \alpha_i^m \mu_i^b \right]} \right) \right) . \dfrac{\pi_i k\beta^* \Lambda_i^h}{\mu_i^b} \\
b = \left[\left(\dfrac{\alpha_i^m \mu_i^b}{\left[(1-\pi_i)\, k\beta_i^* \Lambda_i^h N_i^m + \alpha_i^m \mu_i^b \right]} \right) \right] \left[\dfrac{\left(k\beta^* \Lambda_i^h \right)^2}{\left(\mu_i^b \right)^3} + (1-\pi_i) \dfrac{k\beta^* \Lambda_i^h}{\mu_i^b} + \dfrac{\left(\pi_i \beta^* \Lambda_i^h \right)^2}{\left(\mu_i^b \right)^2 \left[\alpha_i^h + \mu_i^h \right]} \right] > 0
\end{cases}
\tag{5.4.18}
$$

Consequently, $a < 0$ and $b > 0$. Implementing Theorem 7.2, item (iv), enables us to establish the following result which is only valid for $\mathcal{R}_0 > 1$ but near 1.

Proposition 5.7. *The unique endemic equilibrium of the multiscale models system (5.2.1) guaranteed by the Center Manifold Theorem 7.2 is locally asymptotically stable for $\mathcal{R}_0 > 1$ near 1.*

5.5 Numerical analysis

This section presents computer simulations for the multiscale model system (5.2.1)'s behaviour performed using Python program version 3.6 on the Windows 10 operation system. The numerical simulations of the multiscale model system (5.2.1) were carried out to explain some of the mathematical results that we obtained. We implemented the estimated parameter values presented in Table 5.1 for sensitivity and numerical analysis. A certain amount of the parameter values implemented in the simulations are results from publications and the others are estimates. The following are initial conditions implemented for these simulations: $R_i^h = \dfrac{\Lambda_i^h}{\mu_i^b}$, $R_i^m = 0$, $M_i^h = 0$, $G_i^h = 0$, $G_i^v = \dfrac{\Lambda_i^v}{\mu_i^g}$, $G_i^m = 0$, $Z_i^v = 0$, $O_i^v = 0$, $P_i^v = 0$ for each individual i.

5.5.1 Sensitivity Analysis

From the sensitivity analysis results of $\mathcal{R}_0$ to the multiscale model system (5.2.1)'s parameters in Figure 5.3, the following deductions are listed below:

Table 5.1: Within-human and within-Mosquito parameter values and their description for i^{th} individual

Parameter	Description	Initial value	Range explored	Units	Source/ Rational
α_i^g	Bursting rate of gametocyte infected erythrocytes	96	90-100	day^{-1}	[145]
Λ_i^h	Supply rate of susceptible erythrocytes	200	100-300	day^{-1}	[146]
μ_i^k	Natural decay rate of oocysts	0.01	0.071-0.143	day^{-1}	[147]
β_i^h	Infection rate of erythrocytes by free merozoites	0.1	2×10^{-9}- 0.2	day^{-1}	[148]; [149]
α_i^z	Rate at which zygotes develop into oocysts	0.4240	0.01-0.05	no.$^{-1}$day^{-1}	[150]
μ_i^b	Natural decay rate of susceptible erythrocytes	0.0083	0.006-0.01	day^{-1}	[149]
N_i^m	Number of merozoites produced per bursting erythrocyte	16	10-30	day^{-1}	[149]
α_i^s	Fertilization rate of gametes	0.08	0.01-0.2	no.$^{-1}$day^{-1}	[145]
μ_i^m	Natural decay rate of free merozoites	0.001	0.001-0.5	day^{-1}	[148]; [149]
μ_i^h	Natural decay rate of gametocyte infected erythrocytes within infected humans	0.0625	0.0600-0.0625	day^{-1}	[151]
π_i	Proportion of gametocyte infected erythrocytes	0.1	0.1-0.5	day^{-1}	Assumed
α_i^m	Bursting rate of erythrocytes to produce merozoites	0.5	0.1-1.0	day^{-1}	[141];[149]
α_i^h	Rate at which gametocytes develop and become infectious	0.02	0.01-0.9	day^{-1}	[151]
μ_i^g	Death rate of gametocytes	0.0625	0.0326-0.0725	day^{-1}	[145]
Λ_i^v	Rate of uptake of gametocytes through super infection of mosquto	300	100-300	day^{-1}	Variable
α_i^v	Rate at whch sporozoites become infectious to humans	0.025	0.167-1.00	no.$^{-1}$day^{-1}	[145]
μ_i^s	Natural decay rate of gametes	58.0	40-129	day^{-1}	[145]
μ_i^z	Natural decay rate of zygotes	1	1-4	day^{-1}	[145]
α_i^k	Bursting rate of oocysts to produce sporozoites	0.2	0-1.0	no.$^{-1}$day^{-1}	Variable
N_i^k	Number of sporozoites produced per bursting oocyst	3000	1000-10000	day^{-1}	[145]
N_i^g	Number of gametes produced per gametocyte infected erythrocyte	2	1-3	day^{-1}	Estimated
μ_i^v	Natural decay rate of sporozoites	0.0001	0.0001-0.01	day^{-1}	[145]

(a) The multiscale model system (5.2.1)'s parameters have both positive PRCCs and negative PRCCs. This implies that parameters with positive PRCCs will increase the value of $\mathcal{R}_0$ as they are increased, where as parameters with negative PRCCs will decrease the value for $\mathcal{R}_0$ as they are increased. For example, an increase in a parameter like infection rate of erythrocytes by free merozoites, β_{ji}^h transmission rate at the between-host will consequently increase the value of $\mathcal{R}_0$, and also increasing a parameter like the natural decay rate of free merozoites, μ^m will result in the reduction in the value of $\mathcal{R}_0$.

(b) The Malaria disease transmission metric $\mathcal{R}_0$ is extremely sensitive to four of the disease parameters of the multiscale model system (5.2.1), $(\Lambda_i^h, N_i^m, \mu_i^m, \beta_{ji}^h)$. We note that $\mathcal{R}_0$ characterizes transmission of Malaria disease at the beginning of the epidemic. We deduce the following from the sensitivity of $\mathcal{R}_0$ to the Malaria disease multiscale model system (5.2.1)'s parameters.

(i) Since $\mathcal{R}_0$ is significantly sensitive to $(\Lambda_i^h, N_i^m, \mu_i^m, \beta_{ji}^h)$, this implies that caution must be applied on the accuracy of these five Malaria disease multiscale model system (5.2.1)'s parameters during the collection of data if the effectiveness and usefulness of the Malaria disease multiscale model system (5.2.1) is to be intensified.

(ii) Since $\mathcal{R}_0$ is responsive to the transmission rate between the humans, β_{ji}^h (the between-host level parameter) this implies that Malaria interventions such as Insecticide-treated nets and indoor residual spraying would have more effect in preventing the transmission of Malaria disease infection at the beginning of the epidemic.

(iii) Since $\mathcal{R}_0$ is significantly sensitive to the rate of supply of susceptible red blood cells, Λ_i^h (the within-host level parameter) and number of merozoites produced per bursting erythrocyte, N_i^m this implies that Malaria disease interventions such as malaria vaccination (which stimulate

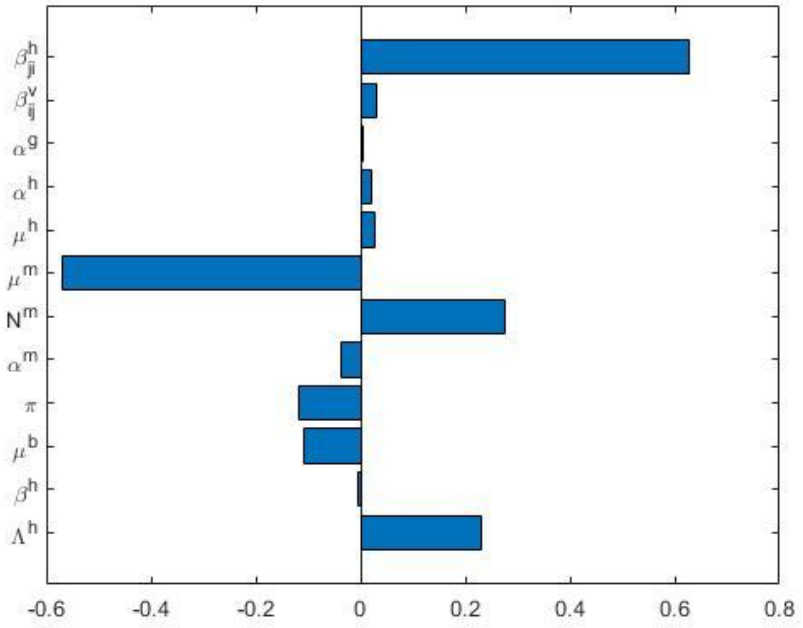

Figure 5.3: *Tornado plot of partial rank correlation coefficients (PRCCs) of the model parameters that influence the Malaria transmission indicator* $\mathcal{R}_0$

immune response to destroy malaria parasite) would be more effective to control the spread of Malaria disease infection at the beginning of the outbreak.

(iv) Since $\mathcal{R}_0$ is significantly sensitive to the rate of natural decay of free merozoites, μ_i^m this implies that Malaria disease interventions such as malaria vaccination (which stimulate immune response to destroy malaria parasite) would be more effective to control the spread of Malaria disease infection at the beginning of the outbreak.

5.5.2 Numerical simulations of the multiscale model of Malaria transmission dynamics

5.5.2.1 Influence of within-host scale parameters of the Malaria multiscale model dynamics

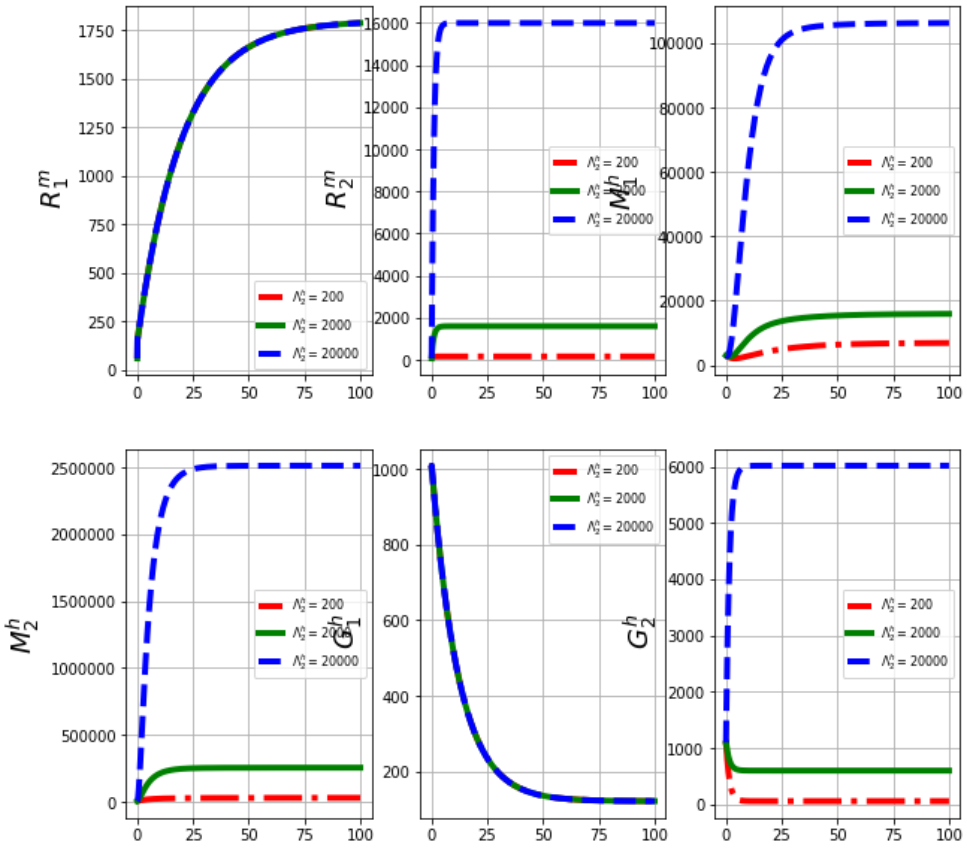

Figure 5.4: Graphs of numerical results of the model system (5.2.1) demonstrating the progression in time of (a) merozoite infected erythrocytes for individual 1, R_1^m, (b) merozoite infected erythrocytes for individual 2, R_2^m, (c) free merozoites in bloodstream for individual 1, M_1^h, (d) free merozoites in bloodstream for individual 2, M_2^h, (e) gametocyte infected erythrocytes for individual 1, G_1^h, (f) gametocyte infected erythrocytes for individual 2, G_2^h for variant values of supply rate of susceptible erythrocytes in individual 2, Λ_2^h : $\Lambda_2^h = 200, \Lambda_2^h = 2000$ and $\Lambda_2^h = 20000$.

Figure 5.4 represents the graphs of numerical results of the model system (5.2.1) demonstrating the progression in time of (a) merozoite infected erythrocytes for individual 1, R_1^m, (b) merozoite infected erythrocytes for individual 2, R_2^m, (c) free merozoites in bloodstream for individual 1, M_1^h, (d) free merozoites in bloodstream for individual 2, M_2^h, (e) gametocyte infected erythrocytes for individual 1, G_1^h, (f) gametocyte infected erythrocytes for individual 1, G_2^h for variant values of supply rate of susceptible erythrocytes in individual 2, Λ_2^h : $\Lambda_2^h = 200, \Lambda_2^h = 2000$ and $\Lambda_2^h = 20000$. From these results we can observe that as the supply rate of susceptible erythrocytes in individual 2 increases there is a remarkable increase in merozoite infected erythrocytes for individual 2, R_2^m, free merozoites in bloodstream for individual 1, M_1^h, free merozoites in bloodstream for individual 2, M_2^h, gametocyte infected erythrocytes for individual

2, G_2^h. This implies that interventions like the use of Insecticide-treated nets and indoor residual spraying will have more effect in preventing spread of the disease.

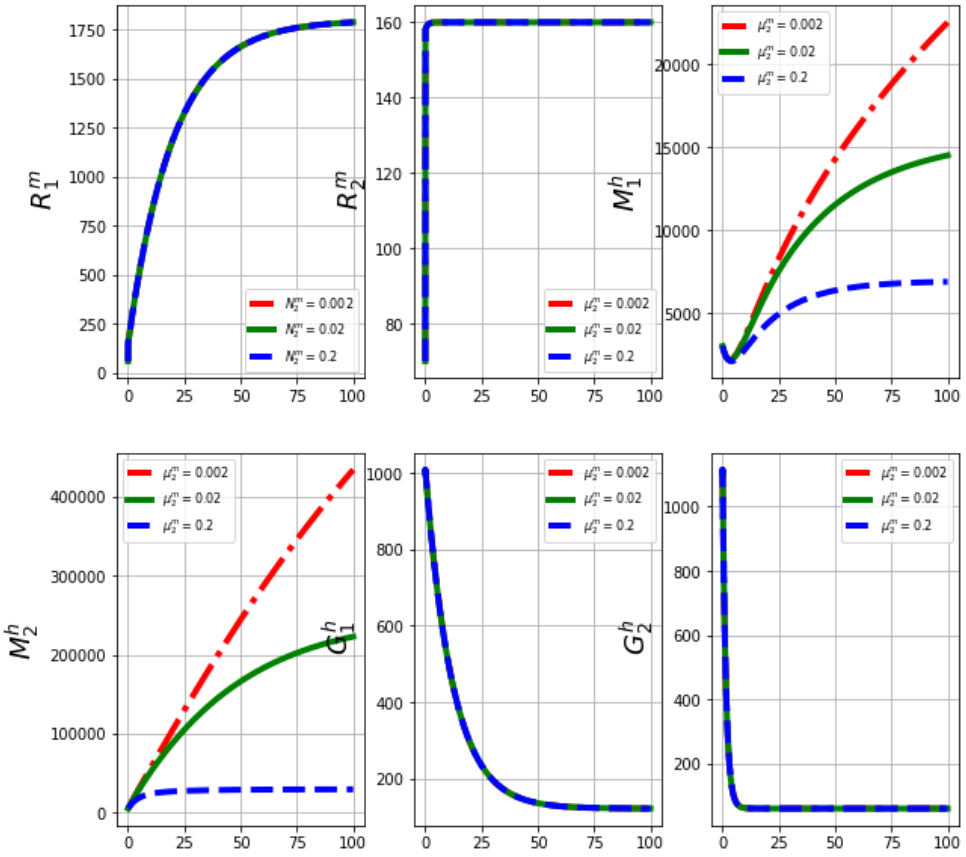

Figure 5.5: Graphs of numerical results of the model system (5.2.1) demonstrating the progression in time of (a) merozoite infected erythrocytes for individual 1, R_1^m, (b) merozoite infected erythrocytes for individual 2, R_2^m, (c) free merozoites in bloodstream for individual 1, M_1^h, (d) free merozoites in bloodstream for individual 2, M_2^h, (e) gametocyte infected erythrocytes for individual 1, G_1^h, (f) gametocyte infected erythrocytes for individual 1, G_2^h for variant values of natural decay rate of free merozoites for individual 2, $\mu_2^m : \mu_2^m = 0.002, \mu_2^m = 0.02$ and $\mu_2^m = 0.2$.

Figure (5.5) represents the graphs of numerical results of the model system (5.2.1) demonstrating the progression in time of (a) merozoite infected erythrocytes for individual 1, R_1^m, (b) merozoite infected erythrocytes for individual 2, R_2^m, (c) free merozoites in bloodstream for individual 1, M_1^h, (d) free merozoites in bloodstream for individual 2, M_2^h, (e) gametocyte infected erythrocytes for individual 1, G_1^h, (f) gametocyte infected erythrocytes for individual 1, G_2^h for variant values of natural decay rate of free merozoites for individual 2, $\mu_2^m : \mu_2^m = 0.002, \mu_2^m = 0.02$ and $\mu_2^m = 0.2$. From these results we can observe that as the natural decay rate of free merozoites for individual 2 increases there is a remarkable decrease in free merozoites in bloodstream for individual 1, M_1^h and free merozoites in bloodstream for individual 2, M_2^h.

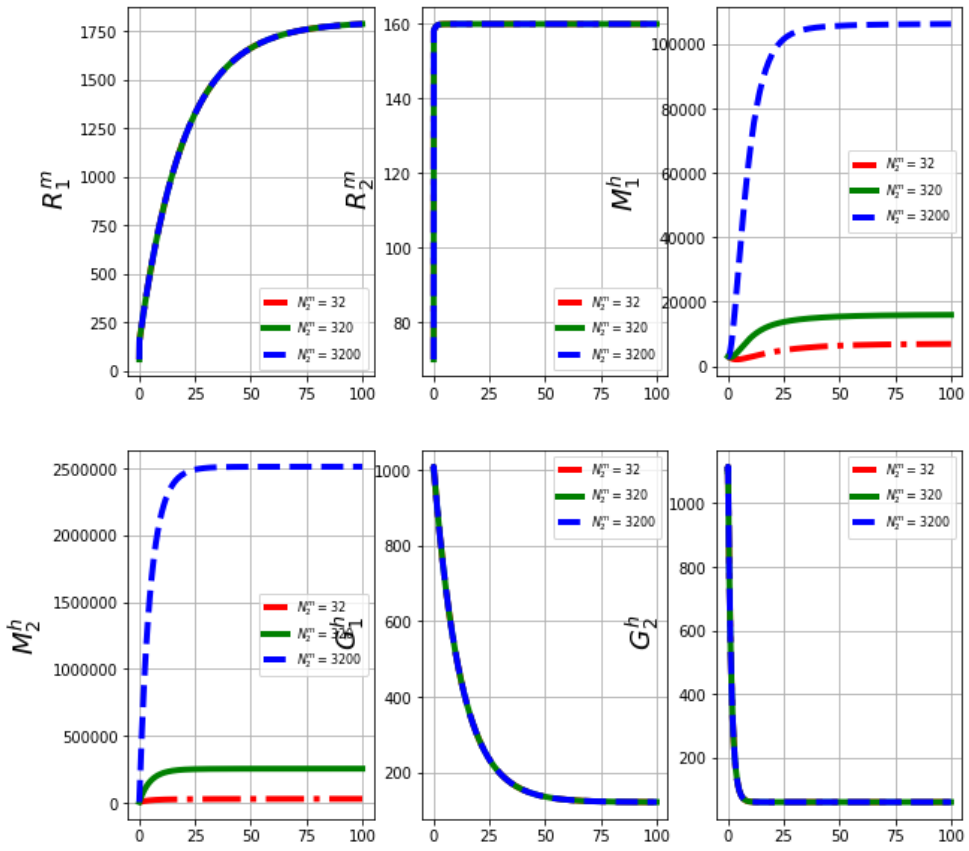

Figure 5.6: Graphs of numerical results of the model system (5.2.1) demonstrating the progression in time of (a) merozoite infected erythrocytes for individual 1, R_1^m, (b) merozoite infected erythrocytes for individual 2, R_2^m, (c) free merozoites in bloodstream for individual 1, M_1^h, (d) free merozoites in bloodstream for individual 2, M_2^h, (e) gametocyte infected erythrocytes for individual 1, G_1^h, (f) gametocyte infected erythrocytes for individual 1, G_2^h for variant values of number of merozoites produced per bursting erythrocyte, N_2^h : $N_2^h = 32, N_2^h = 320$ and $N_2^h = 3200$.

Figure (5.6) represents the graphs of numerical results of the model system (5.2.1) demonstrating the progression in time of (a) merozoite infected erythrocytes for individual 1, R_1^m, (b) merozoite infected erythrocytes for individual 2, R_2^m, (c) free merozoites in bloodstream for individual 1, M_1^h, (d) free merozoites in bloodstream for individual 2, M_2^h, (e) gametocyte infected erythrocytes for individual 1, G_1^h, (f) gametocyte infected erythrocytes for individual 1, G_2^h for variant values of number of merozoites produced per bursting erythrocyte, N_2^h : $N_2^h = 32, N_2^h = 320$ and $N_2^h = 3200$. From these results we can observe that as the number of merozoites produced per bursting erythrocyte increases there is a remarkable increase in free merozoites in bloodstream for individual 1, M_1^h and free merozoites in bloodstream for individual 2, M_2^h.

5.5.2.2 Influence of between-host scale parameters of the Malaria multiscale model dynamics

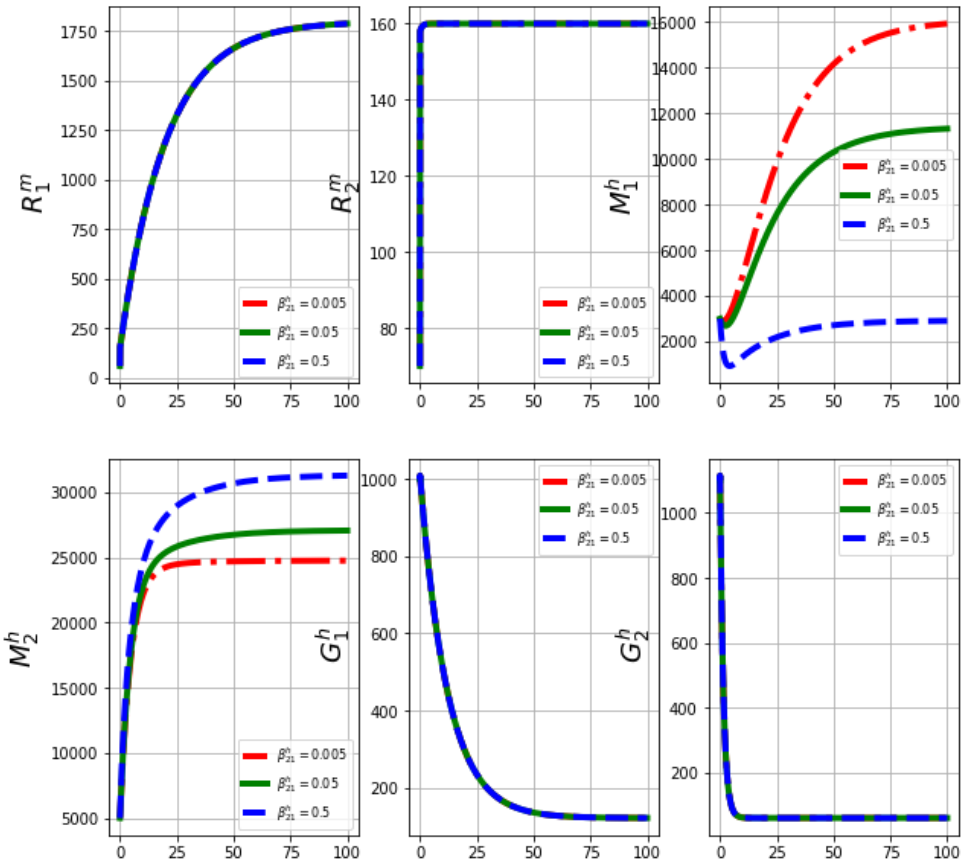

Figure 5.7: Graphs of numerical results of the model system (5.2.1) demonstrating the progression in time of (a) merozoite infected erythrocytes for individual 1, R_1^m, (b) merozoite infected erythrocytes for individual 2, R_2^m, (c) free merozoites in bloodstream for individual 1, M_1^h, (d) free merozoites in bloodstream for individual 2, M_2^h, (e) gametocyte infected erythrocytes for individual 1, G_1^h, (f) gametocyte infected erythrocytes for individual 1, G_2^h for variant values of infection rate of individual 2 by individual 1 through a mosquito vector, $\beta_{21}^h : \beta_{21}^h = 0.005, \beta_{21}^h = 0.05$ and $\beta_{21}^h = 0.5$.

Figure 5.7 represents the graphs of numerical results of the model system (5.2.1) demonstrating the progression in time of (a) merozoite infected erythrocytes for individual 1, R_1^m, (b) merozoite infected erythrocytes for individual 2, R_2^m, (c) free merozoites in bloodstream for individual 1, M_1^h, (d) free merozoites in bloodstream for individual 2, M_2^h, (e) gametocyte infected erythrocytes for individual 1, G_1^h, (f) gametocyte infected erythrocytes for individual 1, G_2^h for variant values of infection rate of individual 2 by individual 1 through a mosquito vector, $\beta_{21}^h : \beta_{21}^h = 0.005, \beta_{21}^h = 0.05$ and $\beta_{21}^h = 0.5$. From these results we can observe that as infection rate of individual 2 by individual 1 through a mosquito vector increases there is a remarkable increase in free merozoites in bloodstream for individual 2, M_2^h and a reduction in free merozoites in bloodstream for individual 1, M_1^h. This implies that interventions like the use of Insecticide-treated nets and indoor residual spraying will have more effect in preventing spread of the disease.

5.5.2.3 Network of human population

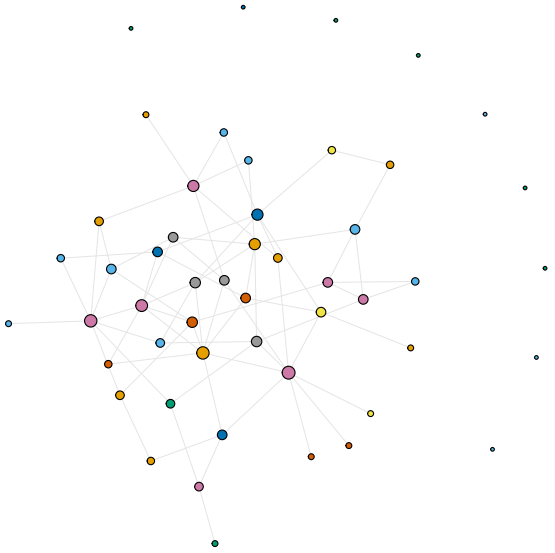

Figure 5.8: Network for the transmission dynamics of malaria through the mosquito vector within a human population.

The epidemic simulations were performed using R programming language as follows. (1) seed 10 random infected nodes; (2) find nodes that are connected through the mosquito vector to the individuals and calculate Bernoulli trials with the probabilities of success based on the viral load of the infected individual, document any new infected individuals if available, (3) proceed to the next step and repeat step 2 until no infected cases remain.

5.6 Effects of stochasticity on the model

In this section we introduce a white noise (dW_Q/dt) (i.e., W(t) is a Brownian motion), where $Q = \{1, 2, 3, 4\}$, into the multiscale model system (5.2.1) which becomes

$$
\begin{cases}
dR_i^h(t) = \left(\Lambda_i^h - \beta_i^h R_i^h(t) M_i^h(t) - \mu_i^b R_i^h(t)\right) dt + \sigma_1 R_i^h dW_1, \\
dR_i^m(t) = \left((1-\pi_i)\beta_i^h R_i^h(t) M_i^h(t) - \alpha_i^m R_i^m(t)\right) dt + \sigma_2 R_i^m dW_2, \\
dM_i^h(t) = \left(N_i^m \alpha_i^m R_i^m(t) - \mu_i^m M_i^h(t) + \sum_{i\neq j=1}^{n} \beta_{ij}^v M_j^h(t) - \sum_{i\neq j=1}^{n} \beta_{ji}^h M_i^h(t)\right) dt + \sigma_3 M_i^h dW_3, \\
dG_i^h(t) = \left(\pi_i \beta_i^h R_i^h(t) M_i^h(t) - \left[\alpha_i^h + \mu_i^h\right] G_i^h(t)\right) dt + \sigma_4 G_i^h dW_4, \\
dG_i^v(t) = \left(\Lambda_i^v - \left[\alpha_i^g + \mu_i^g\right] G_i^v(t) + \sum_{i\neq j=1}^{n} \beta_{ij}^h G_j^v(t) - \sum_{i\neq j=1}^{n} \beta_{ji}^v G_i^v(t)\right) dt, \\
dG_i^m(t) = \left(N_i^g \alpha_i^g G_i^v(t) - \left[\alpha_i^s + \mu_i^s\right] G_i^m(t)\right) dt, \\
dZ_i^v(t) = \left(\frac{1}{2}\alpha_i^s G_i^m(t) - \left[\alpha_i^z + \mu_i^z\right] Z_i^v(t)\right) dt, \\
dO_i^v(t) = \left(\alpha_i^z Z_i^v(t) - \left[\alpha_i^k + \mu_i^k\right] O_i^v(t)\right) dt, \\
dP_i^v(t) = \left(N_i^k \alpha_i^k O_i^v(t) - \left[\alpha_i^v + \mu_i^v\right] P_i^v(t)\right) dt
\end{cases}
\tag{5.6.1}
$$

We set $W(t) = W_1(t), W_2(t), W_3(t), W_4(t)$ an 4-dimensional Wiener process that is defined on this probability space. Further, the constants $\sigma_1, \sigma_2, \sigma_3, \sigma_4$ are non-negative and describe the intensities of the stochastic pertubations. Let us assume that the components of the 1-dimensional Wiener process W_i are mutually independent. It can be shown that the SDE model (5.6.1) has at least a unique global solution in order for the model to have meaning and also that the solution will always remain positive whenever the initial conditions are positive. Let us consider the following theorem.

Proposition 5.8. *For multiscale model system (5.6.1) and any initial value in $\mathbb{R}_+^{9n}$, there is a unique solution*
$L = \left(R_i^h, R_i^m, M_i^h, G_i^h, G_i^v, G_i^m, Z_i^v, O_i^v, P_i^v\right)_{i=1,\ldots,n}$ *of the multiscale SDE system (5.6.1) for $t \geq 0$ which will remain in $\mathbb{R}_+^{9n}$ with probability one.*

Figure 5.9 shows the randomness in (i) susceptible erythrocytes in humans, R_i^h, (ii) merozoite infected erythrocytes, R_i^m, (iii) free merozoites in bloodstream, M_i^h, (iv) gametocyte infected erythrocytes, G_i^h

for two individuals for a multiscale stochastic model system (5.6.1). Parameter values for diagram (a) are $\Lambda_1^h = 100$, $\beta_1^h = 0.01$, $\mu_1^b = 0.006$, $\pi_1 = 0.1$, $\alpha_1^m = 0.1$, $N_1^m = 10$, $\mu_1^m = 0.001$, $\beta_{12}^v = 0.01$, $\beta_{21}^h = 0.005$, $\alpha_1^h = 0.01$, $\mu_1^h = 0.06$. On the other hand, parameter values for diagram (b) are $\Lambda_2^h = 200$, $\beta_2^h = 0.1$, $\mu_2^b = 0.0083$, $\pi_2 = 0.3$, $\alpha_2^m = 0.5$, $N_2^m = 16$, $\mu_2^m = 0.01$, $\beta_{21}^v = 0.1$, $\beta_{12}^h = 0.05$, $\alpha_2^h = 0.02$, $\mu_2^h = 0.0625$. The numerical method used here to approximate the solutions of the stochastic model is the Milsten method.

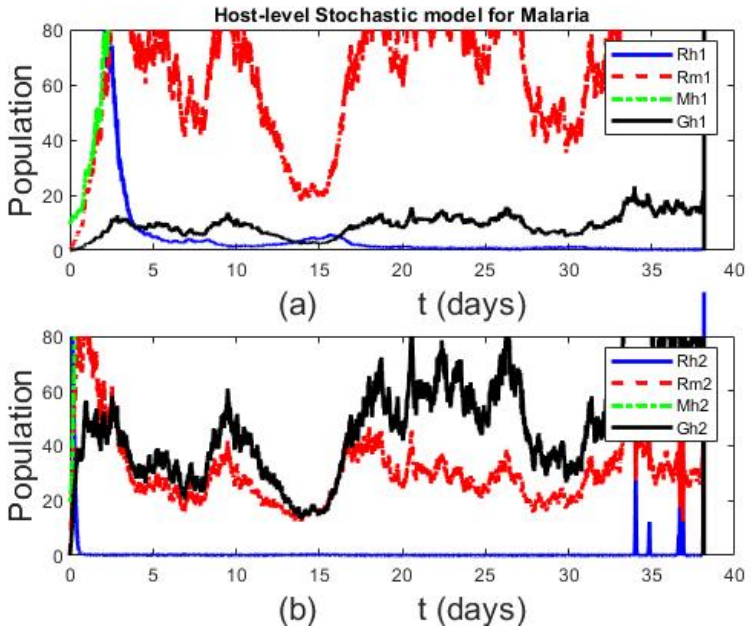

Figure 5.9: Graphs of numerical simulations of the multiscale stochastic model system (5.6.1) showing the evolution in time fortwo humans of (i) susceptible erythrocytes in humans, R_i^h, (ii) merozoite infected erythrocytes, R_i^m, (iii) free merozoites in bloodstream, M_i^h, (iv) gametocyte infected erythrocytes, G_i^h. Parameter values for diagram (a) are $\Lambda_1^h = 100$, $\beta_1^h = 0.01$, $\mu_1^b = 0.006$, $\pi_1 = 0.1$, $\alpha_1^m = 0.1$, $N_1^m = 10$, $\mu_1^m = 0.001$, $\beta_{12}^v = 0.01$, $\alpha_1^h = 0.01$, $\mu_1^h = 0.06$. On the other hand, parameter values for diagram (b) are $\Lambda_2^h = 200$, $\beta_2^h = 0.1$, $\mu_2^b = 0.0083$, $\pi_2 = 0.3$, $\alpha_2^m = 0.5$, $N_2^m = 16$, $\mu_2^m = 0.01$, $\beta_{21}^v = 0.1$, $\alpha_2^h = 0.02$, $\mu_2^h = 0.0625$.

Figure 5.10 shows the graphs of numerical solutions of the Susceptible Erythrocytes, R_1^h of the multiscale SDE model system (5.6.1) with the ODE multiscale model system (5.2.1) solutions. The solution for the stochastic multiscale model is obtained using the Milsten method.

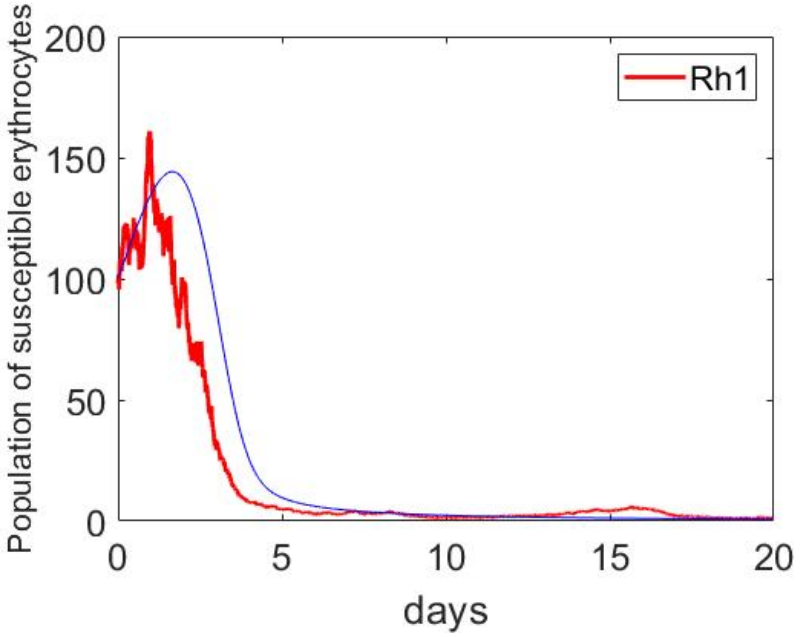

Figure 5.10: Graphs of numerical solutions of the Susceptible Erythrocytes, R_1^h of the multiscale SDE model system (5.6.1) with the ODE multiscale model system (5.2.1) solutions.

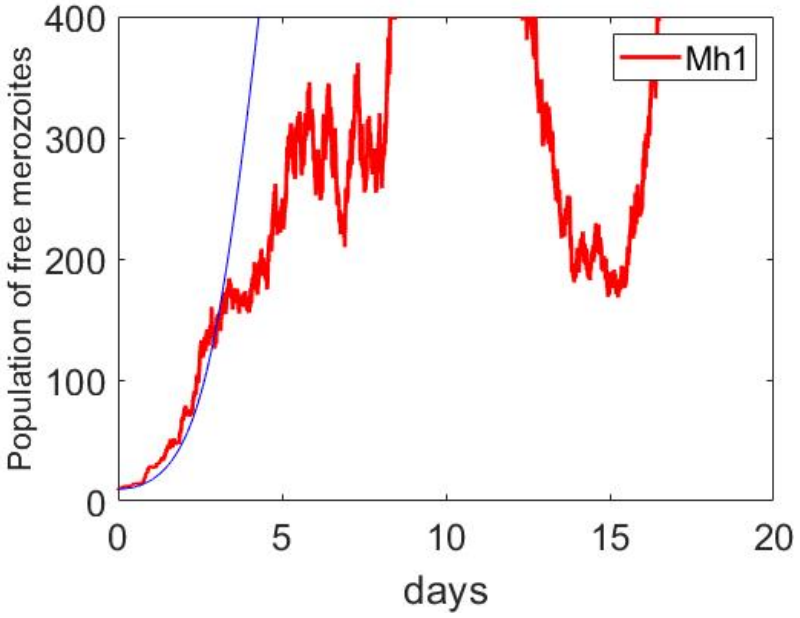

Figure 5.11: Graphs of numerical solutions of the Free Merozoites, M_1^h of the multiscale SDE model system (5.6.1) with the ODE multiscale model system (5.2.1) solutions.

Figure 5.11 shows the graphs of numerical solutions of the Free Merozoites, M_1^h of the multiscale SDE model system (5.6.1) with the ODE multiscale model system (5.2.1) solutions. The solution for the stochastic multiscale model is obtained using the Milsten method. Therefore, the SDE multiscale model system (5.6.1) would be suitable when taking randonmess into account.

5.7 Summary

In this chapter, we chacterised an individual-based network modelling multiscale model of Malaria at Whole organism -level. The mathematical model we developed consisted of the within-human malaria parasite dynamics and within-mosquito malaria parasite dynamics where the humans were connected by a spatial network of n individuals. The framework separated between-organ spread dynamics (inflow and outflow) and the within-organs infection dynamics (replication) for the whole transmission-replication loop. The model demonstrated the time progression of within infected mosquito host as well as within the infected human host. The populations in the infected human host included the erythrocytes infected by gametocytes G_i^h, free merozoites in blood M_i^h, susceptible erythrocytes R_i^h, erythrocytes infected by merozoites R_i^m. In addition, the populations in the infected mosquito include the sporozoites, P_i^v, gametes, G_i^m, infected erythrocytes, G_i^v, oocysts, O_i^v, zygotes. Z_i^v. Through mathematical analysis the model was determined to be epidemiologically and mathematically sound. The analysis of sensitivity of the Malaria indicator $\mathcal{R}_0$, in relation to the variation of Malaria model parameters was carried out by implementing Latin Hypercube Sampling (LHS) and Partial Rank Correlation Coefficients (PRCCs). The results from analysis of sensitivity of $\mathcal{R}_0$ indicated that variation of the between-organ scale parameters in particalar the transmission rate of Malaria parasite through blood, β_{ji}^h had significant effect on the transmission risk of Malaria in humans at whole organism-level and this is confirmed by the Tornado plot in Figure 5.3. Furthermore, Figure 5.4 - Figure 5.7 showed the impact in the variation of four parameters $(\Lambda_i^h, N_i^m, \mu_i^m, \beta_{ji}^h)$ on the variables $\left(R_i^h, R_i^m, M_i^h, G_i^h, G_i^v, G_i^m, Z_i^v, O_i^v, P_i^v\right)$. In addition, Figure 5.9-Figure 5.11 shows the graphs of the stochastic models in comparison to the ODE multiscale models.

In conclusion, we established that the individual-based network modelling multiscale model we developed cannot be extended to a higher level of organisation using graph-theoretic methods. Furthermore, we established that the global transmission of the Malaria parasite between organs can be represented by graph-theoretic methods. Finally, the model presented has a secondary level multiscale cycle with both local exchange and global exchange of pathogen.

Chapter 6

Community-level Multiscale modelling of Malaria disease

6.1 Introduction

In this chapter, we characterise a coupled modelling multiscale model of Malaria disease at community-level using graph-theoretic approach. The model is established applying the same approach that was implemented in chapter 4. In other words, we consider a whole organism scale model of Malaria and then extend the model to a community level model of Malaria using graph-theoretic approach. At community level, within the community there is direct transmission of Malaria disease when infected cells/tissues/hosts come into direct contact with susceptible cells/tissues/hosts or environmental transmission when the plasmodium parasite comes in contact with susceptible cells/tissues/hosts. This is local transmission that can be represented by ordinary differential equations. At between-community there is movement of infected individuals between communities. This movement is global transmission and can be represented using graph theoretic approach. This is a new aspect that is characterised in this chapter. We aim to characterise the spread of Malaria disease taking into account both the dynamics of Malaria disease at within-community scale (microscale) and the interactions (direct contact) between communities at between-community scale (macroscale).

We may consider within a community like a province where humans can infect each other via the mosquito vector. The SIR-type model is implemented to characterise the local transmission of the parasite. Suppose an infected individual travels to another province. This individual introduces the Malaria parasite to the new province. The process of transporting an infected individual to a new province characterizes the global transmission of the parasite at macrocommunity-level. The graph theoretic approach is useful

in modelling the global transmission of Malaria parasite. Most of the models rarely represent the local transmission and global transmission mechanisms of infectious disease systems together. The majority of the models available have modelled local transmission of infectious diseases based on the transmission mechanism theory involving systems of differential equations at single scale. However, this is not enough when modelling the entire infectious disease progression.

Current modelling frameworks established from compartmentalizing hosts into SIRS type models have been implemented to give insights of local transmission mechanisms or global transmission mechanisms of Malaria separately [5, 8, 26, 140–142]. Additionally, various mathematical models have been developed giving insights of transmission mechanisms of Malaria disease at single scale using graph theoretic methods however, to the best of my knowledge there is no model that addresses local transmission and global transmission mechanisms of pathogen at macrocommunity level using graph theoretic methods. The latest work that has been done which is more appropriate in modelling the progression of infectious disease systems based on replication-transmission relativity theory is the multiscale modelling appproach [1]. The multiscale modelling of global transmission mechanisms of infectious diseases is better achieved through the use of graph theoretic methods while the standard SIR models address the local transmission mechanisms. The mathematical framework we propose models the local transmission and global transmission mechanisms of Malaria. This enables us to characterise the transmission dynamics of Malaria within-community and between-community. In this study, the main ideas are centred on developing a multiscale modelling approach using graph theoretic methods at macrocommunity level. Nodes represent communities (patches) which could be geographical distant places and possible transmissions (transportation) are represented by edges. Furthermore, we seek to establish if this model can be extended to higher levels of organisation using graph-theoretic methods.

6.2 The Multiscale model for Malaria

The model we formulate is derived from submodels of Malaria disease from chapter 5 by applying the same approach that was implemented in chapter 3 and chapter 4. To formulate the multiscale model, assume that the environment under consideration is divided into n patches, which may be cities, geographic regions or communities. We assume that there is homogeneity within each patch. We partition the human population in patch i, into compartments of susceptible and infective individuals with the number in each compartment denoted by S_i^H and I_i^H, respectively, for $i = 1, ..., n$. Let the total number of individuals in patch i be represented by $N_i^H = S_i^H + I_i^H$. Presume that the rates of human migration between patches hinges on disease status, and that the infection status of individuals does not change during migration. The rate of migration of humans from patch j to patch i is represented by $\psi_{j,i}^S, \psi_{j,i}^I$ for susceptible and infective individuals, respectively, where $\psi_{i,i}^S = \psi_{i,i}^I = 0$. This structure illustrates a multi-digraph where nodes represent patches and the links represent the rates of migration, described by the nonnegative matrices $\Psi^S = [\psi_{j,i}^S]$ and $\Psi^I = [\psi_{j,i}^I]$. These matrices are presumed to be irreducible. Suppose that the natural

death rate is independent of disease status with $\mu_i^H > 0$ for susceptible and infected populations. Once infected, a susceptible individual (S_i^H) in patch i harbors Malaria parasite, develops clinical infection and progresses into the infectious compartment I_i^H as the individual can now spread the infection at the rate λ_i^V . Upon recovery, an individual moves to the susceptible compartment as disease immunity fades at a rate γ_i^H. The death rate induced by Malaria disease is denoted by δ_i^H. P_i^V is the community sporozoite load and G_i^H is the community gametocyte load.

Therefore the multiscale model we propose is as follows:

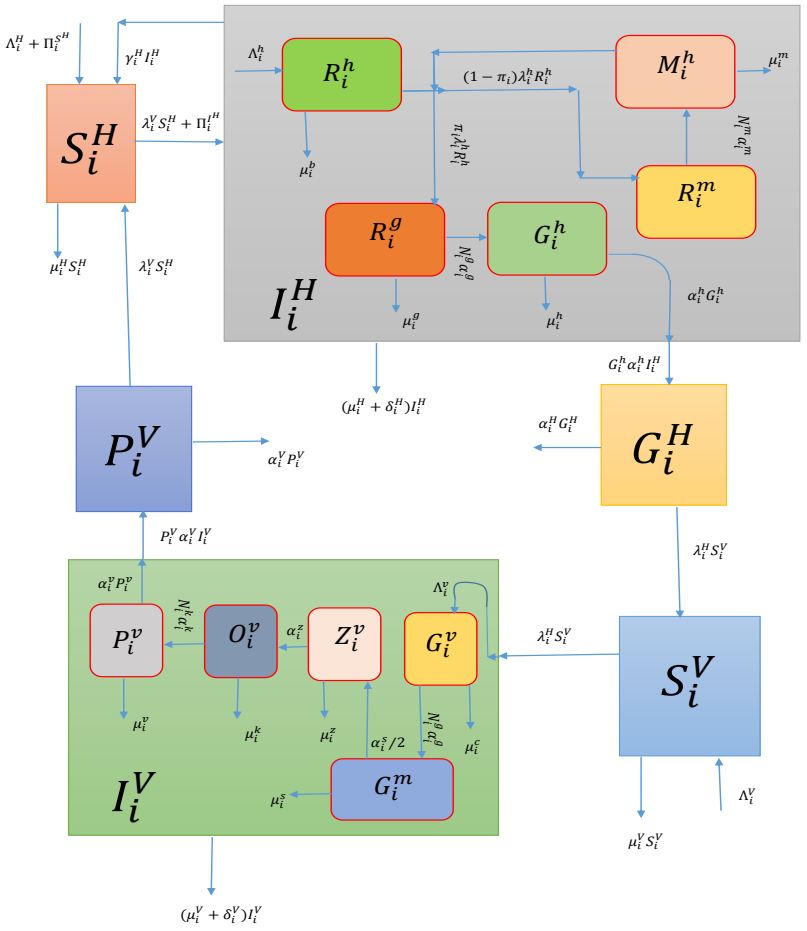

Figure 6.1: Schematic diagram of the community-level model for Malaria with human migration where $\Pi_i^Q = \sum_{j\neq i=1}^{n} \psi_{j,i}^Q Q_j - \sum_{j\neq i=1}^{n} \psi_{i,j}^Q Q_i$, represents movement between provinces, with $Q \in \{S_i^H, I_i^H\}$

$$
\begin{aligned}
\frac{dS_i^H(t)}{dt} &= \Lambda_i^H - \lambda_i^V(t)S_i^H(t) - \mu_i^H S_i^H + \gamma_i^H I_i^H(t) + \sum_{j\neq i=1}^{n} \psi_{j,i}^S S_j^H - \sum_{j\neq i=1}^{n} \psi_{i,j}^S S_i^H, ...(1)\\
\frac{dI_i^H(t)}{dt} &= \lambda_i^V(t)S_i^H(t) - (\mu_i^H + \delta_i^H + \gamma_i^H)I_i^H + \sum_{j\neq i=1}^{n} \psi_{j,i}^I I_j^H - \sum_{j\neq i=1}^{n} \psi_{i,j}^I I_i^H, ...(2)\\
\frac{dP_i^V(t)}{dt} &= N_i^v \alpha_i^v I_i^V(t) - \alpha_i^V P_i^V(t), ...(3)\\
\frac{dS_i^V(t)}{dt} &= \Lambda_i^V - \lambda_i^H(t)S_i^V(t) - \mu_i^V S_i^V, ...(4)\\
\frac{dI_i^V(t)}{dt} &= \lambda_i^H(t)S_i^V(t) - (\mu_i^V + \delta_i^V)I_i^V(t), ...(5)\\
\frac{dG_i^H(t)}{dt} &= N_i^h \alpha_i^h I_i^H(t) - \alpha_i^H G_i^H(t), ...(6)
\end{aligned}
\tag{6.2.1}
$$

where

$$
\begin{cases}
\lambda_i^V(t) = \dfrac{\beta_i^V P_i^V(t)}{P_i^0 + P_i^V(t)},\ \lambda_i^H(t) = \dfrac{\beta_i^H G_i^H(t)}{G_i^0 + G_i^H(t)} \\[2ex]
N_i^h = \dfrac{\pi_i \Lambda_i^h}{\left(\alpha_i^h + \mu_i^h\right)\mathfrak{R}_{0i}}\left[\mathfrak{R}_{0i} - 1\right] \\[2ex]
N_i^v = \dfrac{1}{2}.\dfrac{\Lambda_i^v}{(\alpha_i^v + \mu_i^v)}.\dfrac{N_i^k \alpha_i^k}{\left(\alpha_i^k + \mu_i^k\right)}.\dfrac{\alpha_i^z}{(\alpha_i^z + \mu_i^z)}.\dfrac{\alpha_i^s}{(\alpha_i^s + \mu_i^s)}.\dfrac{N_i^g \alpha_i^g}{(\alpha_i^g + \mu_i^g)} \\[2ex]
\delta_i^H = \hat{\delta_i^H}\left(\tilde{M_i^h}\right),\ \delta_i^V = \hat{\delta_i^V}\left(\tilde{P_i^v}\right),\ \gamma_i^H = \hat{\gamma_i^H}\left(\tilde{M_i^h}\right) \text{ which are all constants.}
\end{cases}
\tag{6.2.2}
$$

Table 6.1: A summary of the variables of the malaria multiscale model for i^{th} patch

Variable	Description	Initial condition
$S_i^H(t)$	Susceptible humans	10,000
$I_i^H(t)$	Infected humans	70
$G_i^H(t)$	Community gametocyte load	60,000
$S_i^V(t)$	Susceptible mosquito vectors	100,000
$I_i^V(t)$	Infected mosquito vectors	200
$P_i^V(t)$	Community sporozoite load	40,000

6.2.1 Mathematical Analysis of the Multiscale model of Malaria Dynamics

$$\Omega = \left\{\Omega_H \times \Omega_V \subset \mathbb{R}_+^{3n} \times \mathbb{R}_+^{3n}\right\} \tag{6.2.1}$$

$$\Omega_H = \left\{\left(S_i^H, I_i^H, P_i^V\right) \in \mathbb{R}_+^{3n}\right\} \text{ and } \quad \Omega_V = \left\{\left(S_i^V, I_i^V, G_i^H\right) \in \mathbb{R}_+^{3n}\right\}, i = 1, 2, ..., n \tag{6.2.2}$$

We let $\hat{\Lambda}^H = \sum_{i=1}^{n} \Lambda_i^H$, $\mu^{H*} = min\left\{\mu_i^H, \mu_i^H + \delta_i^H + \gamma_i^H | i = 1, 2, ..., n\right\}$, $N^H = \sum_{i=1}^{n}\left(S_i^H + I_i^H\right)$ and $N^P = \sum_{i=1}^{n} P_i^V$. Similarly, we let $\hat{\Lambda}^V = \sum_{i=1}^{n} \Lambda_i^V$, $\mu^{V*} = min\left\{\mu_i^V, \mu_i^V + \delta_i^V | i = 1, 2, ..., n\right\}$, $N^V = \sum_{i=1}^{n}\left(S_i^V + I_i^V\right)$ and $N^G = \sum_{i=1}^{n} G_i^H$.

When we add equation (1) and equation (2) of the multiscale model system (6.2.1) we get $\dot{N}^H \leq \hat{\Lambda}^H - \mu^{H*} N^H$, suggesting that $\limsup_{t\to\infty} N^H \leq \hat{\Lambda}^H / \mu^{H*}$

$$\frac{dN_1}{dt} = \left(\frac{dN^H}{dt}, \frac{dN^P}{dt}\right) = \left(\sum_{i=1}^{n} \dot{S}_i^H + \dot{I}_i^H, \dot{P}_i^V\right) \tag{6.2.3}$$

This gives

$$\frac{dN^H}{dt} \leq \hat{\Lambda}^H - \mu^{H*} N^H \leq 0, \quad \text{for} \quad N^H \geq \hat{\Lambda}^H / \mu^{H*} N^H \tag{6.2.4}$$

$$\frac{dN^P}{dt} = \sum_{i=1}^{n} N_i^v \alpha_i^v \dot{I}^V - \alpha_i^V \dot{P}_i^V \leq 0 \quad \text{for} \quad N^P \geq \frac{N_k^v \alpha_k^v \Lambda_k^H}{\alpha_k^V \mu_k^H} \tag{6.2.5}$$

where

$$\frac{N_k^v \alpha_k^v \Lambda_k^H}{\alpha_k^V \mu_k^H} = min\left\{\frac{N_i^v \alpha_i^v \Lambda_i^H}{\alpha_i^V \mu_i^H}, i = 1, 2, ..., n\right\}$$

$$N^H = N^H(0) e^{-\mu^{H*} t} + \frac{\hat{\Lambda}^H}{\mu^{H*}}\left[1 - e^{-\mu^{H*} t}\right] \tag{6.2.6}$$

$$N^P = N^P(0) e^{-\alpha_k^V t} + \frac{N_k^v \alpha_k^v \Lambda_k^H}{\alpha_k^V \mu_k^H}\left[1 - e^{-\alpha_k^V t}\right] \tag{6.2.7}$$

Similarly, from equation (4) and equation (5) we get

$$N^V = N^V(0) e^{-\mu^{V*} t} + \frac{\hat{\Lambda}^V}{\mu^{V*}}\left[1 - e^{-\mu^{V*} t}\right] \tag{6.2.8}$$

$$N^G = N^G(0) e^{-\alpha_l^H t} + \frac{N_l^h \alpha_l^h \Lambda_l^V}{\alpha_l^H \mu_l^V}\left[1 - e^{-\alpha_l^H t}\right] \tag{6.2.9}$$

$N^H(0), N^P(0), N^V(0)$ and $N^G(0)$ describe the initial values of N^H, N^P, N^V and N^G respectively. Thus for $t \to \infty$

$$0 \leq (N^H, N^P) \leq \left(\frac{\hat{\Lambda}^H}{\mu^{H*}}, \frac{N_k^v \alpha_k^v \Lambda_k^H}{\alpha_k^V \mu_k^H} \right) \quad \text{and} \quad 0 \leq (N^V, N^G) \leq \left(\frac{\hat{\Lambda}^V}{\mu^{V*}}, \frac{N_l^h \alpha_l^h \Lambda_l^V}{\alpha_l^H \mu_l^V} \right) \tag{6.2.10}$$

Therefore, this assures non-negativity and boundedness of all the state variables and their solutions respectively, in the region Ω □

Theorem 6.1. *The region* $\Omega = \left\{ \Omega_H \times \Omega_V \subset \mathbb{R}_+^{3n} \times \mathbb{R}_+^{3n} \right\}$ *is positively invariant for the multiscale model system (6.2.1) with nonnegative initial conditions in* $\mathbb{R}_+^{6n}$.

6.3 Determination of the disease free equilibrium and its stability

6.3.1 Uniqueness of disease-free equilibrium of multiscale model system

For the purpose of finding the disease-free equilibrium of the multiscale model (6.2.1), there is need to assess the linear system below

$$\Lambda_i^H - \mu_i^H S_i^H + \sum_{j \neq i=1}^{n} \psi_{j,i}^S S_j^H - \sum_{j \neq i=1}^{n} \psi_{i,j}^S S_i^H = 0, \quad i = i, 1, 2, ..., n, \tag{6.3.1}$$

Expressing the equation above in matrix system form gives,

$$\begin{cases} \Lambda_i^H - \cancelto{0}{\lambda_i^V(t) S_i^H(t)} - \mu_i^H S_i^H + \cancelto{0}{\gamma_i^H I_i^H(t)} + \sum_{j \neq i=1}^{n} \psi_{j,i}^S S_j^H - \sum_{j \neq i=1}^{n} \psi_{i,j}^S S_i^H = 0 \\ \Lambda_i^H - \mu_i^H S_i^H + \sum_{j \neq i=1}^{n} \psi_{j,i}^S S_j^H - \sum_{j \neq i=1}^{n} \psi_{i,j}^S S_i^H = 0 \\ \Lambda_i^H - \left(\mu_i^H + \sum_{j \neq i=1}^{n} \psi_{i,j}^S \right) S_i^H + \sum_{j \neq i=1}^{n} \psi_{j,i}^S S_j^H = 0 \end{cases} \tag{6.3.2}$$

From (6.3.2) we obtain the solution

$$\sum_{j=1}^{n} \varphi_{i,j}^S S_j^H = \Lambda_i^H \tag{6.3.3}$$

where

$$\begin{cases} \varphi^S_{i,j} = -\psi^S_{i,j} \quad \text{for} \quad j = 1; 2; ...; n; j \neq i \\ \varphi^S_{i,j} = \mu^H_i + \sum_{j \neq i=1}^{n} \psi^S_{i,j} \quad \text{for} \quad j = i \end{cases} \tag{6.3.4}$$

By the matricial form we have

$$\varphi^S S^H = \Lambda^H \tag{6.3.5}$$

where $\varphi^S = \left(\varphi^S_{i,j}\right)_{1 \leq i,j \leq n}$; $S^H = \left(S^H_1; S^H_2; ...; S^H_n\right)$ and $\Lambda^H = \left(\Lambda^H_1; \Lambda^H_2; ...; \Lambda^H_n\right)^T$

We can demonstrate that the matrix φ^S is an invertible Z-matrix where the off-diagonal entries are nonzero, which results in the multiscale model system (6.2.1) having a unique solution $S^H = S^H_0 = (\varphi^S)^{-1}\Lambda^H$.

Let us now demonstrate uniqueness of the disease-free equilibrium. In the disease-free case we deduce from the multiscale model system (6.2.1) that:

In the case of human hosts:

$$\Lambda^H_i - \left(\mu^H_i + \sum_{j \neq i=1}^{n} \psi^S_{i,j}\right) S^H_i + \sum_{j \neq i=1}^{n} \psi^S_{j,i} S^H_j = 0 \tag{6.3.6}$$

$$\left(\mu^H_i + \sum_{j \neq i=1}^{n} \psi^S_{i,j}\right) S^H_i - \sum_{j \neq i=1}^{n} \psi^S_{j,i} S^H_j = \Lambda^H_i \tag{6.3.7}$$

$$\begin{bmatrix} \mu^H_1 + \sum_{j \neq i=1}^{n} \psi^S_{1j} & -\psi^S_{12} & \cdots & -\psi^S_{1n} \\ -\psi^S_{21} & \ddots & \cdots & -\psi^S_{2n} \\ \vdots & \vdots & \ddots & \vdots \\ -\psi^S_{n1} & -\psi^S_{n2} & \cdots & \mu^H_n + \sum_{j=1}^{n} \psi_{jn} \end{bmatrix} \begin{bmatrix} S^H_{01} \\ S^H_{02} \\ \vdots \\ S^H_{0n} \end{bmatrix} = \begin{bmatrix} \Lambda^H_1 \\ \Lambda^H_2 \\ \vdots \\ \Lambda^H_n \end{bmatrix} \tag{6.3.8}$$

i.e. $\varphi^S S^H_0 = \Lambda^H$ where $\varphi^S = diag\left(\mu^H_i + \sum_{j \neq i=1}^{n} \psi^S_{i,j}\right) - M^S$;

$$M^S = \begin{bmatrix} 0 & \psi^S_{1,2} & \cdots & \psi^S_{1,n} \\ \psi^S_{2,1} & 0 & \cdots & \psi^S_{2,n} \\ \vdots & \vdots & \ddots & \vdots \\ \psi^S_{n,1} & \psi^S_{n,2} & \cdots & 0 \end{bmatrix}$$

$\Lambda^H = \left(\Lambda^H_1, \Lambda^H_2, ..., \Lambda^H_n\right)^T$, $S^H_0 = \left(S^H_{01}; S^H_{02}; ...; S^H_{0n}\right)^T$

In the case of the vector hosts:

$$\begin{bmatrix} \mu^V_1 & 0 & .. & 0 \\ 0 & \mu^V_2 & .. & 0 \\ .. & .. & .. & .. \\ 0 & 0 & 0 & \mu^V_n \end{bmatrix} \begin{bmatrix} S^V_{01} \\ S^V_{02} \\ .. \\ S^V_{0n} \end{bmatrix} = \begin{bmatrix} \Lambda^V_1 \\ \Lambda^V_2 \\ .. \\ \Lambda^V_n \end{bmatrix} \tag{6.3.9}$$

that is,

$$CS^V = \Lambda^V \tag{6.3.10}$$

where,

$$C = diag\left(\mu^V_i\right),\ S^V_0 = \left[S^V_{01}, S^V_{02}, ..., S^V_{0n}\right]^T, \Lambda^V = \left[\Lambda^V_1, \Lambda^V_2, ..., \Lambda^V_n\right] \tag{6.3.11}$$

From equation (6.3.8) all the off-diagonal entries of φ^S are non-positive and the total of all the entries in every column of φ^S is positive. Furthermore, φ^S is an irreducible non-singular M-matrix and so φ^S must have positive inverse, that is, $\left(\varphi^S\right)^{-1} > 0$, [131]. Consequently, this implies uniqueness of a positive solution $S^H_0 = \left(\varphi^S\right)^{-1}\Lambda^H > 0$. Equivalently, C is an irreducible non-singular M-matrix and so C must have positive inverse, that is, $S^V_0 = C^{-1}\Lambda^V > 0$, [131]. Consequently, $S^V_0 = C^{-1}\Lambda^V > 0$ is a unique solution of $CS^V = \Lambda^V$. Therefore, the results demonstrate the existence of a unique disease-free equilibrium.

$$E_0 = \left(S^H_0, \mathbf{0, 0, 0, 0}, ..., S^V_0, .. \mathbf{0, 0}\right) \tag{6.3.12}$$

where $\mathbf{0} = \underbrace{(0, ..., 0)}_{n \quad times}$, $S^H_0 = \left(\varphi^S\right)^{-1}\Lambda^H$ and $S^V_0 = (C)^{-1}\Lambda^V$ □

Therefore we now have the following result.

Theorem 6.2. *The multiscale model system (6.2.1) always has a unique disease-free equilibrium point* E_0.

6.3.2 The model reproduction number, $\mathcal{R}_0$

The reproductive number, $\mathcal{R}_0$ is described as the average number of secondary infections generated by an infectious individual host brought into an entirely susceptible population [101, 102]. It's an important parameter which helps to examine outbreak of disease. For the vast majority of disease outbreaks, if $\mathcal{R}_0 < 1$, this implies that the outbreak dies out. However, when $\mathcal{R}_0 > 1$, this implies that the outbreak persists. For Malaria infection in humans, $\mathcal{R}_0$ describes the anticipated number of human Malaria infections generated by an individual human host throughout the whole cycle of virulence of the human placed in a totally susceptible human population. Hence, $\mathcal{R}_0$ quantifies spread of Malaria from human to human through the mosquito vector. In order to evaluate the basic reproductive number we implement the next generation operator approach [101]. The multiscale model system (6.2.1) can be expressed as follows:

$$\begin{aligned} \frac{dX}{dt} &= f(X,Z), \\ \frac{dZ}{dt} &= h(X,Z), \end{aligned} \tag{6.3.1}$$

where

$$X = \left(S_i^H, S_i^V\right) \tag{6.3.2}$$

$$Z = (I_i^H, P_i^V, I_i^V, G_i^H) \tag{6.3.3}$$

The elements of X stand for the number of susceptibles as well as other classes of non-infectious individuals. The elements of Z stand for the number of infected individuals able to transmit the disease.

The model's disease compartments are I_i^H, P_i^V, I_i^V and G_i^H. The infected class equations from the model can be represented as follows

$\left(I_1^H, I_2^H, ..., I_n^H, P_1^V, P_2^V, ..., P_n^V, I_1^V, I_2^V, ..., I_n^V, G_1^H, G_2^H, ..., G_n^H\right)$ as

$$\begin{cases} \dfrac{dI_i^H(t)}{dt} = \lambda_i^V(t)S_i^H(t) - (\mu_i^H + \delta_i^H + \gamma_i^H)I_i^H + \sum\limits_{j\neq i=1}^{n} \psi_{j,i}^I I_j^H - \sum\limits_{j\neq i=1}^{n} \psi_{i,j}^I I_i^H \\ \dfrac{dP_i^V(t)}{dt} = N_i^v \alpha_i^v I_i^V(t) - \alpha_i^V P_i^V(t) \\ \dfrac{dI_i^V(t)}{dt} = \lambda_i^H(t)S_i^V(t) - (\mu_i^V + \delta_i^V)I_i^V(t), \\ \dfrac{dG_i^H(t)}{dt} = N_i^h \alpha_i^h I_i^H(t) - \alpha_i^H G_i^H(t) \end{cases} \tag{6.3.4}$$

$$\begin{cases} \dfrac{dI_i^H(t)}{dt} = \lambda_i^V(t)S_i^H(t) - \left(\mu_i^H + \delta_i^H + \gamma_i^H + \sum\limits_{j\neq i=1}^{n} \psi_{i,j}^I\right) I_i^H + \sum\limits_{j\neq i=1}^{n} \psi_{j,i}^I I_j^H \\ \dfrac{dP_i^V(t)}{dt} = N_i^v \alpha_i^v I_i^V(t) - \alpha_i^V P_i^V(t) \\ \dfrac{dI_i^V(t)}{dt} = \lambda_i^H(t)S_i^V(t) - (\mu_i^V + \delta_i^V)I_i^V(t), \\ \dfrac{dG_i^H(t)}{dt} = N_i^h \alpha_i^h I_i^H(t) - \alpha_i^H G_i^H(t) \end{cases} \tag{6.3.5}$$

$$\begin{cases} \dfrac{dI_i^H(t)}{dt} = \lambda_i^V(t)S_i^H(t) - \sum\limits_{j\neq i=1}^{n} \varphi_{j,i}^I I_j^H \\ \dfrac{dP_i^V(t)}{dt} = N_i^v \alpha_i^v I_i^V(t) - \alpha_i^V P_i^V(t) \\ \dfrac{dI_i^V(t)}{dt} = \lambda_i^H(t)S_i^V(t) - (\mu_i^V + \delta_i^V)I_i^V(t), \\ \dfrac{dG_i^H(t)}{dt} = N_i^h \alpha_i^h I_i^H(t) - \alpha_i^H G_i^H(t) \end{cases} \tag{6.3.6}$$

where

$$\begin{cases} \varphi_{i,j}^{I} = -\psi_{i,j}^{I} \quad \text{for} \quad j = 1, ..., n, j \neq i \\ \\ \varphi_{i,i}^{I} = \mu_i^H + \delta_i^H + \gamma_i^H + \sum\limits_{j \neq i=1}^{n} \psi_{i,j}^{I} \end{cases} \tag{6.3.7}$$

The vector of the rates of new infections and the vector of the rates of other transfers between disease states from (6.3.6) are respectively represented by

$$\mathbf{F} = \begin{bmatrix} \left[\lambda_i^V S_i^H\right]_{i=1,...,n} \\ 0_n \\ \left[\lambda_i^H S_i^V\right]_{i=1,...,n} \\ 0_n \end{bmatrix} \quad \text{and} \quad \mathbf{V} = \begin{bmatrix} \left[\sum\limits_{j=1}^{n} \varphi_{i,j}^{I} I_j^H\right]_{i=1,..,n} \\ \left[-N_i^v \alpha_i^v I_i^V + \alpha_i^V P_i^V\right]_{i=1,...,n} \\ \left[\left[\mu_i^V + \delta_i^V\right] I_i^V\right]_{i=1,...,n} \\ \left[-N_i^h \alpha_i^h I_i^H + \alpha_i^H G_i^H\right]_{i=1,...,n} \end{bmatrix} \tag{6.3.8}$$

With respect to the infected classes $\left(I_i^H, P_i^V, I_i^V, G_i^H\right)$ evaluated at the disease-free equilibrium point ε_0, the Jacobian matrices of $\mathbf{F}$ and $\mathbf{V}$ are respectively described as

$$\mathbf{F} = \begin{bmatrix} \mathbb{O} & F_{1,2} & \mathbb{O} & \mathbb{O} \\ \mathbb{O} & \mathbb{O} & \mathbb{O} & \mathbb{O} \\ \mathbb{O} & \mathbb{O} & \mathbb{O} & F_{3,4} \\ \mathbb{O} & \mathbb{O} & \mathbb{O} & \mathbb{O} \end{bmatrix} \tag{6.3.9}$$

where

$$\begin{cases} F_{1,2} = diag\left\{\dfrac{\beta_1^V \Lambda_1^H}{P_{01}^V \mu_1^H}, \dfrac{\beta_2^V \Lambda_2^H}{P_{02}^V \mu_2^H}, ..., \dfrac{\beta_n^V \Lambda_n^H}{P_{0n}^V \mu_n^H}\right\} \\ \\ F_{3,4} = diag\left\{\dfrac{\beta_1^H \Lambda_1^V}{G_{01}^H \mu_1^V}, \dfrac{\beta_2^H \Lambda_2^V}{G_{02}^H \mu_2^V}, ..., \dfrac{\beta_n^H \Lambda_n^V}{G_{0n}^H \mu_n^V}\right\} \end{cases} \tag{6.3.10}$$

and

$$\mathbf{V} = \begin{bmatrix} V_{1,1} & \mathbb{O} & \mathbb{O} & \mathbb{O} \\ \mathbb{O} & V_{2,2} & V_{2,3} & \mathbb{O} \\ \mathbb{O} & \mathbb{O} & V_{3,3} & \mathbb{O} \\ V_{4,1} & \mathbb{O} & \mathbb{O} & V_{4,4} \end{bmatrix} \tag{6.3.11}$$

where

$$\begin{cases} V_{1,1} = \left(\varphi_{ij}^{I}\right)_{1\leq i,j\leq n} \\ V_{2,2} = diag\left(\alpha_1^V, \alpha_2^V, ..., \alpha_n^V\right) \\ V_{2,3} = diag\left(-N_1^v\alpha_1^v, -N_2^v\alpha_2^v, ..., -N_n^v\alpha_n^v\right) \\ V_{3,3} = diag\left(\mu_1^V + \delta_1^V, \mu_2^V + \delta_2^V, ..., \mu_n^V + \delta_n^V\right) \\ V_{4,1} = diag\left(-N_1^h\alpha_1^h, -N_2^h\alpha_2^h, ..., -N_n^h\alpha_n^h\right) \\ V_{4,4} = diag\left(\alpha_1^H, \alpha_2^H, ..., \alpha_n^H\right) \end{cases} \tag{6.3.12}$$

We define $\mathbb{O}$ as the $n \times n$ matrix with all entries being zero. Furthermore, we define the matrix $\mathbf{F}$ to be non-negative of rank one and that can be written as the product of vectors. The matrices $V_{1,1}, V_{2,3}, V_{3,3}, V_{4,1}$ and $V_{4,4}$ are non-singular irreducible M-matrices and can be inverted. We now determine the inverse of matrix $\mathbf{V}$.

$$\mathbf{V}^{-1} = \begin{bmatrix} V_{1,1}^{-1} & \mathbb{O} & \mathbb{O} & \mathbb{O} \\ \mathbb{O} & V_{2,2}^{-1} & -V_{2,2}^{-1}V_{2,3}V_{3,3}^{-1} & \mathbb{O} \\ \mathbb{O} & \mathbb{O} & V_{3,3}^{-1} & \mathbb{O} \\ -V_{4,4}^{-1}V_{4,1}V_{1,1}^{-1} & \mathbb{O} & \mathbb{O} & V_{4,4}^{-1} \end{bmatrix} \tag{6.3.13}$$

$$\mathbf{K} = \mathbf{F}\mathbf{V}^{-1} = \begin{bmatrix} \mathbb{O} & F_{1,2} & \mathbb{O} & \mathbb{O} \\ \mathbb{O} & \mathbb{O} & \mathbb{O} & \mathbb{O} \\ \mathbb{O} & \mathbb{O} & \mathbb{O} & F_{3,4} \\ \mathbb{O} & \mathbb{O} & \mathbb{O} & \mathbb{O} \end{bmatrix} \begin{bmatrix} V_{1,1}^{-1} & \mathbb{O} & \mathbb{O} & \mathbb{O} \\ \mathbb{O} & V_{2,2}^{-1} & -V_{2,2}^{-1}V_{2,3}V_{3,3}^{-1} & \mathbb{O} \\ \mathbb{O} & \mathbb{O} & V_{3,3}^{-1} & \mathbb{O} \\ -V_{4,4}^{-1}V_{4,1}V_{1,1}^{-1} & \mathbb{O} & \mathbb{O} & V_{4,4}^{-1} \end{bmatrix} \tag{6.3.14}$$

$$\mathbf{K} = \mathbf{F}\mathbf{V}^{-1} = \begin{bmatrix} \mathbb{O} & F_{1,2}V_{2,2}^{-1} & -F_{1,2}V_{2,2}^{-1}V_{2,3}V_{3,3}^{-1} & \mathbb{O} \\ \mathbb{O} & \mathbb{O} & \mathbb{O} & \mathbb{O} \\ -F_{3,4}V_{4,4}^{-1}V_{4,1}V_{1,1}^{-1} & \mathbb{O} & \mathbb{O} & F_{3,4}V_{4,4}^{-1} \\ \mathbb{O} & \mathbb{O} & \mathbb{O} & \mathbb{O} \end{bmatrix} \tag{6.3.15}$$

$$\mathbf{K} = \mathbf{F}\mathbf{V}^{-1} = \begin{bmatrix} \mathbb{O} & K_{1,2} & K_{1,3} & \mathbb{O} \\ \mathbb{O} & \mathbb{O} & \mathbb{O} & \mathbb{O} \\ K_{3,1} & \mathbb{O} & \mathbb{O} & K_{3,4} \\ \mathbb{O} & \mathbb{O} & \mathbb{O} & \mathbb{O} \end{bmatrix} \tag{6.3.16}$$

where

$$\begin{cases} K_{1,2} := F_{1,2}V_{2,2}^{-1} \\ K_{1,3} := -F_{1,2}V_{2,2}^{-1}V_{2,3}V_{3,3}^{-1} \\ K_{3,1} := -F_{3,4}V_{4,4}^{-1}V_{4,1}V_{1,1}^{-1} \\ K_{3,4} := F_{3,4}V_{4,4}^{-1} \end{cases} \tag{6.3.17}$$

Therefore, $\mathcal{R}_0$ defined by the spectral radius of $\mathbf{F}\mathbf{V}^{-1}$, is

$$\mathcal{R}_0 = \rho\left(A\right) \tag{6.3.18}$$

where A is the $n \times n$ positive matrix illustrated by

$$A = K_{1,3}K_{3,1} = F_{1,2}V_{2,2}^{-1}V_{2,3}V_{3,3}^{-1}F_{3,4}V_{4,4}^{-1}V_{4,1}V_{1,1}^{-1} \tag{6.3.19}$$

where

$$F_{1,2}V_{2,2}^{-1}V_{2,3}V_{3,3}^{-1} = diag\left\{-\frac{\beta_1^V\Lambda_1^H N_1^v\alpha_1^v}{P_{01}^V\mu_1^H\alpha_1^V\left(\mu_1^V+\delta_1^V\right)}, ..., -\frac{\beta_n^V\Lambda_n^H N_n^v\alpha_n^v}{P_{0n}^V\mu_n^H\alpha_n^V\left(\mu_n^V+\delta_n^V\right)}\right\} \tag{6.3.20}$$

and

$$F_{3,4}V_{4,4}^{-1}V_{4,1}V_{1,1}^{-1} = diag\left\{-\frac{\beta_1^H\Lambda_1^V N_1^h\alpha_1^h}{G_{01}^H\mu_1^V\alpha_1^H},...,-\frac{\beta_n^H\Lambda_n^V N_n^h\alpha_n^h}{G_{0n}^H\mu_n^V\alpha_n^H}\right\}\left(\varphi^I\right)^{-1} \tag{6.3.21}$$

Therefore

$$A = diag\left\{\frac{\beta_1^V\Lambda_1^H N_1^v\alpha_1^v\beta_1^H\Lambda_1^V N_1^h\alpha_1^h}{P_{01}^V\mu_1^H\alpha_1^V\left(\mu_1^V+\delta_1^V\right)G_{01}^H\mu_1^V\alpha_1^H},...,\frac{\beta_n^V\Lambda_n^H N_n^v\alpha_n^v\beta_n^H\Lambda_n^V N_n^h\alpha_n^h}{P_{0n}^V\mu_n^H\alpha_n^V\left(\mu_n^V+\delta_n^V\right)G_{0n}^H\mu_n^V\alpha_n^H}\right\}\left(\varphi^I\right)^{-1} \tag{6.3.22}$$

We now consider some particular situations.

(i) **Situation 1:** Suppose there is no migration between patches, hence, $\psi_{i,j}^I = \psi_{j,i}^I = 0$ for $j = 1,2,...,n, j \neq i$, we obtain

$$\begin{cases} \varphi_{i,j}^I = -\psi_{i,j}^I \quad \text{for} \quad j = 1,...,n, j \neq i \\ \\ \varphi_{i,i}^I = \mu_i^H + \delta_i^H + \gamma_i^H \end{cases} \tag{6.3.23}$$

Therefore,

$$F_{1,2}V_{2,2}^{-1}V_{2,3}V_{3,3}^{-1} = diag\left\{-\frac{\beta_1^V\Lambda_1^H N_1^v\alpha_1^v}{P_{01}^V\mu_1^H\alpha_1^V\left(\mu_1^V+\delta_1^V\right)},...,-\frac{\beta_n^V\Lambda_n^H N_n^v\alpha_n^v}{P_{0n}^V\mu_n^H\alpha_n^V\left(\mu_n^V+\delta_n^V\right)}\right\} \tag{6.3.24}$$

and

$$F_{3,4}V_{4,4}^{-1}V_{4,1}V_{1,1}^{-1} = diag\left\{-\frac{\beta_1^H\Lambda_1^V N_1^h\alpha_1^h}{G_{01}^H\mu_1^V\alpha_1^H},...,-\frac{\beta_n^H\Lambda_n^V N_n^h\alpha_n^h}{G_{0n}^H\mu_n^V\alpha_n^H}\right\}\left(\varphi^I\right)^{-1} \tag{6.3.25}$$

Consequently,

$$A = diag\left\{\frac{\beta_1^V\Lambda_1^H N_1^v\alpha_1^v\beta_1^H\Lambda_1^V N_1^h\alpha_1^h}{P_{01}^V\mu_1^H\alpha_1^V\left(\mu_1^V+\delta_1^V\right)G_{01}^H\mu_1^V\alpha_1^H\varphi_{11}^I},...,\frac{\beta_n^V\Lambda_n^H N_n^v\alpha_n^v\beta_n^H\Lambda_n^V N_n^h\alpha_n^h}{P_{0n}^V\mu_n^H\alpha_n^V\left(\mu_n^V+\delta_n^V\right)G_{0n}^H\mu_n^V\alpha_n^H\varphi_{nn}^I}\right\} \tag{6.3.26}$$

Therefore

$$\mathcal{R}_0 = \max\mathcal{R}_{0i} \tag{6.3.27}$$

where

$$\mathcal{R}_{0i} = \frac{\beta_i^V \Lambda_i^H N_i^v \alpha_i^v \beta_i^H \Lambda_i^V N_i^h \alpha_i^h}{P_{0i}^V \mu_i^H \alpha_i^V \left(\mu_i^V + \delta_i^V\right) G_{0i}^H \mu_i^V \alpha_i^H \left(\mu_i^H + \delta_i^H + \gamma_i^H\right)} \tag{6.3.28}$$

Accordingly, when $\mathcal{R}_{0i} > 1$ for all i, the disease-free equilibrium is unstable resulting in Malaria disease invading the population. This is verified by proving the global stability of the endemic equilibrium of Malaria in section (6.4.2). However, when $\mathcal{R}_{0i} < 1$ for all i, the disease-free equilibrium is asymptotically stable and Malaria disease may be eliminated. Therefore, it is essential to diminish $\mathcal{R}_{0i}$ in each patch i in order to control Malaria disease. This is verified by proving the global stability of the disease-free equilibrium in section (6.3.4).

(ii) **Situation 2:** Suppose there is migration in a model with two patches where the migration rates of the human populations are nonzero.

$$\begin{cases} F_{1,2} = diag\left\{\dfrac{\beta_1^V \Lambda_1^H}{P_{01}^V \mu_1^H}, \dfrac{\beta_2^V \Lambda_2^H}{P_{02}^V \mu_2^H}\right\} \\ F_{3,4} = diag\left\{\dfrac{\beta_1^H \Lambda_1^V}{G_{01}^H \mu_1^V}, \dfrac{\beta_2^H \Lambda_2^V}{G_{02}^H \mu_2^V}\right\} \end{cases} \tag{6.3.29}$$

and

$$\begin{cases} V_{1,1} = \left(\varphi_{ij}^I\right)_{1\leq i,j\leq 2} \\ V_{2,2} = diag\left(\alpha_1^V, \alpha_2^V\right) \\ V_{2,3} = diag\left(-N_1^v \alpha_1^v, -N_2^v \alpha_2^v\right) \\ V_{3,3} = diag\left(\mu_1^V + \delta_1^V, \mu_2^V + \delta_2^V\right) \\ V_{4,1} = diag\left(-N_1^h \alpha_1^h, -N_2^h \alpha_2^h\right) \\ V_{4,4} = diag\left(\alpha_1^H, \alpha_2^H\right) \end{cases} \tag{6.3.30}$$

In otherwords

$$
\begin{cases}
F_{1,2} = \begin{bmatrix} \dfrac{\beta_1^V \Lambda_1^H}{P_{01}^V \mu_1^H} & 0 \\ 0 & \dfrac{\beta_2^V \Lambda_2^H}{P_{02}^V \mu_2^H} \end{bmatrix} \\
F_{3,4} = \begin{bmatrix} \dfrac{\beta_1^H \Lambda_1^V}{G_{01}^H \mu_1^V} & 0 \\ 0 & \dfrac{\beta_2^H \Lambda_2^V}{G_{02}^H \mu_2^V} \end{bmatrix} \\
V_{2,3} = \begin{bmatrix} -N_1^v \alpha_1^v & 0 \\ 0 & -N_2^v \alpha_2^v \end{bmatrix} \\
V_{4,1} = \begin{bmatrix} -N_1^h \alpha_1^h & 0 \\ 0 & -N_2^h \alpha_2^h \end{bmatrix} \\
V_{1,1}^{-1} = \dfrac{1}{\varphi_{11}^I \varphi_{22}^I - \varphi_{12}^I \varphi_{21}^I} \begin{bmatrix} \varphi_{22}^I & -\varphi_{12}^I \\ -\varphi_{21}^I & \varphi_{11}^I \end{bmatrix} \\
V_{2,2}^{-1} = \begin{bmatrix} \dfrac{1}{\alpha_1^V} & 0 \\ 0 & \dfrac{1}{\alpha_2^V} \end{bmatrix} \\
V_{4,4}^{-1} = \begin{bmatrix} \dfrac{1}{\alpha_1^H} & 0 \\ 0 & \dfrac{1}{\alpha_2^H} \end{bmatrix} \\
V_{3,3}^{-1} = \begin{bmatrix} \dfrac{1}{\alpha_1^V + \delta_1^V} & 0 \\ 0 & \dfrac{1}{\alpha_2^V + \delta_2^V} \end{bmatrix}
\end{cases}
\tag{6.3.31}
$$

$$A=\frac{1}{\left(\varphi_{11}^{I}\varphi_{22}^{I}-\varphi_{12}^{I}\varphi_{21}^{I}\right)}\begin{bmatrix}\dfrac{\beta_1^V\Lambda_1^H N_1^v\alpha_1^v\beta_1^H\Lambda_1^V N_1^h\alpha_1^h\varphi_{22}^I}{P_{01}^V\left(\mu_1^H\right)^2\alpha_1^V\left(\mu_1^V+\delta_1^V\right)G_{01}^H\mu_1^V} & -\dfrac{\beta_1^V\Lambda_1^H N_1^v\alpha_1^v\beta_1^H\Lambda_1^V N_1^h\alpha_1^h\varphi_{12}^I}{P_{01}^V\left(\mu_1^H\right)^2\alpha_1^V\left(\mu_1^V+\delta_1^V\right)G_{01}^H\mu_1^V}\\ -\dfrac{\beta_2^V\Lambda_2^H N_2^v\alpha_2^v\beta_2^H\Lambda_2^V N_2^h\alpha_2^h\varphi_{21}^I}{P_{02}^V\left(\mu_2^H\right)^2\alpha_2^V\left(\mu_2^V+\delta_2^V\right)G_{02}^H\mu_2^V} & \dfrac{\beta_2^V\Lambda_2^H N_2^v\alpha_2^v\beta_2^H\Lambda_2^V N_2^h\alpha_2^h\varphi_{11}^I}{P_{02}^V\left(\mu_2^H\right)^2\alpha_2^V\left(\mu_2^V+\delta_2^V\right)G_{02}^H\mu_2^V}\end{bmatrix} \tag{6.3.32}$$

Therefore

$$A=F_{1,2}V_{2,2}^{-1}V_{2,3}V_{3,3}^{-1}F_{3,4}V_{4,4}^{-1}V_{4,1}V_{1,1}^{-1}=\begin{bmatrix}A_{11} & A_{12}\\ A_{21} & A_{22}\end{bmatrix} \tag{6.3.33}$$

where

$$\begin{cases}A_{11}=\dfrac{1}{\left(\varphi_{11}^{I}\varphi_{22}^{I}-\varphi_{12}^{I}\varphi_{21}^{I}\right)}\left(\dfrac{\beta_1^V\Lambda_1^H N_1^v\alpha_1^v\beta_1^H\Lambda_1^V N_1^h\alpha_1^h\varphi_{22}^I}{P_{01}^V\left(\mu_1^H\right)^2\alpha_1^V\left(\mu_1^V+\delta_1^V\right)G_{01}^H\mu_1^V}\right)\\ A_{12}=-\dfrac{1}{\left(\varphi_{11}^{I}\varphi_{22}^{I}-\varphi_{12}^{I}\varphi_{21}^{I}\right)}\left(\dfrac{\beta_1^V\Lambda_1^H N_1^v\alpha_1^v\beta_1^H\Lambda_1^V N_1^h\alpha_1^h\varphi_{12}^I}{P_{01}^V\left(\mu_1^H\right)^2\alpha_1^V\left(\mu_1^V+\delta_1^V\right)G_{01}^H\mu_1^V}\right)\\ A_{21}=-\dfrac{1}{\left(\varphi_{11}^{I}\varphi_{22}^{I}-\varphi_{12}^{I}\varphi_{21}^{I}\right)}\left(\dfrac{\beta_2^V\Lambda_2^H N_2^v\alpha_2^v\beta_2^H\Lambda_2^V N_2^h\alpha_2^h\varphi_{21}^I}{P_{02}^V\left(\mu_2^H\right)^2\alpha_2^V\left(\mu_2^V+\delta_2^V\right)G_{02}^H\mu_2^V}\right)\\ A_{22}=\dfrac{1}{\left(\varphi_{11}^{I}\varphi_{22}^{I}-\varphi_{12}^{I}\varphi_{21}^{I}\right)}\left(\dfrac{\beta_2^V\Lambda_2^H N_2^v\alpha_2^v\beta_2^H\Lambda_2^V N_2^h\alpha_2^h\varphi_{11}^I}{P_{02}^V\left(\mu_2^H\right)^2\alpha_2^V\left(\mu_2^V+\delta_2^V\right)G_{02}^H\mu_2^V}\right)\end{cases} \tag{6.3.34}$$

Taking the characteristic polynomial

$$\begin{vmatrix}A_{11}-\Lambda & A_{12}\\ A_{21} & A_{22}-\Lambda\end{vmatrix}=0 \tag{6.3.35}$$

$$\Lambda^2-(A_{11}+A_{22})\Lambda+A_{11}A_{22}-A_{12}A_{21}=0 \tag{6.3.36}$$

Applying the quadratic formula

$$\Lambda=\frac{1}{2}\left[(A_{11}+A_{22})\pm\sqrt{A_{11}^2+2A_{11}A_{22}+A_{22}^2-4A_{11}A_{22}+4A_{12}A_{21}}\right] \tag{6.3.37}$$

$$\Lambda = \frac{1}{2}\left[(A_{11} + A_{22}) \pm \sqrt{A_{11}^2 - 2A_{11}A_{22} + A_{22}^2 + 4A_{12}A_{21}}\right] \tag{6.3.38}$$

$$\Lambda = \frac{1}{2}\left[(A_{11} + A_{22}) \pm \sqrt{(A_{11} - A_{22})^2 + 4A_{12}A_{21}}\right] \tag{6.3.39}$$

Take

$$\Lambda = \frac{1}{2}\left[(A_{11} + A_{22}) + \sqrt{(A_{11} - A_{22})^2 + 4A_{12}A_{21}}\right] \tag{6.3.40}$$

Hence

$$\mathcal{R}_0 = \frac{1}{2}\left[(A_{11} + A_{22}) + \sqrt{(A_{11} - A_{22})^2 + 4A_{12}A_{21}}\right] \tag{6.3.41}$$

6.3.3 Local Stability of the Malaria disease free equilibrium (DFE)

From Theorem 4.2 of van den Driessche and Watmough [103], if $\mathcal{R}_0 < 1$ then the Malaria disease-free equilibrium is locally asymptotically stable and the disease cannot persist in the human population. We summarize this result below.

Theorem 6.3. *The disease-free equilibrium point E^0 of the multi-scale model system (6.2.1) is locally asymptotically stable whenever $\mathcal{R}_0 < 1$ and unstable otherwise.*

Proof Let J_{12} be the matrices of the partial derivatives evaluated at the disease-free equilibrium. The Jacobian matrix for the linearization of the system about the disease free equilibrium is obtained as the block structure.

$$J = \begin{bmatrix} J_{11} & J_{12} \\ 0 & F - V \end{bmatrix} \tag{6.3.1}$$

The matrix J is triangular. Therefore, the eigenvalues of J are those of the partition matrices J_{11} and $F - V$ where J_{11} is expressed as follows:

$$J = \begin{bmatrix} -\varphi^{S_C} & 0 \\ 0 & -C \end{bmatrix} \tag{6.3.2}$$

The matrices φ^{S_C} and C are irreducible non-singular M-matrices as defined in section (6.3.1). Hence, special abcissa, $s(-\varphi^{S_C}) < 0$, $s(-C) < 0$ and the eigenvalues of the matrix J_{11} have negative real parts. Therefore, the matrix J will has eigenvalues all with negative real parts if the matrix $F - V$ has all eigenvalues with negative real parts. In addition, F is non-negative matrix and V is a non-singular M-matrix. Thus, the eigenvalues of $F - V$ will have negative real parts if and only if $\rho(FV^{-1}) < 1$,

that is, the disease free equilibrium is locally asymptotically stable if and only if the basic reproduction number $\mathcal{R}_0 = \rho(FV^{-1}) < 1$. If $\mathcal{R}_0 > 1$, then $s(F - V) > 0$. This shows that at least one eigenvalue lies in the right half plane. So, the disease free equilibrium is unstable if $\mathcal{R}_0 > 1$. □

Lemma 6.4. *The matrix $(F - V)$ has a real spectrum. Moreover, if $\rho\left(FV^{-1}\right) < 1$, all eigenvalues of $(F - V)$ are negative.*

6.3.4 Global Stability of the disease free equilibrium

For the purpose of establishing the global stability of DFE of the model system (6.2.1), we implement Theorem 2 in van den Driessche and Watmough [103] to establish that the disease-free equilibrium is globally asymptotically stable whenever $\mathcal{R}_0 < 1$ and unstable when $\mathcal{R}_0 > 1$. We identify two conditions that warrant the global asymptotic stability of the disease-free state. The model system (6.2.1) can be written as follows:

$$\begin{cases} \dfrac{dX}{dt} = F(X, Z), \\ \\ \dfrac{dZ}{dt} = G(X, Z), \quad G(X, 0) = 0 \end{cases} \tag{6.3.1}$$

where $X = \left(S_i^H, S_i^V\right)$ denotes all uninfected components and $Z = (I_i^H, P_i^V, I_i^V, G^H)$ denotes all infected and infectious components;

$$E_0 = \left(S_0^H, \mathbf{0, 0, 0, 0}, ..., S_0^V, .. \mathbf{0, 0}\right) \tag{6.3.2}$$

where $\mathbf{0} = \underbrace{(0, ..., 0)}_{n \quad times}$, $S_0^H = \left(\varphi^S\right)^{-1} \Lambda^H$ and $S_0^V = (C)^{-1} \Lambda^V$
denotes the disease-free equilibrium of the system. To warrant global asymptotic stability, the conditions $(H1)$ and $(H2)$ below must be met [101]:

(H1) For $\dfrac{dX}{dt} = F(X, 0), X^*$ is globally asymptotically stable (g.a.s);

(H2) $G(X, Z) = AZ - \hat{G}(X, Z), \hat{G}(X, Z) \geq 0$ for $(X, Z) \in \mathbb{R}^3_+$, where the Jacobian $A = \dfrac{\partial G}{\partial Z} = D_Z G(X^*, 0)$ is an M-matrix (the off diagonal elements of A are nonnegative) and $\mathbb{R}^9_+$ is the region where the model makes biological sense.

$$\frac{dX}{dt} = F(X,Z) = \Lambda_i^H - \lambda_i^V(t)S_i^H(t) - \mu_i^H S_i^H + \gamma_i^H I_i^H(t) + \sum_{j\neq i=1}^{n} \psi_{j,i}^S S_j^H - \sum_{j\neq i=1}^{n} \psi_{i,j}^S S_i^H, \quad (6.3.3)$$

At the disease-free equilibrium $Z = 0$

$$F(X,0) = \Lambda_i^H - \mu_i^H S_i^H \quad (6.3.4)$$

Hence, since Φ is an invariant set for model system (6.2.1) and in view of Theorem 6.3, it is sufficient to show that for all $E^0 \in \Phi$

$$\lim_{t\to\infty} S_i^H(t) = S_{0i}^H, \lim_{t\to\infty} I_i^H(t) = 0, \lim_{t\to\infty} P_i^v(t) = 0, \lim_{t\to\infty} S_i^V(t) = S_{0i}^V, \lim_{t\to\infty} I_i^v(t) = 0, \lim_{t\to\infty} G_i^V(t) = 0 \quad (6.3.5)$$

where S_{0i}^H and S_{0i}^V are as in (6.3.2) , it follows that

$$\frac{dS_i^H(t)}{dt} \leq \Lambda_i^H - \mu_i^H S_i^H(t) \quad (6.3.6)$$

and

$$\frac{dS_i^V(t)}{dt} \leq \Lambda_i^V - \mu_i^V S_i^V(t) \quad (6.3.7)$$

It is easy to see that S_{0i}^H and S_{0i}^V are globally asymptotically stable equilibria for the comparison equations

$$\frac{dy_1(t)}{dt} \leq \Lambda_i^H - \mu_i^H y_1(t) \quad (6.3.8)$$

and

$$\frac{dy_2(t)}{dt} \leq \Lambda_i^V - \mu_i^V y_2(t) \quad (6.3.9)$$

Therefore, for any $\varepsilon > 0$, there exists $\bar{t} > 0$, such that for all $t \geq \bar{t}$, it holds $S_i^H(t) \leq S_{0i}^H + \varepsilon$ and $S_i^V(t) \leq S_{0i}^V + \varepsilon$

$$\lim_{t\to\infty} \sup S_i^H(t) \leq S_{0i}^H \text{ and } \lim_{t\to\infty} \sup S_i^V(t) \leq S_{0i}^V \quad (6.3.10)$$

From (5.3.10) and the equations (2)-(3) and (5)-(6) of the model system (6.2.1) we have that for $t \geq \bar{t}$

$$
\begin{aligned}
\frac{dS_i^H(t)}{dt} &\leq \Lambda_i^H - \left(\lambda_i^V(t) + \mu_i^H\right)\left(S_{0i}^H + \varepsilon\right) + \gamma_i^H I_i^H(t) + \sum_{j\neq i=1}^{n} \psi_{j,i}^S S_j^H - \sum_{j\neq i=1}^{n} \psi_{i,j}^S S_i^H, \\
\frac{dI_i^H(t)}{dt} &\leq \lambda_i^V(t)\left(S_{0i}^H + \varepsilon\right) - (\mu_i^H + \delta_i^H + \gamma_i^H) I_i^H + \sum_{j\neq i=1}^{n} \psi_{j,i}^I I_j^H - \sum_{j\neq i=1}^{n} \psi_{i,j}^I I_i^H \\
\frac{dP_i^V(t)}{dt} &= N_i^v \alpha_i^v I_i^V(t) - \alpha_i^V P_i^V(t) \\
\frac{dS_i^V(t)}{dt} &\leq \Lambda_i^V - \lambda_i^H(t)\left(S_{0i}^V + \varepsilon\right) - \mu_i^V S_i^V, \\
\frac{dI_i^V(t)}{dt} &\leq \lambda_i^H(t)\left(S_{0i}^V + \varepsilon\right) - (\mu_i^V + \delta_i^V) I_i^V(t), \\
\frac{dG_i^H(t)}{dt} &= N_i^h \alpha_i^h I_i^H(t) - \alpha_i^H G_i^H(t)
\end{aligned}
\tag{6.3.11}
$$

Let us consider the comparison system

$$
\begin{aligned}
\frac{dw_1(t)}{dt} &\leq \Lambda_i^H - \left(\lambda_i^V(t) + \mu_i^H\right)\left(S_{0i}^H + \varepsilon\right) + \gamma_i^H w_2(t) + \sum_{j\neq i=1}^{n} \psi_{j,i}^S S_j^H - \sum_{j\neq i=1}^{n} \psi_{i,j}^S S_i^H, \\
\frac{dw_2(t)}{dt} &\leq \lambda_i^V(t)\left(S_{0i}^H + \varepsilon\right) - (\mu_i^H + \delta_i^H + \gamma_i^H) w_2 + \sum_{j\neq i=1}^{n} \psi_{j,i}^I I_j^H - \sum_{j\neq i=1}^{n} \psi_{i,j}^I I_i^H \\
\frac{dw_3(t)}{dt} &= N_i^v \alpha_i^v w_5(t) - \alpha_i^V w_3(t) \\
\frac{dw_4(t)}{dt} &\leq \Lambda_i^V - \lambda_i^H(t)\left(S_{0i}^V + \varepsilon\right) - \mu_i^V w_4, \\
\frac{dw_5(t)}{dt} &\leq \lambda_i^H(t)\left(S_{0i}^V + \varepsilon\right) - (\mu_i^V + \delta_i^V) w_5(t), \\
\frac{dw_6(t)}{dt} &= N_i^h \alpha_i^h w_2(t) - \alpha_i^H w_6(t), w_1(\bar{t}) = S_i^H(\bar{t}), w_2(\bar{t}) = I_i^H(\bar{t}), w_3(\bar{t}) = P_i^v(\bar{t}), w_4(\bar{t}) = S_i^V(\bar{t}), \\
& \quad w_5(\bar{t}) = I_i^V(\bar{t}), w_6(\bar{t}) = G_i^H(\bar{t})
\end{aligned}
\tag{6.3.12}
$$

that we can re-write as

$$
\frac{dw(t)}{dt} = (F_\varepsilon - V_\varepsilon)\, w(t) \tag{6.3.13}
$$

where $w(t) = (w_1(t), w_2(t), w_3(t), w_4(t))^T$ and $(F_\varepsilon - V_\varepsilon)$ is a matrix in (6.3.8) computed in $E^0(\varepsilon) = \left(S_{0i}^H + \varepsilon, 0, 0, , S_{0i}^V + \varepsilon, 0, 0\right)$. Let us note that if $\mathcal{R}_0 = \rho\left(FV^{-1}\right) < 1$, we can choose a sufficiently small $\varepsilon > 0$ such that $\rho\left(F_\varepsilon V_\varepsilon^{-1}\right) < 1$. Then by applying Lemma 6.4 to $(F_\varepsilon - V_\varepsilon)$ we obtain that it has a real spectrum and all its eigenvalues are negative. It follows that $\lim_{t\to\infty} w(t) = 0$, whatever the initial conditions are, from which

$$\lim_{t\to\infty} I_i^H(t) = 0, \lim_{t\to\infty} P_i^V(t) = 0, \lim_{t\to\infty} I_i^V(t) = 0, \lim_{t\to\infty} G_i^H(t) = 0 \tag{6.3.14}$$

Now, for any $\varepsilon > 0$, there exists $\bar{t}_1$ such that for any $t \geq \bar{t}_1$, $I_i^H(t) < \varepsilon$, $P_i^V(t) < \varepsilon$, $I_i^V(t) < \varepsilon$, $G_i^H(t) < \varepsilon$. So, for $t \geq \bar{t}_1$ we have

$$\frac{dS_i^H(t)}{dt} \geq \Lambda_i^H - \frac{\beta_i^V \varepsilon}{P_i^0 + \varepsilon} S_i^H - \mu_i^H S_i^H(t), \tag{6.3.15}$$

It is easy to see that $\dfrac{\Lambda_i^H}{\left[\frac{\beta_i^V \varepsilon}{P_i^0+\varepsilon} + \mu_i^H\right]}$ is a global asymptotically stable equilibrium for the comparison equation

$$\frac{dy(t)}{dt} \geq \Lambda_i^H - \frac{\beta_i^V \varepsilon}{P_i^0 + \varepsilon} y(t) - \mu_i^H y(t), \tag{6.3.16}$$

Thus, for any $\chi > 0$, there exists $\bar{t}_2 > 0$ such that for all $t \geq \bar{t}_2$

$$S_i^H(t) \geq \frac{\Lambda_i^H}{\left[\frac{\beta_i^V \varepsilon}{P_i^0+\varepsilon} + \mu_i^H\right]} - \chi \tag{6.3.17}$$

Therefore, for any $\varepsilon > 0$, we have

$$\lim_{t\to\infty} \inf S_i^H(t) \geq \frac{\Lambda_i^H}{\left[\frac{\beta_i^V \varepsilon}{P_i^0+\varepsilon} + \mu_i^H\right]} \tag{6.3.18}$$

Letting $t \to \infty$, we get $\lim_{t\to\infty} \inf S_i^H(t) \geq S_{0i}^H$ and combining this with (6.3.10) gives us

$$\lim_{t\to\infty} S_i^H(t) = S_{0i}^H \tag{6.3.19}$$

A similar argument ensures that

$$\lim_{t\to\infty} S_i^V(t) = S_{0i}^V \tag{6.3.20}$$

Therefore, $E^0 = \left(\dfrac{\Lambda_i^H}{\mu_i^H}, 0, 0, \dfrac{\Lambda_i^V}{\mu_i^V}, 0, 0\right), i = 1, .., n$ is a global asymptotically stable equilibrium point satisfying condition **H1**.

Since $S_i^H \leq S_{0i}^H$ and $S_i^V \leq S_{0i}^V$, we can obtain from the multiscale model system (6.2.1)

$$\begin{cases} \dfrac{dI_i^H(t)}{dt} \leq \lambda_i^V(t)S_{0i}^H(t) - (\mu_i^H + \delta_i^H + \gamma_i^H)I_i^H(t) + \sum\limits_{j\neq i=1}^{n} \psi_{j,i}^I I_j^H(t) - \sum\limits_{j\neq i=1}^{n} \psi_{i,j}^I I_i^H(t) \\ \dfrac{dP_i^V(t)}{dt} \leq N_i^v \alpha_i^v I_i^V(t) - \alpha_i^V P_i^V(t) \\ \dfrac{dI_i^V(t)}{dt} \leq \lambda_i^H(t)S_{0i}^V(t) - (\mu_i^V + \delta_i^V)I_i^V(t), \\ \dfrac{dG_i^H(t)}{dt} \leq N_i^h \alpha_i^h I_i^H(t) - \alpha_i^H G_i^H(t) \end{cases} \tag{6.3.21}$$

We consider the linear system

$$\begin{cases} \dfrac{dI_i^H(t)}{dt} = \lambda_i^V(t)S_{0i}^H(t) - (\mu_i^H + \delta_i^H + \gamma_i^H)I_i^H(t) + \sum\limits_{j\neq i=1}^{n} \psi_{j,i}^I I_j^H(t) - \sum\limits_{j\neq i=1}^{n} \psi_{i,j}^I I_i^H(t) \\ \dfrac{dP_i^V(t)}{dt} = N_i^v \alpha_i^v I_i^V(t) - \alpha_i^V P_i^V(t) \\ \dfrac{dI_i^V(t)}{dt} = \lambda_i^H(t)S_{0i}^V(t) - (\mu_i^V + \delta_i^V)I_i^V(t), \\ \dfrac{dG_i^H(t)}{dt} = N_i^h \alpha_i^h I_i^H(t) - \alpha_i^H G_i^H(t) \end{cases} \tag{6.3.22}$$

Therefore, the system of equations (6.3.22) can be written as

$$\frac{d\mathbf{u}}{dt} = \mathbf{A}\mathbf{u} \tag{6.3.23}$$

where, $\mathbf{u} = \left[I_1^H, I_2^H, ..., I_n^H, P_1^V, P_2^V, ..., P_n^V, I_1^V, I_2^V, ..., I_n^V, G_1^H, G_2^H, ..., G_n^H\right]^T$, $\mathbf{A} = \mathbf{F} - \mathbf{V}$. In this case, $\mathbf{F}$ is a non-negative matrix from (6.3.9) and $\mathbf{V}$ is a non-negative M-matrix from (6.3.11). Hence,

$$s(\mathbf{F} - \mathbf{V}) < 0 \iff \rho\left\{\mathbf{F}\mathbf{V}^{-1}\right\} < 1 \tag{6.3.24}$$

In other words, the eigenvalues of $\mathbf{F} - \mathbf{V}$ lie on the left half plane if $\mathcal{R}_0 < 1$. Therefore, each positive solution of (6.3.23) satisfies

$$\lim_{t\to\infty} \mathbf{u} = 0 \tag{6.3.25}$$

that is, $\lim_{t\to\infty} I_i^H = 0, \lim_{t\to\infty} P_i^V = 0, \lim_{t\to\infty} I_i^V = 0, \lim_{t\to\infty} G_i^H = 0 \quad \text{for all} \quad i = 1, 2, ..., n$

Since all the variables of the multiscale model system (6.2.1) are non-negative, then the use of Comparison theorem [132, 133]

$$\lim_{t\to\infty} I_i^H = 0, \lim_{t\to\infty} P_i^V = 0, \lim_{t\to\infty} I_i^V = 0, \lim_{t\to\infty} G_i^H = 0 \quad \text{for all} \quad i = 1, 2, ..., n \tag{6.3.26}$$

Furthermore, as $t \to \infty$

$$\begin{cases} \dfrac{dS_i^H}{dt} = \Lambda_i^H - \mu_i^H S_i^H + \displaystyle\sum_{j\neq i=1}^{n} \psi_{j,i}^S S_j^H - \sum_{j\neq i=1}^{n} \psi_{i,j}^S S_i^H, \\ \dfrac{dS_i^V}{dt} = \Lambda_i^V - \mu_i^V S_i^V, \end{cases} \tag{6.3.27}$$

In the matrix form

$$\frac{d}{dt}\left[S^H\right] = \Lambda^H - \varphi^S S^H, \tag{6.3.28}$$

$$\frac{d}{dt}\left[S^V\right] = \Lambda^V - CS^V \tag{6.3.29}$$

Therefore, the matrices φ^S and C are non-singular M-matrices, where all their eigenvalues lie in the left half plane. Consequently, if S_h^H and S_h^V are the homogeneous solutions of system equations (6.3.28) and (6.3.29) respectively, then we have

$$\lim_{t\to\infty} S_h^H = 0 \quad \text{and} \quad \lim_{t\to\infty} S_h^V = 0 \tag{6.3.30}$$

From section (6.3.1) matrix φ^S is an irreducible, non-singular M-matrix. Therefore, the matrix φ has a positive inverse. $S_0^H = \left(\varphi^S\right)^{-1} \Lambda^H$ is a particular solution and $S^H = S_h^H + S_0^H$ is the general solution of equation (6.3.28). Similarly, the matrix C is a diagonal matrix with positive diagonal elements. Hence, C has an inverse with positive diagonal elements. Consequently, $S_0^V = (C)^{-1} \Lambda^V$ is a positive particular solution and $S^V = S_h^V + S_0^V$ is the general solution of equation (6.3.29). In addition,

$$\lim_{t\to\infty} S_i^H = S_{0i}^H, \lim_{t\to\infty} I_i^H = 0, \lim_{t\to\infty} P_i^V = 0, \lim_{t\to\infty} S_i^V = S_{0i}^V, \lim_{t\to\infty} I_i^V = 0, \lim_{t\to\infty} G_i^H = 0 \tag{6.3.31}$$

for all $\quad i = 1, 2, ..., n$

Therefore, as $t \to \infty$, we obtain the equilibrium point

$$E_0 = \left(S_0^H, \mathbf{0, 0, 0, 0}, ..., S_0^V, .. \mathbf{0, 0}\right) \tag{6.3.32}$$

where $\mathbf{0} = \underbrace{(0, ..., 0)}_{n \quad times}$, $S_0^H = \left(\varphi^S\right)^{-1} \Lambda^H$ and $S_0^V = (C)^{-1} \Lambda^V$ Therefore, the disease-free equilibrium is globally asymptotically stable if $\mathcal{R}_0 < 1$ and unstable if $\mathcal{R}_0 > 1$ □

Theorem 6.5. *If $\mathcal{R}_0 < 1$, then the disease-free equilibrium is globally asymptotically stable and unstable if $\mathcal{R}_0 > 1$*

6.4 The endemic equilibrium and its stability

6.4.1 The endemic equilibrium

When the equilibrium is endemic then the human population is infected by Malaria. The endemic equilibrium point of the multiscale model system (6.2.1) is defined by

$$E^* = (S_1^{H*}, I_1^{H*}, P_1^{V*}, S_1^{V*}, I_1^{V*}, G_1^{H*}, ..., S_n^{H*}, I_n^{H*}, P_n^{V*}, S_n^{V*}, I_n^{V*}, G_n^{H*}) \tag{6.4.1}$$

The six equations of the multiscale model system (6.2.1) are set to zero on the left-hand side to give:

$$\begin{aligned}
0 &= \Lambda_i^H - \lambda_i^V(t) S_i^H(t) - \mu_i^H S_i^H + \gamma_i^H I_i^H(t) + \sum_{j \neq i=1}^{n} \psi_{j,i}^S S_j^H - \sum_{j \neq i=1}^{n} \psi_{i,j}^S S_i^H, \\
0 &= \lambda_i^V(t) S_i^H(t) - (\mu_i^H + \delta_i^H + \gamma_i^H) I_i^H + \sum_{j \neq i=1}^{n} \psi_{j,i}^I I_j^H - \sum_{j \neq i=1}^{n} \psi_{i,j}^I I_i^H \\
0 &= N_i^v \alpha_i^v I_i^V(t) - \alpha_i^V P_i^V(t) \\
0 &= \Lambda_i^V - \lambda_i^H(t) S_i^V(t) - \mu_i^V S_i^V, \\
0 &= \lambda_i^H(t) S_i^V(t) - (\mu_i^V + \delta_i^V) I_i^V(t), \\
0 &= N_i^h \alpha_i^h I_i^H(t) - \alpha_i^H G_i^H(t)
\end{aligned} \tag{6.4.2}$$

The endemic equilibrium is denoted by $E^* = (S_1^{H*}, I_1^{H*}, P_1^{V*}, S_1^{V*}, I_1^{V*}, G_1^{H*}, ..., S_n^{H*}, I_n^{H*}, P_n^{V*}, S_n^{V*}, I_n^{V*}, G_n^{H*})$. The endemic value of the susceptible humans in patch i is given by

$$S_i^{H*} = \frac{\Lambda_i^H + \gamma_i^H I_i^{H*} + \sum_{j \neq i=1}^{n} \psi_{j,i}^S S_j^{H*}}{\left[\lambda_i^{V*} + \mu_i^H + \sum_{j \neq i=1}^{n} \psi_{i,j}^S\right]} \tag{6.4.3}$$

We deduce from equation (6.4.3) the endemic value of the susceptible human population in patch i is proportional to the mean time stayed in the susceptible compartments, the supply rate of new susceptibles via birth and rate of migration from another patch j. The individuals leave this compartment either through death, infection or migration of susceptible humans from patch i to patch j. The endemic value of the infected humans in patch i is defined by

$$I_i^{H*} = \frac{\lambda_i^{V*} S_i^{H*} + \sum_{j\neq i=1}^{n} \psi_{j,i}^{I} I_j^{H*}}{\left[\mu_i^H + \delta_i^H + \gamma_i^H + \sum_{j\neq i=1}^{n} \psi_{i,j}^{I}\right]} \tag{6.4.4}$$

We deduce from equation (6.4.4) that the value of infected humans in patch i is defined by the average time stayed in the infected compartment, the infection rate of susceptible humans and the number of susceptible hosts. The number of infected individuals is increased through migration from patch j to patch i and reduced through migration from patch i to patch j. The endemic value of the community sporozoite load in patch i is defined by

$$P_i^{V*} = \frac{N_i^v \alpha_i^v I_i^{V*}}{\alpha^V} \tag{6.4.5}$$

We deduce from equation (6.4.5) that the community sporozoite load in patch i is defined by the number of infected mosquitoes, the average sporozoite load within an infected mosquito and the elimination rate of community sporozoite load. The endemic value of infected mosquitoes in patch i is expressed as:

$$I_i^{V*} = \frac{\lambda_i^{H*} S_i^{V*}}{\left[\mu_i^V + \delta_i^V\right]} \tag{6.4.6}$$

We deduce from the expression (6.4.6) of the endemic value of mosquitoes that this quantity is the product of the infection rate of mosquitoes and the average life span of an infected mosquito. The endemic value of susceptible mosquitoes in patch i is described by

$$S_i^{V*} = \frac{\Lambda_i^V}{\left[\lambda_i^V + \mu_i^V\right]} \tag{6.4.7}$$

From the expression of the susceptible mosquitoes (6.4.7) that the quantity is a product of the supply rate of new susceptible mosquitoes and the mean time stayed in the susceptible class. The endemic value of the community gametocyte load in humans in patch i is given by

$$G_i^{H*} = \frac{N_i^h \alpha_i^h I_i^{H*}}{\alpha_i^H} \tag{6.4.8}$$

We deduce from equation (6.4.8) that the endemic value of the community gametocyte load depends on the number of infected humans and the mean gametocyte load within each infected human and the elimination rate of the community gametocyte load. The information above describes the endemic state of Malaria disease illustrated quantitatively by the endemic values of the multiscale model system (6.2.1).

Proposition 6.6. *Suppose that $\Psi^I = \left(\psi^I_{ij}\right)$ is irreducible. If $\mathcal{R}_0 > 1$, then the model system (6.2.1) is uniformly persistent and there exists an endemic equilibrium E^* in $\hat{\Omega}$.*

6.4.2 Global stability of the endemic equilibria and uniqueness

Theorem 6.7. *For $\mathcal{R}_0 > 1$ and claim an endemic equilibrium $E^* = (S_1^{H*}, I_1^{H*}, P_1^{V*}, S_1^{V*}, I_1^{V*}, G_1^{H*}, S_2^{H*}, I_2^{H*}, P_2^{V*}, S_2^{V*}, I_2^{V*}, G_2^{H*} ..., S_n^{H*}, I_n^{H*}, P_n^{V*}, S_n^{V*}, I_n^{V*}, G_n^{H*})$ exists. Suppose that one of the following assumptions is satisfied.*

(1) $\Psi^S = 0$ and Ψ^I is irreducible;

(2) $\Psi^I = 0$ and Ψ^S is irreducible;

(3) Ψ^S and Ψ^I are irreducible, and there exists $\lambda > 0$ such that $\psi^S_{j,i} S_j^{H*} = \lambda \psi^I_{j,i} I_j^{H*}$ for all $1 \leq i, j \leq n$.

where $\Psi^S = \left(\psi^S_{ij}\right)$ and $\Psi^I = \left(\psi^I_{ij}\right)$ are migration matrices for susceptible and infected humans respectively. Then E^* is unique and asymptotically stable in $\hat{\Omega}$.

By Proposition (6.6), the existence of a endemic equilibrium E^* is ensured if the assumption (1) or assumption (3) is satisfied.

Proof. This proof is completed through the implementation of the approach by [137]. In the proof we consider assumption (3) is fulfilled and then the remaining assumptions can be proved the same way. We now deduce the global asymptotic stability of E^* in $\hat{\Omega}$ which implies that E^* is necessarily unique.

$$
\begin{aligned}
1.\frac{dS_i^H(t)}{dt} &= \Lambda_i^H - \lambda_i^V(t) S_i^H(t) - \mu_i^H S_i^H + \gamma_i^H I_i^H(t) + \sum_{j \neq i=1}^{n} \psi^S_{j,i} S_j^H - \sum_{j \neq i=1}^{n} \psi^S_{i,j} S_i^H, \\
2.\frac{dI_i^H(t)}{dt} &= \lambda_i^V(t) S_i^H(t) - (\mu_i^H + \delta_i^H + \gamma_i^H) I_i^H + \sum_{j \neq i=1}^{n} \psi^I_{j,i} I_j^H - \sum_{j \neq i=1}^{n} \psi^I_{i,j} I_i^H \\
3.\frac{dP_i^V(t)}{dt} &= N_i^v \alpha_i^v I_i^V(t) - \alpha_i^V P_i^V(t) \qquad (6.4.1) \\
4.\frac{dS_i^V(t)}{dt} &= \Lambda_i^V - \lambda_i^H(t) S_i^V(t) - \mu_i^V S_i^V, \\
5.\frac{dI_i^V(t)}{dt} &= \lambda_i^H(t) S_i^V(t) - (\mu_i^V + \delta_i^V) I_i^V(t), \\
6.\frac{dG_i^H(t)}{dt} &= N_i^h \alpha_i^h I_i^H(t) - \alpha_i^H G_i^H(t)
\end{aligned}
$$

Set

$$V_i\left(S_i^H, I_i^H\right) = S_i^H - S_i^{H*} - S_i^{H*}\ln\frac{S_i^H}{S_i^{H*}} + I_i^H - I_i^{H*} - \ln\frac{I_i^H}{I_i^{H*}} \tag{6.4.2}$$

From equilibrium equations of (6.4.1), we obtain

$$0 = \Lambda_i^H - \lambda_i^V(t)S_i^H(t) - \mu_i^H S_i^H + \gamma_i^H I_i^H(t) + \sum_{j\neq i=1}^{n}\psi_{j,i}^S S_j^H - \sum_{j\neq i=1}^{n}\psi_{i,j}^S S_i^H, \tag{6.4.3}$$

$$\mu_i^H S_i^H = \Lambda_i^H - \lambda_i^V(t)S_i^H(t) + \gamma_i^H I_i^H(t) + \sum_{j\neq i=1}^{n}\psi_{j,i}^S S_j^H - \sum_{j\neq i=1}^{n}\psi_{i,j}^S S_i^H \tag{6.4.4}$$

$$\mu_i^H S_i^{H*} = \Lambda_i^H - \lambda_i^{V*}(t)S_i^{H*}(t) + \gamma_i^H I_i^{H*}(t) + \sum_{j\neq i=1}^{n}\psi_{j,i}^S S_j^{H*} - \sum_{j\neq i=1}^{n}\psi_{i,j}^S S_i^{H*} \tag{6.4.5}$$

$$0 = \lambda_i^V(t)S_i^H(t) - (\mu_i^H + \delta_i^H + \gamma_i^H)I_i^H + \sum_{j\neq i=1}^{n}\psi_{j,i}^I I_j^H - \sum_{j\neq i=1}^{n}\psi_{i,j}^I I_i^H \tag{6.4.6}$$

$$(\mu_i^H + \delta_i^H + \gamma_i^H)I_i^H = \lambda_i^V(t)S_i^H(t) + \sum_{j\neq i=1}^{n}\psi_{j,i}^I I_j^H - \sum_{j\neq i=1}^{n}\psi_{i,j}^I I_i^H \tag{6.4.7}$$

$$(\mu_i^H + \delta_i^H + \gamma_i^H)I_i^{H*} = \lambda_i^{V*}(t)S_i^{H*}(t) + \sum_{j\neq i=1}^{n}\psi_{j,i}^I I_j^{H*} - \sum_{j\neq i=1}^{n}\psi_{i,j}^I I_i^{H*} \tag{6.4.8}$$

We can highlight that $1 - x + \ln x \leq 0$ for $x > 0$ and equality holds if and only if $x = 1$. When we differentiate V_i along the solution of system (6.4.1), gives

$$\frac{dV_i}{dt} = \frac{\partial V_i}{\partial S_i^H}.\frac{dS_i^H}{dt} + \frac{\partial V_i}{\partial I_i^H}.\frac{dI_i^H}{dt} \tag{6.4.9}$$

$$\frac{dV_i}{dt} = \left(1 - \frac{S_i^{H*}}{S_i^H}\right).\frac{dS_i^H}{dt} + \left(1 - \frac{I_i^{H*}}{I_i^H}\right).\frac{dI_i^H}{dt} \tag{6.4.10}$$

Substituting equations in (6.4.1) into (6.4.10) we get

$$\frac{dV_i}{dt} = \left(1 - \frac{S_i^{H*}}{S_i^H}\right).\left(\Lambda_i^H - \lambda_i^V(t)S_i^H(t) - \mu_i^H S_i^H + \gamma_i^H I_i^H(t) + \sum_{j\neq i=1}^{n}\psi_{j,i}^S S_j^H - \sum_{j\neq i=1}^{n}\psi_{i,j}^S S_i^H\right)$$

$$+\left(1 - \frac{I_i^{H*}}{I_i^H}\right).\left(\lambda_i^V(t)S_i^H(t) - (\mu_i^H + \delta_i^H + \gamma_i^H)I_i^H + \sum_{j\neq i=1}^{n}\psi_{j,i}^I I_j^H - \sum_{j\neq i=1}^{n}\psi_{i,j}^I I_i^H\right) \tag{6.4.11}$$

$$\frac{dV_i}{dt} = \Lambda_i^H - \lambda_i^V(t)S_i^H(t) - \mu_i^H S_i^H + \gamma_i^H I_i^H(t) + \sum_{j\neq i=1}^{n} \psi_{j,i}^S S_j^H - \sum_{j\neq i=1}^{n} \psi_{i,j}^S S_i^H - \frac{S_i^{H*}}{S_i^H}\Lambda_i^H + \frac{S_i^{H*}}{S_i^H}\lambda_i^V S_i^H + \frac{S_i^{H*}}{S_i^H}\mu_i^H S_i^H$$

$$- \frac{S_i^{H*}}{S_i^H}\gamma_i^H I_i^H - \frac{S_i^{H*}}{S_i^H}\sum_{j=1}^{n}\psi_{ji}^S S_j^H + \frac{S_i^{H*}}{S_i^H}\sum_{j=1}^{n}\psi_{ij}^S S_i^H + \lambda_i^V(t)S_i^H(t) - (\mu_i^H + \delta_i^H + \gamma_i^H)I_i^H + \sum_{j\neq i=1}^{n}\psi_{j,i}^I I_j^H$$

$$- \sum_{j\neq i=1}^{n}\psi_{i,j}^I I_i^H - \frac{I_i^{H*}}{I_i^H}\lambda_i^V S_i^H + \frac{I_i^{H*}}{I_i^H}\left(\mu_i^H + \delta_i^H + \gamma_i^H\right)I_i^H - \frac{I_i^{H*}}{I_i^H}\sum_{j=1}^{n}\psi_{ji}^I I_j^H + \frac{I_i^{H*}}{I_i^H}\sum_{j=1}^{n}\psi_{ij}^I I_i^H \quad (6.4.12)$$

$$\frac{dV_i}{dt} = \Lambda_i^H - \lambda_i^V(t)S_i^H(t) - \mu_i^H S_i^H + \gamma_i^H I_i^H(t) + \sum_{j\neq i=1}^{n}\psi_{j,i}^S S_j^H - \sum_{j\neq i=1}^{n}\psi_{i,j}^S S_i^H - \Lambda_i^H\frac{S_i^{H*}}{S_i^H} + \lambda_i^V S_i^{H*} + \mu_i^H S_i^{H*}$$

$$- \gamma_i^H\frac{S_i^{H*}}{S_i^H}I_i^H - \sum_{j=1}^{n}\psi_{ji}^S S_j^H\frac{S_i^{H*}}{S_i^H} + \sum_{j=1}^{n}\psi_{ij}^S S_i^{H*} + \lambda_i^V(t)S_i^H(t) - (\mu_i^H + \delta_i^H + \gamma_i^H)I_i^H + \sum_{j\neq i=1}^{n}\psi_{j,i}^I I_j^H - \sum_{j\neq i=1}^{n}\psi_{i,j}^I I_i^H$$

$$- \lambda_i^V\frac{I_i^{H*}}{I_i^H}S_i^H + \left(\mu_i^H + \delta_i^H + \gamma_i^H\right)I_i^{H*} - \sum_{j=1}^{n}\psi_{ji}^I I_j^H\frac{I_i^{H*}}{I_i^H} + \sum_{j=1}^{n}\psi_{ij}^I I_i^{H*} \quad (6.4.13)$$

$$\begin{cases} \mu_i^H S_i^{H*} = \Lambda_i^H - \lambda_i^{V*}(t)S_i^{H*}(t) + \gamma_i^H I_i^{H*}(t) + \sum_{j\neq i=1}^{n}\psi_{j,i}^S S_j^{H*} - \sum_{j\neq i=1}^{n}\psi_{i,j}^S S_i^{H*} \\ \mu_i^H S_i^H = \Lambda_i^H\frac{S_i^H}{S_i^{H*}} - \lambda_i^{V*}(t)S_i^H(t) + \gamma_i^H I_i^{H*}(t)\frac{S_i^H}{S_i^{H*}} + \sum_{j=1}^{n}\psi_{ji}^S S_j^{H*}\frac{S_i^H}{S_i^{H*}} - \sum_{j=1}^{n}\psi_{ij}^S S_i^H \\ (\mu_i^H + \delta_i^H + \gamma_i^H)I_i^{H*} = \lambda_i^{V*}(t)S_i^{H*}(t) + \sum_{j\neq i=1}^{n}\psi_{j,i}^I I_j^{H*} - \sum_{j\neq i=1}^{n}\psi_{i,j}^I I_i^{H*} \\ (\mu_i^H + \delta_i^H + \gamma_i^H)I_i^H = \lambda_i^{V*}(t)S_i^{H*}(t)\frac{I_i^H}{I_i^{H*}} + \sum_{j\neq i=1}^{n}\psi_{j,i}^I I_j^{H*}\frac{I_i^H}{I_i^{H*}} - \sum_{j\neq i=1}^{n}\psi_{i,j}^I I_i^H \end{cases} \quad (6.4.14)$$

Substituting equations in (6.4.14) into (6.4.13) we get

$$\frac{dV_i}{dt} = \Lambda_i^H - \lambda_i^V(t)S_i^H(t) - \left(\Lambda_i^H \frac{S_i^H}{S_i^{H*}} - \lambda_i^{V*}(t)S_i^H(t) + \gamma_i^H I_i^{H*}(t)\frac{S_i^H}{S_i^{H*}} + \sum_{j=1}^{n}\psi_{ji}^S S_j^{H*}\frac{S_i^H}{S_i^{H*}} - \sum_{j=1}^{n}\psi_{ij}^S S_i^H\right)$$

$$+\gamma_i^H I_i^H(t) + \sum_{j\neq i=1}^{n}\psi_{j,i}^S S_j^H - \sum_{j\neq i=1}^{n}\psi_{i,j}^S S_i^H - \Lambda_i^H\frac{S_i^{H*}}{S_i^H} + \lambda_i^V S_i^{H*}$$

$$+\left(\Lambda_i^H - \lambda_i^{V*}(t)S_i^{H*}(t) + \gamma_i^H I_i^{H*}(t) + \sum_{j\neq i=1}^{n}\psi_{j,i}^S S_j^{H*} - \sum_{j\neq i=1}^{n}\psi_{i,j}^S S_i^{H*}\right)$$

$$-\gamma_i^H\frac{S_i^{H*}}{S_i^H}I_i^H - \sum_{j=1}^{n}\psi_{ji}^S S_j^H\frac{S_i^{H*}}{S_i^H} + \sum_{j=1}^{n}\psi_{ij}^S S_i^{H*} + \lambda_i^V(t)S_i^H(t)$$

$$-\left(\lambda_i^{V*}(t)S_i^{H*}(t)\frac{I_i^H}{I_i^{H*}} + \sum_{j\neq i=1}^{n}\psi_{j,i}^I I_j^{H*}\frac{I_i^H}{I_i^{H*}} - \sum_{j\neq i=1}^{n}\psi_{i,j}^I I_i^H\right) + \sum_{j\neq i=1}^{n}\psi_{j,i}^I I_j^H - \sum_{j\neq i=1}^{n}\psi_{i,j}^I I_i^H$$

$$-\lambda_i^V\frac{I_i^{H*}}{I_i^H}S_i^H + \left(\lambda_i^{V*}(t)S_i^{H*}(t) + \sum_{j\neq i=1}^{n}\psi_{j,i}^I I_j^{H*} - \sum_{j\neq i=1}^{n}\psi_{i,j}^I I_i^{H*}\right) - \sum_{j=1}^{n}\psi_{ji}^I I_j^H\frac{I_i^{H*}}{I_i^H} + \sum_{j=1}^{n}\psi_{ij}^I I_i^{H*} \tag{6.4.15}$$

Simplifying (6.4.15) we obtain

$$\frac{dV_i}{dt} = \Lambda_i^H - \lambda_i^V(t)S_i^H(t) - \Lambda_i^H\frac{S_i^H}{S_i^{H*}} + \lambda_i^{V*}(t)S_i^H(t) - \gamma_i^H I_i^{H*}(t)\frac{S_i^H}{S_i^{H*}} - \sum_{j=1}^{n}\psi_{ji}^S S_j^{H*}\frac{S_i^H}{S_i^{H*}} + \sum_{j=1}^{n}\psi_{ij}^S S_i^H$$

$$+\gamma_i^H I_i^H(t) + \sum_{j\neq i=1}^{n}\psi_{j,i}^S S_j^H - \sum_{j\neq i=1}^{n}\psi_{i,j}^S S_i^H - \Lambda_i^H\frac{S_i^{H*}}{S_i^H} + \lambda_i^V S_i^{H*}$$

$$+\Lambda_i^H - \lambda_i^{V*}(t)S_i^{H*}(t) + \gamma_i^H I_i^{H*}(t) + \sum_{j\neq i=1}^{n}\psi_{j,i}^S S_j^{H*} - \sum_{j\neq i=1}^{n}\psi_{i,j}^S S_i^{H*}$$

$$-\gamma_i^H\frac{S_i^{H*}}{S_i^H}I_i^H - \sum_{j=1}^{n}\psi_{ji}^S S_j^H\frac{S_i^{H*}}{S_i^H} + \sum_{j=1}^{n}\psi_{ij}^S S_i^{H*} + \lambda_i^V(t)S_i^H(t)$$

$$-\lambda_i^{V*}(t)S_i^{H*}(t)\frac{I_i^H}{I_i^{H*}} - \sum_{j\neq i=1}^{n}\psi_{j,i}^I I_j^{H*}\frac{I_i^H}{I_i^{H*}} + \sum_{j\neq i=1}^{n}\psi_{i,j}^I I_i^H + \sum_{j\neq i=1}^{n}\psi_{j,i}^I I_j^H - \sum_{j\neq i=1}^{n}\psi_{i,j}^I I_i^H$$

$$-\lambda_i^V \frac{I_i^{H*}}{I_i^H} S_i^H + \lambda_i^{V*}(t) S_i^{H*}(t) + \sum_{j\neq i=1}^{n} \psi_{j,i}^I I_j^{H*} - \sum_{j\neq i=1}^{n} \psi_{i,j}^I I_i^{H*} - \sum_{j=1}^{n} \psi_{ji}^I I_j^H \frac{I_i^{H*}}{I_i^H} + \sum_{j=1}^{n} \psi_{ij}^I I_i^{H*} \quad (6.4.16)$$

$$\frac{dV_i}{dt} = \Lambda_i^H - \cancelto{0}{\lambda_i^V(t) S_i^H(t)} - \Lambda_i^H \frac{S_i^H}{S_i^{H*}} + \lambda_i^{V*}(t) S_i^H(t) - \gamma_i^H I_i^{H*}(t) \frac{S_i^H}{S_i^{H*}} - \sum_{j=1}^{n} \psi_{ji}^S S_j^{H*} \frac{S_i^H}{S_i^{H*}} + \sum_{j=1}^{n} \cancelto{0}{\psi_{ij}^S S_i^H}$$

$$+\gamma_i^H I_i^H(t) + \sum_{j\neq i=1}^{n} \psi_{j,i}^S S_j^H - \sum_{j\neq i=1}^{n} \cancelto{0}{\psi_{i,j}^S S_i^H} - \Lambda_i^H \frac{S_i^{H*}}{S_i^H} + \lambda_i^V S_i^{H*}$$

$$+\Lambda_i^H - \cancelto{0}{\lambda_i^{V*}(t) S_i^{H*}(t)} + \gamma_i^H I_i^{H*}(t) + \sum_{j\neq i=1}^{n} \psi_{j,i}^S S_j^{H*} - \sum_{j\neq i=1}^{n} \cancelto{0}{\psi_{i,j}^S S_i^{H*}}$$

$$-\gamma_i^H \frac{S_i^{H*}}{S_i^H} I_i^H - \sum_{j=1}^{n} \psi_{ji}^S S_j^H \frac{S_i^{H*}}{S_i^H} + \sum_{j=1}^{n} \cancelto{0}{\psi_{ij}^S S_i^{H*}} + \cancelto{0}{\lambda_i^V(t) S_i^H(t)}$$

$$-\lambda_i^{V*}(t) S_i^{H*}(t) \frac{I_i^H}{I_i^{H*}} - \sum_{j\neq i=1}^{n} \psi_{j,i}^I I_j^{H*} \frac{I_i^H}{I_i^{H*}} + \sum_{j\neq i=1}^{n} \cancelto{0}{\psi_{i,j}^I I_i^{H*}} + \sum_{j\neq i=1}^{n} \psi_{j,i}^I I_j^H - \sum_{j\neq i=1}^{n} \cancelto{0}{\psi_{i,j}^I I_i^H}$$

$$-\lambda_i^V \frac{I_i^{H*}}{I_i^H} S_i^H + \cancelto{0}{\lambda_i^{V*}(t) S_i^{H*}(t)} + \sum_{j\neq i=1}^{n} \psi_{j,i}^I I_j^{H*} - \sum_{j\neq i=1}^{n} \cancelto{0}{\psi_{i,j}^I I_i^{H*}} - \sum_{j=1}^{n} \psi_{ji}^I I_j^H \frac{I_i^{H*}}{I_i^H} + \sum_{j=1}^{n} \cancelto{0}{\psi_{ij}^I I_i^{H*}} \quad (6.4.17)$$

$$\frac{dV_i}{dt} = \Lambda_i^H - \Lambda_i^H \frac{S_i^H}{S_i^{H*}} + \Lambda_i^H - \Lambda_i^H \frac{S_i^{H*}}{S_i^H}$$

$$+\lambda_i^{V*} S_i^H + \lambda_i^V S_i^{H*} - \lambda_i^V \frac{I_i^{H*}}{I_i^H} S_i^H - \lambda_i^{V*}(t) S_i^{H*}(t) \frac{I_i^H}{I_i^{H*}}$$

$$+\gamma_i^H I_i^H(t) - \gamma_i^H \frac{S_i^{H*}}{S_i^H} I_i^H - \gamma_i^H I_i^{H*}(t) \frac{S_i^H}{S_i^{H*}} + \gamma_i^H I_i^{H*}(t)$$

$$-\sum_{j=1}^{n} \psi_{ji}^S S_j^{H*} \frac{S_i^H}{S_i^{H*}} - \sum_{j=1}^{n} \psi_{ji}^S S_j^H \frac{S_i^{H*}}{S_i^H} + \sum_{j\neq i=1}^{n} \psi_{j,i}^S S_j^H + \sum_{j\neq i=1}^{n} \psi_{j,i}^S S_j^{H*}$$

$$-\sum_{j\neq i=1}^{n} \psi_{j,i}^I I_j^{H*} \frac{I_i^H}{I_i^{H*}} + \sum_{j\neq i=1}^{n} \psi_{j,i}^I I_j^H + \sum_{j\neq i=1}^{n} \psi_{j,i}^I I_j^{H*} - \sum_{j=1}^{n} \psi_{ji}^I I_j^H \frac{I_i^{H*}}{I_i^H} \quad (6.4.18)$$

Therefore

$$\frac{dV_i}{dt} = \Lambda_i^H - \Lambda_i^H \frac{S_i^H}{S_i^{H*}} + \Lambda_i^H - \Lambda_i^H \frac{S_i^{H*}}{S_i^H} + \Lambda_i^H \ln \frac{S_i^H}{S_i^{H*}} - \Lambda_i^H \ln \frac{S_i^H}{S_i^{H*}}$$

$$+\lambda_i^{V*} S_i^H \left[1 - \frac{S_i^{H*} I_i^H}{S_i^H I_i^{H*}} + \ln \frac{S_i^{H*} I_i^H}{S_i^H I_i^{H*}} - \ln \frac{S_i^{H*} I_i^H}{S_i^H I_i^{H*}}\right] + \lambda_i^V S_i^{H*} \left[1 - \frac{S_i^H I_i^{H*}}{S_i^{H*} I_i^H} + \ln \frac{S_i^H I_i^{H*}}{S_i^{H*} I_i^H} - \ln \frac{S_i^H I_i^{H*}}{S_i^{H*} I_i^H}\right]$$

$$+\gamma_i^H I_i^H(t) \left[1 - \frac{S_i^{H*}}{S_i^H} + \ln \frac{S_i^{H*}}{S_i^H} - \ln \frac{S_i^{H*}}{S_i^H}\right] + \gamma_i^H I_i^{H*}(t) \left[1 - \frac{S_i^H}{S_i^{H*}} + \ln \frac{S_i^H}{S_i^{H*}} - \ln \frac{S_i^H}{S_i^{H*}}\right]$$

$$+ \sum_{j \neq i=1}^{n} \psi_{j,i}^S S_j^{H*} \left[1 - \frac{S_i^H}{S_i^{H*}} + \frac{S_j^H}{S_j^{H*}} - \frac{S_j^H S_i^{H*}}{S_j^{H*} S_i^H} + \ln \frac{S_j^H S_i^{H*}}{S_j^{H*} S_i^H} - \ln \frac{S_j^H S_i^{H*}}{S_j^{H*} S_i^H}\right]$$

$$+ \sum_{j \neq i=1}^{n} \psi_{j,i}^I I_j^{H*} \left[1 - \frac{I_i^H}{I_i^{H*}} + \frac{I_j^H}{I_j^{H*}} - \frac{I_j^H I_i^{H*}}{I_j^{H*} I_i^H} + \ln \frac{I_j^H I_i^{H*}}{I_j^{H*} I_i^H} - \ln \frac{I_j^H I_i^{H*}}{I_j^{H*} I_i^H}\right] \tag{6.4.19}$$

$$\frac{dV_i}{dt} = \Lambda_i^H \left[1 - \frac{S_i^H}{S_i^{H*}} + 1 - \frac{S_i^{H*}}{S_i^H} + \ln \frac{S_i^H}{S_i^{H*}} - \ln \frac{S_i^H}{S_i^{H*}}\right]$$

$$+\lambda_i^{V*} S_i^H \left[1 - \frac{S_i^{H*} I_i^H}{S_i^H I_i^{H*}} + \ln \frac{S_i^{H*} I_i^H}{S_i^H I_i^{H*}}\right] - \lambda_i^{V*} S_i^H \ln \frac{S_i^{H*} I_i^H}{S_i^H I_i^{H*}} + \lambda_i^V S_i^{H*} \left[1 - \frac{S_i^H I_i^{H*}}{S_i^{H*} I_i^H} + \ln \frac{S_i^H I_i^{H*}}{S_i^{H*} I_i^H}\right]$$

$$-\lambda_i^V S_i^{H*} \ln \frac{S_i^H I_i^{H*}}{S_i^{H*} I_i^H} + \gamma_i^H I_i^H(t) \left[1 - \frac{S_i^{H*}}{S_i^H} + \ln \frac{S_i^{H*}}{S_i^H}\right] - \gamma_i^H I_i^H(t) \ln \frac{S_i^{H*}}{S_i^H} + \gamma_i^H I_i^{H*}(t) \left[1 - \frac{S_i^H}{S_i^{H*}} + \ln \frac{S_i^H}{S_i^{H*}}\right]$$

$$-\gamma_i^H I_i^{H*}(t) \ln \frac{S_i^H}{S_i^{H*}} + \sum_{j \neq i=1}^{n} \psi_{j,i}^S S_j^{H*} \left[1 - \frac{S_i^H}{S_i^{H*}} + \frac{S_j^H}{S_j^{H*}} - \frac{S_j^H S_i^{H*}}{S_j^{H*} S_i^H} + \ln \frac{S_j^H S_i^{H*}}{S_j^{H*} S_i^H} - \ln \frac{S_j^H S_i^{H*}}{S_j^{H*} S_i^H}\right]$$

$$+ \sum_{j \neq i=1}^{n} \psi_{j,i}^I I_j^{H*} \left[1 - \frac{I_i^H}{I_i^{H*}} + \frac{I_j^H}{I_j^{H*}} - \frac{I_j^H I_i^{H*}}{I_j^{H*} I_i^H} + \ln \frac{I_j^H I_i^{H*}}{I_j^{H*} I_i^H} - \ln \frac{I_j^H I_i^{H*}}{I_j^{H*} I_i^H}\right] \tag{6.4.20}$$

$$\frac{dV_i}{dt} = \Lambda_i^H \left[1 - \frac{S_i^H}{S_i^{H*}} + 1 - \frac{S_i^{H*}}{S_i^H} + \ln \frac{S_i^H}{S_i^{H*}} - \ln \frac{S_i^H}{S_i^{H*}}\right]$$

$$+\lambda_i^{V*} S_i^H \left[1 - \frac{S_i^{H*} I_i^H}{S_i^H I_i^{H*}} + \ln \frac{S_i^{H*} I_i^H}{S_i^H I_i^{H*}}\right] + \lambda_i^V S_i^{H*} \left[1 - \frac{S_i^H I_i^{H*}}{S_i^{H*} I_i^H} + \ln \frac{S_i^H I_i^{H*}}{S_i^{H*} I_i^H}\right] + \ln \frac{S_i^{H*} I_i^H}{S_i^H I_i^{H*}} \left(\lambda_i^V S_i^{H*} - \lambda_i^{V*} S_i^H\right)$$

$$+\gamma_i^H I_i^H(t)\left[1-\frac{S_i^{H*}}{S_i^H}+\ln\frac{S_i^{H*}}{S_i^H}\right]+\gamma_i^H I_i^{H*}(t)\left[1-\frac{S_i^H}{S_i^{H*}}+\ln\frac{S_i^H}{S_i^{H*}}\right]+\gamma_i^H\ln\frac{S_i^H}{S_i^{H*}}\left(I_i^H(t)-I_i^{H*}(t)\right)$$

$$+\sum_{j\neq i=1}^{n}\psi_{j,i}^S S_j^{H*}\left[1-\frac{S_j^H S_i^{H*}}{S_j^{H*}S_i^H}+\ln\frac{S_j^H S_i^{H*}}{S_j^{H*}S_i^H}\right]+\sum_{j\neq i=1}^{n}\psi_{j,i}^S S_j^{H*}\left[-\frac{S_i^H}{S_i^{H*}}+\frac{S_j^H}{S_j^{H*}}-\ln\frac{S_j^H}{S_j^{H*}}-\ln\frac{S_i^{H*}}{S_i^H}\right]$$

$$+\sum_{j\neq i=1}^{n}\psi_{j,i}^I I_j^{H*}\left[1-\frac{I_j^H I_i^{H*}}{I_j^{H*}I_i^H}+\ln\frac{I_j^H I_i^{H*}}{I_j^{H*}I_i^H}\right]+\sum_{j\neq i=1}^{n}\psi_{j,i}^I I_j^{H*}\left[-\frac{I_i^H}{I_i^{H*}}+\frac{I_j^H}{I_j^{H*}}-\ln\frac{I_j^H}{I_j^{H*}}-\ln\frac{I_i^{H*}}{I_i^H}\right] \tag{6.4.21}$$

where $\lambda_i^V S_i^{H*}\leq\lambda_i^{V*}S_i^H$ and $I_i^H(t)\leq I_i^{H*}(t)$

$$\frac{dV_i}{dt}=\Lambda_i^H\left[1-\frac{S_i^H}{S_i^{H*}}+1-\frac{S_i^{H*}}{S_i^H}+\ln\frac{S_i^H}{S_i^{H*}}-\ln\frac{S_i^H}{S_i^{H*}}\right]$$

$$+\lambda_i^{V*}S_i^H\left[1-\frac{S_i^{H*}I_i^H}{S_i^H I_i^{H*}}+\ln\frac{S_i^{H*}I_i^H}{S_i^H I_i^{H*}}\right]+\lambda_i^V S_i^{H*}\left[1-\frac{S_i^H I_i^{H*}}{S_i^{H*}I_i^H}+\ln\frac{S_i^H I_i^{H*}}{S_i^{H*}I_i^H}\right]+\ln\frac{S_i^{H*}I_i^H}{S_i^H I_i^{H*}}\left(\lambda_i^V S_i^{H*}-\lambda_i^{V*}S_i^H\right)$$

$$+\gamma_i^H I_i^H(t)\left[1-\frac{S_i^{H*}}{S_i^H}+\ln\frac{S_i^{H*}}{S_i^H}\right]+\gamma_i^H I_i^{H*}(t)\left[1-\frac{S_i^H}{S_i^{H*}}+\ln\frac{S_i^H}{S_i^{H*}}\right]+\gamma_i^H\ln\frac{S_i^H}{S_i^{H*}}\left(I_i^H(t)-I_i^{H*}(t)\right)$$

$$+\sum_{j\neq i=1}^{n}\psi_{j,i}^S S_j^{H*}\left[1-\frac{S_j^H S_i^{H*}}{S_j^{H*}S_i^H}+\ln\frac{S_j^H S_i^{H*}}{S_j^{H*}S_i^H}\right]+\sum_{j\neq i=1}^{n}\psi_{j,i}^S S_j^{H*}\left[\frac{S_j^H}{S_j^{H*}}+\ln\frac{S_j^{H*}}{S_j^H}-\frac{S_i^H}{S_i^{H*}}-\ln\frac{S_i^{H*}}{S_i^H}\right]$$

$$+\sum_{j\neq i=1}^{n}\psi_{j,i}^I I_j^{H*}\left[1-\frac{I_j^H I_i^{H*}}{I_j^{H*}I_i^H}+\ln\frac{I_j^H I_i^{H*}}{I_j^{H*}I_i^H}\right]+\sum_{j\neq i=1}^{n}\psi_{j,i}^I I_j^{H*}\left[\frac{I_j^H}{I_j^{H*}}+\ln\frac{I_j^{H*}}{I_j^H}-\frac{I_i^H}{I_i^{H*}}-\ln\frac{I_i^{H*}}{I_i^H}\right] \tag{6.4.22}$$

$$\leq\sum_{j\neq i=1}^{n}\psi_{j,i}^S S_j^{H*}\left[\frac{S_j^H}{S_j^{H*}}+\ln\frac{S_j^{H*}}{S_j^H}-\frac{S_i^H}{S_i^{H*}}-\ln\frac{S_i^{H*}}{S_i^H}\right]+\sum_{j\neq i=1}^{n}\psi_{j,i}^I I_j^{H*}\left[\frac{I_j^H}{I_j^{H*}}+\ln\frac{I_j^{H*}}{I_j^H}-\frac{I_i^H}{I_i^{H*}}-\ln\frac{I_i^{H*}}{I_i^H}\right] \tag{6.4.23}$$

$$= \sum_{j\neq i=1}^{n} \lambda\psi_{j,i}^{I} I_j^{H*} \left[\frac{S_j^H}{S_j^{H*}} + \ln \frac{S_j^{H*}}{S_j^H} - \frac{S_i^H}{S_i^{H*}} - \ln \frac{S_i^{H*}}{S_i^H} \right] + \sum_{j\neq i=1}^{n} \psi_{j,i}^{I} I_j^{H*} \left[\frac{I_j^H}{I_j^{H*}} + \ln \frac{I_j^{H*}}{I_j^H} - \frac{I_i^H}{I_i^{H*}} - \ln \frac{I_i^{H*}}{I_i^H} \right] \tag{6.4.24}$$

$$= \sum_{j\neq i=1}^{n} \psi_{j,i}^{I} I_j^{H*} \left[\left(\lambda \frac{S_j^H}{S_j^{H*}} + \lambda \ln \frac{S_j^{H*}}{S_j^H} + \frac{I_j^H}{I_j^{H*}} + \ln \frac{I_j^{H*}}{I_j^H} \right) - \left(\lambda \frac{S_i^H}{S_i^{H*}} + \lambda \ln \frac{S_i^{H*}}{S_i^H} + \frac{I_i^H}{I_i^{H*}} + \ln \frac{I_i^{H*}}{I_i^H} \right) \right] \tag{6.4.25}$$

$$= \sum_{j=1}^{n} \psi_{j,i}^{I} I_j^{H*} \left[H_j(S_j^H, I_j^H) - H_i(S_i^H, I_i^H) \right] \tag{6.4.26}$$

where

$$H_i(S_i^H, I_i^H) = \lambda \frac{S_i^H}{S_i^{H*}} + \lambda \ln \frac{S_i^{H*}}{S_i^H} + \frac{I_i^H}{I_i^{H*}} + \ln \frac{I_i^{H*}}{I_i^H} \tag{6.4.27}$$

We let a weight matrix $\mathcal{W} = (w_{ij})$ with entry $w_{ij} = \psi_{j,i}^{I} I_j^{H*}$ and indicate the equivalent weighted digraph as $(\mathcal{H}, \mathcal{W})$. Letting $c_i = \sum_{\mathcal{T}\in\mathbb{T}_i} w(\mathcal{T}) \geq 0$ be as expressed in (B.1) in the Appendix 7.3 with $(\mathcal{H}, \mathcal{W})$. Therefore, by (B.2) in Appendix 7.3, the identity below is satisfied

$$\sum_{i=1}^{n} c_i \sum_{j=1}^{n} \psi_{j,i}^{I} I_j^{H*} \left[H_j(S_j^H, I_j^H) - H_i(S_i^H, I_i^H) \right] = 0 \tag{6.4.28}$$

Setting

$$V\left(S_1^H, I_1^H, S_2^H, I_2^H, ..., S_n^H I_n^H\right) = \sum_{i=1}^{n} c_i V_i\left(S_i^H, I_i^H\right) \tag{6.4.29}$$

Taking (6.4.13) and (6.4.28) we get

$$\frac{dV}{dt} = c_i \frac{dV_i}{dt} \leq \sum_{i=1}^{n} c_i \sum_{j=1}^{n} \psi_{j,i}^{I} I_j^{H*} \left[H_j(S_j^H, I_j^H) - H_i(S_i^H, I_i^H) \right] = 0 \tag{6.4.30}$$

for all $(S_1^H, I_1^H, ..., S_n^H I_n^H) \in \tilde{\Omega}$. Consequently, V is a Lyapunov function for the system (6.4.1). In view of the fact that $\Psi^I = \left(\psi_{ij}^I\right)$ is irreducible, we know that $c_i > 0 \; \forall \; i$ (see the Appendix 7.3), and therefore $dV_i/dt = 0$ suggests that $S_i^H = S_i^{H*}$ for all i. From the first equation of system (6.4.1), we obtain

$$0 = \frac{dS_i^H(t)}{dt} = \Lambda_i^H - \lambda_i^V(t) S_i^H(t) - \mu_i^H S_i^H + \gamma_i^H I_i^H(t) + \sum_{j\neq i=1}^{n} \psi_{j,i}^{S} S_j^H - \sum_{j\neq i=1}^{n} \psi_{i,j}^{S} S_i^H \tag{6.4.31}$$

$i = 1, 2, ..., n$, suggesting that $I_i^H = I_i^{H*}$ for all i. The only invariant set on which $dV_i/dt = 0$ is the singleton $\{P^*\}$. Hence, by LaSalle Invariance Principle [138], P^* is globally asymptotically stable in $\tilde{\Omega}$. □

6.4.3 Uniqueness and global solution of stochastic model

We consider a stochastic model adopted from (6.2.1) and implementing the same approach used in (4.5.1) of chapter 4

$$\begin{cases} dS_i^H(t) = \left(\Lambda_i^H - \dfrac{\beta_i^V P_i^V(t)}{P_{0i} + P_i^V(t)} S_i^H(t) - \mu_i^H S_i^H(t) + \gamma_i^H I_i^H(t) + \displaystyle\sum_{j\neq i=1}^{n} \psi_{j,i}^S S_j^H - \sum_{j\neq i=1}^{n} \psi_{i,j}^S S_i^H\right) dt + S_i^H(t)\sigma_{S^H} dW_{S^H} \\ dI_i^H(t) = \left(\dfrac{\beta_i^V P_i^V(t)}{P_{0i} + P_i^V(t)} S_i^H(t) - (\mu_i^H + \delta_i^H + \gamma_i^H) I_i^H + \displaystyle\sum_{j\neq i=1}^{n} \psi_{j,i}^I I_j^H - \sum_{j\neq i=1}^{n} \psi_{i,j}^I I_i^H\right) dt + I_i^H(t)\sigma_{I^H} dW_{I^H} \\ dP_i^V(t) = \left(N_i^v \alpha_i^v I_i^V(t) - \alpha_i^V P_i^V(t)\right) dt \\ dS_i^V(t) = \left(\Lambda_i^V - \dfrac{\beta_i^H G_i^H(t)}{G_{0i} + G_i^H(t)} S_i^V(t) - \mu_i^V S_i^V\right) dt \\ dI_i^V(t) = \left(\dfrac{\beta_i^H G_i^H(t)}{G_{0i} + G_i^H(t)} S_i^V(t) - (\mu_i^V + \delta_i^V) I_i^V(t)\right) dt \\ dG_i^H(t) = \left(N_i^h \alpha_i^h I_i^H(t) - \alpha_i^H G_i^H(t)\right) dt \end{cases} \tag{6.4.1}$$

In this section, we first prove that all the solutions of the system are positive. Suppose $\left(\Omega; \mathcal{F}; \{\mathcal{F}\}_{t\geq t_0} P\right)$ is a complete probability space with filtration $\{\mathcal{F}_t\}_{t\geq 0}$ meeting the usual conditions (i.e. it is increasing and continuous while $\{\mathcal{F}_0\}$ contains all P-null sets). Set $C^{2,1}\left(\mathbb{R}^4 \times [0,\infty); \mathbb{R}_+\right)$ to be the family of all nonnegative functions $V(x,t)$ defined on $\mathbb{R}^4 \times [0,\infty)$ which are continuously twice differentiable in x and once in t. Suppose $W(t) = (W_{S^H}(t), W_{I^H}(t))$ a 2-dimensional Wiener process defined on this probability space. The non-negative constants σ_{S^H} and σ_{I^H} define the intensities of the stochastic pertubations. Let us presume that the components of the 1-dimensional Wiener process W_i are mutually independent. We have to demonstrate that the stochasic differential equation model (6.4.1) has at least a unique global solution for the model to make sense and also that the solution will remain positive whenever the initial conditions are positive.

Theorem 6.8. *For multiscale model (6.4.1) and any initial value in $\mathbb{R}_+^{6n}$, there is a unique solution $L = \left(S_i^H(t), I_i^H(t), P_i^V(t), S_i^V(t), I_i^V(t), G_i^H\right)_{i=1,2,...,n}$, of the multiscale system (6.4.1) for $t \geq 0$ which will remain in $\mathbb{R}_+^{6n}$ with probability one.*

Proof. The total human host population in the multiscale model system (6.4.1) is given by $N_i^H = S_i^H + I_i^H$. Therefore we have

$$dN_i^H = dS_i^H + dI_i^H \tag{6.4.2}$$

$$= \left(\Lambda_i^H - \frac{\beta_i^V P_i^V(t)}{P_{0i} + P_i^V(t)} S_i^H(t) - \mu_i^H S_i^H(t) + \gamma_i^H I_i^H(t) + \sum_{j \neq i=1}^{n} \psi_{j,i}^S S_j^H - \sum_{j \neq i=1}^{n} \psi_{i,j}^S S_i^H \right) dt$$

$$+ S_i^H(t)\sigma_{S^H} dW_{S^H} + \left(\frac{\beta_i^V P_i^V(t)}{P_{0i} + P_i^V(t)} S_i^H(t) - (\mu_i^H + \delta_i^H + \gamma_i^H) I_i^H + \sum_{j \neq i=1}^{n} \psi_{j,i}^I I_j^H - \sum_{j \neq i=1}^{n} \psi_{i,j}^I I_i^H \right) dt$$

$$+ I_i^H(t)\sigma_{I^H} dW_{I^H} \tag{6.4.3}$$

$$= \left(\Lambda_i^H - \mu_i^H S_i^H(t) + \sum_{j \neq i=1}^{n} \psi_{j,i}^S S_j^H - \sum_{j \neq i=1}^{n} \psi_{i,j}^S S_i^H \right) dt + S_i^H(t)\sigma_{S^H} dW_{S^H}$$

$$+ \left(-(\mu_i^H + \delta_i^H) I_i^H + \sum_{j \neq i=1}^{n} \psi_{j,i}^I I_j^H - \sum_{j \neq i=1}^{n} \psi_{i,j}^I I_i^H \right) dt + I_i^H(t)\sigma_{I^H} dW_{I^H} \tag{6.4.4}$$

$$= \left[\Lambda_i^H - \mu_i^H N_i^H - \delta_i^H I_i^H + \sum_{j \neq i=1}^{n} \psi_{j,i}^Q N_j^H - \sum_{j \neq i=1}^{n} \psi_{i,j}^Q N_i^H \right] dt + S_i^H(t)\sigma_{S^H} dW_{S^H} + I_i^H(t)\sigma_{I^H} dW_{I^H} \tag{6.4.5}$$

$$dN_i^H < \left[\Lambda_i^H + \sum_{j \neq i=1}^{n} \psi_{j,i}^Q N_j^H - \left(\mu_i^H N_i^H + \sum_{j \neq i=1}^{n} \psi_{i,j}^Q N_i^H \right) \right] \tag{6.4.6}$$

$$dN_i^H < \left[\Lambda_i^H - \varphi N_i^H \right] a.s \tag{6.4.7}$$

where

$$\begin{cases} \Lambda_i^H = \sum_{j \neq i=1}^{n} \psi_{j,i}^Q N_j^H + \Lambda_i^H \quad \text{for} \quad Q = S, \quad \text{and} \quad j = 1, .., n, j \neq i \\ \varphi = \mu_i^H + \sum_{j \neq i=1}^{n} \psi_{i,j}^Q \end{cases} \tag{6.4.8}$$

The total human population in the multiscale model system (6.4.1) validates the equation (6.4.7) with the initial value $N_i^H(0) = S_i^H(0) + I_i^H(0)$, if $\left(S_i^H(s), I_i^H(s)\right)_{i=1,2,...n} \in \mathbb{R}_+^{2n} \; \forall \, 0 \leq s \leq t$ almost surely (a.s)

Therefore, through integration we can verify

$$N_i^H \leq \frac{\Lambda_i^H}{\varphi} + \left(N_i^H(0) - \frac{\Lambda_i^H}{\varphi}\right) exp\left(-\varphi s\right) \text{ for all } s \in [0,1] \text{ a.s} \tag{6.4.9}$$

Therefore, $N_i^H \leq \frac{\Lambda_i^H}{\varphi}$ if we assume $N_i^H(0) \leq \frac{\Lambda_i^H}{\varphi}$ such that

$$\left(S_i^H(s), I_i^H(s)\right)_{i=1,2,\ldots n} \in \left(0, \frac{\Lambda_i^H}{\varphi}\right) \text{ for all } s \in [0,1] \text{ a.s} \tag{6.4.10}$$

We remark that the coefficients of the multiscale model system (6.4.1) are locally Lipschitz continuous, for any given initial value, there is a unique maximal local solution $L = \left(S_i^H(t), I_i^H(t), P_i^V(t), S_i^V(t), I_i^V(t), G_i^H\right)_{i=1,2,\ldots,n}$ on $t \in [0, \tau_e)$, where τ_e is the explosion time (see example, [152]).

In order to demonstrate that this solution is global, we have to reveal that $\tau_e = \infty$ almost surely (a.s). We let $m_0 > 0$ such that $\left(S_i^H(0), I_i^H(0), P_i^V(0), S_i^V(0), I_i^V(0), G_i^H(0)\right)_{i=1,2,\ldots,n} \in [\frac{1}{m_0}, m_0)$. For each integer $m \geq m_0$, define a sequence of stopping times by

$$\tau_m = \inf\left\{t \in [0, \tau_e) : S^H(t), I^H(t) \notin \left(\frac{1}{m}, m\right)\right\} \tag{6.4.11}$$

setting $\inf \emptyset = \infty$. Therefore, since τ_m is non-decreasing, the following limit exists: $\tau_\infty = \lim_{m\to\infty} \tau_m$, and $\tau_{infty} \leq \tau_e$ (a.s). We have to demonstrate that $\tau_{infty} = \infty$ a.s. If this statement is infringed, then there exists $T > 0$ and $\epsilon \in (0,1)$ such that

$$\mathbb{P}\left\{\tau_\infty \leq T\right\} \geq \epsilon \tag{6.4.12}$$

Therefore, there is an integer $m_1 \geq m_0$ such that $\mathbb{P}\left\{\tau_m \leq T\right\} \geq \epsilon$, for all $m \geq m_1$. Define a C^2-function $V : \mathbb{R}_+^{2n}$ by

$$V(L) = \sum_{i=1}^{n} \left[\left(S_i^H - 1 - \ln S_i^H\right) + \left(I_i^H - 1 - \ln I_i^H\right) + \left(P_i^V - 1 - \ln P_i^V\right)\right]$$

$$+ \left[\left(S_i^V - 1 - \ln S_i^V\right) + \left(I_i^V - 1 - \ln I_i^V\right) + \left(G_i^H - 1 - \ln G_i^H\right)\right] \tag{6.4.13}$$

Implementing Itô's formula gives,

$$
\begin{aligned}
dV(L) &= \sum_{i=1}^{n}\left[\left(1-\frac{1}{S_i^H}\right)dS_i^H+\frac{1}{2S_i^{H^2}}dS_i^H dS_i^H+\left(1-\frac{1}{I_i^H}\right)dI_i^H+\frac{1}{2I_i^{H^2}}dI_i^H dI_i^H\right]\\
&+\left[\left(1-\frac{1}{P_i^V}\right)dP_i^V+\frac{1}{2P_i^{V^2}}dP_i^V dP_i^V+\left(1-\frac{1}{S_i^V}\right)dS_i^V+\frac{1}{2S_i^{V^2}}dS_i^V dS_i^V\right]\\
&+\left[\left(1-\frac{1}{I_i^V}\right)dI_i^V+\frac{1}{2I_i^{V^2}}dI_i^V dI_i^V+\left(1-\frac{1}{G_i^H}\right)dG_i^H+\frac{1}{2G_i^{H^2}}dG_i^H dG_i^H\right] \quad (6.4.14)
\end{aligned}
$$

and using SDE multiscale model system (6.4.1) we get

$$
\begin{aligned}
dV(L) &= \sum_{i=1}^{n}\left[\left(1-\frac{1}{S_i^H}\right)dS_i^H+\frac{1}{2S_i^{H^2}}\sigma_{S^H}^2 S_i^{H^2}dW_{S^H}^2+\left(1-\frac{1}{I_i^H}\right)dI_i^H+\frac{1}{2I_i^{H^2}}\sigma_{I^H}^2 I_i^{H^2}dW_{I^H}^2\right]\\
&+\left[\left(1-\frac{1}{P_i^V}\right)dP_i^V+\left(1-\frac{1}{S_i^V}\right)dS_i^V+\left(1-\frac{1}{I_i^V}\right)dI_i^V+\left(1-\frac{1}{G_i^H}\right)dG_i^H\right] \quad (6.4.15)
\end{aligned}
$$

$$
\begin{aligned}
dV(L) &= \sum_{i=1}^{n}\left[\left(1-\frac{1}{S_i^H}\right)dS_i^H+\frac{1}{2}\sigma_{S^H}^2 dW_{S^H}^2+\left(1-\frac{1}{I_i^H}\right)dI_i^H+\frac{1}{2}\sigma_{I^H}^2 dW_{I^H}^2\right]\\
&+\left[\left(1-\frac{1}{P_i^V}\right)dP_i^V+\left(1-\frac{1}{S_i^V}\right)dS_i^V+\left(1-\frac{1}{I_i^V}\right)dI_i^V+\left(1-\frac{1}{G_i^H}\right)dG_i^H\right] \quad (6.4.16)
\end{aligned}
$$

$$
\begin{aligned}
dV(L) &= \sum_{i=1}^{n}\left[\left(1-\frac{1}{S_i^H}\right)dS_i^H+\frac{1}{2}\sigma_{S^H}^2 dt+\left(1-\frac{1}{I_i^H}\right)dI_i^H+\frac{1}{2}\sigma_{I^H}^2 dt\right]\\
&+\left[\left(1-\frac{1}{P_i^V}\right)dP_i^V+\left(1-\frac{1}{S_i^V}\right)dS_i^V+\left(1-\frac{1}{I_i^V}\right)dI_i^V+\left(1-\frac{1}{G_i^H}\right)dG_i^H\right] \quad (6.4.17)
\end{aligned}
$$

and making use of model system (6.4.1) we get

$$
dV(L) = \mathcal{G}V dt+\left(1-\frac{1}{S_i^H}\right)\sigma_{S^H}S_i^H dW_{S^H}(t)+\left(1-\frac{1}{I_i^H}\right)\sigma_{i^H}I_i^H dW_{I^H}(t) \quad (6.4.18)
$$

where

$$\begin{aligned}\mathcal{G}V &= \sum_{i=1}^{n}\Lambda_i^H - \frac{\Lambda_i^H}{S_i^H} + \frac{\beta_i^V P_i^V(t)}{P_i^0 + P_i^V(t)} + 2\mu_i^H - \frac{\gamma_i^H I_i^H}{S_i^H} - \delta_i^H I_i^H - \frac{\beta_i^V P_i^V(t)}{P_i^0 + P_i^V(t)}\frac{S_i^H}{I_i^H} - \delta_i^H + \gamma_i^H \\ &+ \sum_{i=1}^{n} N_i^v \alpha_i^v I_i^V - \alpha_i^V P_i^V - \frac{N_i^v \alpha_i^v I_i^V}{P_i^V} + \alpha_i^V + \Lambda_i^V - \mu_i^V N_i^V - \frac{\Lambda_i^H}{S_i^H} + \frac{\beta_i^H G_i^H(t)}{G_i^0 + G_i^H(t)} + 2\mu_i^V \\ &+ \sum_{i=1}^{n} N_i^h \alpha_i^h I_i^H - \alpha_i^H G_i^H - \frac{N_i^h \alpha_i^h I_i^H}{G_i^H} + \alpha_i^H - \delta_i^V I_i^V - \frac{\beta_i^H G_i^H(t)}{G_i^0 + G_i^H(t)}\frac{S_i^V}{I_i^V} + \delta_i^V \\ &+ \frac{1}{2}\left(\sigma_{S^H}^2 + \sigma_{I^H}^2\right) \qquad (6.4.19)\end{aligned}$$

Therefore, from (6.4.10) we can state that $\left(S_i^H(s), I_i^H(s)\right)_{i=1,2,\ldots n} \in \left(0, \frac{\Lambda_i^H}{\varphi}\right)$ for all $s \in [0, t \wedge \tau_m]$ a.s. Henceforth, $\frac{\beta_i^V P_i^V(t)}{P_i^0 + P_i^V(t)} + 2\mu_i^H < \frac{\Lambda_i^H}{\varphi}$ and $\frac{\beta_i^H G_i^H(t)}{G_i^0 + G_i^H(t)} < \frac{\Lambda_i^H}{\varphi}$. Consequently,

$$\begin{aligned}\mathcal{G}V &\leq \sum_{i=1}^{n}\frac{2\Lambda_i^H}{\varphi} + \Lambda_i^H + 2\mu_i^H + \delta_i^H + \gamma_i^H + \alpha_i^V + \Lambda_i^V + 2\mu_i^V + \alpha_i^H + \delta_i^V \\ &+ \frac{1}{2}\left(\sigma_{S^H}^2 + \sigma_{I^H}^2\right) =: \wp \qquad (6.4.20)\end{aligned}$$

We can denote by $\zeta = \min(\tau_m, T)$, then

$$\int_0^{\zeta} dV\left(S_i^H(s), I_i^H(s)\right) \leq \int_0^{\zeta} \wp ds + \mathcal{H}(\zeta) \qquad (6.4.21)$$

where

$$\mathcal{H}(s) = \int_0^s (S^H(a) - 1)\sigma_{S^H} dW_{S^H}(a) + \int_0^s (I^H(a) - 1)\sigma_{I^H} dW_{I^H}(a) \qquad (6.4.22)$$

Taking expectation, yields

$$\begin{aligned}&\mathbb{E}\left[V\left(S_i^H(\zeta), I_i^H(\zeta), P_i^V(\zeta), S_i^V(\zeta), I_i^V(\zeta), G_i^H(\zeta)\right)\right] \\ &\leq V\left(S_i^H(0), I_i^H(0), P_i^V(0), S_i^V(s), G_i^H(s)\right) + \mathbb{E}\int_0^{\zeta} \wp ds \\ &\leq V\left(S_i^H(0), I_i^H(0), P_i^V(0), S_i^V(s), G_i^H(s)\right) + \wp T. \qquad (6.4.23)\end{aligned}$$

We set $\Omega_m = \{\omega \in \Omega : \tau_m < T\}$ for each $m \geq m_1$ and from equation (6.4.12), giving $\mathbb{P}(\Omega_m) \geq \varepsilon$. We remark $\forall\ \nu \in \Omega_m$, with these two bounds gives

$$\left[S_i^H(\tau_{m,\nu}), I_i^H(\tau_{m,\nu})\right] \cap \left[m, \frac{1}{m}\right] \neq \emptyset. \tag{6.4.24}$$

Consequently,

$$V\left((S_i^H(\zeta), I_i^H(\zeta))_{i=1,\ldots,n}\right) \geq U_m \tag{6.4.25}$$

where

$$U_m = \min_{a\in[1,b_0]} \left[m - a - a\ln\frac{m}{a}, \frac{1}{m} - a - a\ln\frac{1}{am}\right]. \tag{6.4.26}$$

we choose $b_0 > 0$ sufficiently small. Therefore we get

$$\begin{aligned} &V\left(\left(S_i^H(0), I_i^H(0), P_i^V(0), S_i^V(s), G_i^H(s)\right)_{i=1,\ldots,n}\right) + \wp T \\ &\geq \mathbb{E}\left(\mathbf{l}_{\Omega_m} V\left(S_i^H(\zeta), I_i^H(\zeta)\right)_{i=1,\ldots,n}\right) \geq \epsilon U_m \end{aligned} \tag{6.4.27}$$

Letting $m \to \infty$ will lead to the contradiction

$$\infty = V\left(\left(S_i^H(0), I_i^H(0), P_i^V(0), S_i^V(s), G_i^H(s)\right)_{i=1,\ldots,n}\right) + \wp T < \infty \tag{6.4.28}$$

Consequently, as $\tau_m \geq \tau_\infty$, gives $\tau_m = \tau_\infty = \infty$ a.s. The proof is complete. □

6.5 Numerical analysis

6.5.1 Sensitivity Analysis

This section presents the analysis of sensitivity for the Malaria transmission indicators obtained from the multiscale model to the model parameters. The transmission indicator we consider is the basic reproductive number, $\mathcal{R}_0$ that generally describes the dynamics for a disease at the beginning of an infection. For any particular epidemic model that illustrates the disease dynamics within a particular population, a sensitivity analysis study is important to perform since it enables us to establish model parameters which can be marked for control, elimination as well as eradication of disease. Therefore, the analysis of sensitivity of the Malaria metric $\mathcal{R}_0$, in relation to the variation of Malaria multiscale model parameters is carried out by implementing Latin Hypercube Sampling and Partial Rank Correlation Coefficients (PRCCs). In order to explore the influence of each model parameter on the basic reproduction number, $\mathcal{R}_0$ we performed 1000 simulations per run. The results of sensitivity of $\mathcal{R}_0$ to the model parameters are presented by the Tornado plots, Figure 6.2.

Table 6.2: Within-human and within-Mosquito parameter values and their description for i^{th} individual

Parameter	Description	Initial value	Range explored	Units	Source/ Rational
α_i^g	Rate at which gametocyte infected erythrocytes burst	96	90-100	day^{-1}	[145]
Λ_i^h	Rate of supply of susceptible erythrocytes	200	100-300	day^{-1}	[146]
μ_i^k	Natural decay rate of oocysts	0.01	0.071-0.143	day^{-1}	[147]
β_i^h	Infection rate of erythrocytes by free merozoites	0.1	2×10^{-9}- 0.2	day^{-1}	[148]; [149]
α_i^z	Rate at which zygotes develop into oocysts	0.4240	0.01-0.05	$no.^{-1} day^{-1}$	[150]
μ_i^b	Natural decay rate of susceptible erythrocytes	0.0083	0.006-0.01	day^{-1}	[149]
N_i^m	Number of merozoites produced per bursting erythrocyte	16	10-30	day^{-1}	[149]
α_i^s	Fertilization rate of gametes	0.08	0.01-0.2	$no.^{-1} day^{-1}$	[145]
μ_i^m	Natural decay rate of free merozoites	0.001	0.001-0.5	day^{-1}	[148]; [149]
μ_i^h	Natural decay rate of gametocyte infected erythrocytes within infected humans	0.0625	0.0600-0.0625	day^{-1}	[151]
π_i	Proportion of gametocyte infected erythrocytes	0.1	0.1-0.5	day^{-1}	Assumed
α_i^m	Rate at which erythrocytes burst to produce merozoites	0.5	0.1-1.0	day^{-1}	[141];[149]
α_i^h	Rate at which gametocytes develop and become infectious	0.02	0.01-0.9	day^{-1}	[151]
μ_i^g	Death rate of gametocytes	0.0625	0.0326-0.0725	day^{-1}	[145]
Λ_i^v	Rate of uptake of gametocytes through super infection of mosquto	300	100-300	day^{-1}	Variable
α_i^v	Rate at whch sporozoites become infectious to humans	0.025	0.167-1.00	$no.^{-1} day^{-1}$	[145]
μ_i^s	Natural decay rate of gametes	58.0	40-129	day^{-1}	[145]
μ_i^z	Natural decay rate of zygotes	1	1-4	day^{-1}	[145]
α_i^k	Bursting rate of oocysts to produce sporozoites	0.2	0-1.0	$no.^{-1} day^{-1}$	Variable
N_i^k	Number of sporozoites produced per bursting oocyst	3000	1000-10000	day^{-1}	[145]
N_i^g	Number of gametes produced per gametocyte infected erythrocyte	2	1-3	day^{-1}	Estimated
μ_i^v	Natural decay rate of sporozoites	0.0001	0.0001-0.01	day^{-1}	[145]

Table 6.3: Between-host (human and mosquito) parameter values and their description for i^{th} patch

Parameter	Description	Initial value	Range explored	Units	Source/ Rational
β_i^V	Contact rate of humans with the infectious reservoir of mosquitoes	0.2	0.1-0.5	day^{-1}	
δ_i^V	Infection induced death rate of mosquitoes	0.00000426	0.00000426-0.00000533	day^{-1}	Assumed
Λ_i^V	Rate of supply of susceptible mosquitoes	6000	5000-7000	day^{-1}	Variable
G_{0i}	Half saturation constant for community gametocyte load	5×10^8	1×10^8-10×10^8	day^{-1}	Variable
μ_i^V	Natural death rate of mosquitoes	0.12	0.033-0.3	day^{-1}	[148];[151]
β_i^H	Contact rate of mosquitoes with the infectious reservoir of humans	0.3	0.1-0.5	day^{-1}	
Λ_i^H	Rate of supply of susceptible humans	1000	1000-2000	day^{-1}	Assumed
μ_i^H	Natural death rate of humans	0.00004	0.00001-0.00008	day^{-1}	[148]
α_i^H	Rate elimination of community gametocytes load	0.0000913	0.0000467-0.000274	day^{-1}	Variable
P_{0i}^V	Half saturation constant for community sporozoite load	1×10^8	1×10^7-5×10^8	day^{-1}	Variable
γ_i^H	Natural recovery rate of humans	0.25	0.1-0.5	day^{-1}	Variable
α_i^V	Rate of elimination of community sporozoite load	0.9	0.09-0.99	day^{-1}	Variable
δ_i^H	Disease induced death rate of humans	0.0027	0.0001-0.5	day^{-1}	Assumed

From the sensitivity analysis results of $\mathcal{R}_0$ to the multiscale model system (6.2.1)'s parameters in Figure 6.2, the following deductions are listed below:

(a) The multiscale model system (6.2.1)'s parameters have both positive PRCCs and negative PRCCs. This implies that parameters with positive PRCCs will increase the value of $\mathcal{R}_0$ as they are increased, where as parameters with negative PRCCs will decrease the value for $\mathcal{R}_0$ as they are increased. For example, an increase in a parameter like natural death rate of humans in patch 1, μ_1^H will consequently decrease the value of $\mathcal{R}_0$.

(b) The Malaria disease transmission metric $\mathcal{R}_0$ is extremely sensitive to six of the disease parameters $(G_{01}^H, \mu_1^V, \mu_1^H, P_{01}^V, \alpha_1^h, \alpha_1^v)$ of the multiscale model system (6.2.1). We note that $\mathcal{R}_0$ characterizes spread of Malaria disease at the beginning of the outbreak. We make the following conclusions regarding the sensitivity of $\mathcal{R}_0$ to the Malaria disease multiscale model system (6.2.1)'s parameters.

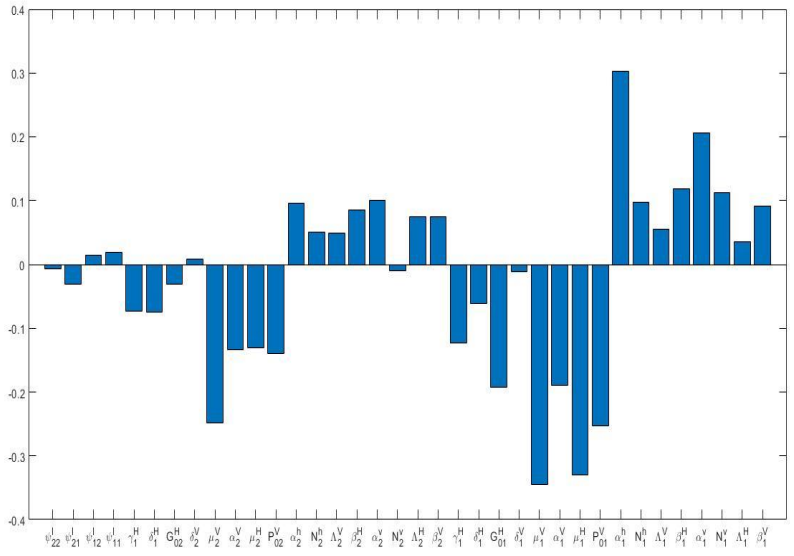

Figure 6.2: *Tornado plot of partial rank correlation coefficients (PRCCs) of the model parameters that influence the Malaria transmission indicator* $\mathcal{R}_0$

(i) Since $\mathcal{R}_0$ is significantly sensitive to impact of six Malaria disease transmission parameters $(G_{01}^H, \mu_1^V, \mu_1^H, P_1^V, \alpha_1^h, \alpha_1^v)$, this implies that caution must be applied on the accuracy of these six Malaria disease multiscale model system (6.2.1)'s parameters during the collection of data if the effectiveness and usefulness of the Malaria disease multiscale model system (6.2.1) is to be intensified.

(ii) Since $\mathcal{R}_0$ is responsive to the half saturation constant for community gametocyte load, G_{01}^H, natural decay rate of mosquitoes μ_1^V, natural decay rate of humans μ_1^H and the half saturation constant for community sporozoite load P_{01}^V this implies that Malaria interventions like Insecticide-treated nets and indoor residual spraying would be more effective in preventing the spread of Malaria infection at the beginning of the outbreak.

(iii) Since $\mathcal{R}_0$ is significantly sensitive to the rate at which gametocyte develop and become infectious α_1^h, elimination rate of community sporozoite load α_1^V and contact rate of humans with the infectious reservoir of mosquitoes interventions such as Malaria vaccination (which stimulate immune response to destroy Malaria parasite) would be more effective to control the spread of Malaria infection at the beginning of the outbreak. Results from Tornado plot in Figure 6.2 also confirmed that the migration rate of infected humans from patch 2 to patch 1, ψ_{12}^I has an impact on $\mathcal{R}_0$. Therefore, mediations such as screening would be more effective in managing the spread of Malaria disease.

6.5.2 Numerical simulations of the multiscale model of Malaria transmission dynamics

This section enables us to implement numerical simulations to substantiate some outcomes obtained from the sensitivity analysis for $\mathcal{R}_0$ and analytical results of the multiscale model. Applying the multiscale model parameter values obtained from Table 6.2 and Table 6.3 we carried out numerical simulations. We demonstrated the impact of six Malaria disease transmission parameters ($G_{01}^H, \mu_1^V, \mu_1^H, P_{01}^V, \alpha_1^h, \alpha_1^v$) on the multiscale model variables $I_1^H(t)$, $I_2^H(t)$, $P_1^V(t)$, $P_2^V(t)$, $I_1^V(t)$, $I_2^V(t)$, $G_1^H(t)$, $G_2^H(t)$ for the two-patch model. These parameters were only selected because they are significantly sensitive to $\mathcal{R}_0$.

6.5.2.1 Influence of within-host scale parameters of the Malaria multiscale model dynamics

In this subsection, we demonstrate by implementing numerical simulations the impact of within-host scale parameters on the between-host scale variables of the coupled multiscale model (6.2.1). Figure 6.3 and Figure 6.4 demonstrate the impact of variation of two within-host scale parameters (α_1^h, α_1^v) on the between-host scale model variables $I_1^H(t)$, $I_2^H(t)$, $P_1^V(t)$, $P_2^V(t)$, $I_1^V(t)$, $I_2^V(t)$, $G_1^H(t)$, $G_2^H(t)$ for the two-patch model.

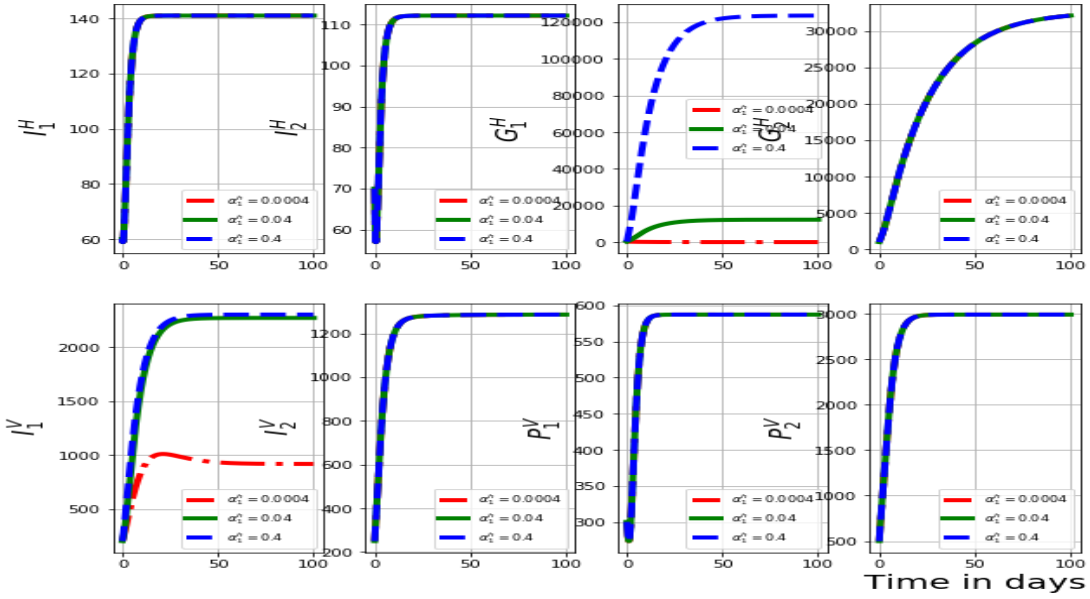

Figure 6.3: Graphs of numerical results of the model system (6.2.1) demonstrating the progression in time of (a) infected humans in patch 1, I_1^H, (b) infected humans in patch 2, I_2^H, (c) community gametocytes load in patch 1, G_1^H, (d) community gametocytes load in patch 2, G_2^H, (e) infected mosquito vectors in patch 1, I_1^V, (f) infected mosquito vectors in patch 2, I_2^V, (g) community sporozoite load in patch 1, P_1^V, (h) community sporozoite load in patch 2, P_2^V, for variant values of the rate at which gametocytes develop and become infectious in patch 1, $\alpha_1^h : \alpha_1^h = 0.0004, \alpha_1^h = 0.004$ and $\alpha_1^h = 0.04$.

Figure (6.3) represents the graphs of numerical results of the model system (6.2.1) demonstrating the progression in time of (a) infected humans in patch 1, I_1^H, (b) infected humans in patch 2, I_2^H, (c) community gametocytes load in patch 1, G_1^H, (d) community gametocytes load in patch 2, G_2^H, (e) infected mosquito

vectors in patch 1, I_1^V, (f) infected mosquito vectors in patch 2, I_2^V, (g) community sporozoite load in patch 1, P_1^V, (h) community sporozoite load in patch 2, P_2^V, for variant values of the rate at which gametocytes develop and become infectious in patch 1, $\alpha_1^h : \alpha_1^h = 0.0004, \alpha_1^h = 0.004$ and $\alpha_1^h = 0.04$. From these results we can see that as the rate at which gametocytes develop and become infectious increases, there is also a remarkable increase in the community gametocyte load in patch 1 and population of infected mosquitoes in patch 1. Furthermore, there is no noticeable change in the other model variables. These results reflect that treatments of individuals from malaria by reducing the rate at which gametocytes develop and become infectious are important for both the individual and the community since the risk of transmission of Malaria for the individual in the community is minimized.

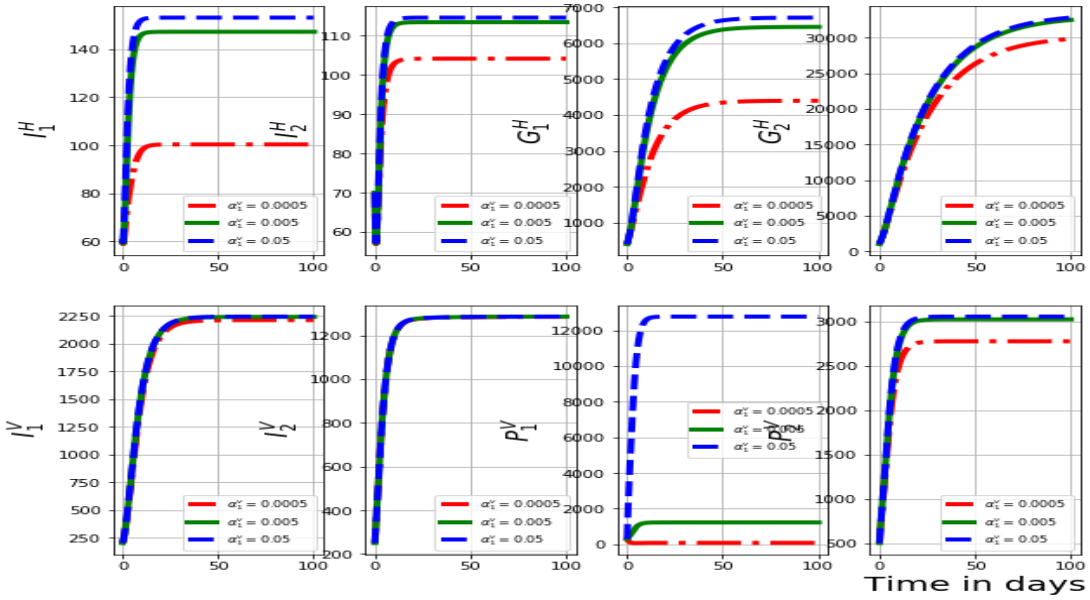

Figure 6.4: Graphs of numerical results of the model system (6.2.1) demonstrating the progression in time of (a) infected humans in patch 1, I_1^H, (b) infected humans in patch 2, I_2^H, (c) community gametocytes load in patch 1, G_1^H, (d) community gametocytes load in patch 2, G_2^H, (e) infected mosquito vectors in patch 1, I_1^V, (f) infected mosquito vectors in patch 2, I_2^V, (g) community sporozoite load in patch 1, P_1^V, (h) community sporozoite load in patch 2, P_2^V, for different values of the rate at which sporozoites become infectious to humans in patch 1, $\alpha_1^v : \alpha_1^v = 0.0005, \alpha_1^v = 0.005$ and $\alpha_1^v = 0.05$.

Figure (6.4) represents the graphs of numerical results of the model system (6.2.1) demonstrating the progression in time of (a) infected humans in patch 1, I_1^H, (b) infected humans in patch 1, I_2^H, (c) community gametocytes load in patch 1, G_1^H, (d) community gametocytes load in patch 2, G_2^H, (e) infected mosquito vectors in patch 1, I_1^V, (f) infected mosquito vectors in patch 2, I_2^V, (g) community sporozoite load in patch 1, P_1^V, (h) community sporozoite load in patch 2, P_2^V, for different values of the rate at which sporozoites become infectious to humans in patch 1, $\alpha_1^v : \alpha_1^v = 0.0005, \alpha_1^v = 0.005$ and $\alpha_1^v = 0.05$. From these results we can observe that as the rate at which sporozoites become infectious to humans increases in patch 1, there is a significant increase in the infected human population in patch 1, the infected human population in patch 2, community sporozoite load in patch 1, community sporozoite load in patch 2, community gametocyte load in patch 1 and community gametocyte load in patch 2. Furthermore, there is no noticeable change in the infected mosquito populations in both patches. These results reflect that

treatments of individuals from malaria by reducing the rate at which sporozoites become infectious to humans are important for both the individual and the community since the risk of transmission of malaria for the individual in the community is reduced.

6.5.2.2 Influence of between-host scale parameters on the Malaria multiscale model dynamics

In this subsection, we demonstrate by implementing numerical simulations the impact of between-host scale parameters on the between-host scale variables of the multiscale model (6.2.1). Figure 6.5 - Figure 6.8 demonstrate the impact of variation of four between-host scale parameters $(\mu_1^V, \mu_1^H, G_{01}^H, P_{01}^V)$ on the between-host scale model variables $I_1^H(t)$, $I_2^H(t)$, $P_1^V(t)$, $P_2^V(t)$, $I_1^V(t)$, $I_2^V(t)$, $G_1^H(t)$, $G_2^H(t)$ for the two-patch model.

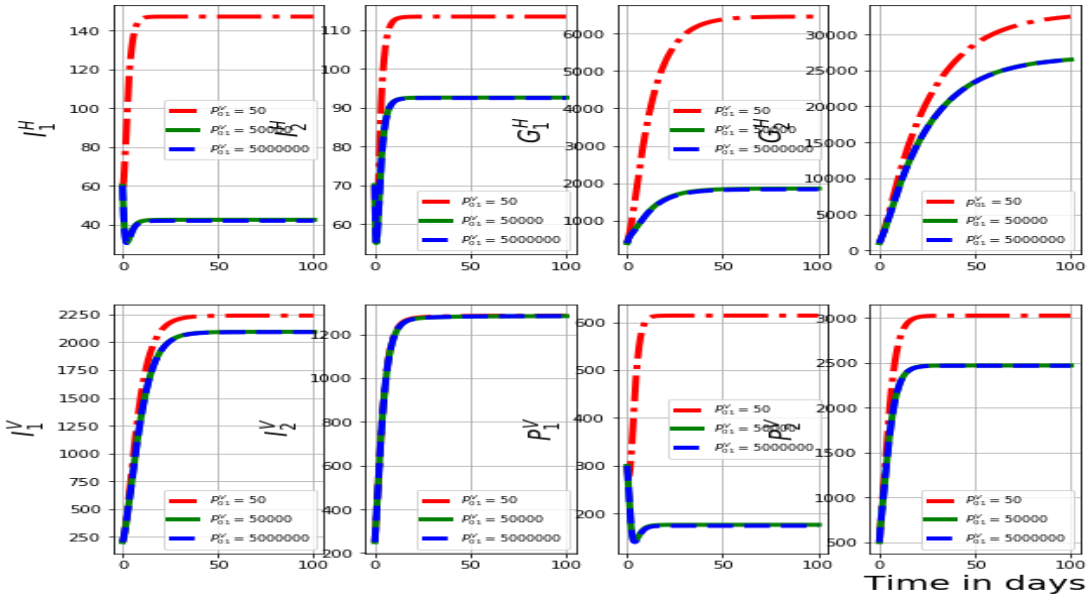

Figure 6.5: Graphs of numerical results of the model system (6.2.1) demonstrating the progression in time of (a) infected humans in patch 1, I_1^H, (b) infected humans in patch 2, I_2^H, (c) community gametocytes load in patch 1, G_1^H, (d) community gametocytes load in patch 2, G_2^H, (e) infected mosquito vectors in patch 1, I_1^V, (f) infected mosquito vectors in patch 2, I_2^V, (g) community sporozoite load in patch 1, P_1^V, (h) community sporozoite load in patch 2, P_2^V, for variant values of the half saturation constant for community sporozoite load in patch 1, P_{01} : $P_{01} = 50, P_{01} = 50000$ and $P_{01} = 5000000$.

Figure (6.5) represents the graphs of numerical results of the model system (6.2.1) demonstrating the progression in time of (a) infected humans in patch 1, I_1^H, (b) infected humans in patch 2, I_2^H, (c) community gametocytes load in patch 1, G_1^H, (d) community gametocytes load in patch 2, G_2^H, (e) infected mosquito vectors in patch 1, I_1^V, (f) infected mosquito vectors in patch 2, I_2^V, (g) community sporozoite load in patch 1, P_1^V, (h) community sporozoite load in patch 2, P_2^V, for variant values of the half saturation constant for community sporozoite load in patch 1, P_{02} : $P_{01} = 50, P_{01} = 50000$ and $P_{01} = 5000000$. From these results we can observe that as the half saturation constant for community sporozoite load increases, there is a decrease in the infected human population in patch 1, the infected human population in patch

2, community gametocyte load in patch 1 and patch 2, infected mosquito population in patch 1, and the community sporozoite load in patch 1 and patch 2. However, there is no noticeable change in the infected mosquito population in patch 1. These results indicate that interventions such as indoor residual spraying (IRS) can be implemented to reduce the half saturation constant for the community sporozoite load minimizing the risk of transmission of Malaria in the community.

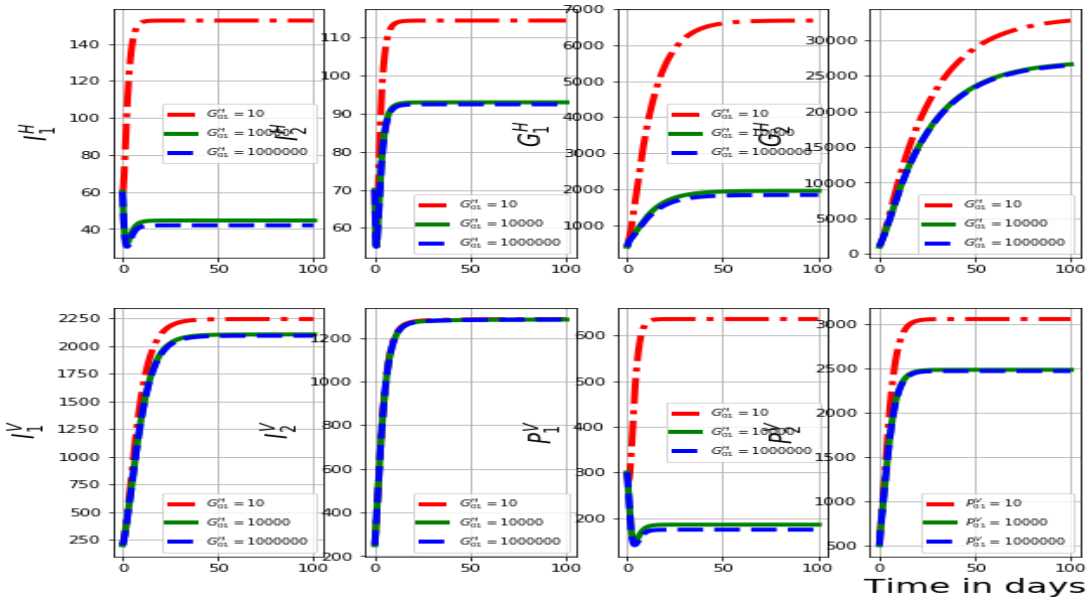

Figure 6.6: Graphs of numerical results of the model system (6.2.1) demonstrating the progression in time of (a) infected humans in patch 1, I_1^H, (b) infected humans in patch 2, I_2^H, (c) community gametocytes load in patch 1, G_1^H, (d) community gametocytes load in patch 2, G_2^H, (e) infected mosquito vectors in patch 1, I_1^V, (f) infected mosquito vectors in patch 2, I_2^V, (g) community sporozoite load in patch 1, P_1^V, (h) community sporozoite load in patch 2, P_2^V, for variant values of the half saturation constant for community gametocyte load in patch 1, $G_{01} : G_{01} = 10, G_{01} = 10000$ and $G_{01} = 1000000$.

Figure (6.6) represents the graphs of numerical results of the model system (6.2.1) demonstrating the progression in time of (a) infected humans in patch 1, I_1^H, (b) infected humans in patch 2, I_2^H, (c) community gametocytes load in patch 1, G_1^H, (d) community gametocytes load in patch 2, G_2^H, (e) infected mosquito vectors in patch 1, I_1^V, (f) infected mosquito vectors in patch 2, I_2^V, (g) community sporozoite load in patch 1, P_1^V, (h) community sporozoite load in patch 2, P_2^V, for variant values of the half saturation constant for community gametocyte load in patch 1, $G_{01} : G_{01} = 10, G_{01} = 10000$ and $G_{01} = 1000000$. From these results we can observe that as the half saturation constant for community gametocyte load increases, there is a decrease in the population of infected mosquitoes in patch 1. Furthermore, there is a remarkable reduction in the infected human population in patch 1 and patch 2, the community gametocyte load in patch 1 and patch 2, and the community sporozoite load in patch 1 and patch 2. These results indicate that interventions such as indoor residual spraying (IRS) and the use of Long-lasting treated nets (LLTNs) can be implemented to reduce the half saturation constant for the community gametocyte load minimizing the risk of transmission of malaria in the community.

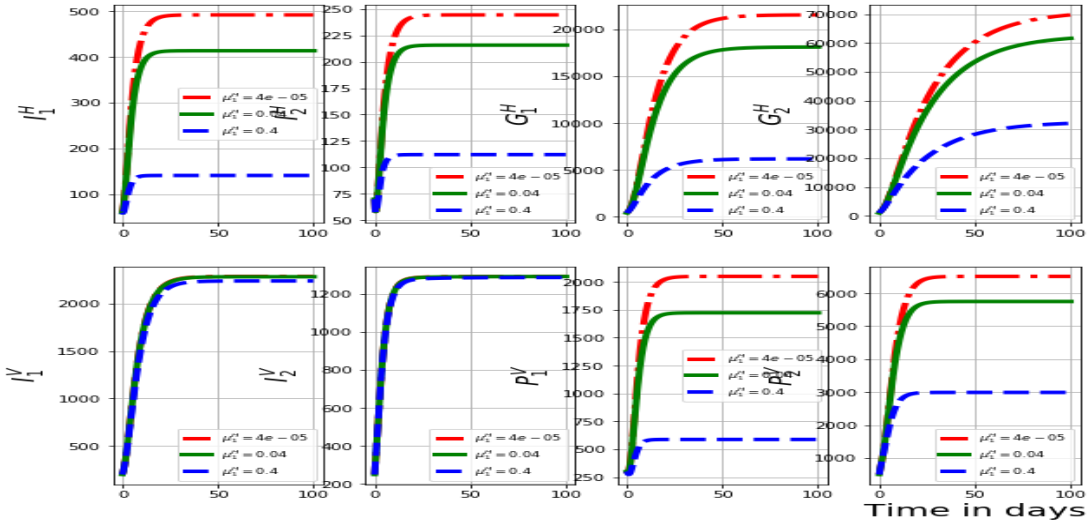

Figure 6.7: Graphs of numerical results of the model system (6.2.1) demonstrating the progression in time of (a) infected humans in patch 1, I_1^H, (b) infected humans in patch 2, I_2^H, (c) community gametocytes load in patch 1, G_1^H, (d) community gametocytes load in patch 2, G_2^H, (e) infected mosquito vectors in patch 1, I_1^V, (f) infected mosquito vectors in patch 2, I_2^V, (g) community sporozoite load in patch 1, P_1^V, (h) community sporozoite load in patch 2, P_2^V, for variant values of the natural death rate of humans in patch 1, $\mu_1^H : \mu_1^H = 4e-05, \mu_1^H = 0.04$ and $\mu_1^H = 0.4$.

Figure (6.7) represents the graphs of numerical results of the model system (6.2.1) demonstrating the progression in time of (a) infected humans in patch 1, I_1^H, (b) infected humans in patch 2, I_2^H, (c) community gametocytes load in patch 1, G_1^H, (d) community gametocytes load in patch 2, G_2^H, (e) infected mosquito vectors in patch 1, I_1^V, (f) infected mosquito vectors in patch 2, I_2^V, (g) community sporozoite load in patch 1, P_1^V, (h) community sporozoite load in patch 2, P_2^V, for variant values of the natural death rate of humans in patch 1, $\mu_1^H : \mu_1^H = 4e-05, \mu_1^H = 0.04$ and $\mu_1^H = 0.4$. From these results we can observe that as the natural death rate of humans increases in patch 1, there is a remarkable reduction in the infected human population in patch 1 and patch 2, the community gametocyte load in patch 1 and patch 2, and the community sporozoite load in patch 1 and patch 2. Furthermore, there is no significant change in the infected mosquito population in patch 1 and patch 2. These results indicate that interventions such as indoor residual spraying (IRS), the use of Long-lasting treated nets (LLTNs) and artemisinin-based combination therapy (ACT) can be implemented to reduce the natural death rate of humans minimizing mortalities due to malaria infection in the community.

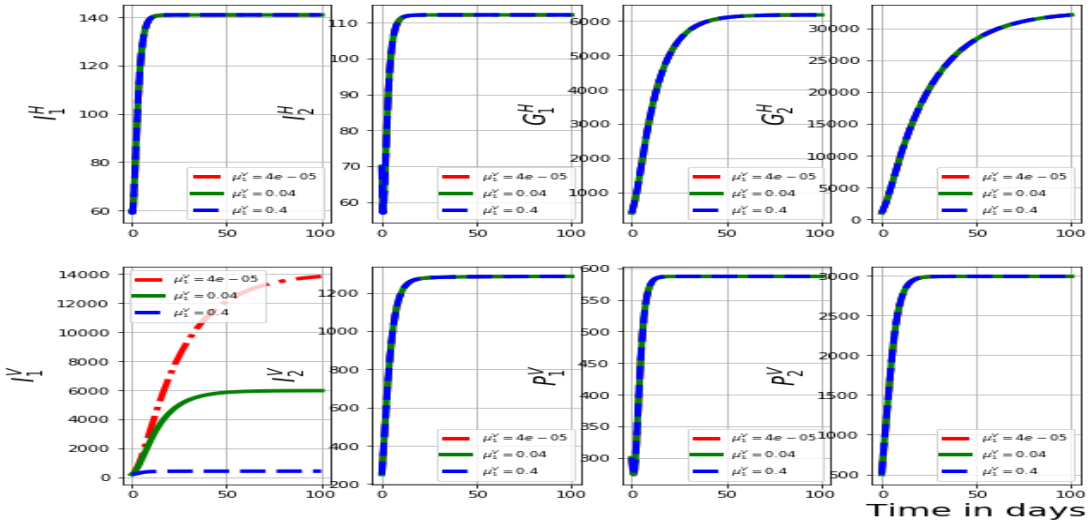

Figure 6.8: Graphs of numerical results of the model system (6.2.1) demonstrating the progression in time of (a) infected humans in patch 1, I_1^H, (b) infected humans in patch 2, I_2^H, (c) community gametocytes load in patch 1, G_1^H, (d) community gametocytes load in patch 2, G_2^H, (e) infected mosquito vectors in patch 1, I_1^V, (f) infected mosquito vectors in patch 2, I_2^V, (g) community sporozoite load in patch 1, P_1^V, (h) community sporozoite load in patch 2, P_2^V, for variant values of the natural death rate of mosquitoes in patch 1, $\mu_1^V : \mu_1^V = 2.4e-05, \mu_1^V = 0.024$ and $\mu_1^V = 0.24$.

Figure (6.8) represents the graphs of numerical results of the model system (6.2.1) demonstrating the progression in time of (a) infected humans in patch 1, I_1^H, (b) infected humans in patch 2, I_2^H, (c) community gametocytes load in patch 1, G_1^H, (d) community gametocytes load in patch 2, G_2^H, (e) infected mosquito vectors in patch 1, I_1^V, (f) infected mosquito vectors in patch 2, I_2^V, (g) community sporozoite load in patch 1, P_1^V, (h) community sporozoite load in patch 2, P_2^V, for variant values of the natural death rate of mosquitoes in patch 1, $\mu_1^V : \mu_1^V = 2.4e-05, \mu_1^V = 0.024$ and $\mu_1^V = 0.24$. From these results we can observe that as the natural death rate of mosquitoes increases, there is a remarkable reduction in the infected mosquito population in patch 1. Furthermore, there is no significant change on the remaining model variables. These results indicate that interventions such as indoor residual spraying (IRS) can be implemented to increase the natural death rate of mosquitoes minimizing the transmission of malaria infection in the community.

6.5.2.3 Influence of between-community scale parameters on the Malaria multiscale model dynamics

In this subsection, we demonstrate by implementing numerical simulations the impact of between-community scale parameters on the individual-based multiscale model (6.2.1) variables. Figure 6.9 demonstrates the impact of variation of between-community scale parameter ψ_{12}^I (which is migration rate between two patches) on the Malaria multiscale model variables $I_i^H(t)$, $P_i^V(t)$, $I_i^V(t)$, $G_i^H(t)$.

Figure 6.9 represents the graphs of numerical results of the multiscale model system (6.2.1) demonstrating the progression in time of (a) infected humans in patch 1, I_1^H, (b) infected humans in patch 2, I_2^H, (c)

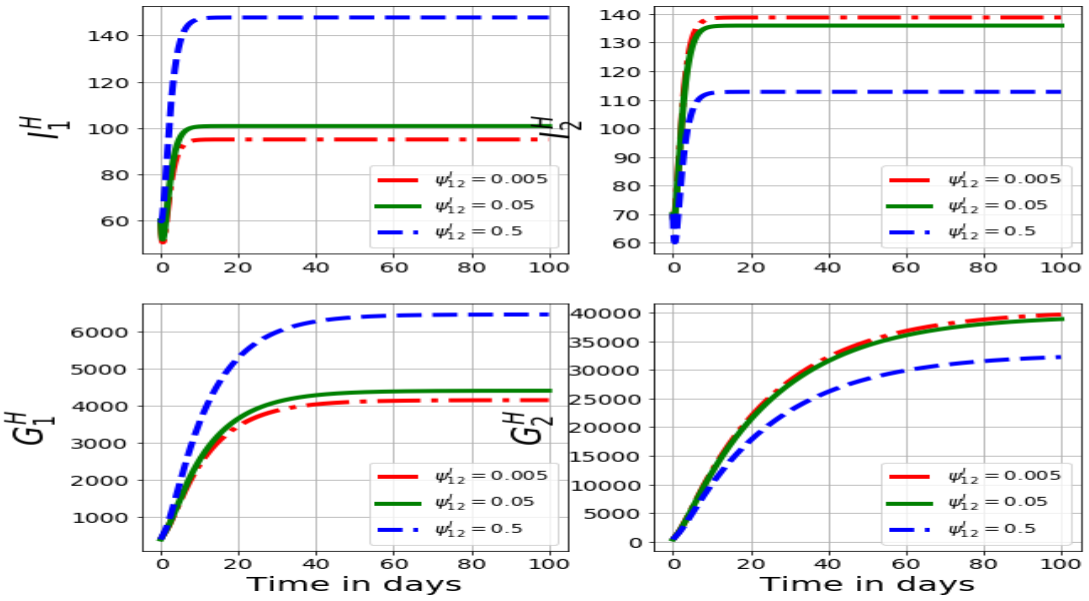

Figure 6.9: Graph of numerical results of the multiscale model system (6.2.1) demonstrating the progression in time of (a) infected humans in patch 1, I_1^H, (b) infected humans in patch 2, I_2^H, (c) community gametocyte load in patch 1, G_1^H, (d) community gametocyte load in patch 2, G_2^H, for different values of the migratrion rate of infected humans from patch 2 to patch 1, $\psi_{12}^I : \psi_{12}^I = 0.005, \psi_{12}^I = 0.05, \psi_{12}^I = 0.5$

community gametocyte load in patch 1, G_1^H, (d) community gametocyte load in patch 2, G_2^H for different values of the migratrion rate of infected humans from patch 2 to patch 1, ψ_{12}^I: $\psi_{12}^I = 0.005$, $\psi_{12}^I = 0.05$, $\psi_{12}^I = 0.5$. From these results we can see that as rate of migration of infected humans from patch 2 to patch 1 increases, there is noticeable increase in the population of infected human population in patch 1 and the community gametocyte load in patch 1. Furthermore, there is a decrease in the infected human population in patch 2 and the community gametocyte load in patch 2. These results indicate that interventions such as border screening of the human populations during migration can be implemented to minimize the rate of migration of infected individuals and therefore reducing global transmission of Malaria infection between different communities.

Figure 6.10 represents the graphs of numerical results of the multiscale model system (6.2.1) demonstrating the progression in time of (a) infected mosquitoes in patch 1, I_1^V, (b) infected mosquitoes in patch 2, I_2^V, (c) community sporozoite load in patch 1, P_1^V, (d) community sporozoite load in patch 2, P_2^V for different values of the migratrion rate of infected humans from patch 2 to patch 1, $\psi_{12}^I : \psi_{12}^I = 0.005, \psi_{12}^I = 0.05, \psi_{12}^I = 0.5$. From these results we can see that as rate of migration of infected humans from patch 2 to patch 1 increases, there is a small increase in the population of infected mosquito population in patch 1 and the community sporozoite load in patch 1. Furthermore, there is no change in the infected mosquito population in patch 2 and these is a decrease in the community sporozoite load in patch 2. These results indicate that interventions such as border screening of the human populations during migration can be implemented to minimize the rate of migration of infected individuals and therefore reducing global transmission of malaria infection between different communities.

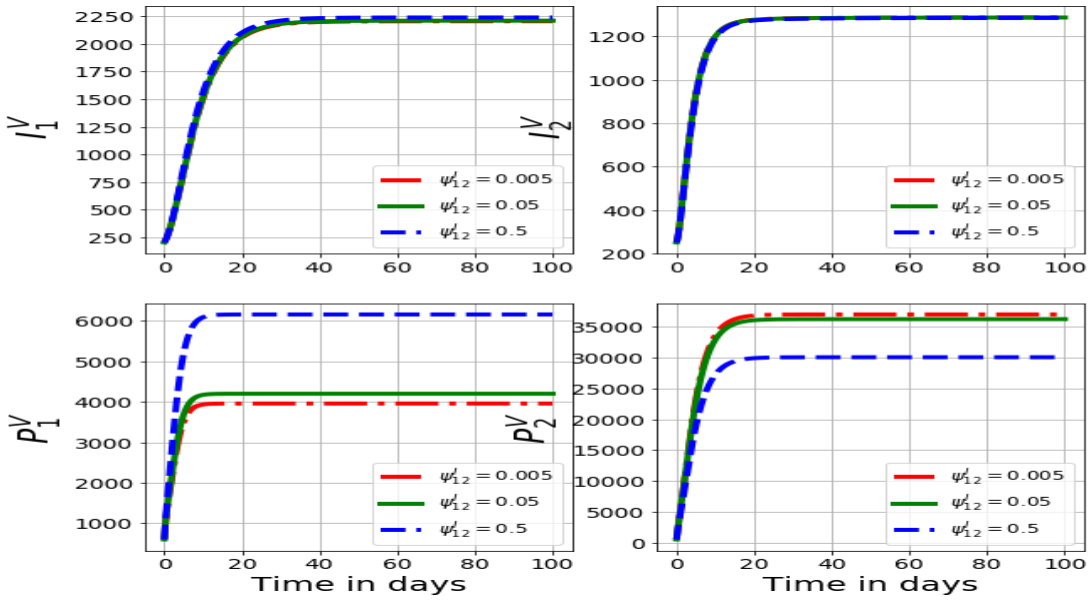

Figure 6.10: Graph of numerical results of the multiscale model system (6.2.1) demonstrating the progression in time of (a) infected mosquitoes in patch 1, I_1^V, (b) infected mosquitoes in patch 2, I_2^V, (c) community sporozoite load in patch 1, P_1^V, (d) community sporozoite load in patch 2, P_2^V for different values of the migratrion rate of infected humans from patch 2 to patch 1, $\psi_{12}^I : \psi_{12}^I = 0.005, \psi_{12}^I = 0.05, \psi_{12}^I = 0.5$

6.6 Incorporating sochasticity into the multiscale model

The multiscale model system (6.2.1) does not take into account the inherent randomness that is associated with Malaria infection. In this section we investigate the effect of the introduction of environmental noise into the multiscale model system (6.2.1). Therefore we present a multiscale model system of stochastic differential equations for modelling Malaria infection obtained when we perturb the multiscale model system (6.2.1) by a Wiener process.

$$
\begin{cases}
dS_i^H(t) = \left(\Lambda_i^H - \dfrac{\beta_i^V P_i^V(t)}{P_{0i} + P_i^V(t)} S_i^H(t) - \mu_i^H S_i^H(t) + \gamma_i^H I_i^H(t) + \displaystyle\sum_{j\neq i=1}^{n} \psi_{j,i}^S S_j^H - \sum_{j\neq i=1}^{n} \psi_{i,j}^S S_i^H\right) dt + S_i^H(t)\sigma_{S^H} dW_{S^H} \\
dI_i^H(t) = \left(\dfrac{\beta_i^V P_i^V(t)}{P_{0i} + P_i^V(t)} S_i^H(t) - (\mu_i^H + \delta_i^H + \gamma_i^H) I_i^H + \displaystyle\sum_{j\neq i=1}^{n} \psi_{j,i}^I I_j^H - \sum_{j\neq i=1}^{n} \psi_{i,j}^I I_i^H\right) dt + I_i^H(t)\sigma_{I^H} dW_{I^H} \\
dP_i^V(t) = \left(N_i^v \alpha_i^v I_i^V(t) - \alpha_i^V P_i^V(t)\right) dt \\
dS_i^V(t) = \left(\Lambda_i^V - \dfrac{\beta_i^H G_i^H(t)}{G_{0i} + G_i^H(t)} S_i^V(t) - \mu_i^V S_i^V\right) dt \\
dI_i^V(t) = \left(\dfrac{\beta_i^H G_i^H(t)}{G_{0i} + G_i^H(t)} S_i^V(t) - (\mu_i^V + \delta_i^V) I_i^V(t)\right) dt \\
dG_i^H(t) = \left(N_i^h \alpha_i^h I_i^H(t) - \alpha_i^H G_i^H(t)\right) dt
\end{cases}
\tag{6.6.1}
$$

dW_{S^H} and dW_{I^H} represent the white noise and σ_{S^H} and σ_{I^H} represent the intensity of the noise. This is a

standard technique that has been implemented in stochastic population modelling and therefore introducing stochasticity into the multiscale model system (6.2.1) (see [109, 153–155]). This section focuses on the investigation of the effect of migration on the SDE multiscale model system (6.6.1) for Malaria infection. Figure (6.11) (a)-(c) show the graphs of numerical results of the model system (6.6.1) demonstrating the variation in time of the infected human populations I_1^H and I_2^H in patch 1 and patch 2 respectively for different migration rates of infected humans from patch 2 to patch 1, ψ_{12}^I: $\psi_{12}^I = 0.05, \psi_{12}^I = 0.5, \psi_{12}^I = 0.9$. From these results we can see that as the rate of migration of infected humans ψ_{12}^I from patch 2 to patch 1 increases, there is noticeable increase in the pupolation of infected human population in patch 1. Therefore, these results indicate that interventions such as border screening of people during migration can help to control the spread of infection globally.

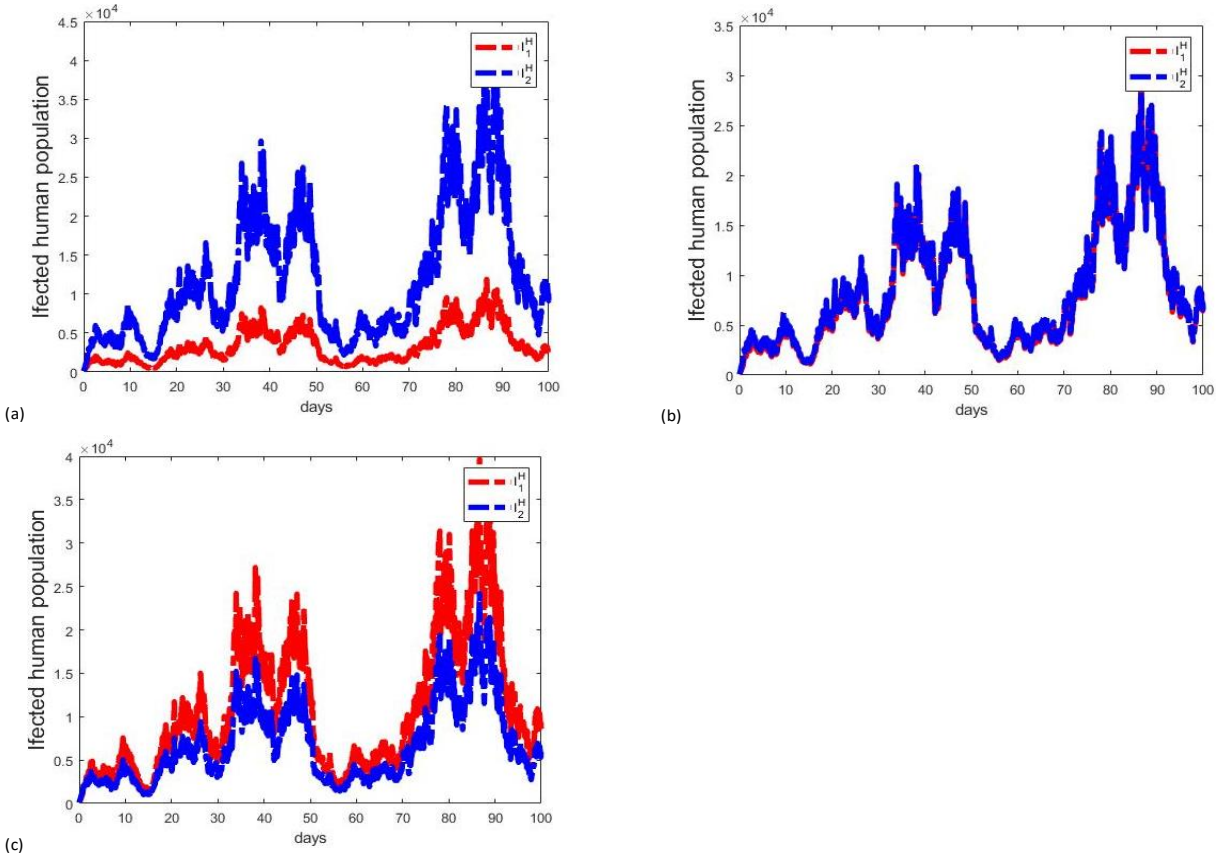

Figure 6.11: (a) shows the graphs of numerical results of the multiscale model system (6.6.1) demonstrating the variation in time of the infected human populations I_1^H and I_2^H in patch 1 and patch 2 respectively for the migration rate of infected humans from patch 2 to patch 1, $\psi_{12}^I = 0.05$. (b) shows the graphs of numerical results of the multiscale model system (6.6.1) demonstrating the variation in time of the infected human populations I_1^H and I_2^H in patch 2 and patch 1 respectively for the migration rate of infected humans from patch 2 to patch 1, $\psi_{12}^I = 0.5$. (c) shows the graphs of numerical results of the multiscale model system (6.6.1) demonstrating the variation in time of the infected human populations I_1^H and I_2^H in patch 1 and patch 2 respectively for the migration rate of infected humans from patch 2 to patch 1, $\psi_{12}^I = 0.9$.

6.7 Summary

In this chapter, we characterised a coupled modelling multiscale model of Malaria at macrocommunity-level, with the main objective of investigating the role of migration on the multiscale dynamics of Malaria in humans. By mathematical analysis the model was determined to be epidemiologically and mathematically sound. The analysis of sensitivity of the Malaria indicator $\mathcal{R}_0$, in relation to the variation of Malaria model parameters was carried out by implementing Latin Hypercube Sampling and Partial Rank Correlation Coefficients (PRCCs). Applying the model parameter values we carried out the numerical simulations to demonstrate the impact of six Malaria disease transmission parameters ($G_{01}^H, \mu_1^V, \mu_1^H, P_{01}^V, \alpha_1^h, \alpha_1^v$) on the multiscale model variables $I_1^H(t)$, $I_2^H(t)$, $P_1^V(t)$, $P_2^V(t)$, $I_1^V(t)$, $I_2^V(t)$, $G_1^H(t)$, $G_2^H(t)$ for the two-patch model. These parameters were only selected because they were significantly responsive to $\mathcal{R}_0$. The results of sensitivity analysis of $\mathcal{R}_0$ indicated that the variation of the within-host scale parameters in particalar the rate at which gametocytes develop and become infectious, α_1^h have significant effect on the transmission risk of Malaria in humans at macrocommunity-level and this is confirmed by the Tornado plot in Figure 6.2. Results from Tornado plot in Figure 6.2 also confirmed that the migration rate of infected humans from patch 1 from patch 2, ψ_{12}^I has some impact on $\mathcal{R}_0$. Figure 6.9-Figure 6.11 demonstrate the variation in the rate of migration of infected human population from patch 2 to patch 1. Results show that an increase in the rate of migration leads to an increase of infected humans in the receiving patch 1.

In conclusion, we established that the model we characterised in this chapter can not be extended to macroecosystem level using graph-theoretic approach. Furthermore, we established that the global transmission of Malaria can be described using graph-theoretic approach. In addition, we established that the distinction between local transmission and global transmission mechanisms of infectious diseases informs us on the appropriate interventions at community level from calculations of the reproduction number. Finally, the model presented has a secondary level multiscale cycle with both local exchange and global exchange of pathogen.

Chapter 7

Conclusions and directions for future research

7.1 Conclusions

In this thesis, we characterised multiscale models based on vector-borne diseases and directly transmitted diseases with Malaria and FMD as paradigms respectively. Initially, we characterised the host level model of FMD using graph-theoretic methods in chapter 2 and chapter 5. We characterised the host level model of FMD in chapter 3 using the nested approach. However, the major challenge was whether we can extend this to community level in chapter 4 since it incorporates local transmission and global transmission. In chapter 4 there are elements of chapter 2 and chapter 3 since it has a host level at each community. My investigation involved establishing this new idea that we can not extend chapter 2 further into a graph-theoretic model at community level. The best way forward is to extend chapter 3 into community level. In chapter 3 the scale of observation is the whole organism scale. In chapter 4 we have a combination of whole organism scale represented in chapter 3 and macrocommunity scale. These scales of observation are the aspects characterised and this was better represented using different methods. Having established this knowledge we then used it for Malaria in chapter 6. We implemented an equivalent of chapter 3 which was a whole-organism scale and extended it to a graph-theoretic at community level in chapter 6.

In Chapter 2 we characterised an individual-based network modelling multiscale model of FMD at host-level. The derivation of the model is achieved by first developing a within-cattle model and then embedding the model into a spatial network of N cattle. Thus, in order to describe the whole disease dynamics we implemented explicitly the within-cattle model. Through mathematical analysis the model was

determined to be epidemiologically and mathematically sound. The analysis of sensitivity of the FMDV indicator $\mathcal{R}_0$, in relation to the variation of FMD model parameters was carried out by implementing Latin Hypercube Sampling and Partial Rank Correlation Coefficients (PRCCs). Applying the model parameter values we carried out the numerical simulations to demonstrate the impact of five FMD transmission parameters ($\beta_{ij}, U^0, \phi, \omega, \epsilon$) on the model variables $V_i, F_i, U_i, P_i, I_i, A_i, C_i, J_i$. These parameters were only selected because they were significantly responsive to $\mathcal{R}_0$. In view of the fact that $\mathcal{R}_0$ was responsive to the transmission rate between the cattle, β_{ij} (the between-host level parameter) it implied that FMD interventions such as quarantines would be more effective to control the spread of FMD infection at the beginning of the outbreak. Furthermore, since $\mathcal{R}_0$ was significantly responsive to the rate of production of antibodies, ϕ_A and rate at which FMDV virus is cleared, ω this implied that FMD interventions such as vaccination (which increases the rate of antibody production and clearance of FMDV virus) would be more effective to control the spread of FMD infection at the beginning of outbreak. The inclusion of a stochastic model enabled us to capture randomness of disease spread. The application of this method may be relevant in managing FMD and can be generalized to numerous directly transmitted diseases.

In Chapter 3 we characterised a nested modelling multiscale model centred on combining two sub-models namely: (i) the within-cattle scale and (ii) between-cattle scale sub-models for FMDV dynamics. Hence, we established a uni-directionally coupled multiscale model in which the within-cattle scale submodel is uni-directionally coupled to the between-cattle scale FMDV transmission dynamics submodel. By performing mathematical analysis the model was determined to be epidemiologically and mathematically sound. Therefore, the analysis of sensitivity of the FMDV metric $\mathcal{R}_0$ and the endemic value of the community viral load V_C^*, in relation to the variation of FMD multiscale model parameters was carried out by implementing Latin Hypercube Sampling and Partial Rank Correlation Coefficients (PRCCs). Applying the model parameter values we carried out the numerical simulations to demonstrate the impact of five FMD disease transmission parameters ($\beta_C, \mu_C^{S_C}, V_0, \alpha_C, \Lambda_C$) on the model variables $S_C(t), I_C(t), V_C(t)$. These parameters were only selected because they were significantly responsive to $\mathcal{R}_0$ and V_C^*. In view of the fact that $\mathcal{R}_0$ was responsive to the rate of infection of susceptible cattle, β_C and birth rate of susceptibles, Λ_C this implied that FMD interventions such as vaccination would be more effective in preventing the spread of FMD disease infection at the beginning of the outbreak. Randomness of disease dynamics was highlighted by implementing a stochastic model.

In Chapter 4 we characterised a nested modelling multiscale model of FMD at community-level, with the main objective of investigating the role of migration on the multiscale model dynamics of FMD in cattle. Through mathematical analysis the model was determined to be epidemiologically and mathematically sound. The analysis of sensitivity of the FMDV indicator $\mathcal{R}_0$, in relation to the variation of FMD model parameters was carried out by implementing Latin Hypercube Sampling (LHS) and Partial Rank Correlation Coefficients (PRCCs). Applying the model parameter values we conducted the numerical simulations to demonstrate the impact of six FMD transmission parameters (N_2, $\mu_{C_2}^{S_C}$, V_{02}, α_{C_2}, α_2, ψ_{12}^I) on the

multiscale model variables $S_{C_i}(t), I_{C_i}(t), V_{C_i}(t)$. These parameters were only selected because they are significantly sensitive to $\mathcal{R}_0$. The results from analysis of sensitivity of $\mathcal{R}_0$ indicated that the variation of the within-community scale parameters in particular the amount of FMD virus available for excretion in patch 2, N_2 have a huge impact on the transmission risk of FMD in cattle at community-level and this was confirmed by the Tornado plot in Figure 4.2. Results from Tornado plot in Figure 4.2 also confirmed that the migration rate of infected cattle from patch 1 from patch 2, ψ_{12}^I has an impact on $\mathcal{R}_0$. Figure (4.8) and Figure 4.13-Figure 4.15 demonstrate the variation in the rate of migration of infected cattle population from patch 1 to patch 2. Results show that an increase in the rate of migration lead to an increase of infected cattle population in the receiving patch 2. Furthermore, Figure 4.3 - Figure 4.7 showed the impact in the variation of the parameter values $(\alpha_2, \mu_{C_2}^{S_C}, V_{02}, \alpha_{C_2}, N_2)$ on the model variables $(S_{C_1}, I_{C_i}, V_{C_i})$. In addition, Figure 4.9- Figure 4.12 described the graphs of the stochastic models in comparison to the ODE multiscale models.

In Chapter 5 we characterised an individual-based network modelling multiscale model of Malaria at Whole organism-level. The mathematical model we developed consisted of the within-human malaria parasite dynamics and within-mosquito malaria parasite dynamics where the humans were connected by a spatial network of n individuals. The framework separated between-organ spread dynamics (inflow and outflow) and the within-organs infection dynamics (replication) for the whole transmission-replication loop. The model demonstrated the time progression of within infected mosquito host as well as within the infected human host. The populations in the infected human host included the erythrocytes infected by gametocytes G_i^h, free merozoites in blood M_i^h, susceptible erythrocytes R_i^h, erythrocytes infected by merozoites R_i^m. In addition, the populations in the infected mosquito include the sporozoites, P_i^v, gametes, G_i^m, infected erythrocytes, G_i^v, oocysts, O_i^v, zygotes. Z_i^v. Through mathematical analysis the model was determined to be epidemiologically and mathematically sound. The analysis of sensitivity of the Malaria indicator $\mathcal{R}_0$, in relation to the variation of Malaria model parameters was carried out by implementing Latin Hypercube Sampling (LHS) and Partial Rank Correlation Coefficients (PRCCs). The results from analysis of sensitivity of $\mathcal{R}_0$ indicated that variation of the between-organ scale parameters in particalar the transmission rate of Malaria parasite through blood, β_{ji}^h had significant effect on the transmission risk of Malaria in humans at whole organism-level and this is confirmed by the Tornado plot in Figure 5.3. Furthermore, Figure 5.4 - Figure 5.7 showed the impact in the variation of four parameters $(\Lambda_i^h, N_i^m, \mu_i^m, \beta_{ji}^h)$ on the variables $\left(R_i^h, R_i^m, M_i^h, G_i^h, G_i^v, G_i^m, Z_i^v, O_i^v, P_i^v\right)$. In addition, Figure 5.9- Figure 5.11 shows the graphs of the stochastic models in comparison to the ODE multiscale models.

In Chapter 6 we characterised a coupled modelling multiscale model of Malaria at macrocommunity-level, with the main objective of investigating the role of migration on the multiscale dynamics of Malaria in humans. By mathematical analysis the model was determined to be epidemiologically and mathematically sound. The analysis of sensitivity of the Malaria indicator $\mathcal{R}_0$, in relation to the variation of Malaria model

parameters was carried out by implementing Latin Hypercube Sampling and Partial Rank Correlation Coefficients (PRCCs). Applying the model parameter values we carried out the numerical simulations to demonstrate the impact of six Malaria disease transmission parameters ($G_{01}^H, \mu_1^V, \mu_1^H, P_{01}^V, \alpha_1^h, \alpha_1^v$) on the multiscale model variables $I_1^H(t)$, $I_2^H(t)$, $P_1^V(t)$, $P_2^V(t)$, $I_1^V(t)$, $I_2^V(t)$, $G_1^H(t)$, $G_2^H(t)$ for the two-patch model. These parameters were only selected because they were significantly responsive to $\mathcal{R}_0$. The results of sensitivity analysis of $\mathcal{R}_0$ indicated that the variation of the within-host scale parameters in particalar the rate at which gametocytes develop and become infectious, α_1^h have significant effect on the transmission risk of Malaria in humans at macrocommunity-level and this is confirmed by the Tornado plot in Figure 6.2. Results from Tornado plot in Figure 6.2 also confirmed that the migration rate of infected humans from patch 1 from patch 2, ψ_{12}^I has some impact on $\mathcal{R}_0$. Figure 6.9-Figure 6.11 demonstrate the variation in the rate of migration of infected human population from patch 2 to patch 1. Results show that an increase in the rate of migration leads to an increase of infected humans in the receiving patch 1.

In conclusion, we established that once you have used a graph-theoretic method at host level it will be difficult to extend this to community level. However, when we used different methods then it was easy to extend to community level. This is the major aspect of characterization that we investigated in this thesis which has not been done before. We also established that at organ level, the within-organ level constitutes local transmission mechanism, that is, direct transmission or environmental transmission which can be modelled using ODEs. However, at between-organ it was difficult to represent direct contact between organs. Therefore the pathogen is moved through blood to other organs. This transport of blood (global transmission) was modelled using graph-theoretic approach. At community level, the within-community level constitutes local transmission through direct contact or environmental transmission. Therefore, the ODEs are used to model this local transmission or local exchange of pathogen. However, at between-community level it was difficult to represent the contact of communities directly. Therefore, individuals moved between communities to achieve contact at community level. This movement of individuals is global transmission or global exchange of pathogen. This global transmission was represented using graph-theoretic approach. Furthermore, we also established distinctions between local transmission and global transmission mechanisms which enabled us to implement interventions targeted towards global transmission such as travel restrictions.

7.2 Future Research Directions

The focus of this study was to characterise multiscale models using different mathematical methods at various levels of organisation with FMD and Malaria as paradigms. Therefore, the following aspects can be considered for future research directions:

(1) It is important to characterise the individual-based network modelling multiscale modelling and nested modelling approaches if they accurately predict the dynamics of infectious disease systems

to the existing empirical data.

(2) The multiscale models we characterised used single pathogen species or single pathogen strain and so they can be extended to incorporated multiple pathogen species or multiple pathogen strains

(3) The multiscale models characterised in Chapter 4 and Chapter 6 did not consider other factors that impact the dynamics of disease systems like climate variations. Therefore, these factors are essential in determining the dynamics of FMD and Malaria.

(4) The multiscale models characterised in this study can be broadened to encorporate mediations that target microscale and macroscale disease dynamics.

(5) The multiscale models characterised in Chapter 4 and Chapter 6 took migration of cattle and humans respectively into account. However, they did not keep track of where a particular person is birthed and often stays as well as the patch where a person is at a particular period. Thus, this is imperative in modelling infectious disease systems like Corona virus.

Appendix A

7.3 Some graph theoretical terminology

(A.1) A *directed graph* or *digraph* $\mathcal{G} = (V, E)$ contains a set $V = 1, 2, ..., n$ of vertices and a set E of arcs (i, j) leading from the initial vertex i to vertex j.

(A.2) A subgraph $\mathcal{H}$ of $\mathcal{G}$ is said to be *spanning* if $\mathcal{H}$ and $\mathcal{G}$ have the same vertex set.

(A.3) A digraph $\mathcal{G}$ is *weighted* if each arc j, i is assigned a positive weight a_{ij}. In our convention, $a_{ij} > 0$ if and only if there exists an arc from vertex j to vertex i in $\mathcal{G}$.

(A.4) The *weight* $w(\mathcal{H})$ of a subgraph $\mathcal{H}$ is the product of the weights on all its arcs.

(A.5) A *directed path* $\mathcal{P}$ in $\mathcal{G}$ is a subgraph with distinct vertices $i_1, i_2, ..., i_m$ such that its set of arcs is $\{(i_k, i_{k+1} : k = 1, 2, ..., m - 1)\}$. If $i_m = i_1$, we call $\mathcal{P}$ a directed cycle.

(A.6) A connected subgraph $\mathcal{T}$ is a *tree* if it contains no cycles, directed or undirected.

(A.7) A tree $\mathcal{T}$ is rooted at vertex i, called the *root*, if i is not a terminal vertex of any arcs, and each of the remaining vertices is a terminal vertex of exactly one arc.

(A.8) Given a weighted digraph $\mathcal{G}$ with n vertices, define the weight matrix $A = (a_{ij})_{n \times n}$ whose entry a_{ij} equals the weight of arc (j, i) if it exists, and 0 otherwise. We denote a weighted digraph as $(\mathcal{G}, A)$.

(A.9) A subgraph $\mathcal{Q}$ is *unicyclic* if it is a disjoint union of rooted trees whose roots form a directed cycle. Note that every vertex of $\mathcal{Q}$ is the terminal vertex of exactly one arc.

Appendix B

7.4 A combinatorial identity

Let $(\mathcal{H}, \mathcal{W})$ be a weighted digraph with $n \geq 2$ vertices, where $\mathcal{W} = (w_{ij})$ is the weighted matrix. A weight $w_{ij} > 0$ if the directed arc (j, i) from vertex j from vertex i exists, otherwise $w_{ij} = 0$. Let $\mathbb{T}_i$ be the set of all spanning trees of $(\mathcal{H}, \mathcal{W})$ rooted at vertex i. For $\mathcal{T} \in \mathbb{T}_i$, the weight of $\mathcal{T}$, denoted by $w(\mathcal{T})$, is the product of weights on all arcs of $\mathcal{T}$. Let

$$c_i = \sum_{\mathcal{T} \in \mathbb{T}} w(\mathcal{T}), \qquad i = 1, 2, ..., n. \tag{B.1}$$

Then $c_i \geq 0$, and for any family of functions $\{H_i(x_i)\}_{i=1}^n$, the following identity holds

$$\sum_{i,j=1}^{n} c_i w_{ij} H_i(x_i) = \sum_{i,j=1}^{n} c_i w_{ij} H_j(x_j) \tag{B.2}$$

If $\mathcal{W} = (w_{ij})$ is irreducible, then $c_i > 0$ for $i = 1, 2, ..., n$.

Theorem 7.1. *Assume $n \geq 2$. Let c_i be given in $(B.1)$. Then the following identity holds:*

$$\sum_{i,j=1}^{n} c_i a_{ij} F_{ij}(x_i, x_j) = \sum_{\mathcal{Q} \in \mathbb{Q}} w(\mathcal{Q}) \sum_{(s,r) \in E(\mathcal{C}_{\mathcal{Q}}))} F_{r,s}(x_r, x_s) \tag{7.4.1}$$

Here $F_{ij}(x_i, x_j), 1 \leq i, j \leq n$, are arbitrary functions, $\mathbb{Q}$ is the set of all spanning unicyclic graphs of $(\mathcal{G}, A)$, $w(\mathcal{Q})$ is the weight of $\mathcal{Q}$ and $\mathcal{C}_{\mathcal{Q}}$ denotes the directed cycle of $\mathcal{Q}$

Proof Following the approach by [136], for a spanning tree $\mathcal{T}$ rooted at vertex i

$$w(\mathcal{T}) a_{ij} = w(\mathcal{Q}), \tag{7.4.2}$$

where $\mathcal{Q}$ is the unicyclic graph obtained from $\mathcal{T}$ by adding an arc (j,i) from vertex j to the root vertex i. Consequently,

$$w(\mathcal{T})a_{ij}F_{ij}(x_i,x_j) = w(\mathcal{Q})F_{ij}(x_i,x_j) \quad \text{, and} \quad (j,i) \in E(\mathcal{C}_{\mathcal{Q}}). \tag{7.4.3}$$

As we execute this operation in all possible ways to all rooted trees in $\mathcal{G}$, we get all unicyclic graphs in $\mathcal{G}$, and each unicyclic graph $\mathcal{Q}$ is created as many times as the number of arcs in its cycle $\mathcal{C}_{\mathcal{Q}}$. The identity 7.4.1 follows from (B.1) if we reorganize the double sum on the left-hand side as a sum over all unicyclic graphs in $\mathcal{G}$. □

Proof of (B.2) Using theorem 7.1, we know that both sides of (B.2) are equal to

$$\sum_{\mathcal{Q}\in\mathbb{Q}} w(\mathcal{Q}) \sum_{k\in V(\mathcal{C}_{\mathcal{Q}})} G_k(x_k), \tag{7.4.4}$$

where $V(\mathcal{C}_{\mathcal{Q}})$ is the vertex set of $\mathcal{C}_{\mathcal{Q}}$. □

Appendix C

Theorem 7.2. *Consider the following general system of ordinary differential equations with parameter* ϕ*:*

$$\frac{dx}{dt} = f(x, \phi) \tag{7.4.5}$$

$$f : \mathbf{R}^n \times \mathbf{R} \to \mathbf{R}. \quad f : \mathbf{C}^2 \left(\mathbf{R}^2 \times \mathbf{R}\right).$$

where 0 is an equilibrium of the system, that is, $f(0, \phi) = 0$ *for all* ϕ*, and assume that*

(A1) $A = D_x f(0,0) = ((\partial f_i/\partial x_j)(0,0))$ *is a linearization matrix of the multiscale model system (5.4.3) around the equilibrium 0 with* ϕ *evaluated at 0. Zero is a simple eigenvalue of* A*, and other eigenvalues have negative real parts.*

(A2) matrix A *has a right eigenvector u and a left eigenvector v corresponding to the zero eigenvalues.*

Let f_k *be the kth component of* f *and*

$$\begin{cases} a = \displaystyle\sum_{k,i,j=1}^{n} u_k v_i v_j \frac{\partial^2 f_k}{\partial x_i \partial x_j}(0,0), \\ \\ b = \displaystyle\sum_{k,i,j=1}^{n} u_k v_i \frac{\partial^2 f_k}{\partial x_i \partial \phi}(0,0), \end{cases} \tag{7.4.6}$$

The local dynamics of multiscale model system (5.4.3) around 0 are totally governed by a *and* b *and are summarized as follows.*

(i) $a > 0$ *and* $b > 0$. *When* $\phi < 0$ *with* $|\phi| \ll 1$, *0 is locally asymptotically stable, and there exists a positive unstable equilibrium: when* $0 < \phi \ll 1$, *0 is unstable and there exists a negative and locally asymptotically stable equilibrium.*

(ii) $a < 0$ *and* $b < 0$. *When* $\phi < 0$ *with* $|\phi| \ll 1$, *0 is unstable, when* $0 < \phi \ll 1$, *0 is asymptotically stable, and there exists a positive unstable equilibrium.*

(iii) $a > 0$ *and* $b < 0$. *When* $\phi < 0$ *with* $|\phi| \ll 1$, *0 is unstable, and there exists a locally asymptotically stable negative equilibrium; when* $0 < \phi \ll 1$, *0 is stable and a positive unstable equilibrium appears.*

(iv) $a < 0$ *and* $b > 0$. *When* ϕ *changes from negative to positive, 0 changes its stability from stable to unstable. Correspondingly a negative unstable equilibrium becomes positive and locally asymptotically stable.*

Bibliography

[1] Winston Garira. the replication-transmission relativity theory for multiscale modelling of infectious disease systems. *Scientific reports*, 9(1):1–17, 2019.

[2] Winston Garira. A complete categorization of multiscale models of infectious disease systems. *Journal of biological dynamics*, 11(1):378–435, 2017.

[3] Marianna Karamanou, George Panayiotakopoulos, Gregory Tsoucalas, Antonis A Kousoulis, and George Androutsos. From miasmas to germs: a historical approach to theories of infectious disease transmission. *Infez Med*, 20(1):58–62, 2012.

[4] Winston Garira. The research and development process for multiscale models of infectious disease systems. *PLoS computational biology*, 16(4):e1007734, 2020.

[5] Anil K Dasanna, Ulrich S Schwarz, Gerhard Gompper, and Dmitry A Fedosov. Multiscale modeling of malaria-infected red blood cells. *Handbook of Materials Modeling: Applications: Current and Emerging Materials*, 2018.

[6] Dmitry A Fedosov, Huan Lei, Bruce Caswell, Subra Suresh, and George E Karniadakis. Multiscale modeling of red blood cell mechanics and blood flow in malaria. *PLoS computational biology*, 7 (12):e1002270, 2011.

[7] Richard Howey, Bartlomiej Bankowski, Nicholas Juleff, Nicholas J Savill, Debi Gibson, John Fazakerley, Bryan Charleston, and Mark EJ Woolhouse. Modelling the within-host dynamics of the foot-and-mouth disease virus in cattle. *Epidemics*, 4(2):93–103, 2012.

[8] Julien Arino and P Van den Driessche. Disease spread in metapopulations. *Fields Institute Communications*, 48(1):1–13, 2006.

[9] Duygu Balcan, Vittoria Colizza, Bruno Gonçalves, Hao Hu, José J Ramasco, and Alessandro Vespignani. Multiscale mobility networks and the spatial spreading of infectious diseases. *Proceedings of the National Academy of Sciences*, 106(51):21484–21489, 2009.

[10] E Bertuzzo, Renato Casagrandi, Marino Gatto, I Rodriguez-Iturbe, and A Rinaldo. On spatially explicit models of cholera epidemics. *Journal of the Royal Society Interface*, 7(43):321–333, 2009.

[11] Dirk Brockmann, Vincent David, and Alejandro Morales Gallardo. Human mobility and spatial disease dynamics. *Reviews of nonlinear dynamics and complexity*, 2:1–24, 2009.

[12] Vittoria Colizza, Alain Barrat, Marc Barthélemy, and Alessandro Vespignani. The role of the airline transportation network in the prediction and predictability of global epidemics. *Proceedings of the National Academy of Sciences*, 103(7):2015–2020, 2006.

[13] Roger Guimera, Stefano Mossa, Adrian Turtschi, and LA Nunes Amaral. The worldwide air transportation network: Anomalous centrality, community structure, and cities' global roles. *Proceedings of the National Academy of Sciences*, 102(22):7794–7799, 2005.

[14] Winston Garira and Faraimunashe Chirove. A general method for multiscale modelling of vector-borne disease systems. *Interface focus*, 10(1):20190047, 2020.

[15] Shi Chen, Yakubu Owolabi, Ang Li, Eugenia Lo, Patrick Robinson, Daniel Janies, Chihoon Lee, and Michael Dulin. Patch dynamics modeling framework from pathogens' perspective: Unified and standardized approach for complicated epidemic systems, 2020.

[16] Alexis Erich S Almocera and Esteban A Hernandez-Vargas. Coupling multiscale within-host dynamics and between-host transmission with recovery (sir) dynamics. *Mathematical biosciences*, 309:34–41, 2019.

[17] Winston Garira, Dephney Mathebula, and Rendani Netshikweta. A mathematical modelling framework for linked within-host and between-host dynamics for infections with free-living pathogens in the environment. *Mathematical biosciences*, 256:58–78, 2014.

[18] Winston Garira. A primer on multiscale modelling of infectious disease systems. *Infectious Disease Modelling*, 3:176–191, 2018.

[19] Winston Garira and Dephney Mathebula. A coupled multiscale model to guide malaria control and elimination. *Journal of theoretical biology*, 475:34–59, 2019.

[20] Rendani Netshikweta and Winston Garira. A multiscale model for the world's first parasitic disease targeted for eradication: guinea worm disease. *Computational and mathematical methods in medicine*, 2017, 2017.

[21] Winston Garira and Martin Kanaan Mafunda. From individual health to community health: towards multiscale modeling of directly transmitted infectious disease systems. *Journal of Biological Systems*, 27(01):131–166, 2019.

[22] Ashutosh N Aggarwal. Quality of life with tuberculosis. *Journal of clinical tuberculosis and other mycobacterial diseases*, 17:100121, 2019.

[23] Alexandre Bittencourt Pigozzo, Gilson Costa Macedo, Rodrigo Weber dos Santos, and Marcelo Lobosco. Computational modeling of microabscess formation. *Computational and mathematical methods in medicine*, 2012, 2012.

[24] Anne Schneeberger, Catherine H Mercer, Simon AJ Gregson, Neil M Ferguson, Constance A Nyamukapa, Roy M Anderson, Anne M Johnson, and Geoff P Garnett. Scale-free networks and sexually transmitted diseases: a description of observed patterns of sexual contacts in britain and zimbabwe. *Sexually transmitted diseases*, 31(6):380–387, 2004.

[25] Richard Howey, Melvyn Quan, Nicholas J Savill, Louise Matthews, Søren Alexandersen, and Mark Woolhouse. Effect of the initial dose of foot-and-mouth disease virus on the early viral dynamics within pigs. *Journal of the Royal Society Interface*, 6(39):835–847, 2009.

[26] Abdulaziz YA Mukhtar, Justin B Munyakazi, and Rachid Ouifki. Assessing the role of human mobility on malaria transmission. *Mathematical biosciences*, 320:108304, 2020.

[27] Matt J Keeling and Ken TD Eames. Networks and epidemic models. *Journal of the Royal Society Interface*, 2(4):295–307, 2005.

[28] Mike J Jeger, Marco Pautasso, Ottmar Holdenrieder, and Mike W Shaw. Modelling disease spread and control in networks: implications for plant sciences. *New Phytologist*, 174(2):279–297, 2007.

[29] Mark DF Shirley and Steve P Rushton. The impacts of network topology on disease spread. *Ecological Complexity*, 2(3):287–299, 2005.

[30] G Witten and G Poulter. Simulations of infectious diseases on networks. *Computers in Biology and Medicine*, 37(2):195–205, 2007.

[31] Duncan J Watts and Steven H Strogatz. Collective dynamics of 'small-world'networks. *nature*, 393 (6684):440, 1998.

[32] James Holland Jones and Mark S Handcock. An assessment of preferential attachment as a mechanism for human sexual network formation. *Proceedings of the Royal Society of London. Series B: Biological Sciences*, 270(1520):1123–1128, 2003.

[33] Réka Albert and Albert-László Barabási. Statistical mechanics of complex networks. *Reviews of modern physics*, 74(1):47, 2002.

[34] Sergei N Dorogovtsev and José FF Mendes. *Evolution of networks: From biological nets to the Internet and WWW*. OUP Oxford, 2013.

[35] Mark EJ Newman. Ego-centered networks and the ripple effect. *Social Networks*, 25(1):83–95, 2003.

[36] Romualdo Pastor-Satorras and Alessandro Vespignani. Epidemic spreading in scale-free networks. *Physical review letters*, 86(14):3200, 2001.

[37] Réka Albert, Hawoong Jeong, and Albert-László Barabási. Error and attack tolerance of complex networks. *nature*, 406(6794):378, 2000.

[38] David A Sanchez. *Ordinary differential equations and stability theory: an introduction*. Courier Corporation, 1979.

[39] Joseph P LaSalle. Stability theory for ordinary differential equations. *Journal of Differential Equations*, 4(1):57–65, 1968.

[40] TA Burton and Tetsuo Furumochi. Fixed points and problems in stability theory for ordinary and functional differential equations. *Dynamic systems and applications*, 10(1):89–116, 2001.

[41] Sung Kyu Choi, Keon-Hee Lee, and Hi Jun Oh. Stability theory for ordinary differential equations. *Journal of the Chungcheong Mathematical Society*, 1(1):11–17, 1988.

[42] Suzete M Afonso, Fernanda Andrade Da Silva, Everaldo M Bonotto, Márcia Federson, Luciene P Gimenes, Rogelio Grau, Jaqueline G Mesquita, and Eduard Toon. Stability theory. *Generalized Ordinary Differential Equations in Abstract Spaces and Applications*, pages 241–294, 2021.

[43] Jack Carr. Center manifold. *Scholarpedia*, 1(12):1826, 2006.

[44] Alberto Bressan. Tutorial on the center manifold theorem. *Hyperbolic systems of balance laws*, 1911:327–344, 2003.

[45] J-P Eckmann and Clarence Eugene Wayne. Propagating fronts and the center manifold theorem. *Communications in mathematical physics*, 136(2):285–307, 1991.

[46] Giuseppe Da Prato and Alessandra Lunardi. Stability, instability and center manifold theorem for fully nonlinear autonomous parabolic equations in banach space. *Arch. Rational Mech. Anal*, 101 (2):115–141, 1988.

[47] Brian Hassard and Yieh Hei Wan. Bifurcation formulae derived from center manifold theory. *Journal of Mathematical Analysis and Applications*, 63(1):297–312, 1978.

[48] Nicholas Karydas and John Schinas. The center manifold theorem for a discrete system. *Applicable Analysis*, 44(3-4):267–284, 1992.

[49] Jack K Hale and Hüseyin Koçak. *Dynamics and bifurcations*, volume 3. Springer Science & Business Media, 2012.

[50] Odo Diekmann and Mirjam Kretzschmar. Patterns in the effects of infectious diseases on population growth. *Journal of Mathematical Biology*, 29(6):539–570, 1991.

[51] Bernt Oksendal. Stochastic differential equations: an introduction with applications. https://link.springer.com/book/10.1007/978-3-642-14394-6, 2013. Accessed: 2022-09-14.

[52] Bernt Øksendal, Agnes Sulem, and Tusheng Zhang. Optimal control of stochastic delay equations and time-advanced backward stochastic differential equations. *Advances in Applied Probability*, 43 (2):572–596, 2011.

[53] Michalis Faloutsos, Petros Faloutsos, and Christos Faloutsos. On power-law relationships of the internet topology. In *ACM SIGCOMM computer communication review*, volume 29, pages 251–262. ACM, 1999.

[54] Alison Gray, David Greenhalgh, Liangjian Hu, Xuerong Mao, and Jiafeng Pan. A stochastic differential equation sis epidemic model. *SIAM Journal on Applied Mathematics*, 71(3):876–902, 2011.

[55] Yoshihiro Maki and Hideo Hirose. Infectious disease spread analysis using stochastic differential equations for sir model. In *2013 4th International Conference on Intelligent Systems, Modelling and Simulation*, pages 152–156. IEEE, 2013.

[56] Amine El Koufi and Nouhaila El Koufi. Stochastic differential equation model of covid-19: Case study of pakistan. *Results in Physics*, 34:105–218, 2022.

[57] Kendall Atkinson, Weimin Han, and David E Stewart. *Numerical solution of ordinary differential equations*. John Wiley & Sons, 2011.

[58] Endre Süli. Numerical solution of ordinary differential equations. http://people.maths.ox.ac.uk/suli/nsodes.pdf, 2010. Accessed: 2022-09-23.

[59] Chenggui Yuan and Xuerong Mao. Convergence of the euler–maruyama method for stochastic differential equations with markovian switching. *Mathematics and Computers in Simulation*, 64 (2):223–235, 2004.

[60] Liangjian Hu, Xiaoyue Li, and Xuerong Mao. Convergence rate and stability of the truncated euler–maruyama method for stochastic differential equations. *Journal of Computational and Applied Mathematics*, 337:274–289, 2018.

[61] Xuerong Mao. Convergence rates of the truncated euler–maruyama method for stochastic differential equations. *Journal of Computational and Applied Mathematics*, 296:362–375, 2016.

[62] Zhiyong Wang and Chengjian Zhang. An analysis of stability of milstein method for stochastic differential equations with delay. *Computers & Mathematics with Applications*, 51(9-10):1445–1452, 2006.

[63] Qian Guo, Wei Liu, Xuerong Mao, and Rongxian Yue. The truncated milstein method for stochastic differential equations with commutative noise. *Journal of Computational and Applied Mathematics*, 338:298–310, 2018.

[64] Lorenzo Mari, Enrico Bertuzzo, Lorenzo Righetto, Renato Casagrandi, Marino Gatto, Ignacio Rodriguez-Iturbe, and Andrea Rinaldo. Modelling cholera epidemics: the role of waterways, human mobility and sanitation. *Journal of the Royal Society Interface*, 9(67):376–388, 2011.

[65] KO Okosun and Oluwole Daniel Makinde. A co-infection model of malaria and cholera diseases with optimal control. *Mathematical biosciences*, 258:19–32, 2014.

[66] Kazeem Oare Okosun, Mirirai Mukamuri, and Oluwole Daniel Makinde. Co-dynamics of trypanosomiasis and cryptosporidiosis. *Appl. Math*, 10(6):2137–2161, 2016.

[67] I Takaidza, OD Makinde, and OK Okosun. Computational modelling and optimal control of ebola virus disease with non-linear incidence rate. In *Journal of Physics: Conference Series*, volume 818, page 012003. IOP Publishing, 2017.

[68] Kazeem Oare Okosun and Oluwole Daniel Makinde. On a drug-resistant malaria model with susceptible individuals without access to basic amenities. *Journal of biological physics*, 38(3):507–530, 2012.

[69] Soon-Hyung Yook, Hawoong Jeong, and Albert-László Barabási. Modeling the internet's large-scale topology. *Proceedings of the National Academy of Sciences*, 99(21):13382–13386, 2002.

[70] Jon Kleinberg. Computing: The wireless epidemic. *Nature*, 449(7160):287, 2007.

[71] Maziar Nekovee. Worm epidemics in wireless ad hoc networks. *New Journal of Physics*, 9(6):189, 2007.

[72] Yongxiang Xia, K Tse Chi, Wai M Tam, Francis CM Lau, and Michael Small. Scale-free user-network approach to telephone network traffic analysis. *Physical Review E*, 72(2):026116, 2005.

[73] Zoltán Dezső and Albert-László Barabási. Halting viruses in scale-free networks. *Physical Review E*, 65(5):055103, 2002.

[74] Nilly Madar, Tomer Kalisky, Reuven Cohen, Daniel Ben-avraham, and Shlomo Havlin. Immunization and epidemic dynamics in complex networks. *The European Physical Journal B*, 38(2): 269–276, 2004.

[75] Vitaly Belik, Theo Geisel, and Dirk Brockmann. Natural human mobility patterns and spatial spread of infectious diseases. *Physical Review X*, 1(1):011001, 2011.

[76] Shunjiang Ni and Wenguo Weng. Impact of travel patterns on epidemic dynamics in heterogeneous spatial metapopulation networks. *Physical review E*, 79(1):016111, 2009.

[77] Lin Wang and Xiang Li. Spatial epidemiology of networked metapopulation: An overview. *Chinese Science Bulletin*, 59(28):3511–3522, 2014.

[78] Tanya Kostova-Vassilevska. On the use of models to assess foot-and-mouth disease transmission and control. Technical report, Lawrence Livermore National Lab.(LLNL), Livermore, CA (United States), 2004.

[79] Arnaud LeMenach, Judith Legrand, Rebecca F Grais, Cécile Viboud, Alain-Jacques Valleron, and Antoine Flahault. Modeling spatial and temporal transmission of foot-and-mouth disease in france: identification of high-risk areas. *Veterinary Research*, 36(5-6):699–712, 2005.

[80] Montiago LaBute, Benjamin McMahon, Mac Brown, Carrie Manore, and Jeanne Fair. A flexible spatial framework for modeling spread of pathogens in animals with biosurveillance and disease control applications. *ISPRS International Journal of Geo-Information*, 3(2):638–661, 2014.

[81] John C Lang, Hans De Sterck, Jamieson L Kaiser, and Joel C Miller. Analytic models for sir disease spread on random spatial networks. *Journal of Complex Networks*, 6(6):948–970, 2018.

[82] Simon M Firestone, Robert M Christley, Michael P Ward, and Navneet K Dhand. Adding the spatial dimension to the social network analysis of an epidemic: Investigation of the 2007 outbreak of equine influenza in australia. *Preventive veterinary medicine*, 106(2):123–135, 2012.

[83] Richard A Bradhurst, Sharon E Roche, Iain J East, Paul Kwan, and M Graeme Garner. A hybrid modeling approach to simulating foot-and-mouth disease outbreaks in australian livestock. *Frontiers in Environmental Science*, 3:17, 2015.

[84] Laura W Pomeroy, Shweta Bansal, Micheal Tildesley, KI Moreno-Torres, Mark Moritz, Ningchuan Xiao, TE Carpenter, and Rebecca B Garabed. Data-driven models of foot-and-mouth disease dynamics: A review. *Transboundary and emerging diseases*, 64(3):716–728, 2017.

[85] Miguel A Acevedo, Olivia Prosper, Kenneth Lopiano, Nick Ruktanonchai, T Trevor Caughlin, Maia Martcheva, Craig W Osenberg, and David L Smith. Spatial heterogeneity, host movement and mosquito-borne disease transmission. *PloS one*, 10(6):e0127552, 2015.

[86] Sehjeong Kim, Abdessamad Tridane, and Dong Eui Chang. Human migrations and mosquito-borne diseases in africa. *Mathematical Population Studies*, 23(2):123–146, 2016.

[87] Michael Eschbaumer, Carolina Stenfeldt, Steven I Rekant, Juan M Pacheco, Ethan J Hartwig, George R Smoliga, Mary A Kenney, William T Golde, Luis L Rodriguez, and Jonathan Arzt. Systemic immune response and virus persistence after foot-and-mouth disease virus infection of naive cattle and cattle vaccinated with a homologous adenovirus-vectored vaccine. *BMC veterinary research*, 12(1):205, 2016.

[88] Donald Thompson, P Muriel, D Russell, P Osborne, A Bromley, M Rowland, S Creigh-Tyte, and C Brown. Economic costs of the foot and mouth disease outbreak in the united kingdom in 2001. *Revue scientifique et technique (International Office of Epizootics)*, 21(3):675–687, 2002.

[89] Simon I Hay, Carlos A Guerra, Peter W Gething, Anand P Patil, Andrew J Tatem, Abdisalan M Noor, Caroline W Kabaria, Bui H Manh, Iqbal R F Elyazar, Simon Brooker, et al. A world malaria map: Plasmodium falciparum endemicity in 2007. *PLoS medicine*, 6(3):e1000048, 2009.

[90] MEJ Woolhouse. Foot-and-mouth disease in the uk: What should we do next time? *Journal of Applied Microbiology*, 94:126–130, 2003.

[91] J Pega, Danilo Bucafusco, Sebastián Di Giacomo, Juan Manuel Schammas, D Malacari, Alejandra Victoria Capozzo, J Arzt, C Pérez-Beascoechea, E Maradei, LL Rodríguez, et al. Early adaptive immune responses in the respiratory tract of foot-and-mouth disease virus-infected cattle. *Journal of virology*, 87(5):2489–2495, 2013.

[92] JS Salt. The carrier state in foot and mouth disease—an immunological review. *British Veterinary Journal*, 149(3):207–223, 1993.

[93] RP Kitching. Global epidemiology and prospects for control of foot-and-mouth disease. *Foot-and-mouth disease virus*, pages 133–148, 2005.

[94] Notice Ringa and Chris T Bauch. Impacts of constrained culling and vaccination on control of foot and mouth disease in near-endemic settings: A pair approximation model. *Epidemics*, 9:18–30, 2014.

[95] SE Roche, MG Garner, RL Sanson, C Cook, C Birch, JA Backer, C Dube, KA Patyk, MA Stevenson, ZD Yu, et al. Evaluating vaccination strategies to control foot-and-mouth disease: a model comparison study. *Epidemiology & Infection*, 143(6):1256–1275, 2015.

[96] TG Rawdon, MG Garner, RL Sanson, MA Stevenson, C Cook, C Birch, SE Roche, KA Patyk, KN Forde-Folle, Caroline Dubé, et al. Evaluating vaccination strategies to control foot-and-mouth disease: a country comparison study. *Epidemiology & Infection*, 146(9):1138–1150, 2018.

[97] Paul Sutmoller, Simon S Barteling, Raul Casas Olascoaga, and Keith J Sumption. Control and eradication of foot-and-mouth disease. *Virus research*, 91(1):101–144, 2003.

[98] Yona Sinkala, Martin Simuunza, John B Muma, Dirk U Pfeiffe, Christopher J Kasanga, and Aaron Mweene. Foot and mouth disease in zambia: Spatial and temporal distributions of outbreaks, assessment of clusters and implications for control. *Onderstepoort Journal of Veterinary Research*, 81(2):1–6, 2014.

[99] TJD Knight-Jones and J Rushton. The economic impacts of foot and mouth disease–what are they, how big are they and where do they occur? *Preventive veterinary medicine*, 112(3-4):161–173, 2013.

[100] Henry C Tuckwell, Laurent Toubiana, and Jean-Francois Vibert. Spatial epidemic network models with viral dynamics. *Physical Review E*, 57(2):2163, 1998.

[101] Carlos Castillo-Chavez, Zhilan Feng, and Wenzhang Huang. On the computation of ro and its role on global stability. *Mathematical approaches for emerging and reemerging infectious diseases: an introduction*, 1:229, 2002.

[102] Odo Diekmann, Johan Andre Peter Heesterbeek, and Johan AJ Metz. On the definition and the computation of the basic reproduction ratio r 0 in models for infectious diseases in heterogeneous populations. *Journal of mathematical biology*, 28(4):365–382, 1990.

[103] Pauline Van den Driessche and James Watmough. Reproduction numbers and sub-threshold endemic equilibria for compartmental models of disease transmission. *Mathematical biosciences*, 180(1-2):29–48, 2002.

[104] Evelyn C Rynkiewicz, Amy B Pedersen, and Andy Fenton. An ecosystem approach to understanding and managing within-host parasite community dynamics. *Trends in parasitology*, 31(5): 212–221, 2015.

[105] Mathieu Sicard, Jessica Dittmer, Pierre Gréve, Didier Bouchon, and Christine Braquart-Varnier. A host as an ecosystem: W olbachia coping with environmental constraints. *Environmental Microbiology*, 16(12):3583–3607, 2014.

[106] Lofgren Eric T, Adrea M Egizi, and Nina H Fefferman. Patients as patches: Ecology and epidemiology in healthcare environments. *infection control & hospital epidemiology*, 37(12):1507–1512, 2016.

[107] Xuerong Mao. *Stability of stochastic differential equations with respect to semimartingales*. Longman, 1991.

[108] Xuerong Mao. *Exponential stability of stochastic differential equations*. Marcel Dekker, 1994.

[109] Xuerong Mao. *Stochastic differential equations and applications*. Elsevier, 2007.

[110] Zishun Zhao, Thomas I Wahl, and Thomas L Marsh. Invasive species management: foot-and-mouth disease in the us beef industry. *Agricultural and Resource Economics Review*, 35(1203-2016-95325):98–115, 2006.

[111] Aurelio H Cabezas, Michael W Sanderson, Majid Jaberi-Douraki, and Victoriya V Volkova. Clinical and infection dynamics of foot-and-mouth disease in beef feedlot cattle: an expert survey. *Preventive veterinary medicine*, 158:160–168, 2018.

[112] PT Thomsen and H Houe. Dairy cow mortality. a review. *Veterinary Quarterly*, 28(4):122–129, 2006.

[113] Steady Mushayabasa, Claver P Bhunu, and Mlamuli Dhlamini. Impact of vaccination and culling on controlling foot and mouth disease: a mathematical modelling approach. 2011.

[114] B Singh, Shiv Prasad, DK Sinha, and Med Ram Verma. Estimation of economic losses due to foot and mouth disease in india. *Indian J. Anim. Sci*, 83(9):964–970, 2013.

[115] Soren Alexandersen, Z Zhang, AI Donaldson, and AJM Garland. The pathogenesis and diagnosis of foot-and-mouth disease. *Journal of comparative pathology*, 129(1):1–36, 2003.

[116] JA Backer, TJ Hagenaars, G Nodelijk, and HJW Van Roermund. Vaccination against foot-and-mouth disease i: epidemiological consequences. *Preventive veterinary medicine*, 107(1-2):27–40, 2012.

[117] M Barasa, A Catley, D Machuchu, H Laqua, E Puot, D Tap Kot, and D Ikiror. Foot-and-mouth disease vaccination in south sudan: Benefit–cost analysis and livelihoods impact. *Transboundary and Emerging Diseases*, 55(8):339–351, 2008.

[118] Konrad Bauer. Foot-and-mouth disease as zoonosis. In *Viral Zoonoses and Food of Animal Origin*, pages 95–97. Springer, 1997.

[119] J Casal, JM Moreso, and E Planas-Cuchi. Simulated airborne spread of aujeszky's disease and foot-and-mouth disease. *Veterinary Record*, 140(26):672–676, 1997.

[120] Sarah J Cox and Paul V Barnett. Experimental evaluation of foot-and-mouth disease vaccines for emergency use in ruminants and pigs: a review. *Veterinary research*, 40(3):1, 2009.

[121] Alex I Donaldson and Soren Alexandersen. Predicting the spread of foot and mouth disease by airborne virus. *Revue Scientifique et Technique-Office International des épizooties*, 21(3):569–578, 2002.

[122] C Dubé, C Ribble, D Kelton, and B McNab. A review of network analysis terminology and its application to foot-and-mouth disease modelling and policy development. *Transboundary and emerging diseases*, 56(3):73–85, 2009.

[123] M Graeme Garner and SD Beckett. Modelling the spread of foot-and-mouth disease in australia. *Australian Veterinary Journal*, 83(12):758–766, 2005.

[124] Marvin J Grubman and Barry Baxt. Foot-and-mouth disease. *Clinical microbiology reviews*, 17(2): 465–493, 2004.

[125] Syed M Jamal and Graham J Belsham. Foot-and-mouth disease: past, present and future. *Veterinary research*, 44(1):1–14, 2013.

[126] Rowland R Kao, Darren M Green, Jethro Johnson, and Istvan Z Kiss. Disease dynamics over very different time-scales: foot-and-mouth disease and scrapie on the network of livestock movements in the uk. *Journal of the Royal Society Interface*, 4(16):907–916, 2007.

[127] Cecilia Langellotti, Gonzalo Cesar, Ivana Soria, Valeria Quattrocchi, Carolina Jancic, Patricia Zamorano, and Mónica Vermeulen. Foot-and-mouth disease virus infection of dendritic cells triggers phosphorylation of erk1/2 inducing class i presentation and apoptosis. *Vaccine*, 33(38):4945–4953, 2015.

[128] MM Rweyemamu and VM Astudillo. Global perspective for foot and mouth disease control. *Revue scientifique et technique-Office international des épizooties*, 21(3):765–769, 2002.

[129] Simon M Firestone, Yoko Hayama, Richard Bradhurst, Takehisa Yamamoto, Toshiyuki Tsutsui, and Mark A Stevenson. Reconstructing foot-and-mouth disease outbreaks: a methods comparison of transmission network models. *Scientific reports*, 9(1):1–12, 2019.

[130] Sibylle Mohr, Michael Deason, Mikhail Churakov, Thomas Doherty, and Rowland R Kao. Manipulation of contact network structure and the impact on foot-and-mouth disease transmission. *Preventive veterinary medicine*, 157:8–18, 2018.

[131] Abraham Berman and Robert J Plemmons. *Nonnegative matrices in the mathematical sciences*. SIAM, 1994.

[132] Vangipuram Lakshmikantham, Srinivasa Leela, and Anatoly A Martynyuk. *Stability analysis of nonlinear systems*. Springer, 1989.

[133] Hal L Smith and Paul Waltman. *The theory of the chemostat: dynamics of microbial competition*, volume 13. Cambridge university press, 1995.

[134] Hongbin Guo, Michael Y Li, and Zhisheng Shuai. Global stability of the endemic equilibrium of multigroup sir epidemic models. *Canadian applied mathematics quarterly*, 14(3):259–284, 2006.

[135] Hongbin Guo, Michael Li, and Zhisheng Shuai. A graph-theoretic approach to the method of global lyapunov functions. *Proceedings of the American Mathematical Society*, 136(8):2793–2802, 2008.

[136] Michael Y Li and Zhisheng Shuai. Global-stability problem for coupled systems of differential equations on networks. *Journal of Differential Equations*, 248(1):1–20, 2010.

[137] Michael Y Li and Zhisheng Shuai. Global stability of an epidemic model in a patchy environment. *Canadian Applied Mathematics Quarterly*, 17(1):175–187, 2009.

[138] Joseph P La Salle. *The stability of dynamical systems*. SIAM, 1976.

[139] Santwana Kar and Santosh Kar. Control of malaria. *Nat Rev Drug Discov*, 9(7):511–512, 2010.

[140] Philip A Eckhoff. A malaria transmission-directed model of mosquito life cycle and ecology. *Malaria journal*, 10(1):1–17, 2011.

[141] Christinah Chiyaka, Winston Garira, and S Dube. Modelling immune response and drug therapy in human malaria infection. *Computational and Mathematical Methods in Medicine*, 9(2):143–163, 2008.

[142] KP Day, RE Hayward, and M Dyer. The biology of plasmodium falciparum transmission stages. *Parasitology*, 116(S1):S95–S109, 1998.

[143] C Hetzel and RM Anderson. The within-host cellular dynamics of bloodstage malaria: theoretical and experimental studies. *Parasitology*, 113(1):25–38, 1996.

[144] Herbert W Hethcote. The mathematics of infectious diseases. *SIAM review*, 42(4):599–653, 2000.

[145] Miranda I Teboh-Ewungkem and Thomas Yuster. A within-vector mathematical model of plasmodium falciparum and implications of incomplete fertilization on optimal gametocyte sex ratio. *Journal of theoretical biology*, 264(2):273–286, 2010.

[146] Zadoki Tabo, Livingstone S Luboobi, and Joseph Ssebuliba. Mathematical modelling of the in-host dynamics of malaria and the effects of treatment. *Journal of Mathematics and Computer Science*, 17(1):1–21, 2017.

[147] RE Howells and EE Davies. Nuclear division in the oocyst of plasmodium berghei. *Annals of Tropical Medicine & Parasitology*, 65(4):451–459, 1971.

[148] Liming Cai, Necibe Tuncer, and Maia Martcheva. How does within-host dynamics affect population-level dynamics? insights from an immuno-epidemiological model of malaria. *Mathematical Methods in the Applied Sciences*, 40(18):6424–6450, 2017.

[149] Barbara Hellriegel. Modelling the immune response to malaria with ecological concepts: short-term behaviour against long-term equilibrium. *Proceedings of the Royal Society of London. Series B: Biological Sciences*, 250(1329):249–256, 1992.

[150] LC Gouagna, S Bonnet, R Gounoue, JP Verhave, W Eling, R Sauerwein, and Christian Boudin. Stage-specific effects of host plasma factors on the early sporogony of autologous plasmodium falciparum isolates within anopheles gambiae. *Tropical Medicine & International Health*, 9(9): 937–948, 2004.

[151] Mathieu Legros and Sebastian Bonhoeffer. A combined within-host and between-hosts modelling framework for the evolution of resistance to antimalarial drugs. *Journal of the Royal Society Interface*, 13(117):20160148, 2016.

[152] Gilberto González Parra, Abraham J Arenas, and Miladys R Cogollo. Positivity and boundedness of solutions for a stochastic seasonal epidemiological model for respiratory syncytial virus (rsv). *Ingeniería y Ciencia*, 13(25):95–121, Escuela de Ciencias y Humanidades y Escuela de Ingeniería de la Universidad.

[153] N. Dalal, D. Greenhalgh, and X. Mao. A stochastic model of aids and condom use. *Journal of Mathematical Analysis and Applications*, 325(1):36–53, 2007.

[154] X. Mao, G. Marion, and E. Renshaw. Environmental brownian noise suppresses exlposions in population dynamics. *Stochastic Processes and their Applications*, 97(1):95–110, 2002.

[155] X. Mao, C. Yuan, and J. Zou. Stochastic differential delay equations of population dynamics. *Journal of Mathematical Analysis and Applications*, 97(1):95–110, 2005.